

Branched and Star Copolymers Based on Poly(glycolic acid) and Poly(lactic acid)

Dissertation zur Erlangung des Grades

"Doktor der Naturwissenschaften"

im Promotionsfach Makromolekulare Chemie

am Fachbereich Chemie, Pharmazie und Geowissenschaften

der Johannes Gutenberg-Universität in Mainz

Anna Magdalena Fischer

Mainz, Juni 2012

Tag der mündlichen Prüfung: 11.07.2012

Hiermit versichere ich gemäß § 10 Abs. 3d der Promotionsordnung vom 24.07.2007, dass ich die als Dissertation vorgelegte Arbeit selbst angefertigt und alle benutzten Hilfsmittel (Literatur, Apparaturen, Material) in der Arbeit angegeben habe.

Die als Dissertation vorgelegte Arbeit wurde in der Zeit vom Mai 2009 bis Juni 2012 am Institut für Organische Chemie der Johannes Gutenberg-Universität Mainz im Arbeitskreis von Univ.-Prof. Dr. Holger Frey angefertigt.

In Dankbarkeit
für alle, die mich unterstützt haben

„Ich habe zwar keine Lösung, aber ich bewundere das Problem.“

Ashleigh Brilliant

Danksagung (Acknowledgments)

Table of Contents

Motivation and Objectives	11
Abstract	15
Graphical Abstract.....	20
Chapter 1: Introduction.....	25
1.1 Poly(glycolic acid): A Status Report on Synthesis, Applications and Limitations	27
Chapter 2: Branched and Star Copolymers Based on Poly(glycolide).....	75
2.1 Soluble Hyperbranched Poly(glycolide) Copolymers	77
Supporting Information.....	96
2.2 One-Pot Synthesis of PLLA Multi-Arm Star Copolymers Based on a Polyester Polyol Macroinitiator	103
Supporting Information.....	117
Chapter 3: Glycerol-Based Poly(glycolide) Copolymers	121
3.1 Poly(glycolide) Multi-Arm Star Polymers: Improved Solubility via Limited Arm Length.....	123
3.2 Synthesis of Branched Glycerol-Based Poly(glycolide) Copolymers via Ring-Opening Polymerization.....	139
Supporting Information.....	158
3.3 Poly(ethylene glycol)-g-Poly(glycolide) Copolymers: A Promising Polymer Surfactant for Microparticle Synthesis	167
Supporting Information.....	185
Chapter 4: Novel Copolymers Based on Poly(lactide).....	191
4.1 Block Copolymers Based on Poly(lactide) and Poly(dimethylsiloxane): Strongly Segregated Systems.....	193
Supporting Information.....	208
4.2 Combining Polysulfides with Polyesters to Degradable Block Copolymers	211
Supporting Information.....	218
Chapter 5: Ongoing Projects	229
5.1 Thermorheological Properties of Hyperbranched Poly(glycolide) Copolymers.....	231
5.2 Synthesis and Characterization of Functional P(HPMA)-block-P(DLLA) Copolymers as Surfactant for Miniemulsion Technique	243

Appendix.....	255
A1. Long-Chain Branched Poly(lactide)s Based on Polycondensation of AB ₂ -type Macromonomers	257
Supporting Information.....	273
A.2 CURRICULUM VITAE – Anna Magdalena Fischer	281
A.3 List of Publications	Fehler! Textmarke nicht definiert.

Motivation and Objectives

Motivation and Objectives

The rapid progress in poly(ester) research as a multi-disciplinary field mainly relies on the biodegradability and ease of synthesis of these materials. Despite the large variety of available poly(ester)s that possess good biocompatibility, a special focus lies on poly(lactide), poly(ϵ -caprolactone) and poly(lactide-co-glycolide) (PLGA) copolymers. With respect to their promising features they are commercially applied in drug delivery systems, tissue engineering, bone fixation devices and sutures. The application of poly(lactide) (PLA) for packaging purpose is pursued by a number of companies at present, since PLA is produced from renewable resources. As an alternative to commodity plastics it contributes to the environmental impact reduction. The lack of side chain functionality, its brittleness and the extent of crystallization have been addressed by designing novel functional lactone monomers, using blends or simply by changing the macromolecular architecture.

Although glycolic acid or glycolide are often applied in PLGA copolymers, poly(glycolide) (PGA) still represents a rather neglected homopolymer in the class of aliphatic poly(ester)s. Biodegradable materials benefit from the fast hydrolysis of the more hydrophilic PGA ester bonds. This peculiar feature of PGA units enables modulation of the degradation rate according to the molar composition. High cell affinity and low inflammation tendency represent key advantages of PGA in tissue regeneration. However, a major drawback hampering synthesis, application and characterization of PGA is its lack of solubility in common organic solvents and its high melting point, limiting processing to the bulk phase. Hence, further developments are crucial to overcome main limitations of PGA.

Besides the manifold advances in the field of linear polymers, the development of new macromolecular structures has been a great issue in recent years ranging from dendrimer-, star- and comb-like polymers to hyperbranched materials. While preserving valuable characteristics of the linear analogue, the introduction of dendritic units in a polyester backbone is a promising approach to tailor materials properties and to increase functionality.

With the increasing demand for biomedical applications a central issue in recent aliphatic poly(ester) research has been the lack of water-solubility and functionality, limiting the application to non-aqueous environment. The design of amphiphilic poly(ester)-based copolymers using poly(ethylene glycol) as a hydrophilic building block enhanced solubility and contributed to a broadening of application fields, i.e., in physiological environment. Especially, polylactones based on metal-free organocatalysis qualify for the design of "smart materials" relying on controlled reaction conditions and reproducible material properties.

The main objective of this thesis is the design and synthesis of poly(glycolide)-based polymers with various topologies. Dendritic and star-shaped topologies are of central interest to (i) overcome the fundamental drawback of insolubility and (ii) to provide access to an increased number of functional end groups at the aliphatic poly(ester) backbone. Different synthetic pathways toward branched poly(glycolide) (PGA) copolymers will be explored with respect to the introduction of branching and also keeping in mind the ease of synthesis for possible industrial scale-up. Branching can be realized employing two different strategies: On the one hand, AB₂ comonomers (e.g., bishydroxy acids) can be used, which serve as initiators in ring-opening polymerization (ROP) of glycolide and participate in subsequent polycondensation. On the other hand, the inimer strategy can be pursued to introduce branching sites via copolymerization of glycolide with a hydroxyl-functional lactone.

Besides material properties, the exploration of mild polymer modification reaction conditions considering the sensitive poly(ester) backbone is of great interest. The addressability of the functional end groups is proved using the dendritic copolymers as macroinitiators for the synthesis of multi-arm star polymers.

Another important aspect of this thesis is the combination of PGA oligomers with hydrophilic and biocompatible building blocks to comb-like and multi-arm star copolymers, targeting amphiphilic poly(ester)-based materials with valuable features like self-aggregation in aqueous solution and partial degradability, which could be relevant in drug delivery systems. In general, different strategies are combined to provide easy access toward soluble PGA copolymers.

The main task of the last part of this thesis is the synthesis of tailor-made poly(lactide) copolymers with flexible building blocks combining different polymerization methods, such as cationic/anionic ROP of cyclosiloxane or anionic ROP of propylene sulfide with lactide ROP. The copolymers benefit from poly(lactide)s' unique property of stereocomplexation and its degradability. The investigation of the material properties, supramolecular structure formation and adsorption behavior is of central interest to establish new fields of application.

Abstract

Abstract

Chapter 1 reviews the synthesis, peculiar features and challenges concomitant with poly(glycolide) (PGA) synthesis and applications both with respect to homo- and copolymers in a comprehensive manner. One central field comprises the synthesis of functional poly(glycolide) copolymers based on star-like and branched architectures, as well as polymer modification reactions. It presents currently established, different fields of applications mainly focusing on the PGA homopolymer, and enlightens the importance of this material in various areas, ranging from biomedical applications to packaging purposes. Drawbacks, recent progress and future developments are being discussed.

In **Chapter 2** the synthesis of branched and star-like poly(glycolide) architectures is presented. The problem of insolubility and high processing temperatures associated with poly(glycolide) is addressed by the introduction of branches and reduction of the PGA chain length. **Chapter 2.1** deals with the first synthesis of hyperbranched poly(glycolide) copolymers, combining ring-opening polymerization (ROP) and AB₂-polycondensation. The ROP of glycolide has been initiated via a functional initiator and yielded bishydroxy acid-functional prepolymers, which were subsequently condensed to obtain polyfunctional hyperbranched (hb) poly(glycolide) copolymers. The introduction of branches into the poly(glycolide) backbone resulted in a suppression of crystallization and permitted incorporation of up to 85 mol% glycolide. Evidence of branching has been gathered by detailed 1D and 2D NMR analysis, accompanied by the synthesis of model compounds resembling the branched and linear repeating units. Hyperbranched polyesters and their derivatives exhibit potential in coating applications, drug delivery systems and as crosslinking agents. The obtained amorphous hb PGA copolymers guarantee degradability and excellent thermal stability (see **Chapter 5.1**). In **Chapter 2.2** poly(L-lactide) multi-arm stars have been synthesized in a grafting-from approach, based on the previously obtained polyester ployols (**Chapter 2.1**), which served as macroinitiators in the ROP of L-lactide. The melting point of the obtained PLLA multi-arm star block copolymers has been significantly reduced, which allows for an adjustment of PLLA's thermal properties solely by changing the architecture. The variation of molar composition and PLLA chain length is a key issue in the modulation of its degradation profile.

Several approaches towards hydrophilic glycerol-based poly(glycolide)s including comb-like, hyperbranched and star-like architectures are presented in **Chapter 3**. **Chapter 3.1** describes the synthesis of poly(glycolide) multi-arm stars based on a hyperbranched poly(glycerol) core. This strategy introduces the concept of "improved solubility via limited PGA chain length" and allowed for glycolide incorporation up to a molecular weight fraction of 91 %. Amphiphilic poly(ether ester)s are

promising vehicles in drug delivery for physical entrapment of drug moieties due to their core-shell characteristics. **Chapter 3.3** represents a further approach towards branched, glycerol-based poly(glycolide), relying on an iminer-promoted ring-opening multibranching copolymerization (ROMBP) of glycolide and a hydroxyl-functional lactone (5HDON). In order to overcome side reactions, such as etherification due to the harsh reaction conditions associated with polycondensation, ROMBP has been chosen for esterification under mild conditions. The formation of branching has been followed by ^1H NMR spectroscopy, and polymer modification enabled the calculation of the degree of branching (DB). Derivatization of the terminal functionalities has been accomplished and is a promising tool in broadening the materials' range of application.

In **Chapter 3.2** the build-up of amphiphilic PGA graft copolymers has been accomplished combining oxyanionic polymerization and glycolide ring-opening. Oxyanionic ROP of ethoxy ethyl glycidyl ether (EEGE) initiated via monofunctional PEG, and subsequent cleavage of the acetal protecting group succeeded in poly(ethylene glycol)-*b*-poly(glycerol) copolymers. These multifunctional precursor have been successfully applied in $\text{Sn}(\text{Oct})_2$ -catalyzed ROP of glycolide. Chain extension of poly(glycerol) concomitant with increased functionality allowed the incorporation of glycolide up to a content of 62 wt%. Solubility of the comb-like polymers has been provided via limited PGA chain length. The amphiphilic graft copolymers represent promising surfactants in emulsion technique and are suitable candidates in tissue engineering due to their hydrophilicity and antifouling properties. TEM analysis revealed the formation of micellar aggregates in aqueous environment.

In cooperation a series of partially degradable poly(lactide) block copolymers with highly incompatible blocks and promising potential in various fields of application has been realized (**Chapter 4**). The design of AB and ABA block copolymers consisting of poly(dimethylsiloxane) (PDMS) and poly(lactide) segments is described in **Chapter 4.1**. The synthesis of mono- and difunctional PDMS blocks has been achieved via two different routes using cationic and anionic ROP of cyclosiloxanes. Hydroxyalkyl functions have been introduced by subsequent hydrosilylation serving as initiation sites in the DBU-catalyzed ROP of L- and D-lactide. As expected, AFM images of the AB-and ABA-type block copolymers revealed phase separation, resulting in lamellar assembly. In order to take advantage of the unique features of poly(lactide), stereocomplexation of the PLA blocks has been introduced, resulting in materials with properties similar to thermoplastic elastomers.

Chapter 4.2 presents the first approach toward poly(propylene sulfide)-*b*-poly(L-lactide) copolymers. Here, poly(propylene sulfide) represents the soft segment, which led to a reduction of PLAs' melting temperature and allowed adhesion to gold nanoparticles. The synthesis of monofunctional poly(propylene sulfide) has been achieved by anionic ROP, and subsequent chain-end termination with bromoethanol followed by ring-opening polymerization of lactide. The block copolymers may be

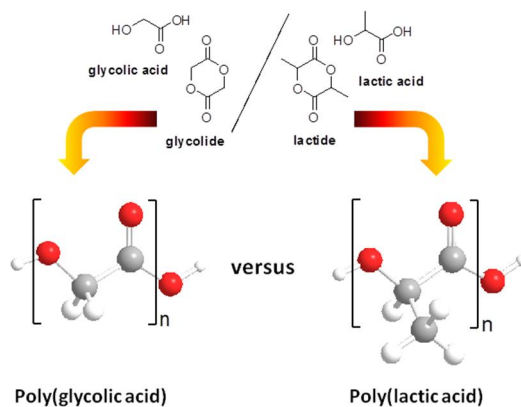
transformed into amphiphilic polymers via oxidation of the PPS backbone, yielding poly(sulfoxide)-*b*-poly(lactide) copolymers. The stimuli-responsive behaviour of the PPS building blocks to oxidants renders the system highly interesting in drug release, which is triggered upon polarity driven change of the morphology.

Chapter 5 summarizes the current status of ongoing collaborative efforts and their future perspectives. Both an investigation of thermo-rheological properties of hyperbranched PGA copolymers (**Chapter 5.1**) based on **Chapter 2.1** and the synthesis and application of poly(N-(2-hydroxypropyl)-methacrylamide)-*b*-poly(lactide) copolymers as surfactant in a miniemulsion are described (**Chapter 5.2**).

Graphical Abstract

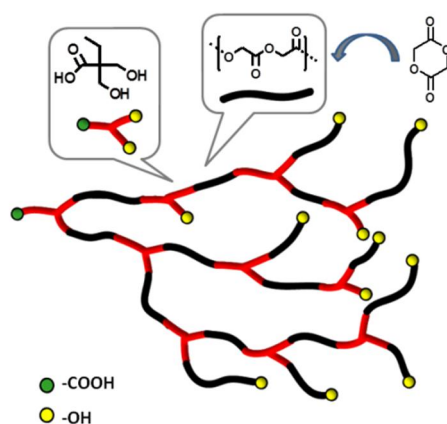
Chapter 1:

Poly(glycolic acid): A Status Report on Synthesis, Applications and Limitations.....27



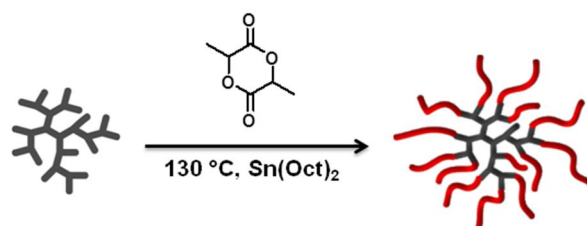
Chapter 2.1:

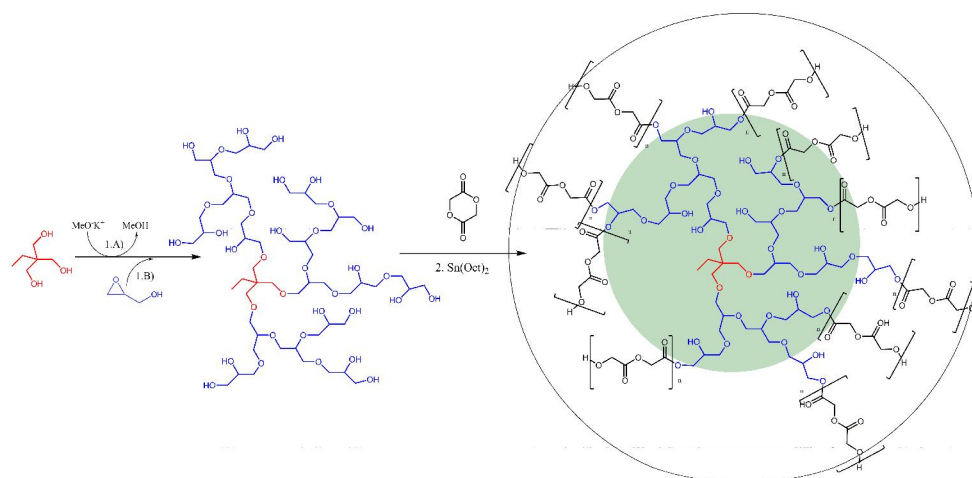
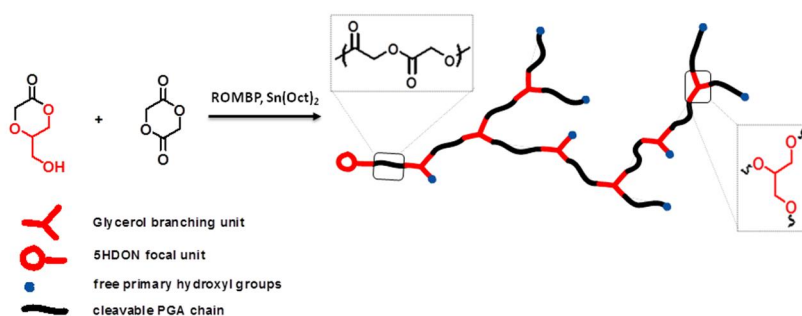
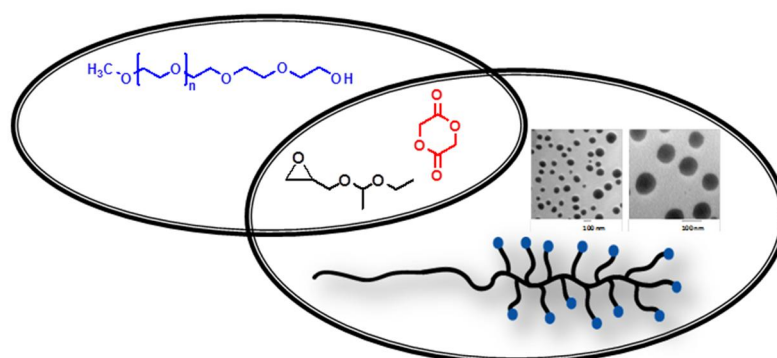
Soluble Hyperbranched Poly(glycolide Copolymers.....77



Chapter 2.2:

One-Pot Synthesis of PLLA Multi-Arm Star Copolymers Based on a Polyester Polyol Macroinitiator.....103

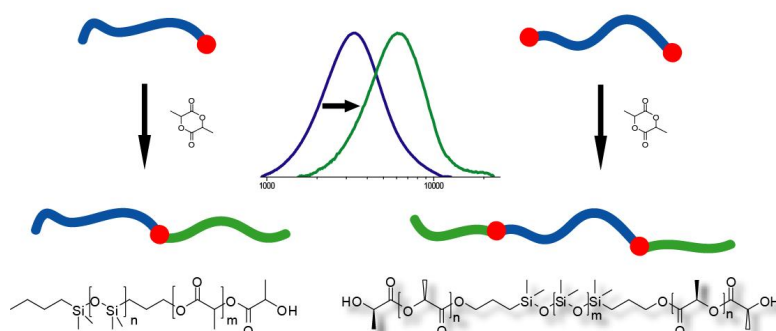


Chapter 3.1:**Poly(glycolide) Multi-Arm Star Polymers: Improved Solubility via Limited Arm Length.....123****Chapter 3.2:****Synthesis of Branched Glycerol-Based Poly(glycolide) Copolymers****via Ring-Opening Polymerization.....139****Chapter 3.3:****Comb-like Poly(ethylene glycol)-g-Poly(glycolide) Copolymers: A promising polymer surfactant in microparticle synthesis.....167**

Chapter 4.1:

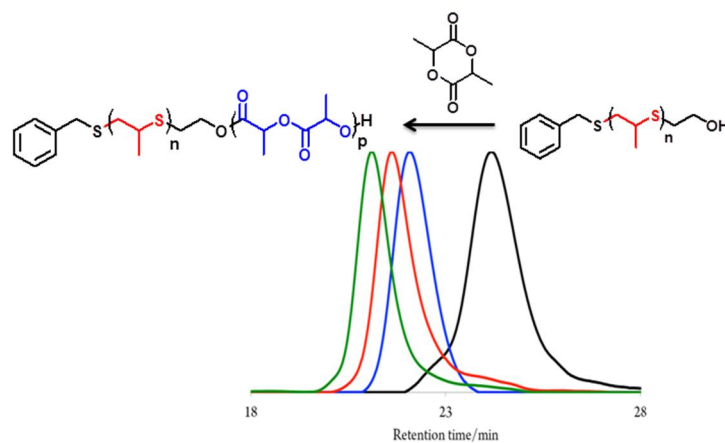
Block Copolymers Based on Poly(lactide) and Poly(dimethylsiloxane):

Strongly Segregated Systems193



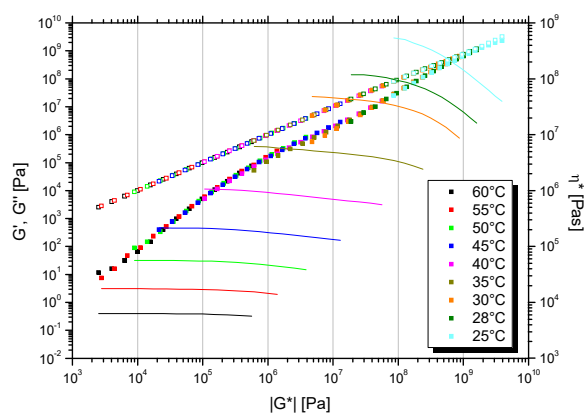
Chapter 4.2:

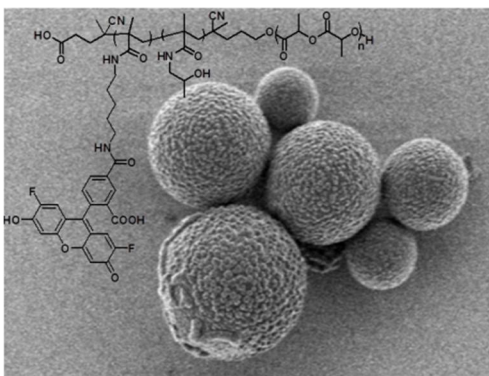
Combining Polysulfides with Polyesters to Degradable Block Copolymers.....211



Chapter 5.1:

Thermorheological Properties of Hyperbranched PGA Copolymers.....231



Chapter 5.2:**Synthesis and Characterization of Functional P(HPMA)-b-P(DLLA) Copolymers as Surfactant for Miniemulsion Technique.....243**

Chapter 1: Introduction

1.1 Poly(glycolic acid): A Status Report on Synthesis, Applications and Limitations

Anna M. Fischer and Holger Frey

Abstract

Apart from poly(lactic acid) (PLA), poly(glycolic acid) (PGA) is one of the most popular aliphatic degradable polyesters and is widely used in biomedical applications. PGA plays a key role in controlling and adjusting degradation times of biomaterials. Most copolymers, such as PLGA, benefit from the fast hydrolysis of the sterically less hindered ester bonds of PGA. However, current research focuses mainly on PLA, because it is produced on an industrial scale from renewable resources and its material properties are easily modulated by copolymerization of the respective stereo-isomers. In contrast, the synthesis of homo- and copolymers with high PGA content is challenging with regard to their insolubility in common organic solvents and their high melting temperatures, limiting processing. This review gives a status report on synthesis, characterization, and modification of glycolic acid-based polymers with PGA as the main structure element. Furthermore, the significance and potential of further work on PGA-based material is highlighted.

Introduction

Poly(glycolic acid) (PGA), composed of glycolic acid (GA) as smallest repeating unit, belongs to the family of the poly(α -hydroxy acids) together with poly(lactic acid) (PLA). Similar to PLA, PGA is a material that is both biocompatible and biodegradable. PGA is commonly defined as a "bioresorbable" material due to its degradation *in vivo* and subsequent elimination or metabolization of the side-products.¹ Application of this aliphatic polyester ranges from its initial use as suture material (Dexon®)^{2,3} and orthopedic device^{4,5,6} to its utilization in drug delivery, tissue engineering,⁷ and last but not least as substitute of conventional commodity plastics. High molecular weight PGA is a highly crystalline (45-52%) thermoplast with a glass transition temperature of 35-45°C and a high melting point of 210-230 °C (160-197 °C for degrees of polymerization $13 \geq DP_n \geq 9$, with $n = \text{GA unit}$)^{8,9} which exhibits a considerably higher modulus (7.0 GPa) and elongation (15-20%) than PLLA (2.7 GPa/5-10%).⁵ By reinforcing PGA fibers, their mechanical properties are significantly improved. The wet-strength half-life of fibers, which is determined by the tensile strength retention after

exposure to water, is 2 weeks for PGA and 6 months for PLLA.⁴ Owing to the additional methyl group in the backbone, PLA exhibits lower hydrophilicity compared to PGA (Figure 1). Thus, the degradation time of PGA ranges from 6 to 12 months in contrast to > 24 months for PLLA, however depending on different factors like prior treatment of the material, temperature, and culture media.⁵ PLA has the advantage of a wide range of products simply by controlled variation of the polymer stereochemistry via enantiomer incorporation, yielding amorphous polymers with high D-lactide content or semi-crystalline materials of high L-lactide content. Further stereocomplexation of enantiomeric PLA structures enhances the mechanical properties and further broadens the field of applications.¹⁰ In contrast, the modulation of properties and modification of PGA is limited to copolymerization, blending and – to a lower extent than in the case of PLA - variation of the macromolecular architecture.

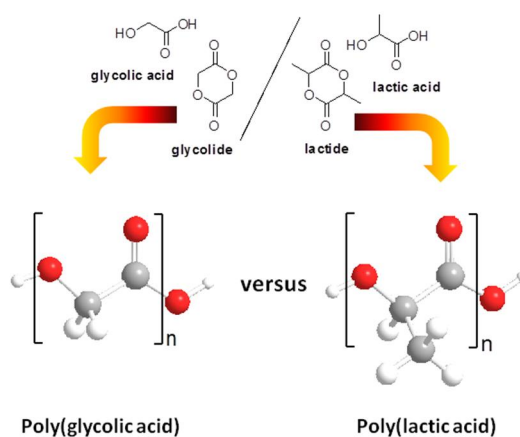


Figure 1. Structural formula of poly(lactic acid), poly(glycolic acid) and their respective precursors.

The crystal structure of PGA consists of two macromolecular chains with a planar zigzag conformation passing an orthorhombic unit cell with the dimensions of $a=5.22 \text{ \AA}$, $b=6.19 \text{ \AA}$, and $c=7.02 \text{ \AA}$ being the fibre axis. The macromolecular chains are arranged in a sheet structure parallel to the ac plane.^{11,12} The dense molecular packing (1.69 g/cm^3) is indicative for a highly crystalline material, which is thought to be responsible for the insolubility of PGA in common organic solvents, with the exception of 1,1,1,3,3,3-hexafluoro-2-propanol (HFIP). In contrast, low-molecular weight PGA ($< 1000 \text{ g/mol}$) is soluble in solvents like N,N-dimethylformamide (DMF), dimethyl sulfoxide (DMSO) and sulfolane. Hence, a suitable mobile phase eluent in size-exclusion chromatography (SEC)¹³ and solubilizer in mass spectrometry (MALDI-ToF MS) is HFIP. Dithranol has been found to be an appropriate matrix for MALDI-ToF characterization of PGA with potassium triflate as a suitable ionizing agent.¹⁴ Deuterated HFIP, a high-cost chemical ($60\text{€}/\text{g}$, Sigma Aldrich), and different solvent mixtures of trifluoroacetic acid- d and chloroform- d have been evaluated for NMR spectroscopy.¹⁵ The lack of convenient solvents for PGA characterization has often motivated bulk phase studies.

Typical solid-state techniques were solid-state NMR spectroscopy,¹⁶ differential scanning calorimetry (DSC),¹⁷ melt rheology,¹⁸ and powder X-ray diffraction.¹⁹ Generally, PGA is shaped by melt processing, i.e., extrusion, injection and compression moulding instead of fabrication from solution, such as electrospinning from HFIP. In drug delivery, solubility problems and high processing temperatures of PGA severely hamper the embedding of relevant drug moieties into the polymer matrix. Blending and prior thermal treatment might be potential strategies to reduce the degree of crystallization and improve material processing.

Since 2002, Kureha Corporation has been operating a plant in Japan, producing 100 million tons PGA per year. In November 2010, Kureha opened a new plant in the U.S. (West Virginia) for food packaging applications with a PGA production capacity of 4000 tons per year. The raw material glycolic acid for PGA production is supplied by DuPont. Higher impermeability to gas and humidity than for poly(ethylene terephthalate) (PET) is one feature of the Kureha PGA commercialized under the tradename Kuredux®.²⁰

1. Industrial Production

Kureha Cooperation has developed the first production technology for PGA manufacturing on commercial scale. More than 30 patents dealing with glycolide and PGA production processes have been published by Kureha to date. Kureha's PGA resins are used in packaging applications for light-weight PET bottles and in biomedical applications. In oil recovery industry, PGA is used as a time release agent for corrosion inhibitors, as dispersants and decomposition inhibitor of lubricants. Owing to the complexing ability of released glycolic acid, iron precipitation can be prevented during cleaning operations. The soluble GA chelates with rust and particulates can easily be pumped from the well. Glycolic acid is less corrosive to metals than mineral acids and minimizes corrosion damage.²¹ The fabrication of Kuredux® includes different forms, such as fibers, sheet/film or barrier layers in multilayer PET bottles to improve moisture, gas and aroma barrier properties (Figure 2). The introduction of 2 wt% PGA into a PET bottle leads to a 35 % reduction in the bottle weight, and during recycling the polyester is chemically separated by basic hydrolysis to recover the valued PET material again.

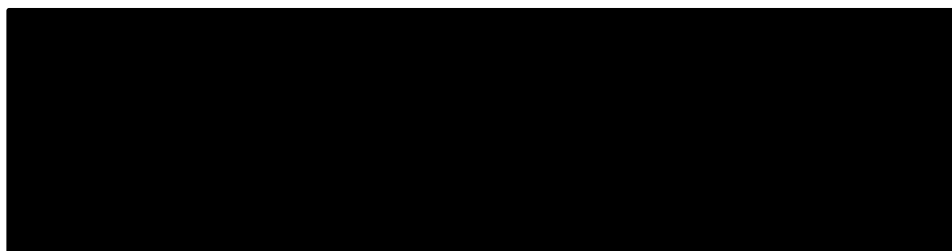


Figure 2. Food packaging and other industrial applications of poly(glycolic acid) marketed as Kuredux®.²²

The mechanical properties of Kuredux® vary upon prior treatment and manufacturing processes. Injection molded specimens exhibit high mechanical strength comparable with commodity engineering plastics. The mechanical properties are significantly improved for oriented films in contrast to non-oriented ones. Mono- and multi-filaments obtained by extrusion show a single-end breaking elongation in the range of 14-16 %. Kuredux® exhibits superior abrasion resistance compared with poly(ether ether ketone) (PEEK) and poly(phenylene sulphide) (PPS) and flexural strength exceeds those of established engineering plastics, especially with the addition of glass fibre. Generally, in flexural strength testing of plastics the resistance of deformation under load is measured.

The heat deflection temperature (HDT) plays an important role in polymer engineering, manufacturing and design and has been investigated for Kuredux® in comparison with other crystalline and non-crystalline polymers. Above the HDT temperature the polymers' mechanical strength deteriorates related with polymer deformation under a specified load. Kuredux® possesses a HDT of 168 °C and a heat resistance beyond its T_g of 40 °C (Figure 3).

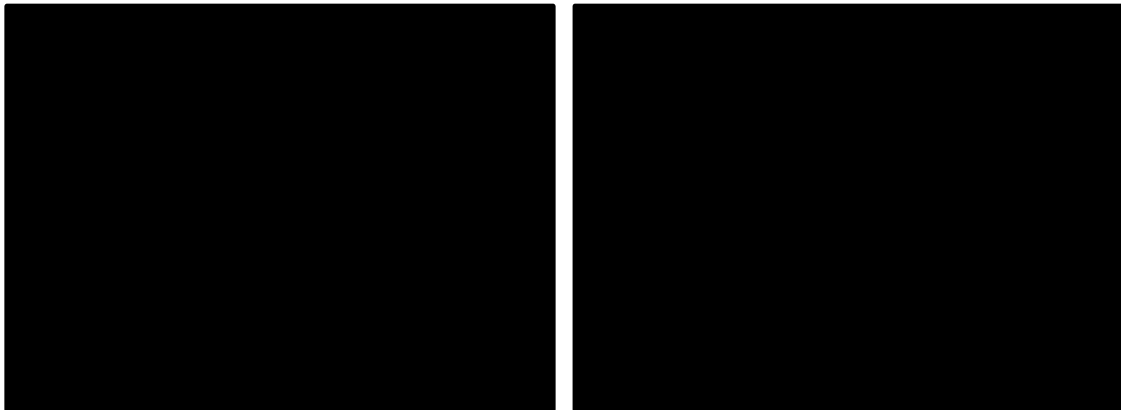


Figure 3. Left: Heat deflection temperature (HDT) of Kuredux® (168 °C); Right: Flexural strength of Kuredux® compared with other polymers.²²

Besides excellent mechanical properties, PGA has additional features which render the material interesting for industrial applications. Owing to its flavour, gas and moisture barrier property it is a desirable packaging material to preserve product quality.

Unique material properties are available by co-extrusion and blending with other polymers, such as PET. Figure 4 gives an overview of the different processing techniques used in PGA production.²²



Figure 4. Examples of Kuredux® thermal processing techniques.²²

Kureha Corporation gives detailed information on Kuredux® processing by extrusion and injection molding with regard to elevated temperatures, as well as stretch molding temperatures for multi-layer films with poly(amide) (PA), poly(ethylene) (PE), PET and PLA. For lamination onto various materials, including polymers and aluminium, the use of a two-component type urethane adhesive is recommended. Kuredux® is approved as biodegradable product in the U.S., Europe and Japan. The features of compostability and barrier performance render PGA a high valued eco-friendly packaging material. Biomedical application relies on the medical-grade Kuresurge®, marketed as resorbable surgical suture, which makes additional surgery for removal from tissue unnecessary.²³

2. Synthesis of Poly(glycolic acid)

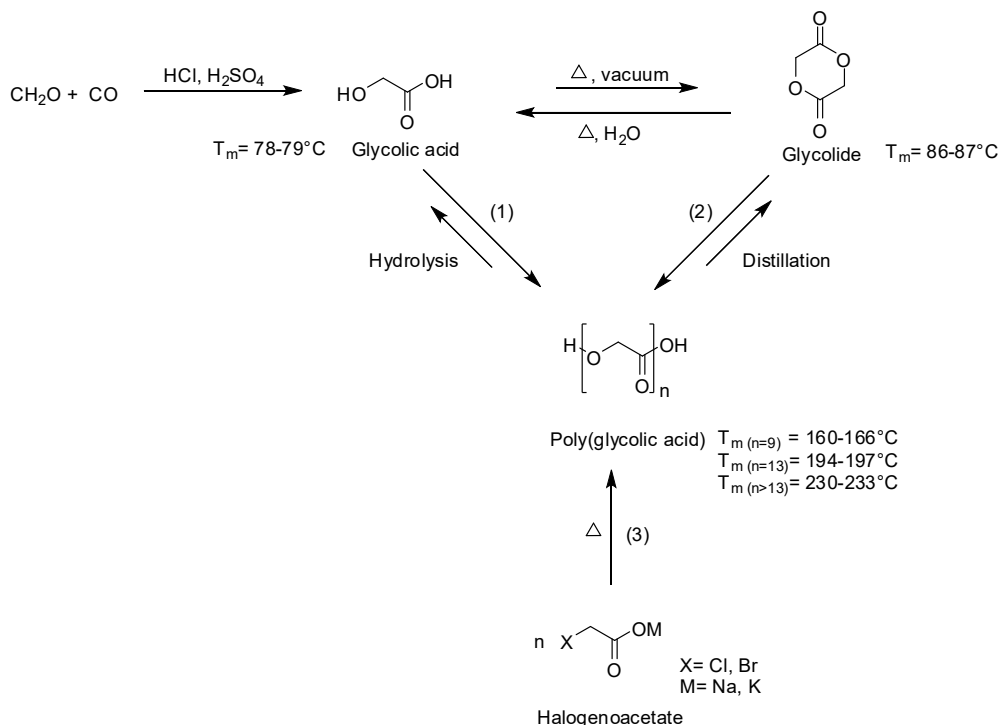
Glycolic acid, the smallest repeating unit in PGA, is widely used in industry as complementary additive in food²⁴ and cosmetics,²⁵ for leather production, metal treatment and PGA preparation. Glycolic acid is prepared by chemical synthesis or extraction from plants. The industrial production is based on an acid-catalyzed reaction of formaldehyde (CH₂O) and carbon monoxide (CO) at high pressure and temperature.²⁶ Further processes to produce glycolic acid include the chemical hydrolysis of chloroacetic acid and the hydrolysis of gluconitrile. Several attempts have been made to produce GA by microorganisms. A microbial approach is the oxidation of ethylene glycol to glycolic acid using different enzymes.²⁷ Glycolic acid is the metabolite of ethylene glycol causing metabolic acidosis in humans associated with the toxicity of ethylene glycol.²⁸ Another chemo-enzymatic process is based on the reaction of formaldehyde and hydrogen cyanide to obtain glycolonitrile, which is converted to ammonium glycolate using an immobilized nitrilase. The ammonium glycolate is then treated with ion exchange chromatography to obtain the pure glycolic acid.²⁹ Both the

enzymatic process³⁰ and the basic pulping of polysaccharides³¹ are not of economic interest with regard to large-scale synthesis at present. Currently, GA can thus not be considered as a sustainable monomer, in contrast to lactic acid, which can be made from starch. However, this may change as a result of current efforts.

Glycolide (1,4-dioxan-2,5-dione), the six-membered cyclic glycolic acid dimer, is used in ring-opening polymerization (ROP) to produce high-molecular weight PGA (Scheme1). In general glycolide is obtained in a depolymerisation process of poly(glycolide).^{8,32} In the first step low molecular weight PGA oligomers are prepared from glycolic acid by step-growth polymerisation. In the second step these oligomers are thermally degraded by intramolecular transesterification to form cyclic dimers in a so-called back-biting mechanism. The hygroscopic glycolide undergoes a monoclinic to orthorhombic phase transition at 42 °C, followed by subsequent melting at 82-87 °C and is easily polymerized upon heating.^{8,33} The purification of glycolide is often carried out by recrystallization from ethyl acetate or ethanol with subsequent removal of the solvent at room temperature or by distillation under high vacuum. In contrast to the PGA homopolymer, glycolide is soluble in a wide range of solvents, i.e., tetrahydrofurane (THF), chloroform, ethyl acetate, acetone, methanol, and water. Unlike PLA, where the rigorous stereocontrol requires additional purification processes, the synthesis of glycolide and PGA is clearly less demanding.

The polymerization of glycolide was first reported by Dessaignes³⁴ and Kékulé³⁵ in the 19th century. They obtained oligomeric PGA by thermal polycondensation of tartronic acid and potassium chloroacetate, respectively. Further studies were focused on the bulk polymerization, mainly by heating of halogenoacetates.^{36,37,38} Detailed studies on poly(glycolide) and the isolation of glycolide via depolymerisation of PGA were reported by Bischoff and Walden.^{39,40} However, most of the data on lactone polymerization reported in literature have been devoted to lactide synthesis, and little attention has been paid to glycolide polymerization. In contrast, it is our aim in this review to focus especially on the literature dealing with PGA homopolymers or polymers consisting of a dominating amount of PGA units.

In principle, the **synthesis of poly(glycolic acid)** can follow three different routes: (1) polycondensation of glycolic acid (GA), (2) ring-opening polymerization of glycolide,^{41,42} or (3) solid-state polymerization of halogenoacetates (displayed in Scheme 1).⁴³



Scheme 1. Synthetic strategies towards PGA and its precursors, glycolic acid and glycolide, the cyclic dimer structure used for ring-opening polymerization.

Although **step-growth polymerization** of GA is the least expensive-expensive route to PGA, the production of high-molecular weight polymer requires high temperatures and long processing times, which promote undesired transesterification reactions and material discoloration. The formation of by-products (water, alcohol) leads to the establishment of an equilibrium, which results in low yields and low molecular weight products. Therefore, in PLA processes, chain coupling agents are added to promote esterification. Chain extenders are used to increase molecular weight. The usage of typical esterification-promoting and chain-extending adjuvants, such as dicyclohexylcarbodiimide (DCC), carbonyl diimidazol (CDI), and diisocyanates raises costs, but often the mechanical properties are improved. The concept of azeotropic condensation of lactic acid was commercialized by Mitsui Toatsu Chemicals and yielded PLA with molecular weights $>300,000$ g/mol.⁴⁴ Based on academic research, Takahashi et al. developed a solvent-free two-step protocol to obtain high molecular weight PGA up to 91,000 g/mol (SEC) via preparing an oligocondensate first, which is subsequently condensed again with zinc acetate dehydrate as catalyst.⁴⁵ This strategy provides a facile route towards large-scale synthesis of PGA. A similar two-step approach deals with the polycondensation

of glycolic acid in ionic liquids in the presence of a catalyst. Dali et al.⁴⁶ reported on the synthesis of oligo-PGA and the subsequent postpolycondensation of the oligomers in ionic liquids, mainly 1,3-dialkylimidazolium salts. Organic salts, which are liquid at room temperature, are suitable solvents for high temperature reactions and solvate a wide range of organic and inorganic compounds. Polymer precipitation in the reaction medium again limited the achievable molar mass of PGA ($DP_n=45$).

The **ring-opening polymerization** (ROP) of the strained, cyclic glycolide monomer can proceed through anionic, cationic, or coordination mechanisms and yields polymers with $M_n > 100,000$ g/mol. Exhaustive purification of glycolide from free acid content is a prerequisite to obtain high molecular weights via controlled reaction conditions. The solvent-mediated ROP is difficult because of the lack of practical solvents with regard to the low solubility of the monomer and the growing polymer. In addition, the increasing melting point with increasing PGA chain length leads to an early polymer precipitation in the reaction medium at low reaction temperatures, which limits conversion.⁴⁷ The solution polymerization of glycolide has been rarely mentioned in literature, and the authors often used non-standard solvents, like nitrobenzene or sulfolane. Therefore, a combination of bulk- and melt-polymerization is a well-established route in industry for the production of sutures. Bulk polymerizations, which are operated below the melting point in the region of the polymers' softening point, allow for the synthesis of high molecular weight polymers that solidify and crystallize from the reaction mixture. In contrast, melt polymerizations are limited to low molecular weights, and the resulting PGA polymer is contaminated with degradation products, such as carbon dioxide, formaldehyde, and the corresponding acid monomer.⁴⁸

A variety of **catalysts** have been evaluated for the ROP of lactide and glycolide.⁴⁹ Numerous investigations concerning mechanism and polymerization variables have been carried out on metal-catalyzed coordination polymerization with $\text{Sn}(\text{Oct})_2$ as catalyst.³² The advantage of the widely used tin catalyst is its solubility in various lactones, the high catalyst activity, and the acceptance as food additive by the U.S. Food and Drug Administration (FDA) at low ppm values. Considerable recent interest has been devoted to catalytic zinc derivatives and organic "superbases" (1,8-diazabicyclo[5.4.0]undec-7-ene (DBU), 1,5,7-triazabicyclo[4.4.0]dec-5-ene (TBD))⁵⁰ as alternatives to metal catalysts with respect to eventual biomedical application. Mazarro et al.⁵¹ studied the suitability of DSC kinetic methods for the $\text{Zn}(\text{Oct})_2$ -catalyzed glycolide homopolymerization in bulk and compared the resulting polymerization rate constants with D,L-lactide homopolymerization at 160 °C. Kinetic parameters obtained from DSC studies were in agreement with those obtained from conversion data of glycolide bulk polymerizations. Dobrzynski⁵² et al. reported the successful application of calcium acetylacetonate in the polymerization of glycolide, accompanied by a low degree of transesterification in contrast to tin compounds.

Recently, tremendous progress has been achieved by Quian et al.,⁵³ who reported the methoxy poly(ethylene glycol) (PEG)-initiated homo- and copolymerization of glycolide by organocatalysis. In case of the PGA homologue only polymers having short oligomeric PGA blocks were studied due to well-known limitations in solubility. In principle, the ROP of a cyclic lactone depends on different factors: ring size, ring strain, steric demand of substituents attached, functionalities in the ring, and temperature conditions. Comparing lactide and glycolide, a decrease of the polymerization rate with increasing substitution at the α -carbon atom is expected due to the elevated proximity of substituents in the linear chain compared to the cyclic molecules.⁵⁴ Thus, kinetic evaluation of the DBU-catalyzed ROP yields a higher rate constant for glycolide in comparison with lactide polymerization (Table 1, Figure 5).

Table 1. Rate constants for glycolide and lactide polymerizations catalyzed with 1,8-diazabicyclo[5.4.0]-undec-7-ene, initiated with m-PEG_{2k} (^aApparent rate constant of pseudo-first order ROP, ^bThird-order rate constant).⁵³

monomer	[mPEG _{2k}] (mM)	[DBU] (mM)	k _{app} ^a (s ⁻¹)	k ^b (10 ⁵ (L/mol) ² s ⁻¹)
Lactide (±)1, 1.3M	5.0	6.6	550	1.7
Glycolide 2, 15mM	5.1	0.033	3100	1800

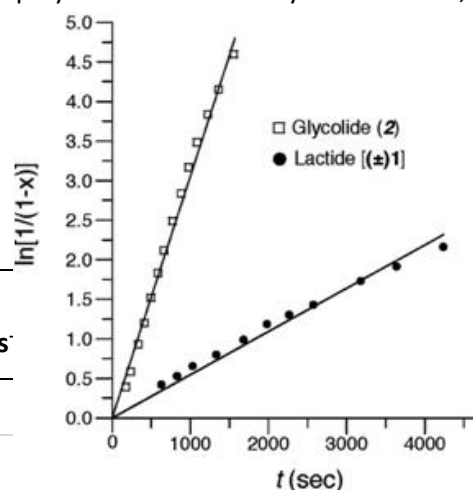


Figure 5. Lactide and glycolide homopolymerization in CDCl₃ at ambient temperature (reaction progress measured by ¹H NMR spectroscopic analysis); Plot of ln[1/(1-x)] vs time (x = monomer conversion).⁵³

A key contribution in the research of the anionic polymerization of glycolide was made by Braun and Kohl, who established a solution polymerization in sulfolane, catalyzed by *N,N*-dibenzylamine at 120 °C.⁴⁷ The simple and rapid preparation of PGA oligomers has been achieved by ROP of glycolide catalyzed by a decamolybdate anion (NH₄)₈[Mo₁₀O₃₄] at 190 °C.⁵⁵ The obtained oligo-esters with number average molecular weight in the range of 1350 to 1830 g/mol (DP_n=11-13 for glycolide) were insoluble in conventional solvents like THF, DMSO and DMF. This data suggests that even PGA with low molecular weight suffers from a lack of practicability with respect to characterization by conventional methods, such as SEC and MALDI-ToF mass spectrometry.

Recently, various classes of cationic catalysts have been applied for the synthesis of PGA homo- and copolymers via ROP, such as protic acids, Lewis acids⁵⁶ or alkylating agents. Systematic studies in terms of temperature and polymerization time revealed methyl triflate to be a suitable initiator (Figure 6). Under mild reaction conditions the reactive chain end allowed build-up of diblock copolymers instead of random PGA copolymers.⁵⁷

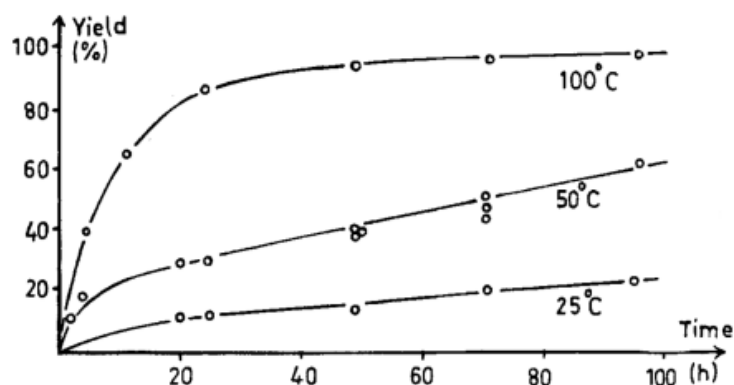


Figure 6. Yield plotted vs. polymerization time for the cationic homopolymerization of glycolide in nitrobenzene catalyzed with methyl triflate (M/I=100:1) at different temperatures.⁵⁷

The cationic glycolide polymerization in melt, catalyzed with antimony trifluoride (SbF_3) revealed important information on the narrow temperature processing window in the range of 160 to 175°C, which permits polymerization under homogenous conditions. Below 160 °C the PGA polymer solidifies during early stages of conversion; above 175 °C, a decay of the active species is observed.⁵⁸ Similar results were obtained in the cationic homopolymerization of PGA catalyzed by a montmorillonite clay catalyst.⁵⁹ Detailed information on ROP, enzymatic, and suspension polymerization, especially of lactide and glycolide copolymers has been reviewed by Singh and Tiwari.⁶⁰

A third approach towards poly(glycolide) represents the thermally induced **solid-state polycondensation** of halogenoacetates, such as sodium chloroacetate, which is a solvent-free process and leads to a quantitative yield of PGA (Scheme 1). The homopolymerization of PGA is accompanied by the formation of sodium chloride. The elimination of the side-product is achieved by simple washing out with water, and residual traces of monomer or catalyst are removed. In comparison to the conventional Sn-catalyzed ROP of glycolide, the solid-state process leads to poly(glycolic acid) with a maximum average chain length of 40 monomer units only. Possible side-reactions are cyclization, forming non-strained lactones, decarboxylation, as well as the formation of unsaturated poly(ester)s by the elimination of HCl. The reaction was investigated with

appropriate solid-state techniques such as thermal analysis (DSC), X-ray diffraction studies, electron microscopy, in-situ IR, and solid-state NMR spectroscopy.^{61,62,63} Poly(glycolide) can be obtained from 11 different halogenoacetate precursors with the formula MOOCCH_2X varying the composition of metal ($\text{M}=\text{Li}, \text{Na}, \text{K}, \text{Rb}, \text{Ag}, \text{Cs}$) and halogen ($\text{X}=\text{Cl}, \text{Br}, \text{I}$). After extraction of the metal halide, a porous morphology remains.⁶⁴ The overall porosity and pore size depend on the respective precursor and the corresponding reaction conditions (Figure 7). Epple et al.⁶⁴ found a strong influence of the treatment of the halogenoacetate prior to polymerization on the final polymer morphology. The pore size was adjustable by simply grinding the precursor before the reaction.

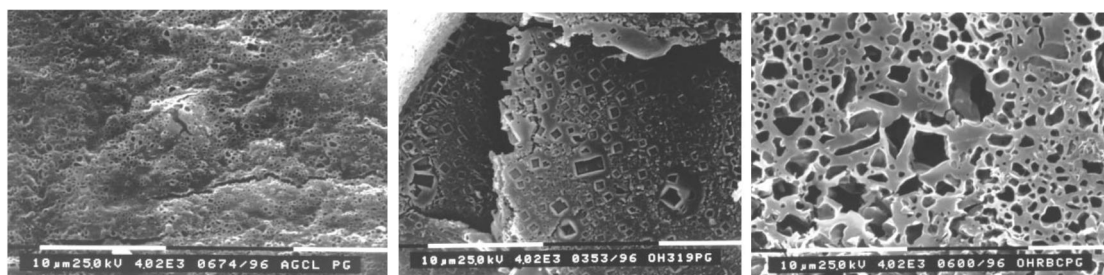


Figure 7. SEM images of porous PGA obtained from silver acetate at 130°C (left), from sodium bromoacetate at 180 °C (middle), and from rubidium chloroacetate at 120 °C.⁶⁴

3. Modification and Characterization of Poly(glycolic acid)

3.1 Modification of PGA

The morphology, degradation pattern and mechanical properties of PGA are influenced by various factors, such as processing methods, prior thermal treatment, production process and storage conditions. Especially, PGA modifications such as surface treatment, blending and copolymerization offer a wide range of applications. The solid-state polycondensation provides a possible pathway to microporous material suitable as a tissue scaffold or bone substituting material.⁶⁵ It possesses the advantage of promoting cell adhesion due to the textured surface and assures hydrophilicity and resorbability. Adjustment of the pore size is crucial to give cells and blood vessels access to the inner part of the implant. Composites of PGA and NaCl were melt-pressed at 190 °C and extracted with water to give three-dimensional microstructured PGA materials. Variation of pore size (0.3-300 μm) and porosity was achieved by mixing PGA/NaCl composites with different amounts of NaCl crystal size. Weight-bearing applications are not recommended due to a significant lack of mechanical properties. A further approach toward rough PGA surfaces is the fabrication of Si templates via photolithography and subsequent pattern transfer onto PGA by casting or injection molding, as reported by Kapure et al.⁶⁶ Surface engineering plays an important role in application of tissue scaffolds to increase hydrophilicity and attach relevant biological ligands to the surface enhancing cell adhesion. Owing to their lack of functionality, the modification of poly(ester) scaffolds

necessitates plasma-based techniques,⁶⁷ coating or surface hydrolysis. Lee et al. generated carboxylic acid groups on PGA fibers via basic hydrolysis with 1N NaOH solution.⁶⁸ In a subsequent step, a biotin-based ligand was covalently attached onto the surface via amide formation to study specific interaction with streptavidin. In a similar approach, Lee et al. modified PGA films via microcontact printing (μ CP).⁶⁹ After basic hydrolysis and surface activation with pentafluorophenyl ester groups, functionalization has been accomplished via amide formation using different amine moieties. Amine-terminated PEG had a clearly cell repellent effect, whereas RGD-peptide patterned PGA films promoted cell adhesion. Typical surface analysis techniques have been applied such as atomic force microscopy (AFM) and fluorescence microscopy to assure successful surface modification. Earlier, Gao et al.⁷⁰ developed surface-hydrolyzed PGA meshes to increase cell seeding density of vascular smooth muscle cells. Non-modified PGA showed solely cell aggregation, whereas the modified surface permitted individual cell attachment. Under prolonged basic treatment degradation led to a reduction of the fiber diameter with 50 % mass loss after 6.2 min (Figure 8).

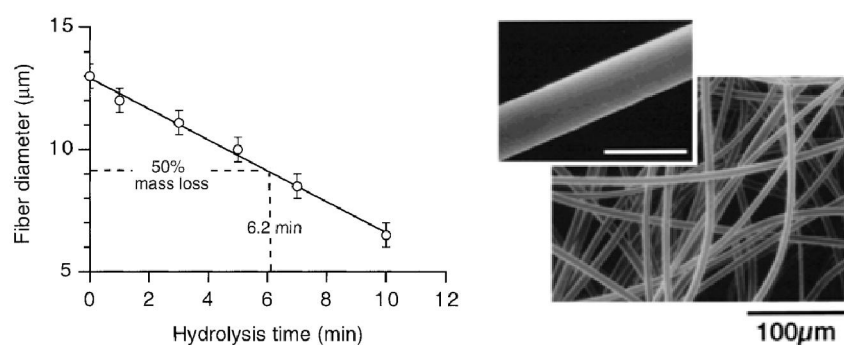


Figure 8. Left: Correlation of fiber diameter with hydrolysis time of the PGA mesh; Right: SEM image of PGA mesh after 10 min in 1N NaOH.⁷⁰

Prior investigations focused on interconnecting networks of non-woven PGA fibers without surface modification.⁷¹ For this, PGA fibers were embedded in a PLLA matrix via dissolution of PLLA in CH_2Cl_2 , wetting of the insoluble fibers with the PLLA solution and subsequent evaporation of the solvent. Thermal treatment induces cross-linking of the fibers. Finally, PLA was simply removed by dissolution in the appropriate solvent. The PGA-PLLA composite appeared to be essential to maintain the three-dimensional structure upon heating. *In vitro* cell seeding studies of hepatocytes grown on non-bonded fibers revealed a preference of cell-cell interaction in contrast to cell-polymer interaction. Freed et al. performed *in vitro* cultivation and *in vivo* transplantation of cartilage cells, such as chondrocytes based on PGA scaffold.⁷² Both, poly(lactide) and poly(glycolide) demonstrated high potential in tissue regeneration.

Melt spinning⁷³ and extrusion⁷⁴ represent feasible processes for PGA fiber manufacturing. Recently, You et al. designed small-diameter PGA fibers by electrospinning from HFIP solution, which undoubtedly represents a current trend in this field.^{75,76} The preparation of solutions containing two polymers yields blends of electrospun fibers.⁷⁷ Unlike to extrusion, this technique allows the formation of fibers in the submicrometer range (~0.15-1.5 μm).⁷⁸ Porous electrospun fibers are obtained by subsequent selective extraction of PLA with chloroform from PGA/PLA blends. Boland et al. attempted to improve the electrospun fiber surface by acidic pre-treatment.⁷⁹ Despite acidic treatment the fiber diameter remained constant. The cleavage of ester bonds at the surface increases hydrophilicity and enhances cell adhesion. Cell studies revealed less inflammation associated with conventional PGA-based materials.⁸⁰ Electrospun composites of PGA and collagen, mimicking the natural cellular environment, showed different cell affinity depending on fiber diameter and composition.⁸¹

The insolubility of PGA and its high melting point hamper its application in pharmaceutical applications. Blending might be one approach of tailoring material properties. In a melt-process Dickers et al. studied different two-component blends of PGA (80 wt%) with respect to miscibility and phase separation.⁸² Unfortunately, blending did not result in a reduction of PGA's melting point. Electrospinning of PCL/PGA homopolymers from HFIP resulted in blended nanofibers, showing miscibility and higher hydrophilicity, tensile strength and porosity upon increasing PGA weight ratio.⁸³ Copolymerization of PEG with PGA either yielded phase-separated or blended materials, depending on the molar composition and segmental chain length.⁹ In summary, a number of studies have been performed to optimize biocompatibility and processing of PGA in various different forms, ranging from PGA films, surfaces, and porous 3D structures to fibers.

3.2 Characterization of PGA

A variety of characterization techniques have been developed to study morphology and other material constants of PGA, also with respect to surface modification and processing techniques employed. A highly sensitive surface characterization tool is time-of-flight secondary ion mass spectrometry (TOF-SIMS), i.e., for the investigation of hydrolytic degradation kinetics of PGA providing mass spectra with low limits of detection.^{84,85} X-ray photoelectron spectroscopy (XPS) is used to study the chemical surface composition of polymers, i.e., to follow successful grafting of biologically active ligands onto films.⁶⁹ These techniques are often combined with fluorescence microscopy, and vibrational spectroscopy, such as IR and Raman spectroscopy.^{86,87} The former give additional information on the amorphous and crystalline phases of PGA together with solid state nuclear magnetic resonance.^{16,19} Typical crystalline-sensitive bands for PGA appear at 1776, 1403, 1248, 998, and 316 cm^{-1} in Raman; and 975, 900, 810, 630, 959 cm^{-1} in IR spectroscopy.

Raman/IR bands of molecular units in amorphous domains appear broader and show different vibration frequencies compared to bands due to the crystalline fraction.⁸⁶ UV/visible spectroscopy has been utilized to follow *in vitro* degradation of PGA via measurement of the absorbance upon chemical reaction of the degradation product, glycolic acid with chromotropic acid.⁸⁸

Scanning electron microscopy (SEM) and atomic force microscopy are surface-sensitive methods, i.e., giving insight into morphological features such as surface erosion during degradation, cell seeding and abrasion of implants.^{68,69,70,89,90} In addition, contact angle measurements are used for the investigation of hydrophobic/hydrophilic surface functionalization.⁶⁶

Molar mass and polydispersity of polymers are commonly determined by size exclusion chromatography (SEC) or solution viscosimetry. However, solution viscosimetry has not been suitable for molar mass determination of PGA since no Mark-Houwink (MH) constants have been reported in literature, yet. In Table 2 several values for PGA's reduced viscosity are given which have been reported in literature.

Table 2. Literature data for reduced viscosity of PGA.

Sample	η_{red} (ml/g)	Conditions	Ref.
PGA, ROP	9.31	HFIP, 25 °C, c=5 g/L	47
PGA, ROP	6.8-11.8	Phenol:trichlorophenol (10:7), 30 °C, c=5 g/L	41

An appropriate eluent for SEC of high molecular weight PGA is HFIP with CF₃COONa as an additive. An alternative eluent for oligomeric PGA is dimethyl formamide (DMF). Other techniques applied in polymer mass characterization, like static dynamic light scattering (SLS) and multiangle laser light scattering (MALLS combined with SEC), have not been reported in literature for PGA homopolymers, yet. Further information on end group analysis and molar composition of PGA copolymers is provided by mass spectrometry (TOF-SIMS, MALDI-ToF MS).¹⁴

Sequence analysis, estimation of molar composition in copolymers and molar mass are implemented by using ¹H NMR spectroscopy. PGA structure-related sequences are sensitive to the surrounding microenvironment. Thus, initiation of glycolide ROP by small traces of water is evidenced by the characteristic proton signal of the methylene group next to the carboxylic end group ($\delta=4.65$ ppm, DMSO-*d*₆ at 300 MHz). ¹H NMR spectroscopy allows for calculation of PGA molar mass from the methylene protons of the PGA backbone ($\delta=4.78-4.87$ ppm, DMSO-*d*₆ at 300 MHz) in reference with the methylene protons next to the hydroxyl end group ($\delta=4.12$ ppm, DMSO-*d*₆ at 300 MHz). Residual monomer impurities or degradation products can be quantified based on their characteristic signals (for glycolide: $\delta=5.05$ ppm, for glycolic acid: $\delta=3.92$ ppm in DMSO-*d*₆ at 300 MHz).⁴⁶ The Hansen solubility parameter (HSP) has been determined for PGA with different methods given in literature.⁹¹

The usage of polymers in sophisticated applications requires the synthesis of materials with defined thermal, mechanical, and degradation properties. The thermal properties of biomedical polymers play an important role from a scientific and a practical point of view, since they determine also the mechanical properties of a material and thus the suitability for a certain application. Typically, thermoplastic polymers are formed in the shape of pellets, fibers or implants by melt processing. Therefore, the processing techniques have to be adjusted according to the PGA's thermal behaviour with respect to thermal decomposition. The high crystallinity of PGA varying between 42-52% results in high mechanical strength of the material. The melting point, determined using differential scanning calorimetry (DSC), is dependent on the average chain length ranging from oligomers with $DP_n=8-13$ to higher molecular weight polymers with $DP_n>13$ (with n =glycoyl unit). Both quenching rate and the molecular weight have a great influence on the degree of crystallization, as reported by Cohn et al.⁹ With increasing PGA chain length the glass temperature (T_g) increases due to the reduced mobility of the rigid crystalline blocks. In Table 3 some of the collected literature data are presented with respect to preparation conditions. Engelberg and Kohn⁹² gave an insight into physico-mechanical properties of degradable polymers with the exception of PGA. Here, the exploration of further material constants was hampered due to the brittleness after PGA film preparation. In addition, the authors studied PGA's thermal properties and observed a thermal decomposition at 254 °C from TGA analysis ($M_n=50,000$, Polyscience Inc.).

Table 3. Literature data for thermal properties of poly(glycolide) prepared by different reaction conditions.

GA units	Synthesis	T_m (°C)	T_g (°C)	T_c (°C)	X_c (%)	H_f (J/g)	Ref.
n=8	PC, HCl ^{a)}	126-128					93
n=9	PC, 170 °C ^{a)}	160-166					93
n=13	PC, 170 °C ^{a)}	194-197					93
n=13	ROP, 130°C ^{b)}	216-218					93
	ROP ^{b)}	227-230					41
	ROP, 220°C ^{b)}	~220	36	80	~50		32
	SSP ^{c)}	216-220					94
	ROP ^{b)}	187-222	10-42	68-104 ^{d)} 108-177 ^{e)}	9.0-52.0	12.6-72.3	9
n>13	PC ^{a)}	220		40	~27-40		45

^{a)} Polycondensation (PC), ^{b)} ring-opening polymerization (ROP), ^{c)} solid-state polycondensation of halogenoacetates (SSP), ^{d)} T_{c1} , ^{e)} T_{c2}

The equilibrium melting point (T_m^0) and the melting enthalpy (ΔH_f) of poly(glycolide) can be estimated by various methods. ΔH_f can be determined by DSC or calculated from the Clausius-Clapeyron equation. T_m^0 is calculated from Flory's models for PLGA or from Hofmann-Weeks plot as reported by Nakafuko et al.⁹⁵ The melting parameters are strongly influenced by optical impurities and prior thermal treatment of the respective material.

Table 4 gives an overview of literature data for PGA's physical properties, revealing a certain ambiguity for the melting enthalpy value for 100% crystalline PGA.

Table 4. Physical properties of poly(glycolide).

Parameter	Value	Ref.
T_m^0 (°C)	213.6	95
dT_m^0/dp (KMPa ⁻¹)	0.32	95
ΔV (cm ³ g ⁻¹)	0.1162	95
ΔH_f (Jg ⁻¹)	183.2 ± 6.0	95
	139.0	9
	180.4	41
	202.1	41
ΔS_f (Jg ⁻¹ K ⁻¹)	0.363 ± 0.012	95
	0.275	9
Density (gcm ⁻³)	1.50-1.69	96,11
σ_B (kgmm ⁻²) ^{b)}	8-100 ^{a)}	96
E (kgmm ⁻²) ^{c)}	400-1400 ^{a)}	96
ϵ_B (%) ^{d)}	30-40 ^{a)}	96

^{a)} Oriented fiber; ^{b)} Tensile strength; ^{c)} Young's modulus; ^{d)} Elongation-at-break

Small-angle X-ray scattering (SAXS), wide-angle X-ray scattering (WAXS) and molecular model calculations have been used to study the crystalline morphology in PGA, often applied in combination with DSC techniques in the characterization of PGA fibers.^{11,12,17,19,97,98} In several studies WAXS profiles were used to investigate the degradation behaviour of PGA, revealing a constant PGA crystallinity in the initial phase due to water penetration predominantly in amorphous domains.⁹⁹

Melt rheology gives information on the linear viscoelastic properties of polymers and the critical molecular weight of entanglement (M_c). Gautier et al.¹⁸ performed an *in situ* polymerization between two parallel rheometer plates and thereby calculated bulk polymerization kinetics of Sn(Oct)₂-catalyzed ROP of glycolide at 200-230 °C. The Fox-Flory equation, with T_g as a function of $1/M_n$,

yielded the value for $T_{g\infty} = 44.8$ °C with the polymeric constant $K = 1.1 \cdot 10^5$ K/g·mol. Melt rheological properties are of importance to define the suitability of application and processing based on shear viscosity. From the molar mass dependency of the zero shear viscosity the critical molecular weight of entanglement has been calculated as $M_c \sim 11,000$ g/mol, using the time-temperature superposition principle. The melt viscosities of high molecular weight PGA are 50 to 6,000 Pa·s at a temperature of 240 °C and a shear rate of 121 sec^{-1} .¹³ Several studies concentrated on the mechanical properties of PGA fibers,^{98,100} especially on their loss of tensile strength during hydrolytic degradation.¹⁰¹ Table 5 gives an overview of relevant mechanical constants of commercially available PGA.

Table 5. Mechanical properties of Kuredux® using different test methods applied from Kureha Cooperation.²²

Sample	Tensile Modulus (GPa)	Tensile strength (MPa)	Tensile elongation (%)
Injection molded	7.0	109	2.1
Un-oriented film (100 µm)	3.3	113	5
Oriented film (20 µm)	7.0/5.5	380/250	40/80
Monofilament ^{a)}	21	1.3	18
Multifilament ^{b)}	21.2	-	21.4

^{a)} Stretch temperature: 57 °C, Stretch ratio:6.0;

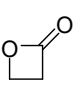
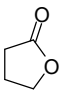
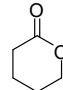
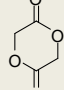
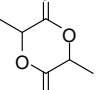
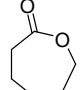
^{b)} Stretch temperature: 64 °C, Stretch ratio:5.0

4. Copolymers of Poly(glycolic acid)

Within the last years a variety of PGA copolymers has been synthesized by polycondensation or ring-opening polymerization. Particularly copolymers of lactide and glycolide have attracted much interest of both scientists in academia as well as researchers in industry aiming at biomedical and pharmaceutical applications. Soon after commercialization of poly(glycolide) as a surgical suture under the tradename Dexon®, Ethicon established a new material composed of glycolide and 8% lactide (Glactine910®, Vicryl®). Further suture materials based on PGA copolymers with trimethylene carbonate (TMC, Maxon®) and ε-caprolactone (CL, Monocryl®) followed. Terpolymers of GL and TMC with CL or dioxanone (Monosyn®, Biosyn®) have also been commercialized as degradable sutures. The synthesis procedure comprises a copolymerization of GL and TMC, giving a random block,

followed by GL addition to attach hard segments to these already formed soft segments. The basic idea behind copolymerization was broadening the field of application by enlarging the range of materials properties. Whereas the glycolide-rich semi-crystalline copolymers are applied for suture and bone fixation devices, the amorphous copolymers are suitable candidates for tissue regeneration and drug delivery systems. The copolymerization of lactones results in random or blocky copolymers due to different monomer reactivities and transesterification rearrangements. The macromolecular architecture and microstructure have a tremendous influence on the resulting degradation profile. In Table 6 the thermodynamic data of polymerization are compared for a series of lactone monomers.¹⁰² These data are of importance to understand the reactivity of the different cyclic monomer structures for copolymerization. In case of three- and four-membered cyclic esters ROP is favorable due to a high ring strain, whereas polymerization of six and higher-membered lactones is merely driven by a decrease of entropy.

Table 6. Thermodynamic data for the polymerization and thermal properties of the most common polyesters.¹⁰²

Monomer	PL	BL	VL	GL	LA	CL
Structure						
Ring size	4	5	6	6	6	7
ΔH_p° (kJ mol ⁻¹)	-82.3	-6.8	-27.4	-34.0	-22.9	-28.8
ΔS_p° (kJ mol ⁻¹)	-74.0	-65	-65	-6.3	-25	-53.9
Polymer	PPL	PBL	PVL	PGA	PLA	PCL
T_g/T_m (°C)	-24/93	-59/65	-63/60	34/225	vide infra*	-60/65

with $\Delta G_p = \Delta H_p - T\Delta S_p$, where T is the absolute temperature and R the gas constant;

* PLLA/PDLA: T_g 55-60/ T_m 170 °C; PmesoLA: T_g 45-55 °C; PDLLA: T_g 45-55 °C

4.1 Design of PGA Copolymers via ROP and Polycondensation

Macromolecular engineering of polymers is of central importance in order to meet the requirements of specific applications. Materials properties may be tailored by copolymerization, blending and also by variation of the macromolecular architecture. Copolymerization of the highly crystalline poly(glycolide) with comonomers such as β -propiolactone (PL), γ -butyrolactone (BL), and ϵ -caprolactone (CL) results in soft-segmented copolymers with reduced degree of crystallization and increased flexibility and therefore improved mechanical properties. Specific variation of reaction conditions, like temperature, catalyst, solvent or bulk polymerization, was performed to obtain information about the parameters influencing the microstructure and molar composition of the copolymers. Anionic initiators promoted exclusively the homopolymerization of one monomer and are therefore not well-suited for the preparation of copolyesters (either glycolide or PL). Especially, ZnCl_2 , dibutyl tin dimethylate and $\text{Al}(\text{OiPr})_3$ showed a preference for glycolide incorporation in the presence of CL.¹⁰³ The application of acidic initiators, such as fluorosulfonic acid (FSO_3H) or ferric chloride (FeCl_3), led to blocky and random sequences depending on the temperature. In addition, complexing agents catalyzed faster incorporation of glycolide, which resulted in a blocky structure. In the case of tin alkoxides rapid transesterification rearrangements yielded segmented or random sequences at temperatures above 100 °C.^{104,105} Interestingly, the glycolic acid units exhibited great sensitivity towards the surrounding microstructure. Thus, apart from triads even tetrads and pentads were detectable in ^1H NMR. Nakayama et al. expected to improve processing and solubilisation of PGA by tetraphenyl tin-catalyzed copolymerization with γ -butyrolactone (BL).¹⁰⁶ The obtained copolymer was only soluble with an incorporation of BL exceeding 65 mol%.

Extensive studies on PGA copolymers with lactide,^{32,104,107} ϵ -caprolactone,^{105,108,109} *p*-dioxanone,¹¹⁰ and trimethylene carbonate^{111,112,113} have been performed, which revealed a predominantly blocky sequence, followed by a random comonomer distribution upon transesterification reactions using $\text{Sn}(\text{Oct})_2$. Recently, Quian et al. developed a controlled strategy, a so-called “semibatch polymerization”, to generate random PLGAs with narrow polydispersity.⁵³ The process is based on organocatalytic ROP and includes the controlled addition of the more reactive glycolide to a lactide polymerization in solution containing the initiator and the 1,8-diazabicyclo[5.4.0]undec-7-ene (DBU) catalyst. By this route the average sequence length of lactic and glycolic acid blocks is reduced, effectively. Note that this review concerns polymers with PGA as a main building unit and purposefully avoids comprehensive coverage of the whole variety of established PGA copolymers.

4.1.1 Random and Semiblock PGA Copolymers

Poly(glycolic acid) copolymers via polycondensation

Due to their commercial availability, glycolic acid has been copolymerized with various hydroxy acids by polycondensation (Figure 9). This reaction is in an equilibrium with its by-products (water, alcohol) limiting the synthesis to relatively low-molecular weight copolyesters. This effect is further enhanced by thermal decomposition of the polymer. ROP most often results in statistically distributed comonomer sequences, whereas the condensation reaction allows for the preparation of alternating copolymers.

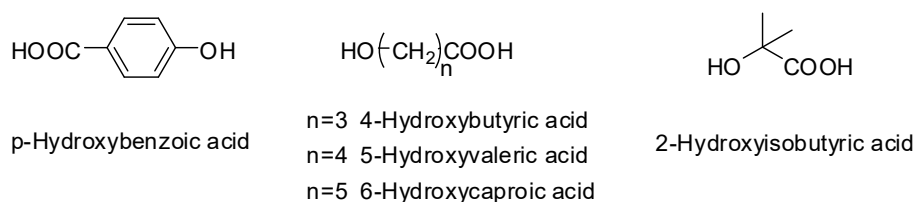


Figure 9. Various comonomers for direct copolycondensation with glycolic acid (GA).

Fukuzaki et al. produced ω -hydroxy acids via hydrolysis of the corresponding cyclic lactones (BL, VL, CL). The subsequent polycondensation was performed without catalyst at 200 °C, and the obtained molecular weights (SEC) of glycolic acid copolyesters were in the range of 1700 to 6000 g/mol.¹¹⁴ Tailoring of the thermal properties has been achieved by changing the molar composition of comonomers and resulted in amorphous (GA/CL, 50/50 mol%) or semi-crystalline (GA/CL, 85/15 mol%) copolymers. The degradation behaviour of poly(GA/ ω -hydroxy acid) formulations based on a melt-processing technique were studied *in vivo* after implantation into rats. GA-rich material showed an initial burst release of the respective drug, whereas amorphous GA/CL formulations resulted in a prolonged constant release over time.

A further route toward alternating copolyesters containing glycolic acid units is the solid-state polycondensation of halogenoacetates (Section 2). The formation of inorganic salt is the driving force of the reaction and leads to porous materials after washing-out with water. Marínez-Palau et al. studied the copolycondensation of 6-hydroxyhexanoic acid (6-HHA)¹¹⁵ and 4-hydroxybutyric acid (4-HBA)^{116,117} with glycolic acid. The observed glass temperature in the case of the GA/6-HHA copolyester (-37 °C) is lower compared to the GA/4-HBA copolymer (-15 °C). This is expected due to the increase of methylene groups, which has an influence on the flexibility of the corresponding material. In contrast to PGA homopolymer the T_m is lowered in both cases. With a decrease of the ionization potential of the alkaline metal the required reaction temperature decreased ($\text{Na}^+ < \text{K}^+ < \text{Cs}^+$). Copolycondensation of GA and 6-HHA resulted in higher molecular weights (2500 to 20500 g/mol) in contrast to GA/4-HBA copolyesters ($M_n = 4200\text{--}8300$ g/mol). Using zinc acetate

dihydrate ($\text{Zn}(\text{CH}_3\text{COO})_2 \cdot 2\text{H}_2\text{O}$) as a catalyst, homo- and copolymers of glycolic acid and 4-hydroxyisobutyric acid (4-HIBA) were synthesized in a step-growth reaction.¹¹⁸ This approach provides molecular weights up to 24,900 g/mol. The copolymers showed similar solubility properties as PGA with HFIP being the best choice of solvent. As expected, the thermal properties are significantly altered due to additional substituents of 4-HIBA introduced into the main chain. The temperature processing window has been enlarged, since the GA/4-HIBA copolyesters show an increased thermal stability in contrast to pure PGA. *p*-Hydroxybenzoic acid (*p*-HBA) and its derivatives are potential building units for thermotropic liquid crystalline polymers. Harsh reaction conditions have been employed in the copolycondensation of GA and *p*-HBA due to the monomer reactivity difference.¹¹⁹ Depending on the structure sequence and molar composition, different phase morphologies were obtained. Copolyesters with 60 to 70 mol% *p*-HBA formed nematic liquid crystalline phases above their melting point (Figure 10).

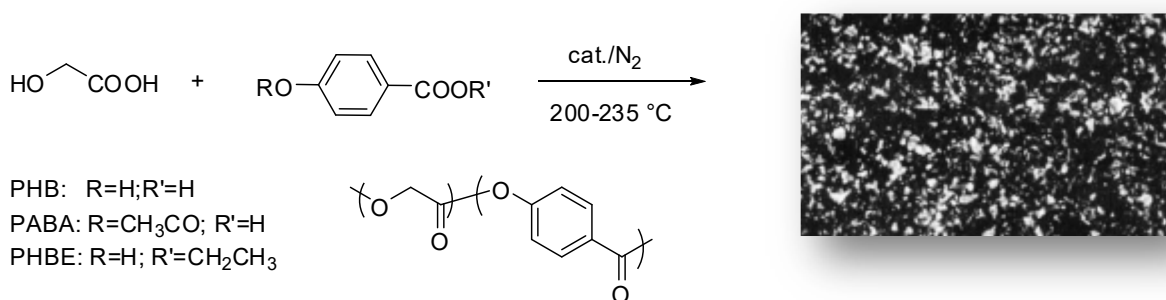


Figure 10. Synthesis pathway of poly(glycolic acid-*co-p*-hydroxybenzoic acid) copolymers and investigation via polarized light microscopy (POM) imaging.¹¹⁹

Poly(ester carbonate)s

Poly(ester carbonate)s, such as poly(TMC-*co*-GL), are well-established in biomedical applications, e.g., as suture material (Maxon®). Generally, poly(carbonate)s exhibit lower degradation rates than aliphatic polyesters, which limits their application and implies the relevance of copolymerization at that point. The advantage of poly(carbonate)s is expressed by their biocompatibility and less acidic degradation products when compared with PGA. The main focus regarding copolymers of glycolide with TMC lies in the synthesis and the tailoring of materials properties. Since conventional poly(TMC-*co*-GL) copolymers show low solubility (GA < 20 mol%) and high crystallinity, Cheng et al. designed a bulky carbonate monomer to overcome this problem.¹²⁰ The synthesis comprises the solvent-mediated $\text{Sn}(\text{Oct})_2$ -catalyzed ROP of glycolide and 5-benzyloxy-trimethylene carbonate (BTMC) (Figure 11). A retardation of crystallization and decreased degradation rate is observed with increasing incorporation of BTMC in the polymer backbone. Surprisingly, the bulky carbonate monomer shows a higher reactivity rate than glycolide. Deprotection of the pendant benzyloxy

groups leading to hydroxyl functions would enhance the significance of these materials, expecting an increase of hydrophilicity and offering the possibility of further post-polymerization modification.

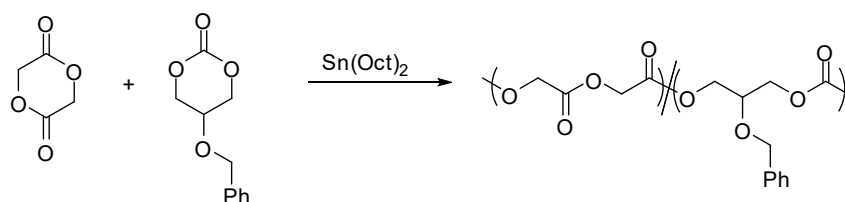


Figure 11. Ring-opening polymerization of glycolide and 5-benzyloxy-trimethylene carbonate catalyzed by $\text{Sn}(\text{Oct})_2$.

Poly(ester amide)s

Unlike poly(ester)s, poly(amide)s are not biodegradable. One reason might be the formation of intermolecular hydrogen bonds leading to a high degree of crystallinity accompanied by a high melting point. Consequently, the incorporation of labile ester bonds into the poly(amide) backbone assures biodegradability and the buffering of the amino acid structures lowers the pH after degradation, which reduces local tissue inflammation. The usage of natural α -amino acids permits the introduction of functional groups, where relevant drugs may be attached. Stability and mechanical properties of the polymers are adjusted via the appropriate amide/ester balance.

Poly(ester amide)s are commonly prepared by condensation of diamines, diols, and dicarboxylic acids. Poly(ester amide)s with alternating glycolic acid and α -amino acids are available from different morpholino-2,5-dione derivatives (**1** and **2**; Figure 12). These cyclic “depsipeptides” have been polymerized via ROP, affording homopolymers as well as copolymers with glycolide.

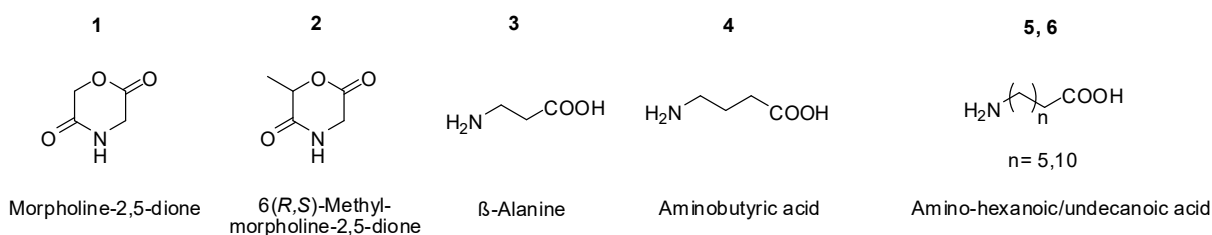


Figure 12. A series of building blocks used for the preparation of poly(ester amide)s based on glycolic acid/glycolide.

In't Veld et al.¹²¹ succeeded in the synthesis of random poly(glycine-co-glycolic acid) copolymers via ROP of glycolide and morpholine-2,5-dione (**1**, Figure 12) in the presence of catalytic amounts of tin octoate ($\text{Sn}(\text{Oct})_2$). The sensitive sequence effects enabled a detailed signal assignment via ^1H NMR analysis. ^{13}C NMR analysis revealed that ROP of **1** in bulk solely starts with the cleavage of the ester

bond. The incorporation of more than 69 mol% glycolide resulted in insoluble material. Depending on the glycolide amount, semi-crystalline or amorphous copolymers were obtained. Homopolymerization of the cyclic ester amide exclusively gives alternating copolymers with poor solubility which might refer to the high melting and glass transition temperatures (T_m : 199 °C; T_g : 67 °C). 6(*R,S*)-Methylmorpholine-2,5-dione (**2**, Figure 12), a six-membered cyclic monomer, consisting of a lactic acid and a glycine building block has also been copolymerized with glycolide by ROP.¹²² Here, Du et al. observed a decrease of the reaction rate with increasing amount of **2**, which might arise due to blocking of the coordination site of the tin atom by the carbonyl oxygen of the amide bond. A similar observation has been made by Ryner et al. who reported on a decrease of $\text{Sn}(\text{Oct})_2$ catalyst activity with the addition of carboxylic acid.¹²³ The comonomers, glycolide and 6(*R,S*)-methylmorpholine-2,5-dione, revealed different reactivity rates and thus resulted in PGM copolymers with a less random microstructure. With increasing incorporation of the amide moiety the overall degree of crystallization is reduced, which has a remarkable influence on the *in vitro* degradation behaviour. A higher content of amorphous regions in the poly(ester amide) copolymers facilitates water penetration, whereas highly crystalline PGA homopolymers show extended degradation times. The high water absorption is accompanied with a fast weight loss in contrast to the pure polyester (Figure 13).

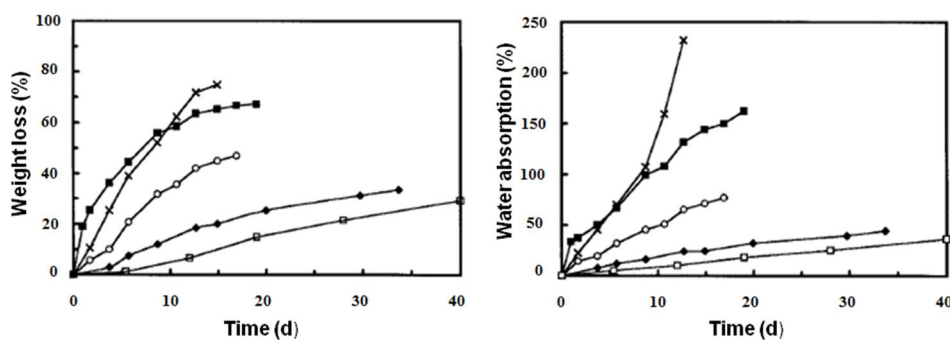


Figure 13. Changes of weight loss (%) and water absorption (%) with degradation of PGM copolymers. ((1) □ PGA; (2) ◆ PGM10; (3) ○ PGM30; (4) ■ PGM50 in distilled water; (5) × PGM30 in PBS buffer.¹²²

Thermal polycondensation of metal salts of N-chloroacetyl amino acids has been the method of choice to synthesize poly(ester amide)s without the elaborate synthesis of cyclic depsipeptides accompanied by moderate yields. The copolycondensation of metabolizable amino acids, such as β -alanine and γ -aminobutyric acid with glycolic acid has been evaluated by the use of the corresponding chloroacetate.¹²⁴ In this three-step protocol, chloroacetyl chloride is reacted with the respective amino acid in basic milieu first. In the next step, the metal salt is formed, which is

subsequently condensed under nitrogen atmosphere. The final poly(ester amide) with microporous morphology is obtained after removal of the inorganic salt. Vera et al. developed a route towards a glycolic acid-based nylon-6 derivative with aminohexanoic acid and a GA-based nylon-6,6 derivative with 1,6-hexanediamine and adipic acid.^{125,126} High molecular weights in the range of 30,000 to 33,000 g/mol (SEC) can be obtained, and the thermal properties can be adjusted for a wide range of applications simply by variation of the molar composition.

Functional Alternating Poly(ester amide)s and Poly(ester ether)s

Despite its good degradability and biocompatibility PGA is known to suffer from (i) fast hydrolysis, (ii) rigidity and (iii) the lack of side-chain functionality. The introduction and addressability of reactive functionalities at the poly(glycolide) backbone is a major aim to attach relevant drug moieties. To this end there are several synthetic strategies available at present: (1) synthesis of a functional monomer, (2) copolymerization with a functional comonomer, (3) post-polymerization modification of the hydroxyl end groups, or (4) the utilization of an initiator bearing functional groups. Alternating copolymers of serine and glycolic acid have been successfully synthesized by ROP of a cyclic depsipeptide bearing a primary hydroxyl group, which can be addressed after release of the protecting group (Figure 14, top).¹²⁷ The reactive side groups have been converted to acrylate functions, and subsequent photopolymerization provides access toward cross-linked gels. These might be potential candidates for injectable drug delivery systems.

Poly(ester ether)s based on glycolic acid (GA) and glycerol (G) represent an interesting class of degradable materials with unique properties. Branched alternating poly(GA/G) copolymers have been synthesized by ring-opening polymerization of a six-membered lactone, called 5-hydroxymethyl-1,4-dioxan-2-one, bearing a functional hydroxyl group (Figure 14, bottom).¹²⁸ In ROP the primary hydroxyl group initiates the chain growth and is incorporated as a monomer at the same time. Upon ring-opening polymerization four different subunits are built-up: the initial focal unit, linear and dendritic units, as well as terminal units. The addressability of the focal unit, resulting in ring-opening, has been successfully applied by Wolf and Frey.¹²⁹ The large number of end groups provides a further platform for derivatization.

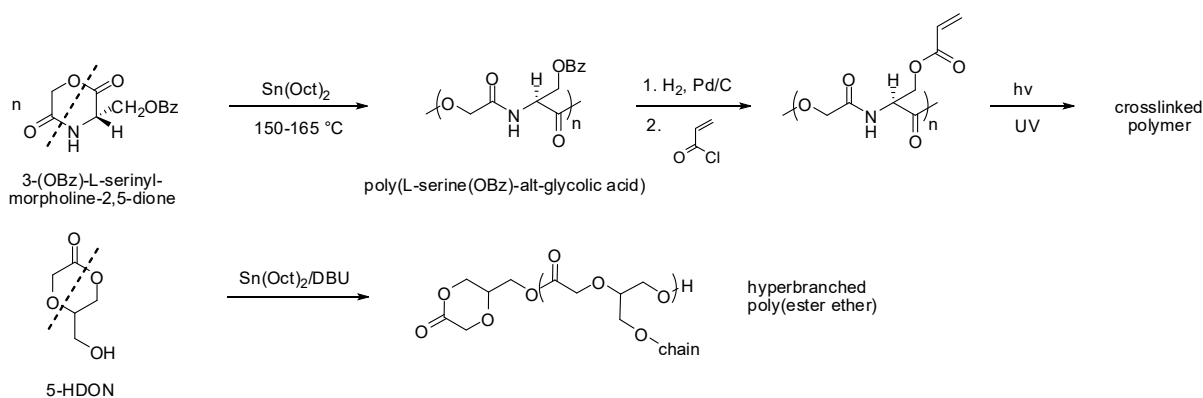


Figure 14. Appropriate monomers for the synthesis of alternating PGA copolymers in form of poly(ester amide)s or poly(ester ether).

4.1.2 Block and Graft Copolymers Based on PGA

The synthesis of block copolymers is accomplished via sequential monomer addition to the active chain end or via initiation⁵⁷ of the ROP with a hydroxy-functional precursor. The first strategy has been applied to prepare poly(ϵ -caprolactone-*block*-glycolide) copolymers initiated with an aluminium alkoxide under mild reaction conditions ($T=25\text{ }^{\circ}\text{C}$).^{130,131}

Typically, bishydroxy-functional PEG is used as a prepolymer to design ABA triblock copolymers via ROP of glycolide (=A block) as reported by Casey et al.¹³² Poly(ethylene glycol) (PEG) is an appropriate candidate as macroinitiator because of its hydrophilicity and water-solubility. Poly(ether ester)s based on PEG and poly(lactone)s are appreciable materials in biomedical applications, since both blocks are non-toxic and non-immunogenic. AB blocks containing hydrophilic PEG segments and hydrophilic PGA segments have been prepared and investigated with regard to their micellar aggregation behavior and cytotoxicity.^{133,134} Very recently, Zhang et al.¹³⁵ developed a polymeric paclitaxel prodrug conjugate based on m-PEG and oligomeric PGA to design targeted drug carriers according to Ringsdorf's concept.¹³⁶ The synthetic strategy comprises the coupling of carboxyl-terminated m-PEG with hydroxyl-terminated PGA octamer, which was obtained by exhaustive protection and deprotection steps. Subsequent covalent linkage to paclitaxel yielded the polymeric anticancer drug conjugate applicable as controlled release system in drug delivery due to the degradable PGA blocks. Graft copolymers are designed in three different ways employing the so-called "macromonomer technique", the grafting-from or the grafting-to approach. An example of the former strategy is the synthesis of a methacrylic PGA macromonomer by ring-opening polymerization, followed by subsequent radical copolymerization with methyl acrylate (Figure 15).¹³⁷

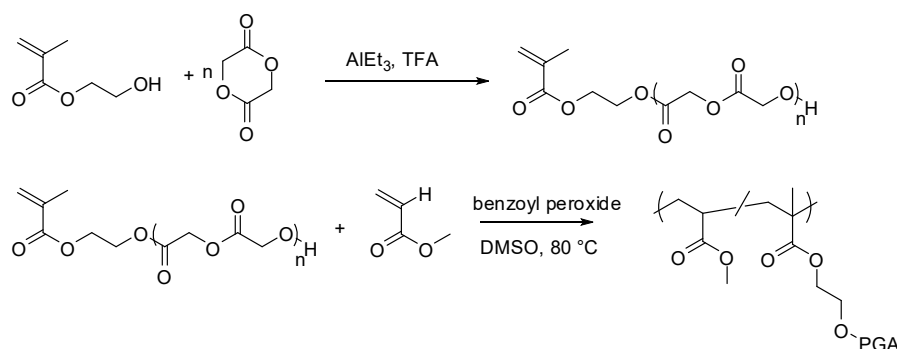


Figure 15. Synthesis of methacrylic PGA macromonomer via AlEt_3 -catalyzed ROP and subsequent free radical copolymerization with methyl acrylate.¹³⁷

In a similar procedure, diacrylate macromonomers were prepared based on a PEG central block extended with oligo(glycolide) and terminated with acrylate functional groups.¹³⁸ The macromonomers had to bear at least 55 mol% PEG to provide water solubility.

The usage of non-toxic initiators in the subsequent photopolymerization allowed for the preparation of bioerodible hydrogels for tissue engineering and provided tissue adhesion.

Brush-type PGA copolymers have been synthesized by grafting PGA onto hydroxy-functional poly- α,β -[N-(2-hydroxyethyl)-L-aspartamide] (PHEA) in the absence of any catalyst (Figure 16).¹³⁹ The potential of drug encapsulation via self-aggregation and degradation behaviour of the amphiphilic graft copolymers has been studied with regard to possible drug delivery applications. The PGA derivative benefits from the degradability of both building blocks and from the hydrophilic PHEA backbone providing water-solubility, non-toxicity and non-antigenicity. Degradation rate and drug release behaviour (*in vitro*) have been successfully modulated by variation of the PGA/PHEA molar ratio.

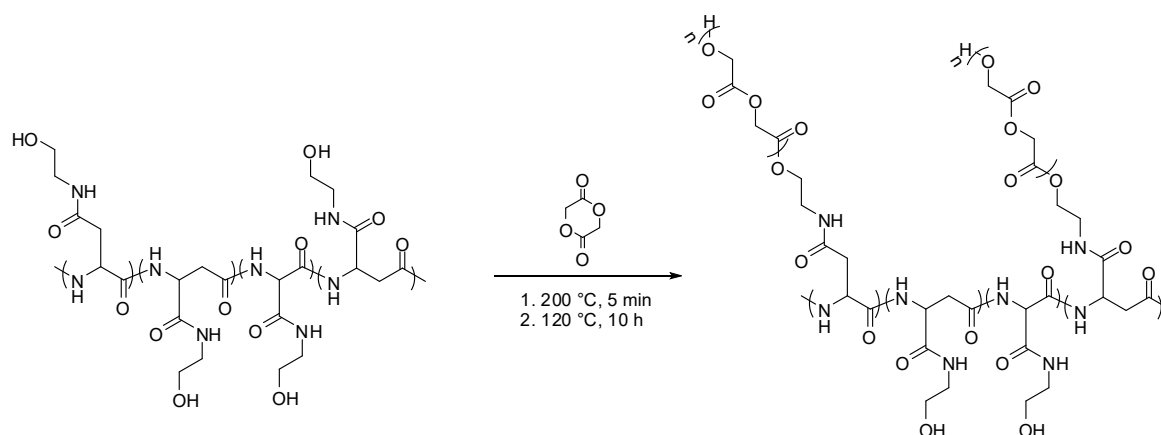


Figure 16. Synthesis of amphiphilic degradable poly- α,β -[N-(2-hydroxyethyl)-L-aspartamide]-g-poly(glycolide) copolymers.

4.1.3 Star-Shaped and Hyperbranched PGA Copolymers

Star polymers can be prepared by ROP of lactones in the presence of multifunctional alcohols (pentaerythritol, glycerol) or by using polyol macroinitiators based on a dendrimer core. In contrast to the above-mentioned grafting-from approach, the so-called grafting-to strategy is based on the covalent linkage of preformed polymer chains to a polyfunctional core or on using the latter as a termination agent for linear reactive chain ends.¹⁴⁰ Copolymers of star-shaped architecture attract considerable interest due to their differing behavior in comparison with their linear counterparts, especially with regard to rheological and mechanical properties.¹⁴¹

On the basis of poly(glycolide), Xie et al.¹⁴² synthesized a hydroxyl-terminated three-arm star in a condensation polymerization of glycolic acid with trimethylolpropane, followed by additional functionalization yielding methacrylate end-groups (Figure 17). The end-capped PGA prepolymers were used to prepare networks and filler-containing composites via photopolymerization. Degradation studies revealed a slower hydrolysis rate of the composites with increasing filler content, retaining their strength up to 45-60 days.

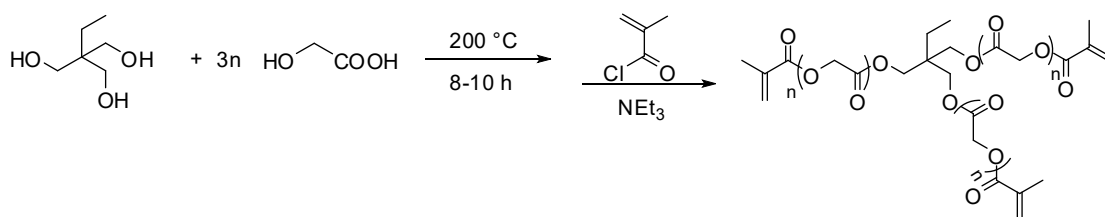


Figure 17. Synthesis route toward injectable and degradable PGA-based composites via photopolymerization of methacrylate-terminated PGA three-arm stars.¹⁴²

Owing to the low solubility of poly(glycolide), Wolf et al. established a promising strategy toward soluble PGA multi-arm stars based on the idea of improving solubility via limited PGA chain length displayed in Figure 18.¹⁴³ These star copolymers exhibit a core-shell structure consisting of a hydrophilic hyperbranched polyglycerol core obtained from oxyanionic ROP of glycidol and a degradable hydrophobic PGA corona. The grafting of glycolide proceeded via $\text{Sn}(\text{Oct})_2$ -catalyzed ROP at 120 °C in bulk. The ease of synthesis and the resulting soluble material up to a weight fraction of 91% glycolide provide a valuable contribution in the research of PGA-based materials. Amphiphilic star polymers are well-known as transport and release systems of hydrophilic drug molecules forming unimolecular micelles.^{144,145}

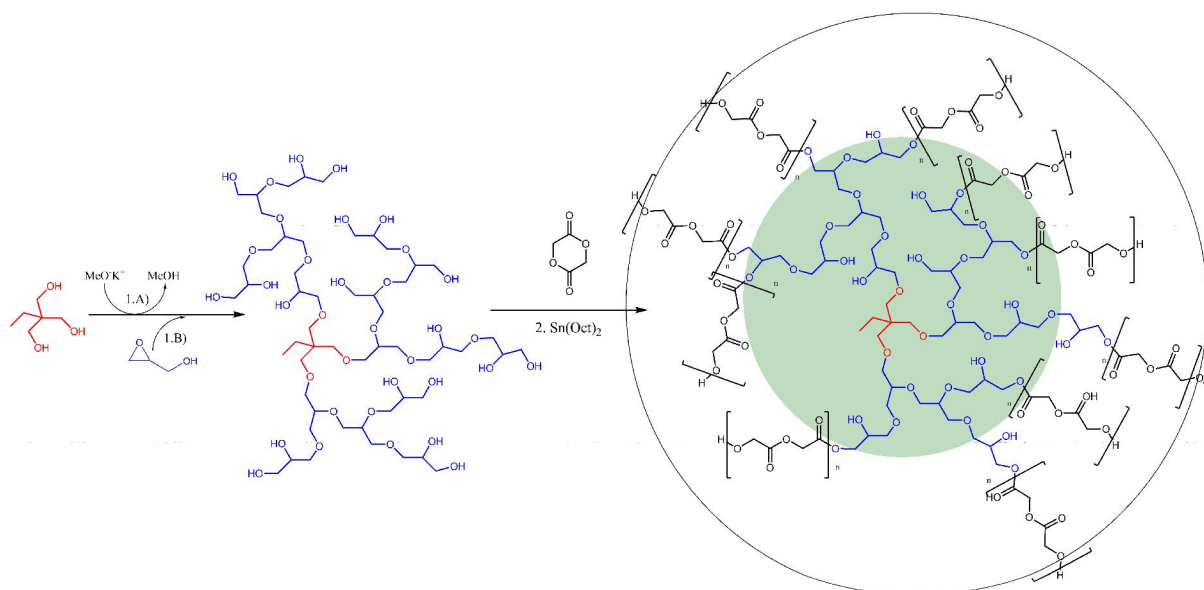


Figure 18. Two-step synthesis toward PGA multi-arm stars based on a polyether polyol macroinitiator as hydrophilic, biocompatible core.¹⁴³

Dendritic macromolecular architectures have been in the focus of extensive research over the past few years.¹⁴⁶ Apart from rheological properties, the viscosity behavior and solubility parameters of linear and branched polymers differ significantly.¹⁴⁷ Recently, Fischer and Frey¹⁴ benefited from the branched topology of poly(glycolide), which afforded amorphous materials with increased solubility and a high number of functional end groups (Figure 19). The synthetic strategy is based on a two-step protocol in a one-pot procedure combining ROP and polycondensation. In the first step, trifunctional prepolymers were obtained via ROP of glycolide initiated with bishydroxy acid. The hydroxyl-terminated chain ends and the single carboxylic acid group in the polymer backbone were subsequently condensed to generate the branched macromolecules. The incorporation of glycolide was successful up to a content of 82 mol%. The obtained polyester polyol was used as a macroinitiator in the lactide polymerization to obtain poly(lactide) multi-arm stars.¹⁴⁸ The authors aimed at adjusting material properties, i.e., degradation time and degree of crystallinity, via the molar composition of PGA and PLLA. The melting point of PLLA was successfully decreased as compared to linear PLLA homopolymers (170-180 °C).

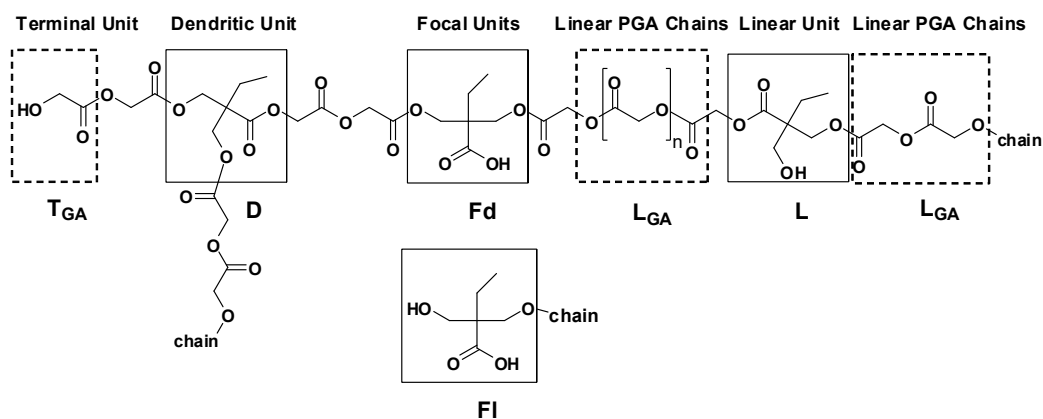


Figure 19. Structure of hyperbranched PGA copolymers formed via ROP/AB₂ polycondensation obtained from glycolide and 2,2-bis(hydroxymethyl)butyric acid showing the predominant units.

4.1.4 Endfunctionalized Poly(glycolide)

Functionalization of poly(ester)s can proceed via three different ways: One strategy is the endcapping of the active chain end following anionic or cationic polymerization. The usage of functional initiators, such as bis hydroxy acids, also leads to the introduction of functionalities and in this special case telechelic polymers are obtained. A further alternative is the post-modification of hydroxyl-terminated poly(glycolide) with methacryloyl chloride, as mentioned in connection with curable materials.

In recent years, PGA has been evaluated for use in biomedical applications, such as tissue scaffolds and wound dressing, but the material played just a passive role and did not really contribute actively, e.g. in wound healing. Lee et al. aimed at designing a biologically active and degradable material based on PGA (Figure 20).¹⁴⁹ They introduced a nitroxyl radical at the end of a PGA chain since NO has a great issue in protection of cells and tissue against oxidative stress. Upon degradation, the NO-derivative is released and the authors observed no toxicity, controlling the proliferation of human smooth muscle cells (SMC) *in vitro*.

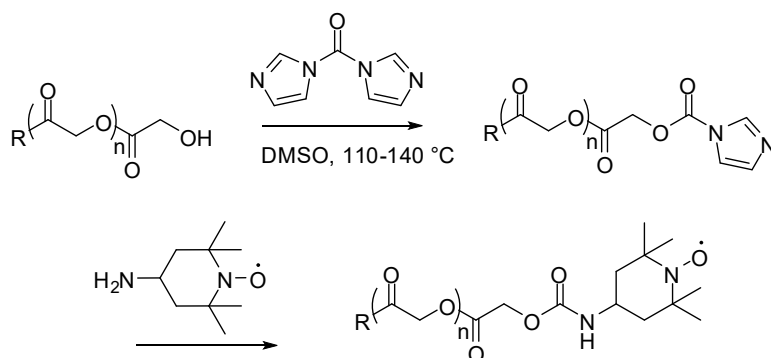


Figure 20. Chemical synthesis of NO--functionalized poly(glycolide).

5. Biomedical Applications

Poly(glycolide) covers a wide range of biomedical applications, which may be subdivided into pharmaceutical and surgical applications. Degradable biomaterials are well-established components in medical research.¹⁵⁰ Key advantages are the resorbability of the device and its biocompatibility, ensuring less inflammatory response. The former feature obviates the need of a second surgical operation for implant removal. In contrast to metal devices, biodegradable implants slowly transfer the load to the healing bone and reduce mechanical stress in the surrounding tissue. The embedding of relevant drug moieties and growth factors in the polymer matrix may enhance the healing process and prevent inflammation.

Since 1970 PGA has been commercially available as degradable surgical suture by American Cyanamid under the tradename Dexon®.^{33,151} The PGA series of Dexon® includes uncoated (Dexon® S) and coated (Dexon® Plus, Dexon® II) fibers. The coating with PCL and calcium stearat (1%) improves knot performance and smooth passage through tissue.³ Today it is marketed as braided multifilament under the tradename Surgicryl® with different resorption time ranging from 42-90 days, respectively.¹⁵² Several monofilaments based on block copolymers consisting of PGA and PLLA (Vicryl®) or PCL (Caprosyn®) have been developed to reduce suture stiffness. Suture studies revealed a better knot reliability for uncoated Dexon® S than Vicryl® despite softening.

PGA of high molecular weight (20,000-145,000 g/mol) can be extruded to form filaments, which are spun to yield multifilament yarns. The final fiber material is obtained after subsequent braiding of the multifilament yarns and exhibits a high modulus of 12.5 GPa.¹⁵³

Braided PGA fibers lose 60% of their tensile strength after 7 days and again 20% after 15 days. The suture material has been completely absorbed after 90-120 days.³ Since PGA loses half of its strength after 2 weeks its suture application is limited to short-time tissue regeneration. Minor tissue reactions are associated with acidic PGA by-products.

The fabrication processes for PGA implants include compression moulding, injection moulding, extrusion and solvent casting to obtain the respective device in the desired shape.⁷ Poly(glycolide) has been employed in load-bearing applications due to its high modulus, tensile strength, and low elongation at break (s. Table 7). Optimized mechanical properties of implants are obtained by self-reinforcing (SR) techniques, using sintering or drawing processes. In the first case, a composite of PGA fibers is obtained by gluing them together. In the other case, fibrillation is generated by orientation drawing.¹⁵³

The application and basic characteristics of PGA implants for bone surgery including SR-PGA screws, pins, plates, and suture anchors are described in detail by Athanasiou et al.,⁴ Ashammakhi et al.,¹⁵³ and Middleton et. al.⁵ Until 1996, PGA has been marketed as internal bone pin under the tradename Biofix®.¹⁵⁴ Recently, Kehoe et al. report on a PGA-based nerve graft conduit, which is commercially

available under the tradename Neurotube®.¹⁵⁵ This peripheral nerve regeneration device received FDA approval and provides most of the clinical data available for surgeons.

Table 7. Mechanical, thermal and degradation properties of PGA compared with bone and steel.⁵

Material	T_m (°C)	T_g (°C)	Modulus^{a)} (GPa)	Elongation (%)	Degradation time^{b)} (month)
PGA	225-230	35-40	7.0	15-20	6-12
PLLA	173-178	60-65	2.7	5-10	>24
Bone			10-20		
Steel			210		

^{a)}Tensile or flexural modulus; ^{b)}Time to complete resorption

Despite the advantages of aliphatic polyesters, their use in fixation devices is limited due to inferior mechanical properties, short life-time and their poor visibility on conventional radiographs compared with metals. Related side-effects are fixation failure and displacements of the fracture. Future applications based on PGA focus more on soft tissue applications, i.e., scaffolds for cartilage¹⁵⁶ and meniscal repair as well as drug release carrier. Even though PGA scaffolds show enhanced cell adhesion, proliferation, differentiation and tissue regeneration biocompatibility is a controversial issue in literature. Foreign body reactions⁸⁰ are suggested to be caused by low pH arising with release of glycolic acid upon degradation and small crystallites of not fully absorbed PGA. Generally, the increased localized acid concentration causes inflammatory response¹⁵⁷ which can be attributed to decelerated diffusion of hydroxy-carboxylic acids from the interior of implants resulting in faster degradation than highly porous implants.¹⁵⁸ Several attempts to reduce acidosis have been achieved by the addition of basic compounds to PGA-based materials. Composites of carbonated apatite and PGA as bone substitution material resulted in stabilization of the pH at 7.2-7.6 upon degradation.¹⁵⁹ Several materials, including PGA, have been investigated for guided tissue regeneration, as described by Hutmacher et al.¹⁹⁰ Scaffolds for tissue engineering are obtained by electrospinning, textile processing or particulate leaching techniques of PGA/NaCl composites, resulting in porous structures after removal of the inorganic salt.¹⁶⁰ These PGA scaffolds have been used for the engineering of cartilage,^{72,161} tendon¹⁶², ureteral stent¹⁶³, intestine¹⁶⁴, blood vessels¹⁶⁵, and other tissues. Polymeric scaffolds were designed for cell seeding *in vitro* or as carrier¹⁶⁶ for cells and growth factors *in vivo*. One approach includes the culturing of cells *in vitro* to regenerate new extracellular matrix in the shape of a biodegradable scaffold for possible transplantation.⁷² Recently, vascular grafts have been obtained by growing smooth muscle cells on a tubular scaffold of poly(glycolic acid). After scaffold

degradation the extracellular matrix tube is implanted as arterial bypass graft in a baboon model.¹⁶⁷ The graft showed excellent mechanical properties and long-term stability at storage conditions of 4 °C. Another approach involves *in vivo* wound healing and tissue formation supported by a fibroblast growth factor embedded in a hybrid matrix of cross-linked collagen and PGA.¹⁶⁸ Eiselt et al.¹⁶⁹ have described technologies and challenges of large tissue-engineering. An overview of biodegradable polymer scaffolds has been given by Agarwal et al.¹⁷⁰ reporting on properties, architecture and cell-polymer interaction.

In recent years, biodegradable poly(ester)s, such as PLA, PGA and PCL, have attracted much interest in controlled drug delivery.^{171,172} Such polymeric drug matrices enhance permeation and retention time of biologically active drug moieties and allow for a controlled release rate. Release of active moieties upon degradation of PGA-based microspheres has been investigated by encapsulation of methylene blue¹⁷³ and prednisolone acetate.¹⁷⁴ Three different methods have been employed for microparticle synthesis including freeze drying, evaporation, and solvent-extraction-precipitation. Radiolabeled PGA microspheres have been achieved by embedding a short-life gamma emitting radioisotope, indium-III, into the polymer matrix.¹⁷⁵ This approach allows *in vivo* monitoring of renal clearance, microsphere administration, tissue distribution and accumulation of particles in organs by gamma scintigraphy. Porous and non-porous PGA matrices have been investigated for controlled release of drugs useful in asthma therapy, such as theophylline.¹⁷⁶ The major concern has been to study the effect of molecular weight and porosity on degradation and release rate. PGA of higher molecular weight and porous material with a high volume-to-pore ratio revealed a slower hydrolysis rate. Tailored drug release is accomplished by blending PGA of different molecular weight.

Especially block copolymers of poly(ester) and PEG are suitable candidates as smart carrier devices. Here, the PEG block provides hydrophilicity and enhances water uptake, whereas controlled drug release proceeds upon degradation of the poly(ester) block. Recently, Zhang et al.¹³⁵ developed a prodrug-polymer conjugate for release of paclitaxel, a useful drug in cancer therapy. In this case, the drug has been covalently linked to diblock copolymers of PEG and PGA instead of being physically entrapped in a polymer matrix. Particularly, drugs with a hydrophobic character are effectively incorporated into amphiphilic copolymers by exploiting their micellar aggregation behaviour in aqueous medium. Such indomethacin-loaded PEG/PGA nanospheres have been investigated in *in vitro* release experiments for anti-inflammatory therapy.¹³³ *In vitro* tests confirmed a constant drug release and biocompatibility of the respective nanospheres.

Several *in vitro* and *in vivo* studies investigated the effect of buffer,^{177,178,179} pH,^{180,181} enzymes,¹⁸² annealing pre-treatment,¹⁸³ carboxyl end groups,¹⁸⁴ and gamma irradiation¹⁸⁵ on degradation behaviour of PGA using various methods, such as magnetic resonance imaging,¹⁸⁶ X-ray scattering¹⁸⁷ and rheological measurements.^{188,189} Some of these aspects are important with regard to packaging

and sterilization of PGA devices. After manufacturing and during processing PGA has to be kept free of moisture due to its hydrolytic instability. Appropriate sterilization techniques have to be used to prevent degradation upon autoclaving and radiation. Gamma irradiation leads to molecular weight loss and thus exposure to ethylene oxide gas is preferred for sterilization of PGA medical devices.⁵ Owing to the research knowledge specific tailoring of the degradation rate of poly(ester)s has become available.

The degradation of semi-crystalline poly(glycolide) proceeds by bulk erosion in a two-stage process. At first water penetrates in the amorphous regions and degrades the polymer into small water-soluble fragments via hydrolysis of the chemically sensitive ester bonds. After erosion of the amorphous parts a crystalline fraction remains. The increased acidic environment in bulk accelerates hydrolysis of the crystalline regions. In the second phase, enzymes with esterase activity attack the ester linkages and chain cleavage of smaller fragments takes place as well by further hydrolysis.⁵ The degradation product glycolic acid is excreted directly in urine or metabolized via the Krebs' cycle into water and carbon dioxide. Oxidation of glycolic acid to glyoxylate yields after subsequent enzymatic conversion glycine, which is converted into serine. After transformation of serine to pyruvic acid, the latter enters the Krebs' cycle (Figure 21).^{3, 7, 190}

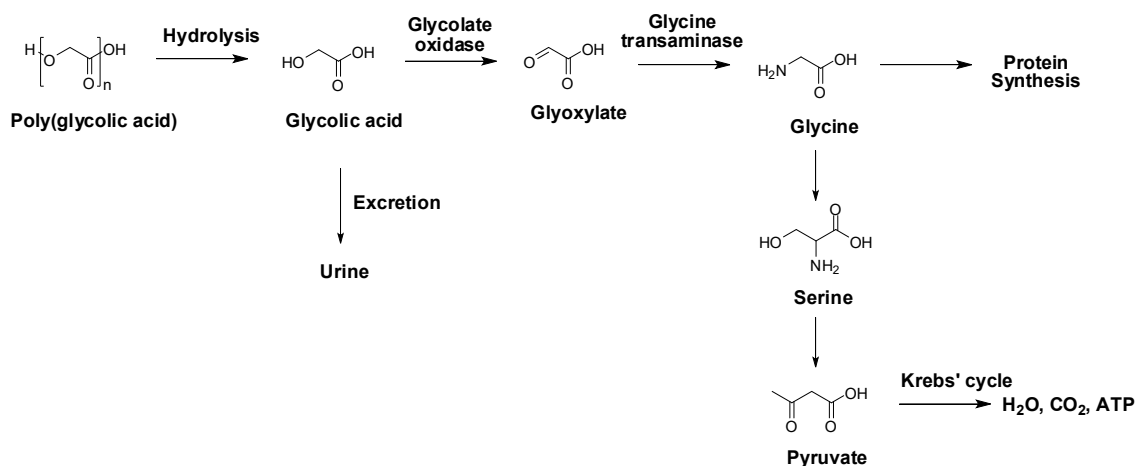


Figure 21. Metabolization via Krebs' cycle or excretion of the degradation end-product, glycolic acid.

Current Challenges and Future Prospects

The present review surveys synthetic procedures, characterization and application developed for poly(glycolide) homo- and copolymers, whereas the main focus lies on PGA as the main building element. Excellent mechanical properties, biodegradability, low tendency for inflammation and high cell affinity represent key advantages of PGA in medical applications. Detailed analysis and advanced characterization methods play an important role to evaluate suitability of PGA in industrial

applications. Investigations on PGA have been preferentially performed in bulk due to its lack of solubility in common organic solvents. Therefore comparison with solution properties of other biodegradable polyesters is not possible. With the increasing demand on tailor-made materials, the accurate determination of materials properties gains increasing importance for novel applications. Hence, advanced research on catalytic systems for “controlled” ring-opening polymerization of glycolide, and detailed evaluation of reaction kinetics is essential to prevent material impurities that accelerate decomposition of the product or residual monomer. Several studies offer solutions to overcome key limitations of PGA, namely hydrolytic and thermal susceptibility, followed by reduced mechanical strength, acidosis of surrounding tissue due to release of hydroxy-carboxylic acids and low solubility. End-user guidelines for PGA processing and storage are provided by industry, advising moisture-free storage and handling to enhance long-term stability and preserve constant quality of the end product. Utilization of basic additives plays a valuable part in contributing to pH stabilization upon PGA degradation.

The exploration of novel PGA-based copolymer architectures, such as multi-arm stars and dendritic macromolecules contributes to broadening the field of applications. The strategy of “Limited PGA chain length” ensures access to a broad variety of soluble materials.

Due to the broad variety of consumer and industrial applications of GA, the replacement of GA production from petroleum-based feedstocks by renewable resources is a global interest regarding sustainability. The availability of GA from renewable raw material contributes in further establishment of PGA-based materials and increases overall popularity.

References

-
1. Vert, M.; Li, M. S.; Spenlehauer, G.; Guerin, P. Bioresorbability and biocompatibility of aliphatic polyesters, *J. Mater. Sci.: Mater. Med.* **1992**, *3*, 432-446.
 2. Dardik, H.; Dardik, I.; Laufman, H. Clinical use of polyglycolic acid polymer as a new absorbable synthetic suture, *Am. J. Surg.* **1971**, *121*, 656-660.
 3. Pillai, C. K. S.; Sharma, C. P. Review paper: absorbable polymeric surgical sutures: chemistry, production, properties, biodegradability, and performance, *J. Biomater. Appl.* **2010**, *25*, 291-366.
 4. Athanasiou, K. A.; Agrawal, C. M.; Barber, F. A.; Burkhart, S. S. Orthopaedic applications for PLA-PGA biodegradable polymers, *Arthroscopy* **1998**, *14*, 726-737

5. Middleton, J. C.; Tipton, A. J. Synthetic biodegradable polymers as orthopaedic devices, *Biomaterials* **2000**, *21*, 2335-2346.
6. Rokkanen, P.; Böstman, O.; Hirvensalo, E.; Partio, E. K.; Mäkelä, E. A.; Pätäälä, H.; Vihtonen, K. Bioabsorbable implants in orthopaedics, *Current Orthopaedics* **1999**, *13*, 223-228.
7. Gunatillake, P. A.; Adhikari, R. Biodegradable synthetic polymers for tissue engineering, *Eur. Cell Mater.* **2003**, *5*, 1-16.
8. Andreas, F.; Sowada, R.; Scholz, J. Darstellung und Eigenschaften von Glykolid, *J. Prakt. Chem.* **1962**, *4*, 141-149.
9. Cohn, D.; Younes, H.; Marom, G. Amorphous and crystalline morphologies in glycolic acid and lactic acid polymers, *Polymer* **1987**, *28*, 2018-2022.
10. Tsuji, H. Poly(lactide) Stereocomplexes: formation, structure, properties, degradation, and applications, *Macromol. Biosci.* **2005**, *5*, 569-597.
11. Chatani, Y.; Suehiro, K.; Okita, Y.; Tadokoro, H.; Chujo, K. Structural studies of polyesters: I. Crystal structure of polyglycolide, *Die Makromolekulare Chemie* **1968**, *113*, 215-229.
12. Marega, C.; Marigo, A.; Zannetti, R.; Paganetto, G. A structural investigation on poly(glycolic acid), *Eur. Polym. J.* **1992**, *28*, 1485-1486.
13. EP 1,550,682 B1 (2003), Kureha Corporation Tokyo, invs.: Sato, H.; Hoshi, T.; Okada, Y.; Suzuki, Y.
14. Fischer, A. M.; Frey, H. Soluble hyperbranched poly(glycolide) copolymers, *Macromolecules* **2010**, *43*, 8539-8548.
15. Hariharan, R.; Pinkus, A. G. Useful NMR solvent mixture for polyesters: trifluoroacetic acid-d/chloroform-d, *Polym. Bull.* **1993**, *30*, 91-95.
16. Montes de Oca, H.; Ward, I. M.; Klein, P. G.; Ries, M. E.; Rose, J.; Farrar D. Solid state nuclear magnetic resonance study of highly oriented poly(glycolic acid), *Polymer* **2004**, *45*, 7261-7272.
17. Montes de Oca, H.; Ward, I. M.; Chivers, R. A.; Farrar, D. F. Structure development during crystallization and solid-state processing of poly(glycolic acid), *J. Appl. Polym. Sci.* **2009**, *113*, 1013-1018.
18. Gautier, E.; Fuertes, P.; Cassagnau, P.; Pascault, J.-P.; Fleury, E. Synthesis and rheology of biodegradable poly(glycolic acid) prepared by melt ring-opening polymerization of glycolide, *J. Polym. Sci.: Part A: Polym. Chem.* **2009**, *47*, 1440-1449.
19. Sekine, S.; Yamauchi, K.; Aoki, A.; Asakura, T. Heterogeneous structure of poly(glycolic acid) fiber studied with differential scanning calorimeter, X-ray diffraction, solid-state NMR and molecular dynamic simulation, *Polymer* **2009**, *50*, 6083-6090.

20. <http://www.chemicals-technology.com/projects/kurehacorporationpol/>
(accessed 19.05.2012)
21. [http://www2.dupont.com/Oil_and_Gas/en_CA/assets/downloads/
DuPont_Oil_Well_Productivity.pdf](http://www2.dupont.com/Oil_and_Gas/en_CA/assets/downloads/DuPont_Oil_Well_Productivity.pdf) (accessed 19.05.2012)
22. Technical Guidebook (Nov 2011); <http://www.kuredux.com/en/about/basicquality.html>
(accessed 19.05.2012)
23. <http://www.kureha.co.jp/en/guidance/division/pgs/index.html> (accessed 19.05.2012)
24. Scientific opinion on the safety evaluation of the substance glycolic acid for use in food contact materials, *European Food Safety Authority (EFSA) Journal* **2010**, *8*, 1927.
25. Cotellessa, C.; Peris, K.; Chimenti, S. Glycolic acid and its use in dermatology, *J. Eur. Acad. Dermatol. Venereol.* **1995**, *5*, 215-217.
26. US Patent 2,443,482 (1948), invs.: M. T. Shattuck, Va, W.
27. Kataoka, M.; Sasaki, M.; Hidalgo, A.-R. G. D.; Nakano, M.; Shimizu, S. Glycolic acid production using ethylene glycol-oxidizing microorganisms, *Biosci. Biotechnol. Biochem.* **2001**, *65*, 2265-2270.
28. http://www.nicnas.gov.au/publications/car/pec/pec12/summary_report.asp
(accessed 19.05.2012)
29. Panova, A.; Mersinger, L. J.; Liu, Q.; Foo, T.; Roe, D. C.; Spillan, W. L.; Sigmund, A. E.; Ben-Bassat, A.; Wagner, L. W.; O'Keefe, D. P.; Wu, S.; Petrillo, K. L.; Payne, M. S.; Breske, S. T.; Gallagher, F. G.; DiCosimo, R. Chemoenzymatic synthesis of glycolic acid, *Adv. Synth. Catal.* **2007**, *349*, 1462-1474.
30. US 7, 198, 927 B2 (2007), E. I. Du Pont de Nemours and Company, invs.: DiCosimo, R.; Payne, M. S.; Panova, A.; Thompson, J.; O'Keefe, D. P. Enzymatic production of glycolic acid.
31. Krochta, J. M.; Tillin, S. J.; Hudson, J. S. Thermochemical conversion of polysaccharides in concentrated alkali to glycolic acid, *Appl. Biochem. Tech.* **1988**, *17*, 23-32.
32. Gilding, D. K.; Reed, A. M. Biodegradable polymers for use in surgery-polyglycolic/poly(actic acid) homo- and copolymers: 1, *Polymer* **1979**, *20*, 1459-1464.
33. Frazza, E. J.; Schmitt, E. E. A new absorbable suture, *J. Biomed. Mater. Res. Symp.* **1971**, *1*, 43-58.
34. Dessaignes, V. Untersuchungen über die von der Nitroweinsäure sich ableitenden Verbindungen, *Liebigs Ann. Chem.* **1854**, *89*, 339-344.
35. Kékule, A. Bildung von Glycolsäure aus Essigsäure, *Liebigs Ann. Chem.* **1858**, *105*, 288-292.
36. Hoffmann, R. Über Monochloressigsäure, *Liebigs Ann. Chem.* **1857**, *102*, 1-20.
37. Heintz, W. Über die Diglycolsäure, *Poggendorffs Ann. Chem. Phys.* **1862**, *115*, 452-465.

38. Beckurts, H.; Otto, R. Studien über das Verhalten der Silbersalze von halogensubstituierten Säuren der Reihe $C_nH_{2n}O_2$ beim Erhitzen mit Wasser und für sich, *Chem. Ber.* **1881**, *14*, 576-591.
39. Bischoff, C. A.; Walden, P. Über Das Glycolid und seine Homologen, *Chem. Ber.* **1893**, *26*, 262-265.
40. Bischoff, C. A.; Walden, P. Über Derivate der Glycolsäure, *Liebigs Ann. Chem.* **1894**, *279*, 45-70.
41. Chujo, K.; Kobayashi, H.; Suzuki, J.; Tokuhara, S.; Tanabe, M. Ring-opening polymerization of glycolide, *Die Makromolekulare Chemie* **1967**, *100*, 262-266.
42. Kohn, F. E.; van Ommen, J. G.; Feijen, J. The mechanism of the ring-opening polymerization of lactide and glycolide, *Eur. Polym. J.* **1983**, *19*, 1081-1088.
43. Herzberg, O.; Epple, M. Formation of polyesters by thermally induced polymerization reactions of molecular solids, *Eur. J. Inorg. Chem.* **2001**, 1395-1406.
44. Garlotta, D. A literature review of poly(lactic acid), *J. Polym. Environ.* **2001**, *9*, 63-84.
45. Takahashi, K.; Taniguchi, I.; Miyamoto, M.; Kimura, Y. Melt/solid polycondensation of glycolic acid to obtain high-molecular-weight poly(glycolic acid), *Polymer* **2000**, *41*, 8725-8728.
46. Dali, S.; Lefebvre, H.; El Garbi, R.; Fradet, A. Synthesis of poly(glycolic acid) in ionic liquids, *J. Polym. Sci.: Part A: Polym. Chem.* **2006**, *44*, 3025-3035.
47. Braun, D.; Kohl, P. R. Anionische Lösungspolymerisation von Glycolid, *Die Angewandte Makromolekulare Chemie* **1986**, *139*, 191-200.
48. Nieuwenhuis, J. Synthesis of polylactides, polyglycolides and their copolymers, *Clin. Mater.* **1992**, *10*, 59-67.
49. Dechy-Cabaret, O.; Martin-Vaca, B.; Bourissou, D. Controlled ring-opening polymerization of lactide and glycolide, *Chem. Rev.* **2004**, *104*, 6147-6176.
50. Kamber, N. E.; Jeong, W.; Waymouth, M. R.; Pratt, R. C.; Lohmeijer, B. G. G.; Hedrick, J. L. Organocatalytic ring-opening polymerization, *Chem. Rev.* **2007**, *107*, 5813-5840.
51. Mazarro R.; de Lucas, A.; Gracia, I.; Rodríguez, J. F. Kinetic study of D,L-lactide and glycolide homopolymerizations by differential scanning calorimetry, *Macromol. Chem. Phys.* **2008**, *209*, 818-824.
52. Dobrzynski, P.; Kasperczyk, J.; Bero, M. Application of Acetylacetonate to the polymerization of glycolide and copolymerization of glycolide with ϵ -caprolactone and L-lactide, *Macromolecules* **1999**, *32*, 4735-4737.

53. Quian H.; Wohl, A. R.; Crow, J. T.; Macosko, C. W.; Hoyer, T. R. A Strategy for control of "random" copolymerization of lactide and glycolide: application to synthesis of PEG-b-PLGA block polymers having narrow dispersity, *Macromolecules* **2011**, *44*, 7132-7140.
54. Saiyasombat, W.; Molloy, R.; Nicholson, T. M.; Johnson, A. F.; Ward, I. M.; Poshyachinda, S. Ring strain and polymerizability of cyclic esters, *Polymer* **1998**, *39*, 5581-5585.
55. Báez, J. E.; Marcos-Fernández, À. A Simple and rapid preparation of poly(glycolide) (PGA) oligomers catalyzed by decamolybdate anion in the presence of aliphatic alcohols, *Int. J. Polym. Anal. Charact.* **2011**, *16*, 269-276.
56. Dobrzynski, P.; Kasperczyk, J.; Janeczek, H.; Bero, M. Synthesis of biodegradable glycolide/L-lactide copolymers using iron compounds as initiators, *Polymer* **2002**, *43*, 2595-2601.
57. Jonté, J. M.; Dunsing, R.; Kricheldorf, H. R. Polylactones. 4. Cationic polymerization of lactones by means of alkylsulfonates, *J. Macromol. Sci.: Part A-Chem.: Appl. Chem.* **1985**, *22*, 495-514.
58. Sanina, G. S.; Fomina, M. V.; Khomyakov, A. K.; Livshits, V. S.; Savin, V. A.; Lyudvig, Ye. B. Cationic polymerization of glycolide in the presence of antimony trifluoride, *Polym. Sci. U.S.S.R.* **1975**, *17*, 3133-3140.
59. Amine, H.; Karima, O.; El Amine, B. M.; Belbachir, M.; Meghabar, R. Cationic ring-opening polymerization of glycolide catalyzed by a montmorillonite clay catalyst, *J. Polym. Res.* **2005**, *12*, 361-365.
60. Singh, V.; Tiwari, M. Structure-processing-property relationship of poly(glycolic Acid) for drug delivery systems 1: synthesis and catalysis, *J. Polym. Sci.* **2010**, 1-23, doi: 10.1155/2010/652719.
61. Epple, M.; Kirschnick, H.; Thomas, J. M. An in situ IR-spectroscopic study of the solid-state formation reaction of polyglycolide, *J. Therm. Anal.* **1996**, *47*, 331-338.
62. Epple, M.; Kirschnick, H. The Thermally induced solid-state polymerization reaction in halogenoacetates, *Chem. Ber.* **1996**, *129*, 1123-1129.
63. Aliev, A. E.; Elizabé, L.; Kariuki, B. M.; Kirschnick, H.; Thomas, J. M.; Epple, M.; Harris, K. D. M. In situ monitoring of solid-state polymerization reactions in sodium chloroacetate and sodium bromoacetate by ²³Na and ¹³C solid-state NMR spectroscopy, *Chem. Eur. J.* **2000**, *6*, 1120-1126.
64. Epple, M.; Herzberg, O. Polyglycolide with controlled porosity: an improved biomaterial, *J. Mater. Chem.* **1997**, *7*, 1037-1042.
65. Schwarz, K.; Epple, M. Hierarchically structured polyglycolide-a biomaterial mimicking natural bone, *Macromol. Rapid Commun.* **1998**, *19*, 613-617.

66. Kapur, R.; Spargo, J. B.; Chen, M.-S.; Calvert, J. M.; Rudolph, A. S. Fabrication and selective surface modification of 3-dimensionally textured biomedical polymers from etched silicon substrates, *J. Biomed. Mater. Res.: Appl. Biomater.* **1996**, *33*, 205-216.
67. Morent, R.; De Geyter, N.; Desmet, T.; Dubruel, P.; Leys, C. Plasma surface modification of biodegradable polymers: a review, *Plasma Process. Polym.* **2011**, *8*, 171-190.
68. Lee, K.-B.; Yoon, K. R.; Woo, S. I.; Choi, I. S. Surface modification of poly(glycolic acid) (PGA) for biomedical applications, *J. Pharm. Sci.* **2003**, *92*, 933–937.
69. Lee, K.-B.; Kim, D. J.; Lee, Z. W.; Woo, S. I.; Choi, I. S. Pattern generation of biological ligands on a biodegradable poly(glycolic acid) film, *Langmuir* **2004**, *20*, 2531-2535.
70. Gao, J.; Niklason, L.; Langer, R. Surface hydrolysis of poly(glycolic acid) meshes increases the seeding density of vascular smooth muscle cells, *J. Biomed. Mater. Res.* **1998**, *42*, 417-424.
71. Mikos, A. G.; Bao, Y.; Cima, L. G.; Ingber, D. E.; Vacanti, J. P.; Langer, R. Preparation of poly(glycolic acid) bonded fiber structures for cell attachment and transplantation, *J. Biomed. Mater. Res.* **1993**, *27*, 183-189.
72. Freed, L. E.; Marquis, J. C.; Nohria, A.; Emmanuel, J.; Mikos, A. G.; Langer, R. Neocartilage formation in vitro and in vivo using cells cultured on synthetic biodegradable polymers, *J. Biomed. Mater. Res.* **1993**, *27*, 11-23.
73. Yang, Q.; Shen, X.; Tan, Z. Investigations of the preparation technology for polyglycolic acid fiber with perfect mechanical performance, *J. Appl. Polym. Sci.* **2007**, *105*, 3444-3447.
74. Freed, L. E.; Vunjak-Novakovic, G.; Biron, R. J.; Eagles, D. B.; Lesnoy, D.C.; Barlow, S. K.; Langer, R. Biodegradable polymer scaffolds for tissue engineering, *Nature Biotechnology* **1994**, *12*, 689-693.
75. You, Y.; Min, B.-M.; Lee, S. J.; Lee, T. S.; Park, W. H. In vitro degradation behavior of electrospun polyglycolide, polylactide, and poly(lactide-co-glycolide), *J. Appl. Polym. Sci.* **2005**, *95*, 193-200.
76. You, Y.; Youk, J. H.; Lee, S. W.; Min, B.-M.; Lee, S. J.; Park, W. H. Preparation of porous ultrafine PGA fibers via selective dissolution of electrospun PGA/PLA blend fibers, *Mater. Lett.* **2006**, *60*, 757-760.
77. Ramdhanie, L. I.; Aubuchon, S. R.; Boland, E. D.; Knapp, D. C.; Barnes, C. P.; Simpson, D. G.; Wnek, G. E.; Bowlin, G. L. Thermal and mechanical characterization of electrospun blends of poly(lactic acid) and poly(glycolic acid), *Polym. J.* **2006**, *38*, 1137-1145.
78. Boland, E. D.; Wnek, G. E.; Simpson, D. G.; Pawlowski, K. J.; Bowlin G. L. Tailoring tissue engineering scaffolds using electrostatic processing techniques: a study of poly(glycolic acid) electrospinning, *J. Macromol. Sci.* **2001**, *38*, 1231-1243.

79. Boland, E. D.; Telemeco, T. A.; Simpson, D. G.; Wnek, G. E.; Bowlin, G. L. Utilizing acid pretreatment and electrospinning to improve biocompatibility of poly(glycolic acid) for tissue engineering, *J. Biomed. Mater. Res. Part B: Appl. Biomater.* **2004**, *71B*, 144-152.
80. Santavirta, S.; Konttinen, Y. T.; Sajto, T.; Grönblad, M.; Partio, E.; Kemppinen, P.; Rokkanen, P. Immune Response to polyglycolic acid implants, *J. Bone Joint Surg.* **1990**, *72B*, 597-600.
81. Tian, F.; Hosseinkhani, H.; Hosseinkhani, M.; Khademhosseini, A.; Yokoyama, Y.; Estrada, G. G.; Kobayashi, H. Quantitative analysis of cell adhesion on aligned micro- and nanofibers, *J. Biomed. Mater. Res.* **2008**, *84A*, 291-299.
82. Dickers, K. J.; Huatan, H.; Cameron, R. E. Polyglycolide-based blends for drug delivery: A differential scanning calorimetry study of the melting behaviour, *J. Appl. Polym. Sci.* **2003**, *89*, 2937-2939.
83. Aghdam, R. M.; Najarian, S.; Shakhesi, S.; Khanlari, S.; Shaabani, K.; Sharifi, S. Investigating the effect of PGA on physical and mechanical properties of electrospun PCL/PGA blend nanofibers, *J. Appl. Polym. Sci.* **2012**, *124*, 123-131.
84. Ha, C.-S.; Gardella, J. A. Surface chemistry of biodegradable polymers for drug delivery systems, *Chem. Rev.* **2005**, *105*, 4205-4232.
85. Lee, J.-W.; Gardella, J. A. In vitro hydrolytic surface degradation of poly(glycolic acid): role of the surface segregated amorphous region in the induction period of bulk erosion, *Macromolecules* **2001**, *34*, 3928-3937.
86. Kister, G.; Cassanas, G.; Vert, M. Morphology of poly(glycolic acid) by IR and Raman spectroscopies, *Spectrochimica Acta Part A* **1997**, *53*, 1399-1403.
87. Agarwal, R.; Misra, R. M.; Tandon, P.; Gupta, V. D. Vibrational dynamics and heat capacity of poly(glycolic acid), *Polymer* **2004**, *45*, 5307-5315.
88. Chu, C. C.; Louie, M. A chemical means to examine the degradation phenomena of polyglycolic acid fibers, *J. Appl. Polym. Sci.* **1985**, *30*, 3133-3141.
89. Suzuki, A.; Shimizu, R. Biodegradable poly(glycolic acid) nanofiber prepared by CO₂ laser supersonic drawing, *J. Appl. Polym. Sci.* **2011**, *121*, 3078-3084.
90. Chu, C.C.; Campbell, N. D. Scanning electron microscopic study of the hydrolytic degradation of poly(glycolic acid) suture, *J. Biomed. Mater. Res.* **1982**, *16*, 417-430.
91. Agrawal, A.; Saran, A. D.; Rath, S. S.; Khanna, A. Constrained nonlinear optimization for solubility parameters of poly(lactic acid) and poly(glycolic acid)—validation and comparison, *Polymer* **2004**, *45*, 8603-8612.
92. Engelberg, I.; Kohn, J. Physico-mechanical properties of degradable polymers used in medical applications: a comparative study, *Biomaterials* **1991**, *12*, 292-304.

93. Schöberl, A.; Wiehler, G. Über die Dehydratisierung von Thioglykolsäure, deren Kondensationspolymere und über Dithioglykolid, *Liebigs Ann. Chem.* **1955**, *595*, 101-130.
94. Pinkus, A. G.; Subramanyan, R. New high-yield, one-step synthesis of polyglycolide from haloacetic acids, *J. Polym. Sci., Polym. Ed.* **1984**, *22*, 1131-1140.
95. Nakafuku, C.; Yoshimura, H. Melting parameters of poly(glycolic acid), *Polymer* **2004**, *45*, 3583-3585.
96. Ikada, Y.; Tsuji, H. Biodegradable polyesters for medical and ecological applications, *Macromol. Rapid Commun.* **2000**, *21*, 117-132.
97. Wang, Z.-G.; Hsiao, B. S.; Zong, X.-H.; Yeh, F.; Zhou, J. J.; Dormier, E.; Jamiolkowski, D. D. Morphological development in absorbable poly(glycolide), poly(glycolide-co-lactide) and poly(glycolide-co-caprolactone) copolymers during isothermal crystallization, *Polymer* **2000**, *41*, 621-628.
98. Montes de Oca, H.; Ward, I. M. Structure and mechanical properties of PGA crystals and fibres, *Polymer* **2006**, *47*, 7070-7077.
99. Hurrel, S.; Cameron, R. E. Polyglycolide: degradation and drug release. Part I: Changes in morphology during degradation, *J. Mater. Sci.: Mater. Med.* **2001**, *12*, 811-816.
100. Hayes, M. J.; Lauren, M. D. Chemical stress relaxation of polyglycolic acid suture, *J. Appl. Biomater.* **1994**, *5*, 215-220.
101. Chu, C. C. Hydrolytic degradation of polyglycolic acid: Tensile strength and crystallinity study, *J. Appl. Polym. Sci.* **1981**, *26*, 1727-1734.
102. Doi, Y.; Steinbüchel, A.; Biopolymers, Vol. 3b, Polyesters II-Properties and chemical synthesis, Wiley-VCH, Weinheim **2002**, p 385.
103. Kricheldorf, H. R.; Mang T.; Jonté, J. M. Kricheldorf, H. R.; Mang T.; Jonté, J. M. Polylactones 1. Copolymerization of glycolide and ϵ -caprolactone, *Macromolecules* **1984**, *17*, 2173-2181.
104. Kricheldorf, H. R.; Jonté, J. M.; Berl, M. Polylactones 3. Copolymerization of glycolide with L, L-lactide and other lactones, *Makromol. Chem. Suppl.* **1985**, *12*, 25-38.
105. Bero, M.; Czaplá, B.; Dobrzynski, P.; Janeczek, H.; Kasperczyk, J. Copolymerization of glycolide and ϵ -caprolactone, 2. Random copolymerization in the presence of tin octoate, *Macromol. Chem. Phys.* **1999**, *200*, 911-916.
106. Nakayama, A.; Kawasaki, N.; Aiba, S.; Meada, Y.; Arvanitoyannis, I.; Yamamoto, N. Synthesis and biodegradability of novel copolyesters containing γ -butyrolactone units, *Polymer* **1998**, *39*, 1213-1222.
107. Kasperczyk, J. Microstructural analysis of poly[(L,L-lactide)-co-(glycolide)] by ^1H and ^{13}C NMR spectroscopy, *Polymer* **1996**, *37*, 201-203.

108. Pack, J. W.; Kim, S. H.; Cho, I.-W.; Park, S. Y.; Kim, Y. H. Microstructure analysis and thermal property of copolymers made of glycolide and ϵ -caprolactone by stannous octoate, *J. Polym. Sci.: Part A: Polym. Chem.* **2002**, *40*, 544-554.
109. (a) Dobrzynski, P.; Li, S.; Kasperczyk, J.; Bero, M.; Gasc, F.; Vert, M. Structure–property relationships of copolymers obtained by ring-opening polymerization of glycolide and ϵ -caprolactone. Part 1. Synthesis and characterization, *Biomacromolecules* **2005**, *6*, 483-488; (b) Li, S.; Dobrzynski, P.; Kasperczyk, J.; Bero, M.; Braud, C.; Vert, M. Structure–property relationships of copolymers obtained by ring-opening polymerization of glycolide and ϵ -caprolactone. Part 2. Influence of composition and chain microstructure on the hydrolytic degradation, *Biomacromolecules* **2005**, *6*, 489-497; (c) Kasperczyk, J. Copolymerization of glycolide and ϵ -caprolactone, 1. Analysis of the copolymer microstructure by means of ^1H and ^{13}C NMR spectroscopy, *Macromol. Chem. Phys.* **1999**, *200*, 903-910.
110. Rodríguez-Galán, A.; Franco, L.; Puiggalí, J. Sequence analysis of glycolide and p-dioxanone copolymers, *J. Polym. Sci.: Part A: Polym. Chem.* **2009**, *47*, 6758-6770.
111. Zurita, R.; Puiggalí, J.; Franco, L.; Rodríguez-Galán, A. Copolymerization of glycolide and trimethylene carbonate, *J. Polym. Sci.: Part A: Polym. Chem.* **2006**, *44*, 993-1013; (b) Celorio-Díaz, E.; Franco, L.; Puiggalí, J. Isothermal crystallization study on a biodegradable segmented copolymer constituted by glycolide and trimethylene carbonate units, *J. Appl. Polym. Sci.* **2010**, *116*, 577-589.
112. Jie, C.; Zhu, J.; Shilin, Y. Preparation, characterization and biodegradable characteristics of poly(1,3-trimethylene carbonate-co-glycolide), *Polym. Int.* **1996**, *41*, 369-375.
113. Lee, S. C.; Kim, K. J.; Kang, S. W.; Kim, C. Microstructural analysis and structure-property relationship of poly(glycolide-co-1,3-trimethylene carbonate), *Polymer* **2005**, *46*, 7953-7960.
114. Fukuzaki, H.; Yoshida, M.; Asano, M.; Kumakura, M. A new biodegradable copolymer of glycolic acid and lactones with relatively low molecular weight prepared by direct copolycondensation in the absence of catalysts, *J. Biomed. Mater. Res.* **1991**, *25*, 315-328.
115. Palau-Martínez, M.; Franco, L.; Puiggalí, J. Polycondensation of metal salts of 6-(2-chloroacetate)hexanoic acid: a new method to synthesize alternating copolyesters constituted by glycolic acid units, *Macromol. Chem. Phys.* **2008**, *209*, 393-403.
116. Palau-Martínez, M.; Franco, L.; Ramis, X.; Puiggalí, J. Poly[(4-hydroxybutyric acid)-alt-(glycolic acid)]: synthesis by thermal polycondensation of metal salts of 4-chlorobutyric acid carboxymethyl ester, *Macromol. Chem. Phys.* **2006**, *207*, 90-103.
117. Palau-Martínez, M.; Franco, L.; Puiggalí, J. Nonisothermal crystallization studies on poly(4-hydroxybutyric acid-alt-glycolic acid), *J. Polym. Sci.: Part B: Polym. Phys.* **2008**, *46*, 121-133.

118. Soccio, M.; Lotti, N.; Finelli, L.; Gazzano, M.; Munari, A. (2-Hydroxy isobutyric) acid containing poly(glycolic acid): structure–properties relationship, *J. Polym. Sci: Part B: Polym. Phys.* **2010**, *48*, 1901-1910.
119. Jin, X.; Carfagna, C.; Nicolais, L.; Lanzetta, R. Synthesis and characterization of potentially biodegradable thermotropic polyesters based on p-hydroxybenzoic acid and glycolic acid, *J. Polym. Sci.: Part A: Polym. Chem.* **1994**, *32*, 3115-3122.
120. Cheng, S.-X.; Miao, Z.-M.; Wang, L.-S.; Zhuo, R.-X. Synthesis and characterization of novel biodegradable copolymers of 5-benzyloxy-1,3-dioxan-2-one and glycolide, *Macromol. Rapid Commun.* **2003**, *24*, 1066-1069.
121. In't Veld, P. J. A.; Shen, Z.-R.; Takens, C. A. J.; Dijkstra, P. J.; Feijen, J. Glycine/glycolic acid based copolymers, *J. Polym. Sci.:Part A: Polym. Chem.* **1994**, *32*, 1063-1069.
122. Du, F.; Ye, W.; Gu, Z.; Yang, J. Synthesis and in vitro degradation of copolymers of glycolide and 6 (R,S)-methylmorpholine-2,5-dione, *J. Appl. Polym. Sci.* **1997**, *63*, 643-650.
123. M. Ryner, K. Stridsberg, A.-C. Albertsson, H. von Schenck, M. Svensson Mechanism of ring-opening polymerization of 1,5-dioxepan-2-one and L-lactide with stannous 2-ethylhexanoate. A theoretical study, *Macromolecules* **2001**, *34*, 3877.
124. Rodríguez-Galán, A.; Vera, M.; Jiménez, K.; Franco, L.; Puiggali, J. Synthesis of poly(ester amide)s derived from glycolic acid and the amino acids: β -alanine or 4-aminobutyric acid, *Macromol. Chem. Phys.* **2003**, *204*, 2078-2089.
125. Vera, M.; Rodríguez-Galán, A.; Puiggali, J. New method of synthesis of poly(ester amide)s derived from the incorporation of glycolic acid residues into aliphatic polyamides, *Macromol. Rapid Commun.* **2004**, *25*, 812-817.
126. Vera, M.; Franco, L.; Puiggali, J. Synthesis and characterization of poly(glycolic acid-alt-6-aminohexanoic acid) and poly(glycolic acid-alt-11-aminoundecanoic acid), *Macromol. Chem. Phys.* **2004**, *205*, 1782-1792.
127. John, G.; Tsuda, S.; Morita, M. Synthesis and modification of new biodegradable copolymers: Serine/glycolic acid based copolymers, *J. Polym. Sci. Part A: Polym. Chem.* **1997**, *35*, 1901-1907.
128. Parchuzowski, P. G.; Grabowska, M.; Tryznowski, M.; Rokicki, G. Synthesis of glycerol based hyperbranched polyesters with primary hydroxyl groups, *Macromolecules* **2006**, *39*, 7181-7186.
129. Wolf, F. K.; Frey, H. Inimer-promoted synthesis of branched and hyperbranched poly(lactide) copolymers, *Macromolecules* **2009**, *42*, 9443-9456.

130. Barakat, I.; Dubois, Ph.; Grandfils, Ch.; Jérôme, R. Poly(ϵ -caprolactone-*b*-glycolide) and poly(D,L-lactide-*b*-glycolide) diblock copolyesters: controlled synthesis, characterization, and colloidal dispersions, *J. Polym. Sci.: Part A: Polym. Chem.* **2001**, *39*, 294-301.
131. Barakat, I.; Dubois, Ph.; Jérôme, R.; Teyssié, Ph.; Mazurek, M. Polymerization of glycolide promoted by ω -Al-alkoxide poly(ϵ -caprolactone) macro-initiators and formation of stable colloidal dispersions, *Macromol. Symp.* **1994**, *88*, 227-244.
132. US Patent 4,716,203, (1987). invs.: Casey, D. J.; Jarrett, P. K.; Rosati, L.
133. Kim, S. Y.; Shin, I. G.; Lee, Y. M. Amphiphilic diblock copolymeric nanospheres composed of methoxy poly(ethylene glycol) and glycolide: properties, cytotoxicity and drug release behaviour, *Biomaterials* **1999**, *20*, 1033-1042.
134. Amine, H.; Karima, O.; El Amine, B. M.; Meghabar, R.; Belbachir, M. Synthesis of biodegradable diblock copolymers of glycolide and poly(oxyethylene) using a montmorillonite clay as catalyst, *J. Polym. Res.* **2005**, *12*, 367-371.
135. Zhang, L.; Fu, J.; Xia, Z.; Wu, P.; Zhang, X. Synthesis and characterization of a well-defined amphiphilic block copolymer and its paclitaxel prodrug from methoxy poly(ethylene glycol) and oligomer of glycolic acid, *J. Appl. Polym. Sci.* **2011**, *122*, 758-766.
136. Ringsdorf, H. Structure and properties of pharmacologically active polymers, *J. Polym. Sci. Symp.* **1975**, *51*, 135-153.
137. Furch, M.; Eguiburu, J. L.; Fernandez-Berridi, San Roman, J. Synthesis and characterization of copolymers of methylacrylate and poly(glycolide) macromonomers, *Polymer* **1998**, *39*, 1977-1982.
138. Sawhney, A. S.; Pathak, C. P.; Hubbell, J. A. Bioerodible hydrogels based on photopolymerized poly(ethylene glycol)-co-poly(alpha-hydroxy acid) diacrylate macromers, *Macromolecules* **1993**, *26*, 581-587.
139. Peng, T.; Su, J.; Lin, G.; Cheng, S.-X.; Zhuo, R.-X. Synthesis and characterization of poly- α,β -[N-(2-hydroxyethyl)-L-aspartamide]-*g*-poly(glycolide) amphiphilic graft copolymers as potential drug carriers, *Colloid Polym. Sci.* **2006**, *284*, 834-842.
140. Cameron, D. J. A.; Shaver, M. P. Aliphatic polyester polymer stars: synthesis, properties and applications in biomedicine and nanotechnology, *Chem. Soc. Rev.* **2011**, *40*, 1761-1776.
141. Fetters, L. J.; Kiss, A. D.; Pearson, D. S. Rheological behavior of star-shaped polymers, *Macromolecules* **1993**, *26*, 647-654.
142. Xie, D.; Park, J.-G.; Zhao, J. Synthesis and evaluation of novel injectable and biodegradable polyglycolide-based composites, *J. Appl. Polym. Sci.* **2007**, *103*, 2977-2984.

143. Wolf, F. K.; Fischer, A. M.; Frey, H. Poly(glycolide) multi-arm stars: improved solubility via limited arm length, *Beilstein J. Org. Chem.* **2010**, *6*, No.67
144. Satoh, T. Unimolecular micelles based on hyperbranched polycarbohydrate cores, *Soft Matter* **2009**, *5*, 1972-1982.
145. Jones, M.-C.; Gao, H.; Leroux, J.-C. Reverse polymeric micelles for pharmaceutical applications, *J. Controlled Release* **2008**, *132*, 208-2015.
146. Irfan, M.; Seiler, M. Encapsulation using hyperbranched polymers: from research and technologies to emerging applications, *Ind. Eng. Chem. Res.* **2010**, *49*, 1169-1196.
147. (a) Voit, B. I.; Lederer, A. Hyperbranched and highly branched polymer architectures – synthetic strategies and major characterization aspects, *Chem. Rev.* **2009**, *109*, 5924-5973; (b) Gao, C.; Yan, D. Hyperbranched polymers: from synthesis to applications, *Prog. Polym. Sci.* **2004**, *29*, 183-275; (c) Jikei, M.; Kakimoto, M. Hyperbranched polymers: a promising new class of materials, *Prog. Polym. Sci.* **2001**, *26*, 1233-1285.
148. Fischer, A. M.; Frey, H. Multi-arm polylactide stars with hyperbranched poly(glycolide) core, *Polymer Preprints (American Chemical Society, Division of Polymer Chemistry)* **2011**, *52* (1).
149. Lee, K.-H.; Chu, C.C.; Quimby, F.; Klaessig, S. Molecular design of biologically active biodegradable polymers for biomedical applications, *Macromol. Symp.* **1998**, *130*, 71-80.
150. Albertsson, A.-C.; Varma, I. K. Recent Developments in ring-opening polymerization of lactones for biomedical applications, *Biomacromolecules* **2003**, *4*, 1466-1486.
151. Herrmann, J. B.; Kelly, R. J.; Higgins, G. A. Polyglycolic acid sutures: Laboratory and clinical evaluation of a new absorbable suture material, *Arch. Surg.* **1970**, *100*, 485-490.
152. <http://www.omega-medical.de/Nahtmaterial/resorbierbar/Surgicryl-PGA-Polyglykolsaeure/> (accessed 20.05.2012)
153. Ashammakhi, N.; Rokkanen P. Absorbable polyglycolide devices in trauma and bone surgery, *Biomaterials* **1997**, *18*, 3-9.
154. Ulery, B. D.; Nair, L. S.; Laurencin, C. T. Biomedical applications of biodegradable polymers, *J. Polym. Sci. Part B: Polym. Phys.* **2011**, *49*, 832–864.
155. Kehoe, S.; Zhang, X. F.; Boyd, D. FDA approved guidance conduits and wraps for peripheral nerve injury: A review of materials and efficacy, *Injury, Int. J. Care Injured* **2012**, *43*, 553-572.
156. Siclari, A.; Mascaro, G.; Gentili, C., Cancedda, R., Boux, E. A Cell-free scaffold-based cartilage repair provides improved function hyaline-like repair at one year, *Clin. Orthop. Relat. Res.* **2012**, *470*, 910-919.
157. Ceonzo, K.; Gaynor, A.; Shaffer, L.; Kojima, K.; Vacanti, C. A.; Stahl, G. L. Polyglycolic acid induced inflammation, *Tissue Eng.* **2006**, *12*, 301-308.

158. Athanasiou, K. A.; Schmitz, J. B.; Agrawal, C. M. The effects of porosity on degradation of PLA-PGA implants, *Tissue Eng.* **1998**, *4*, 53-63.
159. Linhart, W.; Peters, F.; Lehmann, W.; Schwarz, K.; Schilling, A. F.; Amling, M.; Rueger, J. M.; Epple, M. Biologically and chemically optimized composites of carbonated apatite and polyglycolide as bone substitution materials, *J. Biomed. Mater. Res.* **2001**, *54*, 162-171.
160. Ma, P. X. Scaffolds for tissue fabrication, *Mater. Today* **2004**, *7*, 30-40.
161. Kim, B.-S.; Putnam, A. J.; Kulik, T. J.; Mooney, D. J. Optimizing seeding and culture methods to engineer smooth muscle tissue on biodegradable polymer matrices, *Biotechnol. Bioeng.* **1998**, *57*, 46-54.
162. Wei, X.; Zhang, P.H.; Wang, W. Z.; an, Z. Q.; Cao, D. J.; Xu, F.; Cui, L.; Liu, W.; Cao, Y. L. Use of polyglycolic acid unwoven and woven fibers for tendon engineering in vitro, *Key Engineering Materials* **2005**, *288-289*, 7-10.
163. Talja, M.; Välimaa, T.; Tammela, T.; Petas, A.; Törmälä, P. Bioabsorbable and biodegradable stents in urology, *J. Endourology* **1997**, *11*, 391-398.
164. Gupta, A.; Dixit, A.; Sales, K. M.; Sales, K. M.; Winslet, M. C.; Seifalian, A. M. Tissue engineering of small intestine-current status, *Biomacromolecules* **2006**, *7*, 2701-2709.
165. Shen, G.; Tsung, H. C.; Wu, C. F.; Liu, X. Y.; Wang, X.; Liu, W.; Cui, L.; Cao, Y. L. Tissue engineering of blood vessels with endothelial cells differentiated from mouse embryonic stem cells, *Cell Research* **2003**, *13*, 335-341.
166. Hollinger, J. O.; Leon, K. Poly(α -hydroxy acids); carriers for bone morphogenetic proteins, *Biomaterials* **1996**, *17*, 187-194.
167. Dahl, S. L.M.; Kypson, A. P.; Lawson, J. H.; Blum, J. L.; Strader, J. T.; Li, Y.; Manson, R. J.; Tente, W. E.; DiBernardo, L.; Hensley, M. T.; Carter, R.; Williams, T. P.; Prichard, H. L.; Dey, M. S.; Begelman, K. G.; Niklason, L. E. Readily available tissue-engineered vascular grafts, *Sci. Transl. Med.* **2011**, *3*, 68ra9.
168. Nagato, H.; Umabayashi, Y.; Wako, M.; Tabata, Y.; Manabe, M. Collagen-polyglycolic acid hybrid matrix with basic fibroblast growth factor accelerated angiogenesis and granulation tissue formation in diabetic mice, *Journal of Dermatology* **2006**, *33*, 670-675.
169. Eiselt, P.; Kim, B.-S.; Chacko, B.; Isenberg, B.; Peters, M. C.; Greene, K. G.; Roland, W. D.; Loeb sack, A. B.; Burg, K. J. L.; Culberson, C.; Halberstadt, C. R.; Holder, W. D.; Mooney, D. J. Development of technologies aiding large-tissue engineering, *Biotechnol. Prog.* **1998**, *14*, 134-140.
170. Agarwal, C. M.; Ray, R. B. Biodegradable polymeric scaffolds for musculoskeletal tissue engineering, *J. Biomed. Mater. Res.* **2001**, *55*, 141-150.

171. Nair, L. S.; Laurencin, C. T. Biodegradable polymers as biomaterials, *Prog. Polym. Sci.* **2007**, *32*, 762-798.
172. Uhrich, K. E.; Cannizzaro, S. M.; Langer, R. S.; Shakesheff, K. M. Polymeric systems for controlled drug release, *Chem. Rev.* **1999**, *99*, 3181-3198.
173. Sato, T.; Kanke M.; Schroeder, H. G.; DeLuca, P.P. Porous biodegradable microspheres for controlled drug delivery. I. Assessment of processing conditions and solvent removal techniques, *Pharm. Res.* **1988**, *5*, 21-30.
174. Redmon, M. P.; Hickey, A. J.; DeLuca, P. P. Prednisolone-21-acetate poly(glycolic acid) microspheres: influence of matrix characteristics on release, *J. Controlled Release* **1989**, *9*, 99-109.
175. Hazrati, A. M.; Akrawi, S.; Hickey, A. J.; Wedlund, P.; Macdonald, J.; DeLuca, P. P. Tissue distribution of indium-111 labeled poly(glycolic acid) matrices following jugular and hepatic portal vein administration, *J. Controlled Release* **1989**, *9*, 205-214.
176. Braunecker, J.; Baba, M.; Milroy, G. E.; Cameron, R. E. The effects of molecular weight and porosity on the degradation and drug release from polyglycolide, *Int. J. Pharm.* **2004**, *282*, 19-34.
177. (a) Hurrell, S.; Milroy, G. E.; Cameron, R. E. The degradation of polyglycolide in water and in deuterium oxide. Part 1: The effect of reaction rate, *Polymer* **2003**, *44*, 1421-1424; (b) Milroy, G. E.; Smith, R. W.; Holland, R.; Clough, A. S.; Mantle, M. D.; Gladden, L. F.; Huatan, H.; Cameron, R. E. The degradation of polyglycolide in water and deuterium oxide. Part II: Nuclear reaction analysis and magnetic resonance imaging of water distribution, *Polymer* **2003**, *44*, 1425-1435; (c) Hurrell, S.; Cameron, R. E. Polyglycolide degradation and drug release. Part I: Changes in morphology during degradation, *J. Mater. Sci.: Mater. Med.* **2001**, *12*, 811-816.
178. Shawe, S.; Buchanan, F.; Harkin-Jones, E.; Farrar, D. A study on the rate of degradation of the bioabsorbable polymer polyglycolic acid (PGA), *J. Mater. Sci.* **2006**, *41*, 4832-4838.
179. Chu, C. C. An in vitro study of the effect of buffer on the degradation of poly(glycolic acid) sutures, *J. Biomed. Mater. Res.* **1981**, *15*, 19-27.
180. Ginde, R. M.; Gupta, R. K. In vitro chemical degradation of poly(glycolic acid) pellets and fibers, *J. Appl. Polym. Sci.* **1987**, *33*, 2411-2429.
181. Chu, C. C. The in-vitro degradation of poly(glycolic acid) sutures-effect of pH, *J. Biomed. Mater. Res.* **1981**, *15*, 795-804.

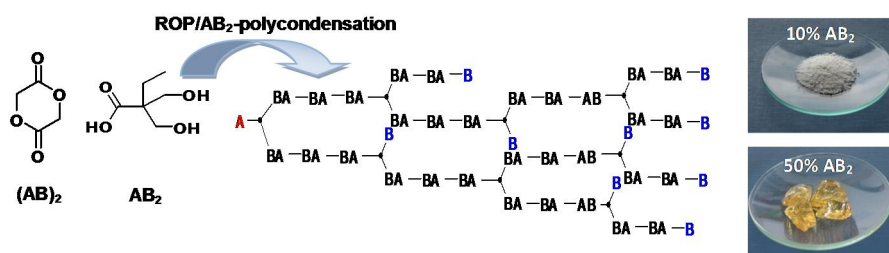
182. Holland, S. J.; Tighe, B. J.; Gould, P. L. Polymers for biodegradable medical devices. 1. The potential of polyesters as controlled macromolecular release systems, *J. Controlled Release* **1986**, *4*, 155-180.
183. Browning, A.; Chu, C. C. The study of thermal and gross morphologic properties of polyglycolic acid upon annealing and degradation treatments, *J. Biomed. Mater. Res.* **1986**, *20*, 613-632.
184. Huff, K. R.; Casey, D. J. Effect of carboxyl end groups on hydrolysis of polyglycolic acid, *J. Polym. Sci.: Polym. Chem. Ed.* **1985**, *23*, 1939-1954.
185. Chu, C. C. The effect of gamma-irradiation on the enzymatic degradation of polyglycolic acid absorbable sutures, *J. Biomed. Mater. Res.* **1983**, *17*, 1029-1040.
186. Milroy, G. E.; Cameron, R. E.; Mantle, M. D.; Gladden, L. F.; Huatan, H. The distribution of water in degrading polyglycolide. Part II: magnetic resonance imaging and drug release, *J. Mater. Sci.: Mater. Med.* **2003**, *14*, 465-473.
187. King, E.; Cameron, R. E. Effect of hydrolytic degradation on the microstructure of poly(glycolic acid): An X-ray scattering and ultraviolet spectrophotometry study of wet samples ultraviolet, *J. Appl. Polym. Sci.* **1997**, *66*, 1681-1690.
188. Montes de Oca, H.; Farrar, D. F.; Ward, I. M. Degradation studies on highly oriented poly(glycolic acid) fibres with different lamellar structures, *Acta Biomaterialia* **2011**, *7*, 1535-1541.
189. Miller, N. D.; Williams, D. F. The in vivo and in vitro degradation of PGA suture material as a function of applied strain, *Biomaterials* **1984**, *5*, 365-368.
190. Hutmacher, D.; Hürzeler, M. B.; Schliephake, H. A review of material properties of biodegradable and bioresorbable polymers and devices for GTR and GBR applications, *Int. J. Oral Maxillofac. Implants* **1996**, *11*, 667-678.

Chapter 2: Branched and Star Copolymers Based on Poly(glycolide)

2.1 Soluble Hyperbranched Poly(glycolide) Copolymers

Anna M. Fischer and Holger Frey

Published in *Macromolecules* **2010**, 43, 8539-8548.



Keywords: poly(glycolide), hyperbranched polyesters, polycondensation

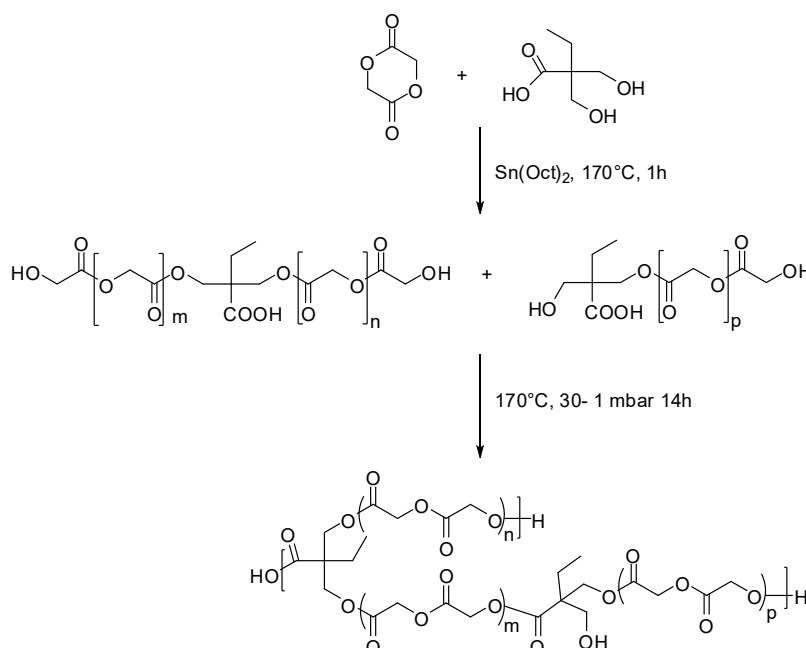
Abstract

A series of (hyper)branched poly(glycolide) copolymers has been prepared by copolymerization of glycolide (GA) with 2,2-bis(hydroxymethyl)butyric acid (BHB) via combined ROP/AB₂-polycondensation. Polymerization was conducted in bulk and catalyzed by stannous-2-ethyl hexanoate (Sn(Oct)₂). The branched topology of the resulting polyesters was studied in detail by 1D- and 2D-NMR spectroscopy and confirmed by the synthesis and characterization of model compounds. The AB₂ monomer BHB was incorporated either as a dendritic or focal unit, but hardly in linear or terminal mode. As expected for multifunctional polycondensation, SEC measurements showed polydisperse products with polydispersity index in the range of 1.88 to 3.40. M_n of the copolymers varied from 1100 to 4000 g/mol. MALDI-TOF MS analysis allowed to verify the main polymeric species. Furthermore, MALDI-TOF evidenced incorporation of several BHB units per macromolecule, confirming a successful condensation reaction and the formation of branched copolymers. Detailed ¹H NMR characterization (1D and 2D methods) permitted calculation of the molar composition, the conversion and the degree of branching (DB), which ranged between 0.12 and 0.44. Differential scanning calorimetry (DSC) measurements showed that in contrast to linear PGA (T_m>220 °C) the melting behavior and the glass-transition temperature of the branched poly(glycolide) copolymers changed drastically. The presence of dendritic units in the polymer backbone resulted in a depression of the melting point and amorphous materials at amounts of BHB exceeding 15%. The amorphous hyperbranched poly(glycolide) copolymers show enhanced solubility in common solvents (e.g., acetone, ethyl acetate, THF) and improved processability in contrast to linear PGA and possess potential for use in slow or controlled drug release systems.

Introduction

Poly(glycolic acid) (PGA) is the most simple aliphatic polyester among the family of the poly(α -hydroxy acid)s. The hydrolysis product glycolic acid is metabolized in the body into pyruvic acid, where it enters the tricarboxylic acid cycle.¹ Homo- and copolymers of PGA are well-known as commercial biodegradable materials (Dexon, Vicryl) for medical applications.^{2,3} These polymers are of considerable interest in view of their biocompatibility and biodegradability.⁴ Comonomers have been introduced to improve both processability and hydrolytic instability of the PGA homopolymer, which is notorious for its high degree of crystallization associated with insolubility in all common organic solvents.⁵ A variety of polymer architectures making use of glycolic acid has been designed, usually with poly(lactic acid) (PLA) and poly(ϵ -caprolactone) (PCL) as main building unit of the polymer backbone.⁶ The introduction of branched units is a well-known strategy to tailor the properties of polymers.^{7,8} In the past decade numerous efforts have been made to improve the preparation of hyperbranched polymers by a variety of synthetic strategies.⁹ However, to date Boltorn®, based on the polycondensation of bis(hydroxymethyl) propionic acid (bis-MPA), is the only commercially available hyperbranched aliphatic polyester synthesized in a one-pot procedure by polycondensation.¹⁰ Several alternative strategies have been devised to prepare branched polyesters in addition to the classical AB_m -polycondensation of carboxylic acids with two or more hydroxyl groups.¹¹ For instance, lactones were functionalized with hydroxyl groups initiating the ring-opening polymerization and at the same time serving as branching units.¹²⁻¹⁵ The polymerization of these initiating monomers, so-called cyclic “inimers” was designated “self condensing cyclic ester polymerization” by Trollsås et al.¹⁶ in analogy to the self-condensing vinyl polymerization pioneered by Fréchet et al.¹⁷ in 1995. Our group presented enzymatic and metal-catalyzed copolymerizations of AB with AB_2 monomers by combination of ring-opening polymerization (ROP) and branching polycondensation steps in the past.^{18,19} Bishydroxy carboxylic acids are employed as AB_2 monomers in combination with lactones as cyclic AB comonomers to generate a hyperbranched structure. This approach was suitable for the preparation of branched poly(ϵ -caprolactone),¹⁸ but it leads to predominantly linear structures for the AB comonomer lactide, although we had initially reported on the synthesis of hyperbranched poly(L-lactide).²⁰ A detailed NMR study by Cooper and Storey showed that the utilized bishydroxy acid mainly acts as an initiator in ROP under the reaction conditions employed.²¹ Esterification of the carboxylic acid with the secondary hydroxyl termini and the formation of dendritic units hardly occurred, and consequently linear PLLA with a single carboxylic acid function was formed. On the basis of current results the failure of the preceding synthesis can be attributed to the considerable difference of the reactivity between primary and secondary hydroxyl termini observed also in conjunction with kinetic measurements with respect to the ring-opening multibranching polymerization (ROMBP) of 5-hydroxymethyl-1,4-dioxane-2-one (5HDON)

with L-lactide.¹² Knauss et al. reported on long-chain branched PLA by initiating Sn(Oct)₂-catalyzed lactide ROP with glycidol. The PLA segments are separated by glycerol branching points.²² In a very recent paper our group presented multi-arm star block copolymers with a hyperbranched polyether core and PGA arms up to an average arm length of 12 glycolic acid units.²³ Since PGA exhibits more difficult processing characteristics than PLA,²⁴⁻²⁶ a branched topology that would ameliorate processing should enhance the range of biomedical applications. However, hyperbranched PGA has not been reported in literature to date. This prompted us to investigate synthetic pathways for the introduction of branching points into the PGA structure, aiming at optimizing the processability of PGA by reducing the degree of crystallization. In the current work we present a solvent-free synthesis of highly branched poly(glycolide) copolymers by combining ROP with AB₂-polycondensation, systematically varying the molar fraction of the AB₂-branching units. In contrast to lactic acid, glycolic acid bears a primary hydroxyl group leading to more rapid esterification of the carboxylic acid group of the 2,2-bis(hydroxymethyl)butyric acid (BHB) employed as an AB₂ building unit (Scheme 1). Using a combination of characterization techniques including detailed one and two-dimensional NMR studies, we demonstrate the successful synthesis of (hyper)branched PGA copolymers with different degree of branching (DB).



Scheme 1. Copolymerization of glycolide with 2,2-bis(hydroxymethyl)butyric acid (BHB) via combined ROP/AB₂-polycondensation.

Results and Discussion

A. Copolymerization, NMR Characterization, and Branching Mechanism.

The ring-opening polymerization of lactide or glycolide catalyzed by Sn(Oct)₂ or strong nucleophilic organobases in the presence of a co-initiator (amines, hydroxyl groups) is well-known.²⁷ In the current paper we use the Sn(Oct)₂-catalyzed ROP/AB₂-polycondensation to synthesize (hyper)branched poly(glycolide) copolymers, avoiding the use of solvents. 2,2-Bis(hydroxymethyl)butyric acid (BHB) is employed as branching AB₂ comonomer unit. The AB₂ monomer has to fulfill several requirements to be applicable in this copolymerization with the objective to achieve a high degree of branching: (1) good solubility in the glycolide melt, which requires sufficiently low melting points of both comonomers and (2) comparable reactivities of the hydroxyl groups. Different reactivity of both monomers leads to undesired homopolymerization, which would be revealed by MALDI-TOF mass spectrometry.

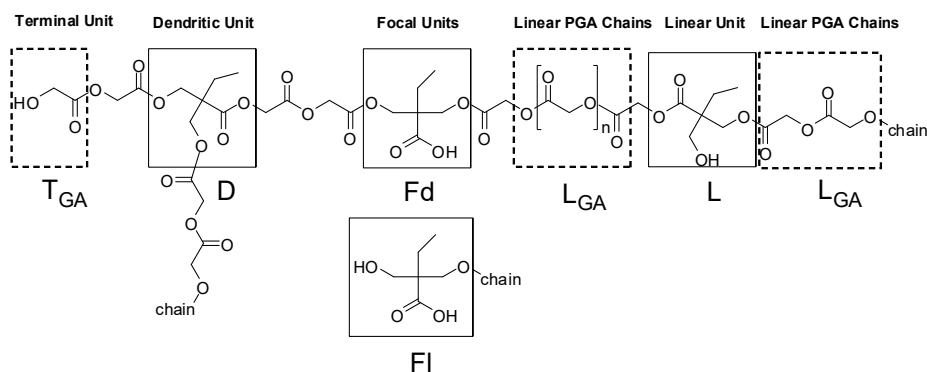
The AB₂ monomer, BHB, contributes to polymer growth in two different ways. It can initiate the polymerization reaction via its hydroxyl groups, and the single carboxylic acid group in the oligomeric backbone can subsequently participate in polycondensation with the hydroxy-functional chain end of another monomer or oligomer. In the ideal case, this synthetic strategy allows the preparation of copolymers with different length of linear poly(glycolide) chain segments between every branching unit in a one-pot synthesis. The copolymer samples prepared will be designated according to the following expressions in the ensuing text: PGAB xx = poly((glycolide)-co-(BHB)) with an amount of xx mol% glycolide (and thus 100 - xx mol% BHB).

In the first series of polymerization experiments, the reaction conditions were evaluated with respect to solvent, temperature, and polymerization time. The polymerization reaction in dimethyl sulfoxide and diphenyl ether at 120 °C stopped after a short time because of polymer precipitation.

In addition, the solution polymerization at higher temperatures resulted in discolored products with a broad molecular weight distribution. On the basis of these results, the bulk copolymerization with glycolide has been pursued. This reaction had to be conducted at elevated temperatures, since even PGA oligomers rapidly phase-separated from the melt at temperatures below 150 °C. Prior to discussing variations in the comonomer composition, we will focus on copolymers from a constant comonomer feed ratio of 50 mol % glycolide and 50 mol % BHB in the following paragraph to detail the general structural elucidation.

Structural Characterization. The complexity of ¹H NMR and ¹³C NMR spectra of the copolymers required detailed 2D-NMR characterization, particularly to confirm the branched structure formed by full reaction of BHB. Thus, model compounds were prepared to distinguish the different modes of BHB incorporation in the copolymer. The NMR experiments were performed in DMSO-d₆, because

the latter provides a broad range of spectral information and was already applied in the structural investigation of poly- and oligoglycolides.²⁸ The signal/structure assignment of the model compounds and the transfer of this information to the present copolymer structure is the first and crucial step in the molecular characterization. Scheme 2 shows the theoretical polyester structure with its possible repeating units.



Scheme 2. Structure of the branched copolymers formed via combined ROP/AB₂-polycondensation, showing the predominant units.

Distinct ¹³C NMR shifts of model compounds present an important foundation for a precise signal to structure assignment. ¹H,¹³C-COSY experiments such as heteronuclear single quantum coherence (HSQC) and hetero multiple bond coherence (HMBC) provide additional information, which is vital for the structural elucidation of the copolyester system formed. Monomer consumption and the formation of dendritic units have also been monitored by detailed kinetic studies.

Model Compounds. Depending on the substitution pattern, five different modes of incorporation of BHB units can be present in the polymer structure. Because of pronounced signal overlap, ¹H NMR spectra do not provide sufficient resolution to distinguish the incorporated units. This problem was approached by focusing on the more specific chemical ¹³C NMR shifts of the BHBs' quaternary carbon and carbonyl atoms. BHB derivatives of focal linear (F_l), focal dendritic (F_d), dendritic (D), linear (L), and terminal (T) units were emulated as esters via selective acetylation, as shown by Kuhlshresta et al.²⁹ Figure 1 displays the ¹³C NMR spectra of the model compounds together with the chemical shifts caused by the quaternary carbons. It is obvious that the chemical environment has a strong influence on the NMR signals. The unambiguous identification of dendritic units (49.64 ppm) is of particular interest to confirm the branched nature of the copolyester.

Generally, some interesting trends can be observed (see Figure 1): (i) by comparing the mono- and diacetylated BHB, we observe an upfield shift of nearly 2 ppm per acyl substituent, (ii) esterification

of the carboxylic acid group causes a downfield shift of nearly 0.5 ppm. Furthermore, the additional signal at ~52 ppm can be assigned to the $-\text{OCH}_3$ group of the methyl ester. The set of copolymer-related ^{13}C NMR signals in the sample PGAB 51 matches those derived for some of the model compounds (see Figure 3). The chemical shifts are 49.28 and 51.18 ppm for the focal dendritic and linear units, 51.66 and 49.75 ppm for the linear and dendritic units, respectively. On the basis of these signals, branching due to esterification of BHB carboxyl groups is confirmed. The carbonyl carbons are also well distinguishable. The esterified carboxyl group present in the dendritic BHB structure shows a chemical shift of 172.25 ppm, in clear contrast to the free carboxylic acid at 174.75 ppm (detailed NMR data are given in the Supporting Information).

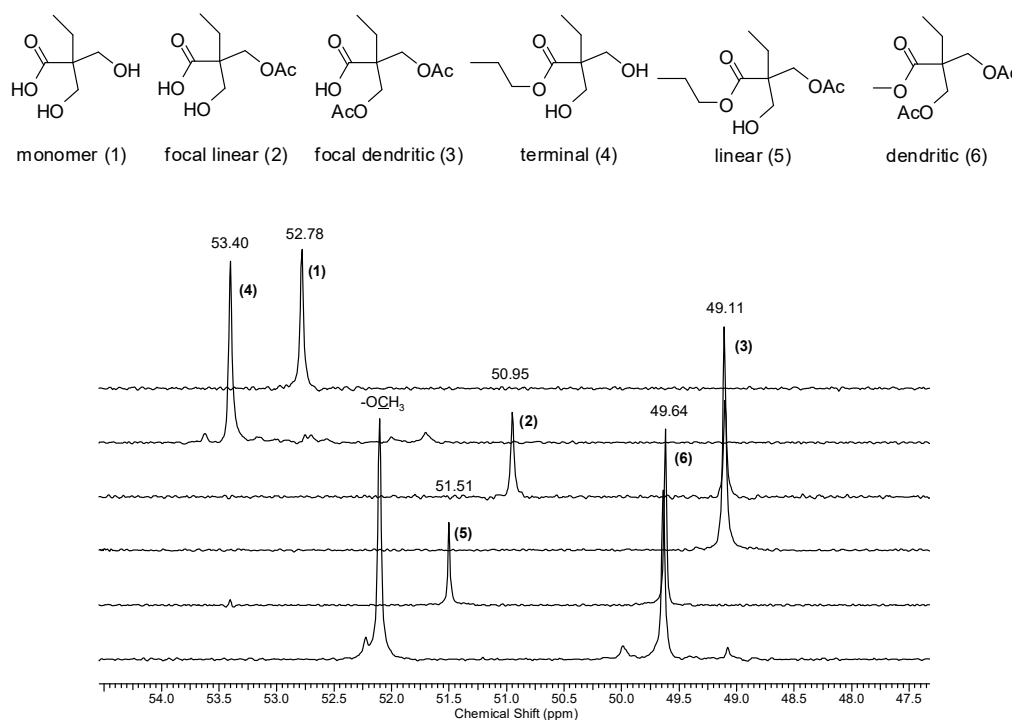


Figure 1. Expanded region of ^{13}C NMR (75 MHz) spectra measured in $\text{DMSO}-d_6$, showing the signals related to the quaternary carbons of the model compounds (1- 6) prepared.

2D-NMR Spectroscopy. Although one-dimensional NMR spectra permit to confirm the branched structure of the copolymers, detailed signal assignment of the ^{13}C NMR spectrum is not possible on the basis of model compounds. Therefore, we used ^1H , ^{13}C correlation spectroscopy (HSQC) to transfer the information obtained by ^1H NMR to ^{13}C NMR spectra (cf. Figure 2). One can immediately identify the signals of the OH-groups (5.50 ppm; 5.35 ppm), because there is no correlation to any carbon present. Likewise, the region of the quaternary carbons (~50 ppm) can be clearly assigned. Unfortunately, there is a superposition in the area of the methylene groups regarding the signals of both monomers ($\text{CH}_2\text{OR}_{\text{GA}}$; $\text{CH}_2\text{OH}_{\text{BHB}}$). This NMR method permits furthermore the visualization of unpreventable side reactions, such as etherification. In this case the free methylene protons

(CH₂OH_{BHB}) suffer from signal superposition together with etherified methylene protons. To verify branching within the polymer structure we also employed ¹H,¹³C correlation spectroscopy (HMBC), permitting visualization of correlations across three or four bonds. By this method we obtained a cross peak (A'/f), which gives evidence of the esterified carboxyl group of BHB with glycolide (further NMR data can be found in the Supporting Information). Table 1 summarizes the results of the detailed structural evaluation of the different structural units for both comonomers.

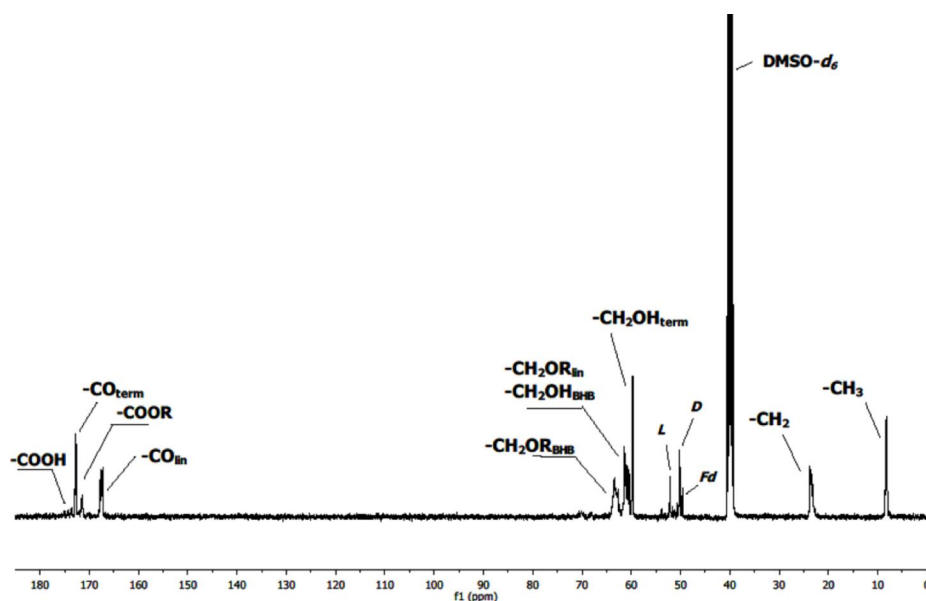


Figure 2. ¹³C NMR spectrum (DMSO-*d*₆; 75 MHz) of PGAB51.

Table 1. Summary of NMR data for model compounds (Figure 1) and the structural repeat units (spectra recorded in DMSO-*d*₆).

Units	BHB	BHB, model compounds	Poly(glycolide)	
	$\delta^{13}\text{C}$ (ppm)	$\delta^{13}\text{C}$ (ppm)	$\delta^1\text{H}$ (ppm) (400 MHz)	$\delta^{13}\text{C}$ (ppm) (75 MHz)
linear (L)	51.66	51.51	4.72-4.90 (CH ₂)	60.33-63.02 (CH ₂) 166.89-167.32 (CO)
terminal (T)	—	53.40	4.00, 4.11 (CH ₂)	59.32; 59.43 (CH ₂) 172.16-173.16 (CO)
dendritic (D)	49.75	49.64	—	—
focal lin (Fl)	51.18	50.95	—	—
focal dend. (Fd)	49.28	49.11	—	—

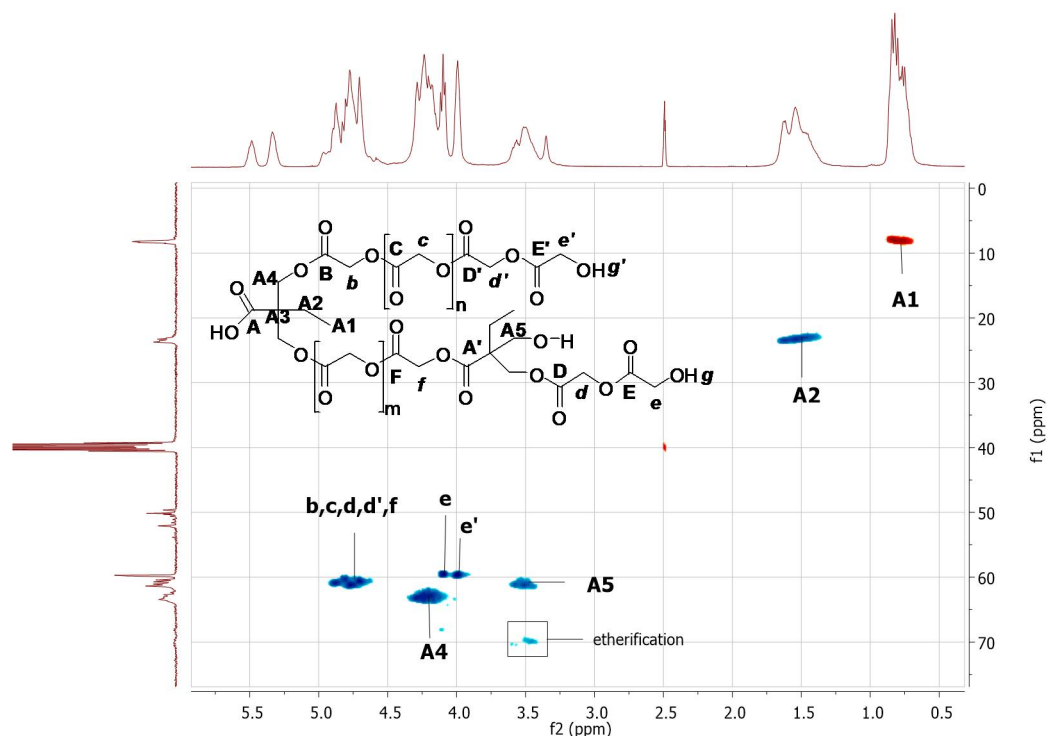
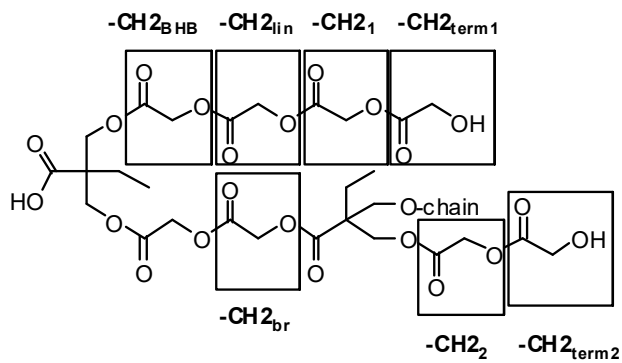


Figure 3. HSQC spectrum ($\text{DMSO-}d_6$) of PGAB 51 from $\text{Sn}(\text{Oct})_2$ -catalyzed ROP/AB₂-polycondensation of glycolide and BHB. Phase information is given by coloration of cross peaks (red= methyl; blue= methylene).

A detailed structural evaluation of the different methylene groups with regard to the glycolic acid units assigned by HMBC is presented in Scheme 3 (further NMR data can be found in the Supporting Information). Special attention was paid to the glycolic acid unit attached to the carboxylic acid group of BHB ($\text{CH}_{2_{br}}$), since it indicates successful esterification by polycondensation. The terminal glycolic acid units ($\text{CH}_{2_{\text{term}1}}/\text{term}2$) are well separated from the other glycolide backbone signal (4.91 ppm). The respective signals can be found at 4.11 and 4.00 ppm. These two signals are related to the glycolic units assigned as CH_{2_2} and CH_{2_1} . In this context one has to differentiate between CH_{2_2} , which represents the special case of an α -unit of a glycolic acid dimer directly attached to the BHB hydroxyl group and CH_{2_1} attached to the linear glycolide backbone. The CH_{2_2} signal is observed predominantly for poly(glycolide) copolymers with a low glycolide fraction. This detailed signal assignment was confirmed by an HMBC-NMR experiment with regard to the cross correlation of the methylene protons with the carbonyl carbons of both comonomers. The evaluation is consistent with previous literature data dealing with linear PGA-co-poly(ϵ -caprolactone),³⁰ as well as multi-arm PGA-PG star copolymers which have been prepared in our group.²³ The structure of the different glycolic acid units may be found in Scheme 3.

Glycolic acid unit	Chemical shift/ ppm
-CH ₂ _{in}	4.90
-CH ₂ _{br}	4.88
-CH ₂ ₁	4.83
-CH ₂ ₂	4.72
-CH ₂ _{BHB}	4.78
-CH ₂ _{term1}	4.11
-CH ₂ _{term2}	4.00



Scheme 3. Structure of the different incorporated glycolic acid units in the (hyper)branched copolymers and the corresponding signal assignment (300 MHz, DMSO-d₆).

Investigation of the Polymerization Process. To confirm the proposed polymerization process presented in Scheme 1, focusing especially on the formation of dendritic units (D), time-dependent NMR measurements have been carried out. This method permits one to follow the combined ROP/polycondensation reaction kinetically. Samples were collected from the polymerization melt and quenched thermally by rapid cooling to at least -20 °C prior to investigation via ¹³C NMR measurements in DMSO-d₆. The synthesis of branched poly(glycolide) copolymers commences with the Sn(Oct)₂-catalyzed ROP of glycolide initiated by 2, 2-bis-(hydroxymethyl)butyric acid (BHB). The first sample collected 1 h after the start of the polymerization reveals the presence of free BHB monomer in the reaction mixture, clearly demonstrated by the presence of the quaternary carbon at 52.78 ppm (see Figure 4). The obtained linear poly(glycolide)s bearing a single carboxylic acid group in the backbone represent two different structures: In this special case we observe the formation of focal linear (FI) as well as focal dendritic (Fd) BHB units. In contrast, when using L-lactide instead of glycolide the BHB hydroxyl groups are completely esterified; i.e., focal dendritic units are formed, as demonstrated by Feijen et al.³¹ The different behavior in the case of glycolide is attributed to the comparable initiation potential and reactivity of the primary hydroxymethylene groups present in BHB and the terminal glycolide units. In the case of lactide secondary hydroxyl groups are formed, which are less reactive. The ROP of glycolide allows in the ideal case the preparation of defined AB₂-macromonomers with adjustable molecular weights by variation of the monomer/initiator ratio. With high amounts of initiator low molecular weight macromonomers are produced that are associated finally with copolymers of a higher degree of branching (DB). The consecutive polycondensation of macromonomers with increased length of linear poly(glycolide) segments is limited because of the increased melting temperature resulting from the formation of linear poly(glycolide) chains. In the early stages of the polycondensation, we observe the incorporation of BHB both as linear (L) and dendritic (D) unit. In contrast, in the late stages of the polycondensation

the fraction of dendritic units increases and some unpreventable side reactions occur that are related to the elevated reaction temperature. For instance, the formation of ether bonds was revealed via ^{13}C NMR spectroscopy. This well-known phenomenon¹⁰ is attributed to the harsh reaction conditions (high temperature, low pressure and prolonged reaction times) and proven by the appearance of a set of signals at ~ 70 ppm (see Figure 2).^{32,33} In addition, the coupling of “focal” carboxylic acid groups leading to formation of anhydrides represents a plausible side reaction. This hypothesis was confirmed via NMR comparison of polymer structure and a model compound mimicking a BHB-based anhydride. The chemical shift for the anhydride is observed at 49.75 ppm for the model compound (see Supporting Information) and 49.89 ppm for the copolymer. The finding that BHB is not incorporated as a terminal unit underlines the proposed polymerization process as shown in Scheme 1.

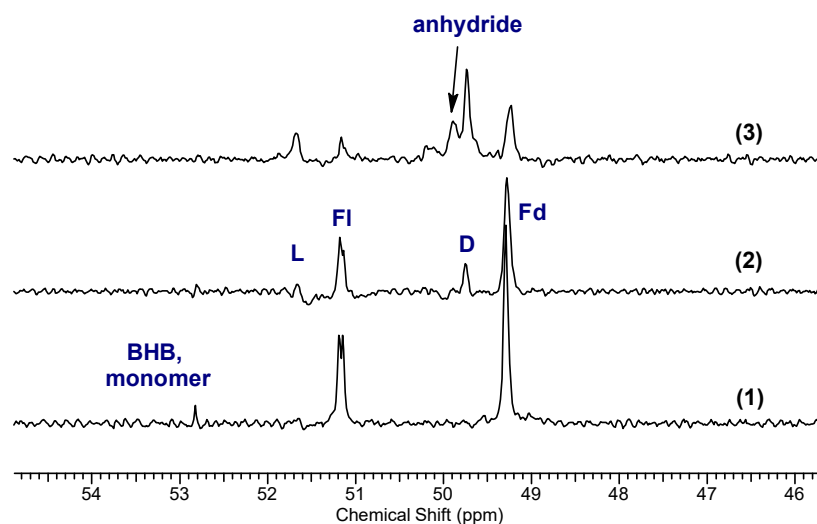


Figure 4. ^{13}C NMR spectra measured in $\text{DMSO-}d_6$ (75 MHz) which show the copolymerization process for the copolymer PGAB 60 at different reaction times: (1) after ROP, 1h at 170 °C; (2) in the early stages of polycondensation (1h, 170 °C, 25 mbar) and at the end of polycondensation (14h, 170 °C, 5 mbar).

Calculation of Different Parameters from ^1H NMR. In Figure 5, the ^1H NMR spectra of the copolymer prepared from a monomer feed ratio of glycolide to BHB of 55:45 is shown. After condensation the obtained comonomer ratio in the polymer shows 45 mol % incorporation of the AB_2 -monomer, as calculated from ^1H NMR spectroscopy. To determine the molar fraction of incorporated BHB by ^1H NMR we used the following eq 1:

$$\chi_{\text{BHB}} = \frac{(A/3)}{[(A/3) + (B-4/4)]} \quad (1)$$

In eq 1, A corresponds to the integral of the BHB CH_3 -proton signal and B represents the integral of free/esterified BHB and glycolide hydroxymethylene protons (cf. Figure 5). On the basis of CH_2OH and CH_2OR groups of BHB and glycolide (GA) we also calculated the fraction of linear and terminal glycolic acid units. In this context, superposition of signals in the region B of the ^1H NMR spectrum had to be taken into account.

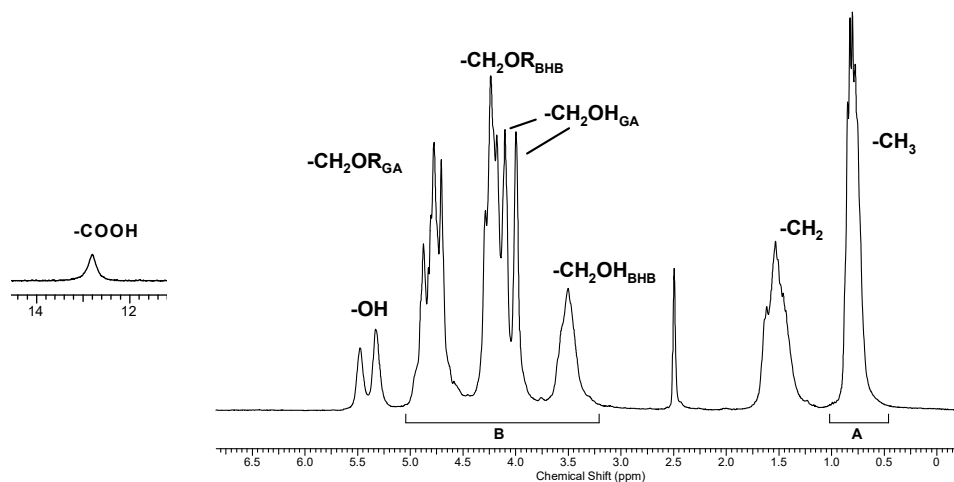


Figure 5. ^1H NMR spectrum (300 MHz, $\text{DMSO}-d_6$) of poly(glycolide) copolymer PGAB 55.

In the late 1990s, our group derived several general equations to calculate the degree of branching (DB) and the average number of branching points (ANB) for hyperbranched polymers, including the copolymerization of AB and AB_2 monomers.³⁴⁻³⁶ In the present case the degree of branching depends on the linear and dendritic units formed by the AB and the AB_2 comonomers. Glycolide is treated as an AB monomer, referring to its ring-opened form. The linear AB units have to be taken into account although they do not represent a potential branching point. The DB for AB/ AB_2 copolycondensation is described by eq. 2³⁴:

$$DB_{AB/AB_2} = \frac{2D}{2D + L_{CO}} \quad (2)$$

$$\text{with } L_{CO} = BHB_{L,Fd,Fl} + GA_{lin} \quad (3)$$

The values for the comonomer ratio were determined by ^1H NMR spectroscopy, whereas the amount of the different BHB units was calculated from inverse gated (IG) decoupled ^{13}C NMR spectroscopy. The ensuing calculation of the DB is based on the prerequisite that the reaction proceeds in a one-pot copolymerization. It should be emphasized that the employed DB-concept does not account for side reactions such as cyclization and etherification. In Table 3 the values for DB calculated according to eq 2 from the integrals of the corresponding ^1H NMR and IG ^{13}C NMR signals are presented. Figure 6 displays the correlation between the degree of branching (DB) and the molar fraction of BHB in the

copolymers. The DB clearly increases with increasing molar fraction of BHB under otherwise unchanged reaction conditions, confirming incorporation of BHB as a dendritic unit (see Figure 6).

Table 3. Characterization of poly(glycolide) copolymers.

sample	GA ^a :BHB ^b Feed ratio mol%	GA:BHB Calc. ^c feed ratio mol%	DB ^c	M _n ^d	M _w /M _n	T _g / T _m [°C]
PGAB 51	50:50	51:49	0.44	3980	1.88	23.7/ --
PGAB 67	67:33	67:33	0.29	1100	3.16	19.8/ --
PGAB 55	55:45	55:45	0.48	1480	2.63	20.0/ --
PGAB 71	70:30	71:29	0.35	1490	3.40	23.3/ --
PGAB 82	80:20	82:18	0.12	1110	2.64	25.9/ --
PGAB 90	90:10	n.d. ^e	n.d.	n.d.	n.d.	28.1/ 196.1

^a)GA = glycolide, ^b)BHB = 2,2-bis(hydroxymethyl)butyric acid, ^c)determined by ¹H NMR and Inverse Gated (IG) decoupled ¹³C NMR, ^d)determined by SEC (size exclusion chromatography), ^e)n.d.= not determined because of insolubility in common organic solvents (DMF; DMSO, etc.)

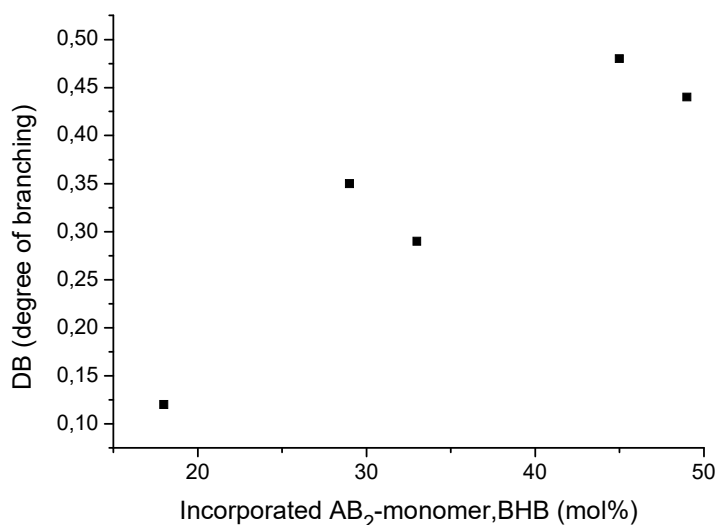


Figure 6. DB vs. the total molar fraction of BHB.

Variation of the Amount of BHB. Size Exclusion Chromatography (SEC). Figure 7 displays the GPC traces of a series of poly(glycolide) copolymers with different amount of BHB incorporated. The materials showed polydispersities in the range of 1.88 to 3.40, as expected for multifunctional polycondensation. The molecular weight M_n of the copolymers varied from 1100 to 4000 g/mol according to SEC.

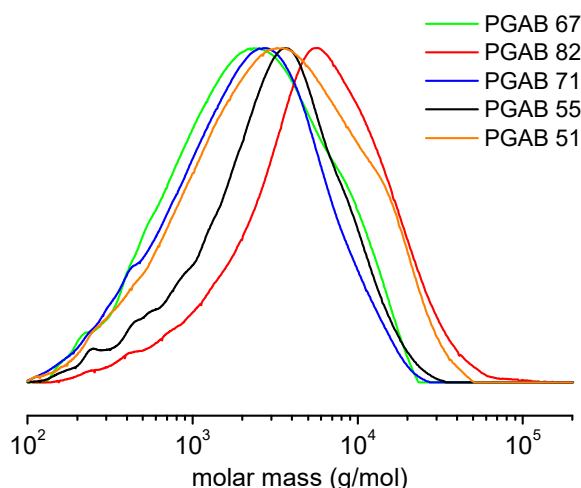


Figure 7. SEC traces (refractive index (RI) detection) of hyperbranched poly(glycolide) derived from the copolymerization of glycolide with different amounts of BHB.

MALDI-ToF Mass Spectrometry. MALDI-TOF MS is a useful method to obtain information on the incorporation of the comonomer and also the extent of cyclization. However, MALDI-TOF MS is known to be limited, when the polydispersity of a polymer exceeds 1.2 because of the well-known mass discrimination effect.³⁷ For this reason, we separated the polydisperse sample into more defined fractions by preparative SEC in DMF. In Figure 8, the MALDI-TOF spectrum of the fractionated sample PGAB 67 is shown. It is important to emphasize that the presence of multiple, distinct distributions, each with mass increment of 58 g/mol (i.e., one glycoyl repeat unit), suggests that the various distributions differ from one another with respect to the number of BHB monomer residues contained in their structure. The observed species are composed of the molar mass of the initiator (BHB; 148.16 g/mol) and the repeating units (glycolide, 116.07 g/mol), ionized as the respective potassium adducts. The distribution curve reveals polymer chains with an odd number of glycolic acid units caused by transesterification reactions, which cannot be avoided due to the harsh reaction conditions during the polymerization. The molar masses of the branched acyclic and cyclic species can be calculated according to the following equations:

$$M = (C_6H_9O_3)_x + (C_2H_2O_2)_n + H_{(x+2)}O + K^+ \quad (4)$$

$$M_{cycle} = M - 18 \text{ g/mol} \quad (5)$$

For the cycles, a mass shift of 18 g/mol is expected in comparison to their linear analogues. Samples with a high amount of BHB monomer in the monomer feed also show a higher amount of

AB₂ comonomer incorporation, evidenced by MALDI-TOF mass spectrometry. MALDI-TOF MS permits one to exclude the possibility of formation of a BHB homopolymer.

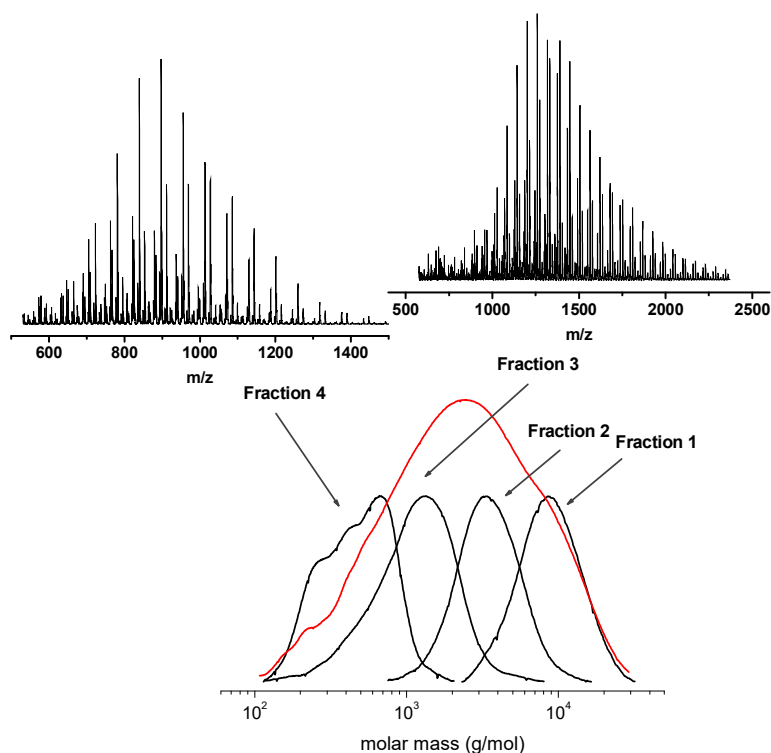


Figure 8. MALDI-ToF mass spectra of preparative SEC fractions 3 and 4 of PGAB 67 together with the corresponding SEC traces, illustrating incorporation of several BHB units.

Thermal Properties. Figure 9 shows DSC thermograms recorded from the second heating scan for the series of copolymers analyzed at a heating rate of 20 °C/min. DSC measurements were conducted to study the impact of the branched topology on the crystallization behavior and the effect of composition on the glass transition (T_g). All samples with a BHB amount exceeding 10 mol % reveal a glass transition in the range 20-26 °C. Only the sample with the lowest amount of BHB (10%) showed a distinct exothermic melting peak. In this case, the ROP stopped after several seconds, and we obtained a white, insoluble product, that was found to be a linear, insoluble macromonomer with a T_m of 196.1 °C. Further polycondensation of this macromonomer was not possible due to its insolubility. Clearly, for higher amounts of BHB the resulting short average linear chain length between the branching points and therefore the significantly higher degree of branching suppress crystallization of the polymer. The influence of DB and the number of end groups on the thermal properties of AB/AB₂ copolymers has been previously studied in literature for other systems, such as hyperbranched polyethers and polyesters.³⁸ Generally, the branched copolymers reveal a decrease of T_g and T_m with increasing degree of branching, as can be expected based on the destabilization and eventually disappearance of the crystalline domains. In our case, the glass transition temperatures of

the amorphous materials are shifted to lower temperatures compared to the linear homopolymer, the T_g for poly(glycolide) being 30- 50 °C.^{39,40} For the series of poly(glycolide) copolymers with varying BHB amount the DSC measurements do not show a linear correlation between the T_g and the copolymer composition. The glass transition of the hyperbranched BHB homopolymer has not been reported in literature to date. However, DSC measurements of a sample prepared in the context of the current study show a T_g of 24 °C for the homopolymer poly(BHB). Because of the fact that the homopolymers PGA and poly(BHB) exhibit similar T_g s, the copolymers show only slight variation in the glass transition temperatures in the range 20-26 °C (Table 3, vide supra). These copolymers are obtained as glassy, transparent, slightly yellow solids at room temperature that flow in the molten state to form a coating layer on metal, a variety of other polymers, and glass. Interestingly, the materials do not show the brittleness that is often associated with hyperbranched polymers. Detailed characterization of the unusual mechanical and rheological properties is in progress.

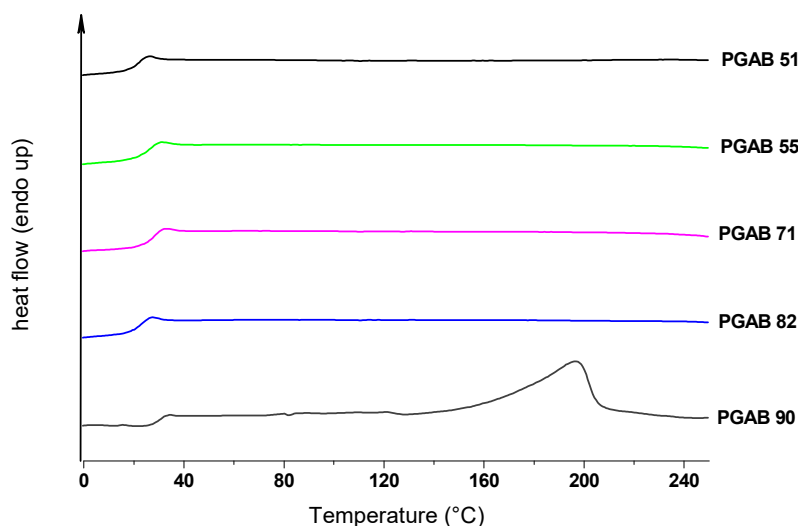


Figure 9. DSC heating traces of poly(glycolide) copolymers with varying BHB molar fraction: heating rate 20 K/min (second run after previous heating to 250 °C and cooling to -20 °C at \pm 20 K/min).

Experimental Section

Materials

Glycolide was purchased from Purac (Groningen, Netherlands) and Sigma-Aldrich, recrystallized twice from dry acetyl acetate and dried in vacuo at 40 °C. 2,2-Bis(hydroxymethyl)-butyric acid (BHB, 98%) was obtained from Sigma-Aldrich and used without further purification. Stannous 2-ethylhexanoate ($\text{Sn}(\text{Oct})_2$) was purchased from Acros Organics and used as received.

Instrumentation

Molecular weights were determined by size exclusion chromatography (SEC) using an instrument consisting of a Waters 717 plus autosampler, a TSP Spectra Series P 100 pump, a set of three PSS-SDV 5A columns with 10^2 , 10^3 and 10^4 Å porosity and a RI detector. DMF was used as the eluent (containing 1 g/L lithium bromide as an additive) at a flow rate of 1 mL/min. Poly(styrene) standards, provided by Polymer Standards Services (PSS, Mainz, Germany), were used for the internal calibration of the SEC system. Preparative SEC was performed with DMF as eluent on an instrument with a Knauer HPLC pump K-501, a refractometer from Shodex RI-71 and a column (300 x 20 mm, MZ-Gelplus, 10 µm) with 103 Å porosity.

All $^1\text{H}/^{13}\text{C}$ NMR spectra were obtained at 25 °C on a Bruker AMX300 spectrometer at 300 MHz or a Bruker Avance-2-400 (400 MHz) spectrometer. The spectra were measured in DMSO-d_6 and the chemical shifts were referred to the internal calibration on the solvents' residual peak. (^1H proton NMR signal: 2.50 ppm; ^{13}C carbon NMR signal: 39.52 ppm). Standard pulse sequences for HSQC and HMBC experiments were used. Deuterated DMSO-d_6 was purchased from Deutero GmbH, dried and stored over molecular sieves. Differential scanning calorimetry (DSC) analyses were obtained using a Perkin-Elmer 7 Series thermal analysis system with autosampler in the temperature range of -80 to 250 °C with heating rates of 1 K/min. The melting points for indium ($T_0 = 156.6$ °C) and Millipore water ($T_0 = 0$ °C) were used for calibration.

Matrix-assisted laser desorption and ionization time-of-flight (MALDI-TOF MS) measurements were performed on a Shimadzu Axima CFR MALDI-TOF mass spectrometer equipped with a nitrogen laser delivering 3 ns laser pulses at 337 nm. Dithranol (1,8,9-trihydroxyanthracene, Aldrich 97%) was used as a matrix, while potassium triflate (Aldrich, 98%) was added to increase ion formation. The samples were prepared from DMSO solutions.

General Procedure for the $\text{Sn}(\text{Oct})_2$ -catalyzed Copolymerization of Glycolide with BHB in Bulk. To a one-necked Schlenk flask equipped with a magnetic stirrer bar and a rubber septum glycolide and BHB were added in the quantities required. The flask was completely immersed in an oil bath preheated to 170 °C. The polymerization was initiated by the addition of 1 mol % $\text{Sn}(\text{Oct})_2$ dissolved in 0.1 mL of toluene. The mixture was stirred at 170 °C for 3 h under argon atmosphere. Then the pressure was reduced to 20 mbar within 3 h, during this time the temperature was maintained at

170 °C. The collected water was removed and the pressure reduced to 1 mbar. The reaction conditions were retained for 15 h. After completion and removal of the oil bath a glassy, slightly yellow solid was obtained.

Synthesis and Characterization of Model Compounds. Mixture of 2 and 3. In a 50 mL round-bottom flask was dissolved 1 g (6.75 mmol) of 2,2-bis(hydroxymethyl)butyric acid in 20 mL of dry dioxane. Then 0.75 g of triethylamine (7.43 mmol) was added. The solution was stirred and cooled to 0 °C. 0.47 g Acetyl chloride (6.08 mmol) were added dropwise. The white precipitate was filtered off and the solvent evaporated in vacuo. The residue was taken up in 20 mL of chloroform, washed twice with water and dried over magnesium sulfate (MgSO₄).

¹H NMR (300 MHz, DMSO-d₆): δ (ppm) 0.75-0.83 (m, -CH₃), 1.34-1.56 (m, CH₂), 1.99 (s, -OCOCH₃), 3.56 (s, -CH₂OH), 4.09 (s, -OCH₂), 4.12 (s, -OCH₂), 12.75 (br, -COOH). ¹³C NMR spectra were identical to that of the model compound **3** except for the following signals. ¹³C NMR (75 MHz, DMSO-d₆): δ (ppm) 8.14 (-CH₃), 20.67 (-OCOCH₃), 22.66 (-CH₂), 49.95 (-C_q), 62.49 (-OCH₂), 60.90 (-CH₂OH), 170.26 (-OCOCH₃), 174.75 (-COOH).

Model Compound 3. To 1 g (6.74 mmol) of 2,2-bis(hydroxymethyl) butyric acid were added 3.44 g (33.7 mmol) of dry distilled acetic anhydride and 7.4 mg (0.06 mmol) of DMAP. The reaction mixture was stirred for 24 h at 37 °C. Upon completion, the mixture was dissolved in water, the product extracted in chloroform, and the organic layer dried over MgSO₄. The solvent was evaporated in vacuo to give a colorless oil (yield: 1.41 g, 90%). ¹H NMR (300 MHz, DMSO-d₆): δ (ppm) 0.81 (t, 3H, -CH₃), 1.53 (q, 2H, -CH₂), 2.00 (s, 6H, -OCOCH₃), 4.12 (s, 4H, -OCH₂), 12.90 (br, 1H, -COOH). ¹³C NMR (75 MHz, DMSO-d₆): δ (ppm) 8.01 (-CH₃), 20.53 (-OCOCH₃), 23.20 (-CH₂), 49.11 (-C_q), 62.62 (-OCH₂), 170.05 (-OCOCH₃), 173.49 (-COOH).

Model Compound 4. To a 100 mL round-bottom flask were added 2 g (13.5 mmol) of 2,2-bis(hydroxymethyl)butyric acid, 5.31 g (43.2 mmol) of 1-bromopropane, 21 g (0.152 mol) of K₂CO₃, 0.71 g (2.67 mmol) of 18-crown-6, and 30 mL of acetone under argon atmosphere. The reaction mixture was heated to reflux for 36 h. After completion, the precipitate was filtered off, and the solvent was removed by rotary evaporation. The residue was taken up in chloroform, washed twice with water and dried over MgSO₄. After evaporation of the solvent in vacuo, the mixture was further purified via column chromatography (ethyl acetate: chloroform (1:2), R_f = 0.51 on silica gel) to obtain product **4** (yield: 0.51 g, 20%). ¹H NMR (300 MHz, chloroform-d₁): δ (ppm) 0.81 (t, 3H, -CH₃/BHB), 0.93 (t, 3H, -CH₂CH₃), 1.50 (q, 2H, -CH₂/BHB) 1.66 (sextet, 2H, -CH₂CH₃), 3.43 (br, 2H, -OH), 3.83 (d, 4H, -CH₂OH), 4.09 (t, 2H, -OCOCH₂). ¹³C NMR (75 MHz, DMSO-d₆): δ (ppm) 8.19 (-CH₃/BHB), 10.34 (-CH₂CH₃), 21.61 (-CH₂CH₃), 22.15 (-CH₂/BHB), 53.40 (-C_q), 60.26 (-CH₂OH), 64.90 (-COOCH₂CH₂CH₃), 174.14 (-COO(CH₂)₂CH₃).

Model Compound 5. To a solution of 128 mg (6.74 mmol) of model compound **4** in 1 mL of dry dioxane and 48 mg (33.7 mmol) of triethylamine was added 37 mg of acetyl chloride dropwise with cooling by an ice bath. The white precipitate was filtered off, the solvent removed in vacuo, and the residue dissolved again in chloroform. The organic layer was washed twice with water, dried over MgSO_4 and the product obtained by evaporation of the solvent. The solvent was evaporated in vacuo to give a colorless oil. A mixture of the linear **5** and the dendritic model compound **6.1** (see Supporting Information) was obtained (40:60). ^1H NMR (300 MHz, DMSO-d_6): δ (ppm) 0.79 (m, $-\text{CH}_3/\text{BHB}$), 0.88 (t, $-\text{CH}_2\text{CH}_3$), 1.51 (m, $-\text{CH}_2\text{CH}_3$), 1.99 (s, $-\text{OCOCH}_3$), 3.53 (m, $-\text{CH}_2\text{OH}$), 4.00 (t, $-\text{COOCH}_2\text{CH}_2\text{CH}_3$ [**6.1**]), 4.05 (t, $-\text{COOCH}_2\text{CH}_2\text{CH}_3$ [**5**]), 4.12 (s, $-\text{OCH}_2$ [**6.1**]), 4.16 (s, $-\text{OCH}_2$ [**5**]).

^{13}C NMR (300 MHz, DMSO-d_6) for linear model compound **5**: δ (ppm) 8.02 ($-\text{CH}_3/\text{BHB}$), 10.22 ($-\text{CH}_2\text{CH}_3$), 20.55 ($-\text{OCOCH}_3$), 21.54 ($-\text{CH}_2\text{CH}_3$), 22.73 ($-\text{CH}_2/\text{BHB}$), 51.50 ($-\text{C}_q$), 60.79 ($-\text{CH}_2\text{OH}$), 62.32 ($-\text{OCH}_2$), 65.43 ($-\text{COOCH}_2\text{CH}_2\text{CH}_3$), 170.12 ($-\text{OCOCH}_3$), 172.93 ($-\text{COOCH}_2\text{CH}_2\text{CH}_3$).

Model Compound 6. In a 50 mL round-bottom flask, 400 mg (1.72 mmol) of model compound **3** and 10 mL of thionyl chloride (SOCl_2) were kept under reflux for 3 h. After completion, the residual SOCl_2 was removed in vacuo and the obtained acid chloride was stored under argon atmosphere. To an ice bath cooled solution of 0.06 g methanol and 0.12 g of triethylamine in 5 mL of dry dioxane was added slowly a solution of 430 mg of acid chloride in 2 mL of dry dioxane. The white precipitate was filtered off, the solvent removed in vacuo, and the residue dissolved again in chloroform. The organic layer was washed twice with water, dried over MgSO_4 and the product obtained after evaporation of the solvent. (yield: 380 mg, 90%) ^1H NMR (300 MHz, chloroform- d_1): δ (ppm) 0.78 (t, 3H, $-\text{CH}_3$), 1.57 (q, 2H, CH_2), 2.00 (s, 6H, $-\text{OCOCH}_3$), 3.67 (s, 3H, $-\text{COOCH}_3$), 4.16 (s, 4H, $-\text{OCH}_2$). ^{13}C NMR (75 MHz, DMSO-d_6): δ (ppm) 7.96 ($-\text{CH}_3$), 20.46 ($-\text{OCOCH}_3$), 23.28 ($-\text{CH}_2$), 49.63 ($-\text{C}_q$), 52.11 ($-\text{COOCH}_3$), 62.42 ($-\text{OCH}_2$), 169.98 ($-\text{OCOCH}_3$), 172.25 ($-\text{COOCH}_3$).

Conclusion

We have demonstrated the preparation of glycolic acid based hyperbranched copolyesters that overcome the well-known solubility limitations of linear poly(glycolide). Hyperbranched poly(glycolide) copolymers based on 2,2-bis(hydroxymethyl)butyric acid (BHB) as AB_2 unit and glycolide have been realized in a one-pot synthesis, involving combined $\text{Sn}(\text{Oct})_2$ -catalyzed ring opening polymerization and melt polycondensation of the in situ produced linear AB_2 macromonomers in a solvent-free procedure under vacuum. $\text{Sn}(\text{Oct})_2$ catalysis afforded two different linear (pre)polymer structures with focal linear (Fl) and focal dendritic (Fd) BHB units, which have been investigated by ^{13}C NMR analysis. The primary nature of the hydroxyl chain-ends of glycolic acid and consequently of the termini of the growing hyperbranched structure is a key issue for the success of the synthetic strategy. In contrast to their linear analogues of comparable molecular

weight, the copolymers exhibit excellent solubility in common polar organic solvents, such as DMF, DMSO as well as acetone and THF. This made detailed 1D-/2D-NMR and SEC characterization possible. Furthermore, the preparation of model compounds corresponding to the different possible modes of incorporation of the AB₂ comonomer evidenced the formation of dendritic units. The hyperbranched poly(glycolide) copolymers prepared possess molecular weights M_n up to 4000 g/mol and high glycolide fraction up to approximately 85 mol%. The molecular weights are similar to previously reported aliphatic polyesters prepared by the classical AB₂ polycondensation route.¹⁰ Amorphous PGA structures were obtained when exceeding 10 mol % of BHB comonomer.

As expected, the short average linear PGA chain length between every branching point impedes crystallization for these materials.

The hyperbranched poly(glycolide) copolymers represent a new class of presumably biodegradable polyester polyols, whose large number of primary hydroxyl termini provides an excellent platform to introduce versatile other functionalities by further modification. Our current research interest focuses on the examination of the mechanical properties and the evaluation of applications in the fields of medicine and pharmacy.

Acknowledgment. A.F. thanks Dr. Florian Wolf for the introduction to the subject of hyperbranched polyesters, particularly with regard to poly(glycolide). Maria Müller is acknowledged for DSC measurements and Heinz Kolshorn for his continuing support with NMR characterization of the materials. We thank Ines Wollmer for her valuable synthetic support. H.F. acknowledges financial support from the Fonds der Chemischen Industrie as well as the German Science Foundation (DFG).

Supporting Information Available: Figures showing additional 2D NMR spectra, relevant information about side reactions, and chemical shifts of model compounds. This material is available free of charge via the Internet at <http://pubs.acs.org>

Supporting Information

I. Additional NMR Data; poly(glycolide) copolymer; model compounds

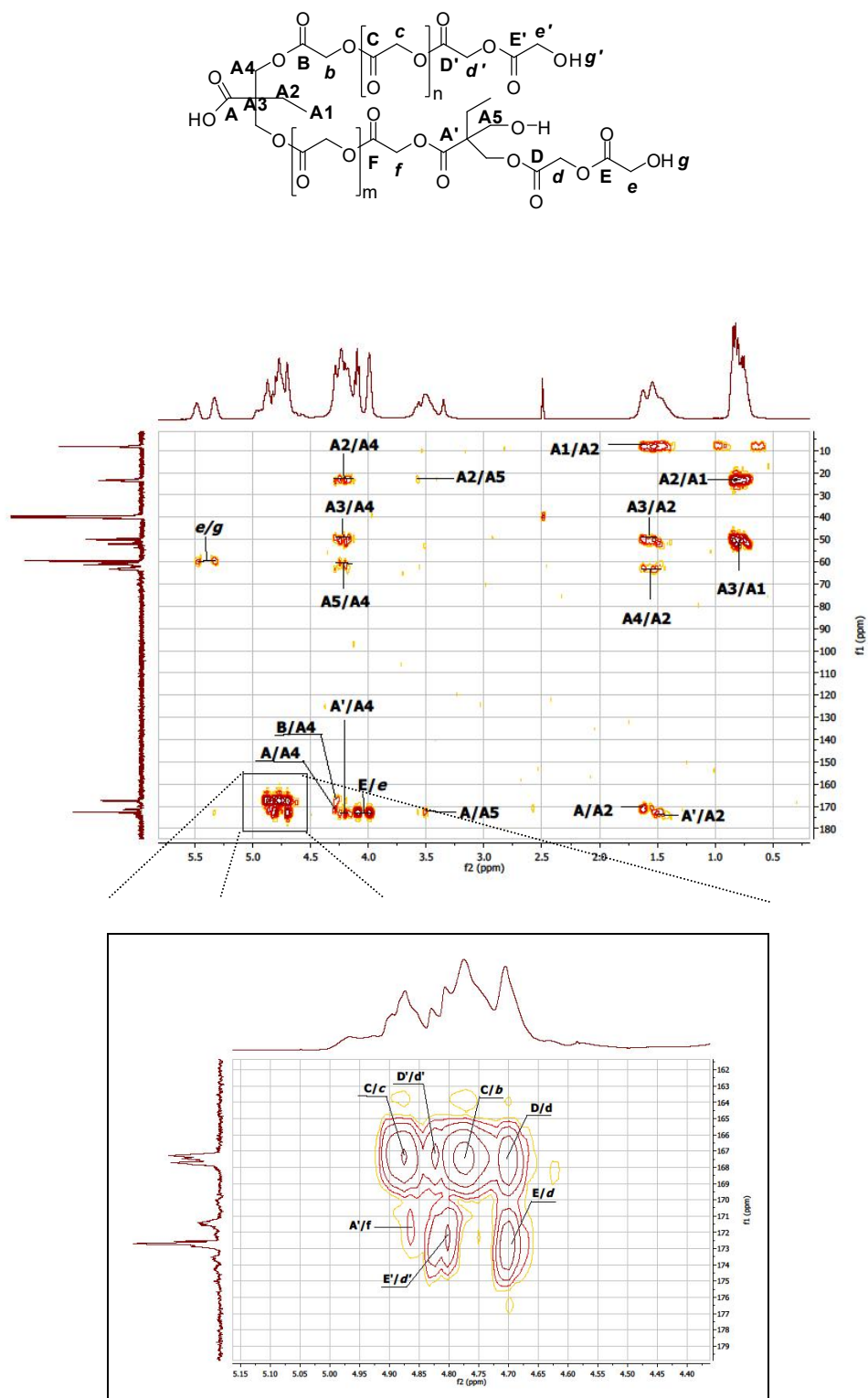


Figure S1. HMBC (Heteronuclear Multiple Bond Correlation Spectroscopy) of PGAB 51 in DMSO- d_6

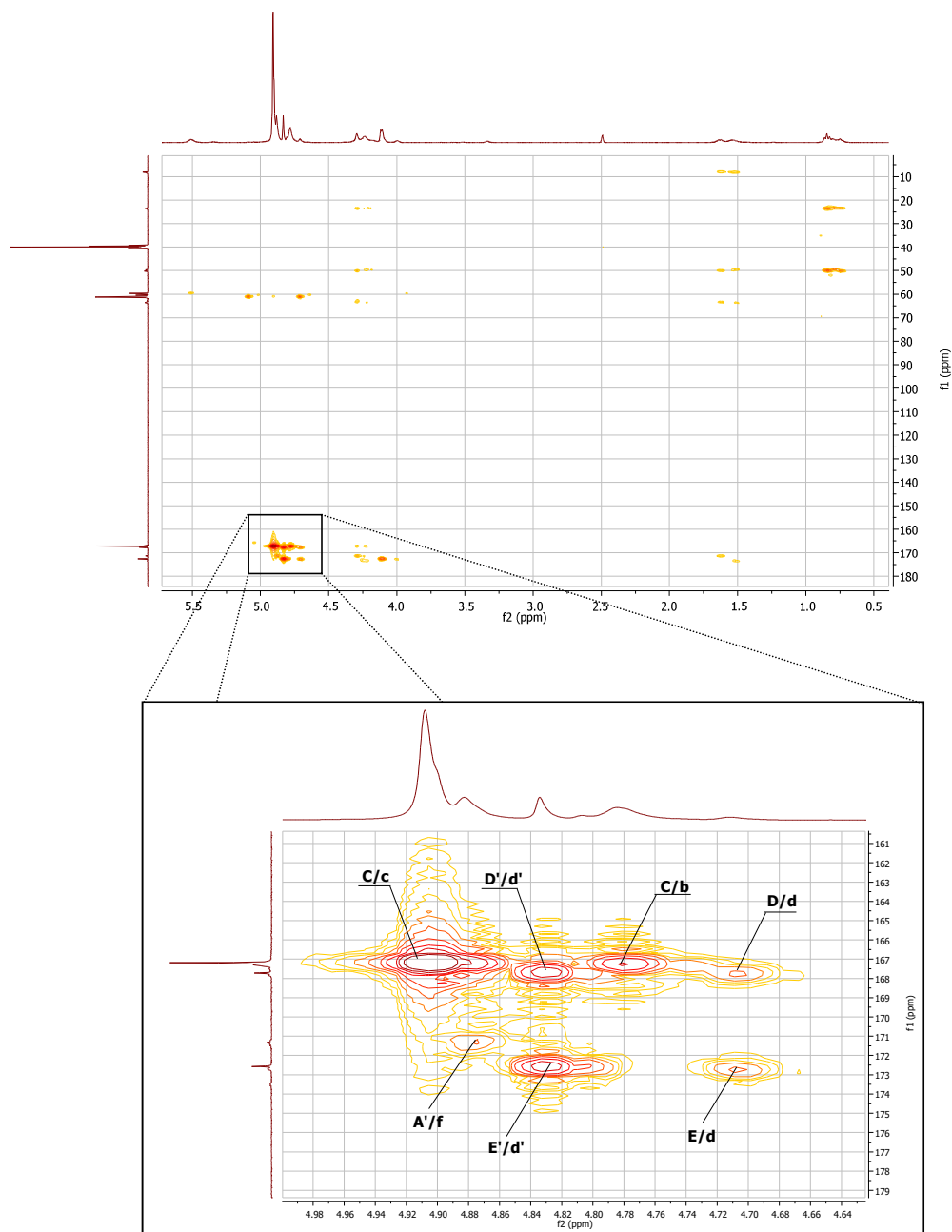


Figure S2. HMBC spectrum for PGAB 80 (precipitated in MeOH) in DMSO-*d*₆ for a better signal assignment

II. Supporting NMR Data for model compounds

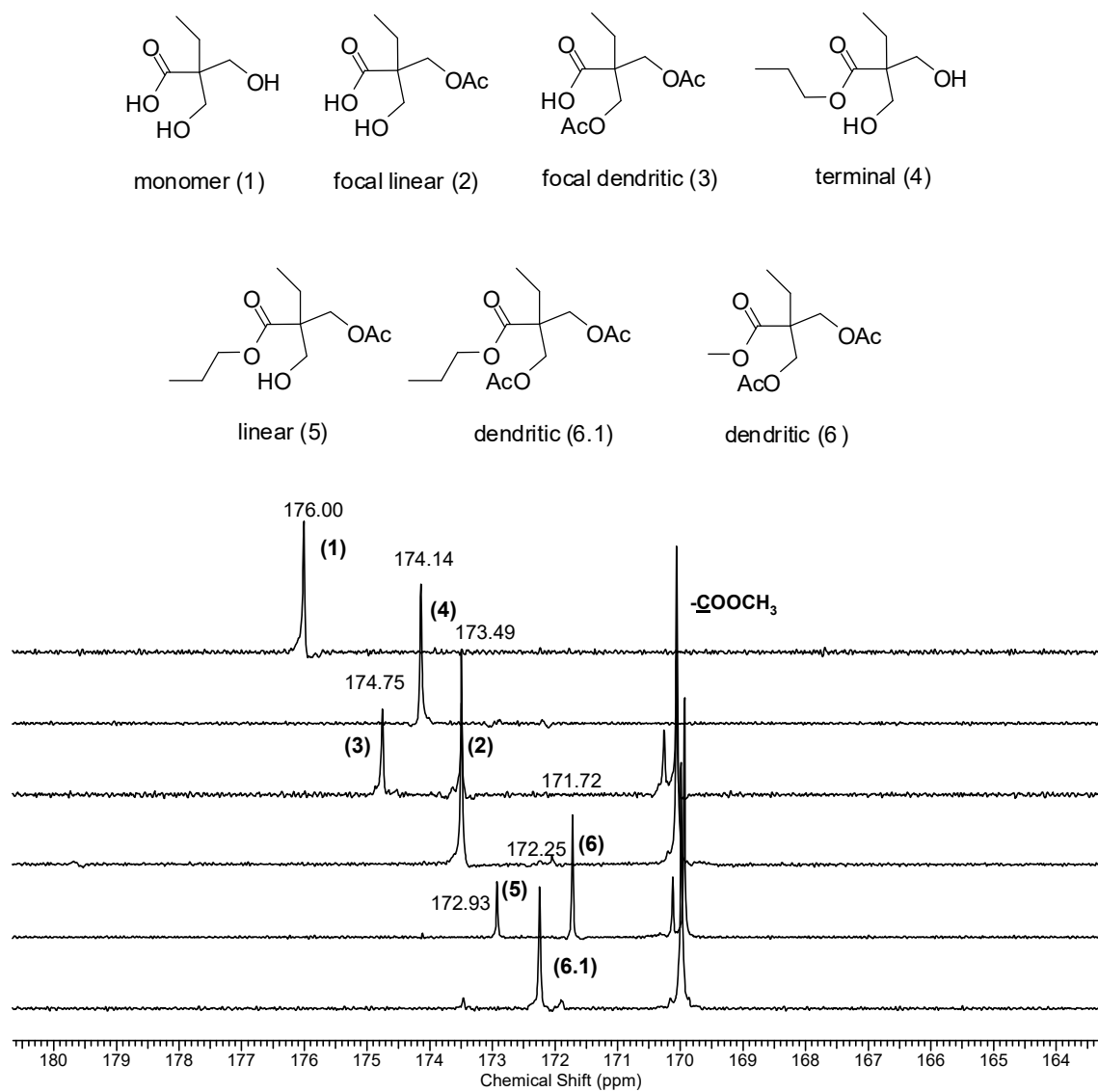


Figure S3. Expanded region of ^{13}C NMR (75 MHz) spectra measured in $\text{DMSO-}d_6$, showing the chemical shifts of the carbonyl carbons for the model compounds prepared.

III. NMR Data for Model compound "Anhydride"

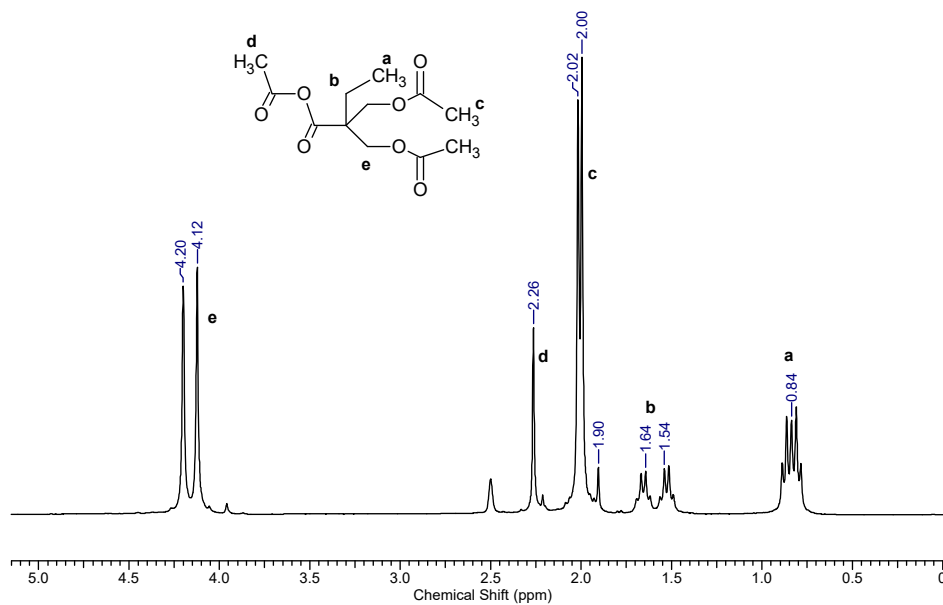


Figure S4. ^1H NMR (DMSO- d_6 , 300 MHz) of a mixture of anhydride and free carboxylic acid.

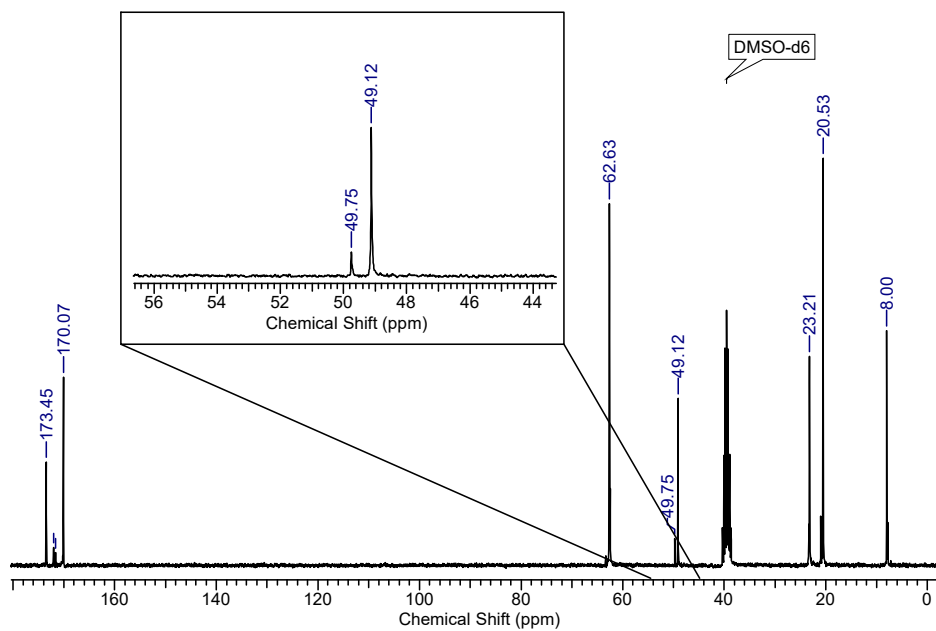


Figure S5. ^{13}C NMR in DMSO- d_6 at 75 MHz, mixture of anhydride and free carboxylic acid.

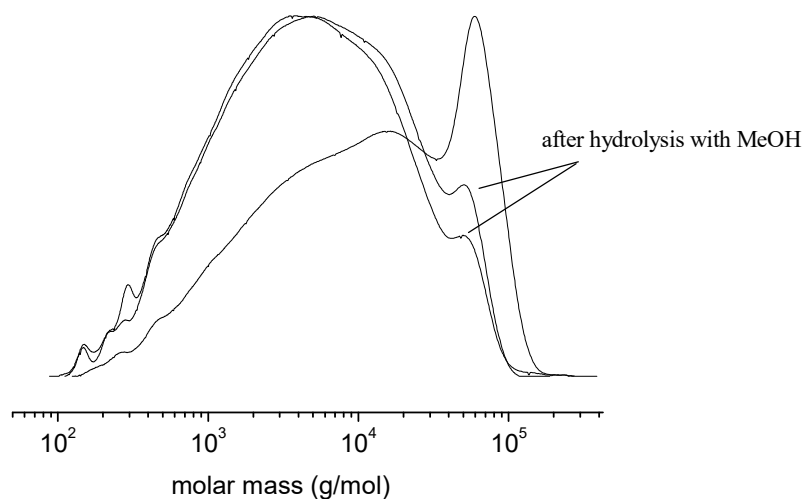


Figure S6. SEC traces (refractive index (RI) detection) of a sample with a high content of anhydride formation in DMF; hydrolysis with MeOH.

References

1. Middleton, J. C.; Tipton, A. J. *Biomaterials* **2000**, *21*, 2335-2346.
2. Dardik, H.; Dardik, I.; Laufmann, H. *Am. J. Surg.* **1971**, *121*, 656-660.
3. Munton, C. G. F.; Phillips, C. I.; Martin, B.; Bartholomew, R. S.; Capperault, I. *Brit. J. Ophthalmol.* **1974**, *58*, 941-947.
4. Vert, M.; Li, S. M.; Spenlehauer, G.; Guerin, P. *J. Mater. Sci.: Mater. Med.* **1992**, *3*, 432-446.
5. Montes de Oca, H.; Ward, I. M. *Polymer* **2006**, *47*, 7070-7077.
6. (a) Kricheldorf, H. R.; Mang, T.; Jonté, J. M. *Macromolecules* **1984**, *17*, 2173-2181. (b) Kasperczyk, J. *Polymer* **1996**, *37*, 201-203.
7. (a) Jikei, M.; Kakimoto, M. *Prog. Polym. Sci.* **2001**, *8*, 1233-1285. (b) Gao, C.; Yan, D. *Prog. Polym. Sci.* **2004**, *29*, 183-275. (c) Yates, C. R.; Hayes, W. *Eur. Polym. J.* **2004**, *40*, 1257-1281. (d) Voit, B.; Beyerlein, D.; Eichhorn, K.-J.; Grundke, K.; Schmaljohann, D.; Loontjens, T. *Chem. Eng. Technol.* **2002**, *25*, 704-707.
8. Hult, A.; Johansson, M.; Malmström, E. *Adv. Polym. Sci.* **1999**, *143*, 1-34.
9. Voit, B.; Lederer, A. *Chem. Rev.* **2009**, *109*, 5924-5973.
10. (a) Magnusson, H.; Malmström, E.; Hult, A. *Macromolecules* **2000**, *33*, 3099-3104. (b) Žagar, E.; Žigon, M.; Podzimek, S. *Polymer* **2006**, *47*, 166-175. (c) Burgath, A.; Sunder, A.; Frey, H. *Macromol. Chem. Phys.* **2000**, *201*, 782-791.
11. (a) Choi, J.; Kwak, S.-Y. *Macromolecules* **2003**, *36*, 8630-8637. (b) Trollsas, M.; Hedrick, J. L. *Macromolecules* **1998**, *31*, 4390-4395.
12. Wolf, F. K.; Frey, H. *Macromolecules* **2009**, *42*, 9443-9456.
13. Lui, M.; Vladimirov, N.; Fréchet, J. M. J. *Macromolecules* **1999**, *32*, 6881-6884.

14. Yu, X.; Feng, J.; Zhuo, R. *Macromolecules* **2005**, *38*, 6244-6247.
15. Parzuchowski, P. G.; Jaroch, M.; Tryznowski, M.; Rockiki, G. *Macromolecules* **2006**, *39*, 7181-7186.
16. Trollsås, M.; Löwenhielm, P.; Lee, V. Y.; Möller, M.; Miller, R. D.; Hedrick, J. L. *Macromolecules* **1999**, *32*, 9062-9066.
17. (a) Fréchet, J. M. J.; Henmi, M.; Gitsov, I.; G.; Sadahito, S.; Leduc, M.; Grubbs, R. B. *Science* **1995**, *269*, 1080-1084. (b) Yan, D.; Müller, A. H. E.; Matyjaszewski, K. *Macromolecules* **1997**, *30*, 7024-7033.
18. Smet, M.; Gottschalk, C.; Skaria, S.; Frey, H. *Macromol. Chem. Phys.* **2005**, *206*, 2421-2428.
19. Skaria, S.; Smet, M.; Frey, H. *Macromol. Rapid Commun.* **2002**, *23*, 292-296.
20. Gottschalk, C.; Frey, H. *Macromolecules* **2006**, *39*, 1719-1723.
21. Cooper, T. R.; Storey, R. F. *Macromolecules* **2008**, *41*, 655-662.
22. Pitet, L. M.; Hait, S. B.; Lanyk, T. J.; Knauss, D. M. *Macromolecules* **2007**, *40*, 2327-2334.
23. Wolf, F. K.; Fischer, A. M.; Frey, H. *Beilstein J. Org. Chem.* **2010**, *6*, No. 67, doi:10.3762/bjoc.6.67.
24. Lim, L.-T.; Auras, R.; Rubino, M. *Prog. Polym. Sci.* **2008**, *8*, 820-852.
25. Sinclair, R. G. *J. Macromol. Sci.: Part A* **1996**, *33*, 585-597.
26. Auras, R.; Harte, B.; Selke, S. *Macromol. Biosci.* **2004**, *4*, 835-864.
27. Dechy-Cabaret, O.; Martin-Vaca, B.; Bourissou, D. *Chem. Rev.* **2004**, *104*, 6147-6176.
28. Dali, S.; Lefebvre, H.; el Gharbi, R.; Fradet, A. *J. Polym. Sci., Part A: Polym. Chem.* **2006**, *44*, 3025-3035.
29. Kuhlshresta, A. S.; Sahoo, B.; Gao, W.; Fu, H.; Gross, R. A. *Macromolecules* **2005**, *38*, 3205-3213.
30. Kasperczyk, J. *Macromol. Chem. Phys.* **1999**, *200*, 903-910.
31. Dijkstra, P. J.; Velthoen, I. W.; Feijen, J. *Macromol. Chem. Phys.* **2009**, *210*, 689-697.
32. Chikh, L.; Tessier, M.; Fradet, A. *Polymer* **2007**, *48*, 1884-1892.
33. Komber, H.; Ziemer, A.; Voit, B. *Macromolecules* **2000**, *35*, 3514-3519.
34. Frey, H.; Hölter, D. *Acta Polym.* **1999**, *50*, 67-76.
35. Frey, H.; Hölter, D. *Acta Polym.* **1997**, *48*, 298-309.
36. Hölter, D.; Burgath, A.; Frey, H. *Acta Polym.* **1997**, *48*, 30-35.
37. Byrd, H. C.; McEven, C. N. *Anal. Chem.* **2000**, *72*, 4568-4576.
38. (a) Sunder, A.; Türk, H.; Haag, R.; Frey, H. *Macromolecules* **2000**, *33*, 7682-7692. (b) Möck, A.; Burgath, A.; Hanselmann, R.; Frey, H. *Macromolecules* **2001**, *34*, 7692-7698. (c) Khalyavina, A.; Schallausky, F.; Komber, H.; Al Sammam, M.; Radke, W.; Lederer, A. *Macromolecules* **2010**, *43*, 3268-3276.

39. Cohn, D.; Younes, H.; Marom, G. *Polymer* **1978**, *28*, 2018-2022.
40. Baker, G. L.; Vogel, E. B.; Smith, M. R., III. *Polym Rev.* **2008**, *48*, 64-84.

2.2 One-Pot Synthesis of PLLA Multi-Arm Star Copolymers Based on a Polyester Polyol Macroinitiator

Anna M. Fischer, Raphael Thiermann, Michael Maskos and Holger Frey

Abstract

On the basis of a hyperbranched poly(glycolide) (*hbPGA*) macroinitiator we present the synthesis of PLLA multi-arm star polyesters via a core-first approach. The star-shaped copolymers were prepared in a one-pot two-step process via Sn(Oct)₂-catalyzed ring-opening polymerization (ROP) conducted in the melt. Complete conversion of the end groups of the polyester polyol is confirmed by the primary hydroxyl termini of the polyester polyol. By adjusting the monomer/initiator ratio different star copolymers with varying PLLA arm length have been obtained with molecular weights in the range of 1500 to 10,000 g/mol (SEC). The successful coupling of the PLLA arms to the *hbPGA* core is confirmed via detailed 1D and 2D NMR spectroscopy. Because of the different hydrodynamic volume of the star polymers in contrast to their linear analogues and in default of a comparable polymer standard, the weight-average molecular weight (M_w) was determined both by SEC and static light scattering (SLS). The star-shaped poly(lactide)s reveal different thermal properties in comparison with linear poly(lactide) homopolymers.

Introduction

Aliphatic poly(ester)s are well-known materials in the field of medical applications and drug delivery systems.^{1,2} Especially, poly(lactide) (PLA) is a widely used material with regard to its biodegradability and biocompatibility.³ The critical issues of petroleum-based plastics together with the fact that the mechanical properties of PLA are comparable with those of poly(styrene) (PS) or poly(ethylene terephthalate) (PET) have led to revived interest in polymers based on renewable resources. Although the popularity of PLA increases, this material bears also disadvantages, e.g. a high degree of crystallization related with a low degradation rate, which limits the field of application. In recent years, several strategies have been developed to optimize materials properties of PLA such as copolymerization, stereocomplexation, variation of architecture or blending. Copolymers of D- and L-lactide⁴ as well as PLLA star polymers⁵ both are well-known to suppress crystallization of PLLA. In addition, blending e.g. with poly(ϵ -caprolactone) provides commercial PLLA blends with an improved toughness.⁶ In the last decades, the interest in complex macromolecular architectures increased especially with regard to hyperbranched,⁷⁻¹¹ star-shaped,¹²⁻¹⁵ brush-like¹⁶ or dendrimer-like

polyesters.¹⁷ In a number of studies, dendritic polymers showed properties clearly different from their linear analogues. One major advantage is their high number of functional end groups, which provide an excellent platform for the introduction of various functionalities via post-polymerization modification. The branched topology leads to improved solubility, low melt viscosity and altered thermal properties.¹⁸⁻²¹ In addition, hyperbranched polyols are favourable macroinitiators for the synthesis of multi-arm star copolymers due to their facile one-step preparation.²² Polyglycerol (PG), a widely used polyether polyol, has been employed in the synthesis of core-shell architectures based on a grafting-from approach via atom transfer radical polymerization (ATRP) or ring-opening polymerization (ROP). Multi-arm star copolymers of hydrophobic ϵ -caprolactone (ϵ CL),²³ glycolide (GA),²⁴ methyl methacrylate (MMA)²⁵ or L-lactide (LLA)^{5,26} with various arm lengths have been prepared with a hydrophilic PG core to obtain reverse micelles capable of encapsulating and releasing drugs. Besides PG, dendritic core molecules such as hyperbranched polyester polyols or dendrimers like poly(amido amine) (PAMAM) and poly(ethylene imine) (PEI) have been used.²⁷⁻²⁹ Derivatization and functionalization of the hydroxyl end groups provide various interesting carrier systems.³⁰ The synthesis of star copolymers may be pursued in two different ways: (1) linear polymer chains are chemically coupled to the core molecule – the “grafting-through” approach. Alternatively, (2) the polymer chains grow directly from the initiating core with its multiple functionalities in a “grafting-from” approach.³¹ The unique properties of star-shaped polyesters in comparison to their linear analogues, particularly with regard to their thermal behaviour and crystallization tendency, motivate further research in this area.³²

In the current work, we present the rapid, one-pot two-step synthesis of PLLA multi-arm stars based on a hyperbranched poly(glycolide) (*hb*PGA) copolymer core via solvent-free, Sn(Oct)₂-catalyzed ROP. The polyol macroinitiator used was prepared by combining ROP and melt AB₂-polycondensation as described recently by our group.³³ The first, rather fundamental intention of our studies was to prevent fast degradation of the amorphous *hb*PGA core via a protective PLLA shell and at the same time an enhancement of solubility in organic solvents. The obtained star block copolymers were investigated with respect to their molecular weight, the average PLLA arm length and their thermal properties.

Experimental Section

Reagents

L-Lactide and glycolide were purchased from Purac (Groningen, Netherlands) and used as received. Tin(II)-2-ethylhexanoate ($\text{Sn}(\text{Oct})_2$, 97% Acros Organics) and 2,2-bis(hydroxymethyl)butyric acid (BHB, 98% Sigma-Aldrich) were used as received. All solvents were of analytical grade and used as received.

Instrumentation

^1H NMR spectra were recorded at 400 MHz on a Bruker AMX400 and are referenced internally to residual proton signals of the deuterated solvent. ^{13}C NMR spectra were recorded at 75 MHz and referenced internally to the solvent signals (^1H NMR signal: 2.50 ppm (DMSO- d_6), 7.27 ppm (CDCl_3); ^{13}C NMR signal: 39.52 ppm (DMSO- d_6), 77.00 ppm (CDCl_3)). For SEC measurements in DMF (containing 1 g/L of lithium bromide as an additive), an Agilent 1100 series was used as an integrated instrument including a PSS Gral column ($10^4/10^4/10^2$ Å porosity) and an RI detector. Calibration was achieved with poly(styrene) standards provided by Polymer Standards Service (PSS).

Differential scanning calorimetry (DSC) analysis was performed on a Perkin-Elmer 7 Series thermal analysis system with autosampler in the temperature range of -180 to +180 °C with heating rates of 1 K/min. The melting points for indium ($T_0=156.6$ °C) and Millipore water ($T_0=0$ °C) were used for calibration.

Dynamic and static light scattering (DLS and SLS) measurements were performed with a helium-neon laser of 623 nm wavelength operating at 22 mW, an ALV/CGS-3 MD goniometer with 8 APD detectors and dual ALV-7004 Multiple-Tau digital correlator. For SLS angle dependent measurements were carried out between 25° and 152° in steps of 1° at a temperature of 23 °C. The DLS measurements were carried out in the range of 26° and 138° in two different angle steps (8 detectors with 16° difference) with 4° difference (26,42,58,74,90,106,122,138 und 30,46,62,78,94,110,126,142).

Data evaluation was achieved with an ALV-Correlator Software for Multi-Detector Goniometer Systems (for WINDOWS-2000/2003/XP/Vista/7). Prior to both DLS and SLS measurements, all the solutions were filtered through 0.02 µm Anotop membrane filters.

General Synthesis of the *hbPGA-g-PLLA* Multi-Arm Stars. The preformed *hbPGA* macroinitiator has been prepared according to literature procedures and has been used in the subsequent ROP of lactide without further prior work-up. To a one-necked Schlenk flask, charged with the precursor and equipped with a magnetic stir bar as well as a rubber septum, L-lactide has been added in the quantities required. The flask was evacuated for 10 min, purged with argon and completely immersed in an oil bath preheated to 120°C. To the homogenous melt 0.1 mol% $\text{Sn}(\text{Oct})_2$ were added as a catalyst for the ROP. The mixture was stirred at 120 °C for 3 h under argon atmosphere. After

cooling, the mixture was dissolved in chloroform (CHCl_3) and precipitated twice in methanol. The purified polymer was isolated by decantation of the solvent and dried in vacuo at 40 °C. The obtained colorless waxy solid (for a shorter PLLA chain length) or powder was soluble in a broad range of solvents e.g. chloroform and tetrahydrofuran (THF). The synthesis has been performed as well in a one-pot procedure without transferring the macroinitiator in a different flask by subsequent addition of the amount of lactide in the quantities required.

^1H NMR (DMSO-d_6): δ (ppm) 5.47-5.49 (OH); 5.11-5.21 (CH_{LA} , linear); 4.78-4.91 ($\text{CH}_2\text{OR}_{\text{GA}}$; CH_{LA} , terminal); 4.10-4.35 ($\text{CH}_2\text{OR}_{\text{BHB}}$); 1.35-1.70 ($\text{CH}_{3,\text{LA}}$, linear; $\text{CH}_{2,\text{BHB}}$); 0.70-0.90 ($\text{CH}_{3,\text{BHB}}$).

^{13}C NMR (DMSO-d_6): δ (ppm)= 174.05 (CO_{LA} terminal); 173.07 (COOH_{BHB}); 170.82 (COOR_{BHB}); 169.23-169.71 (CO_{LA} linear); 166.70 (CO_{GA} linear); 68.51-67.76 (CH_{LA} linear); 65.52 (CH_{LA} terminal); 63.28 ($\text{CH}_2\text{OR}_{\text{BHB}}$); 60.70-60.79 ($\text{CH}_2\text{OR}_{\text{GA}}$); 49.84 (C_{q} , dendritic); 49.21 (C_{q} , focal dendritic); 23.10 ($\text{CH}_{2,\text{BHB}}$); 20.33 ($\text{CH}_{3,\text{LA}}$ terminal); 16.46-16.57 ($\text{CH}_{3,\text{LA}}$ linear); 7.73-7.86 ($\text{CH}_{3,\text{BHB}}$).

Results and Discussion

The hyperbranched poly(glycolide) copolymers with various poly(lactide) arms were prepared in a one-pot two step approach as shown in Figure 1. First, the hyperbranched poly(glycolide) (*hb*PGA) core was synthesized by the combined ROP/ AB_2 -polycondensation in melt using 2,2-bis(hydroxymethyl)butyric acid (BHB) as a branching unit, as described previously in literature.³³ The polymerization starts with $\text{Sn}(\text{Oct})_2$ -catalyzed ring-opening polymerization of glycolide, initiated from BHB followed by a melt polycondensation of the *in-situ* preformed AB_2 macromonomers. In contrast to the linear PGA homopolymer, the hyperbranched copolymers are soluble in a wide range of organic solvents as for example acetone, ethyl acetate and dimethyl sulfoxide (DMSO). In addition, the introduction of branches in the polymer backbone results in an amorphous material with a low glass temperature (T_g).³³

In a subsequent step, the raw polyester polyol formed was used as a macroinitiator for the ring-opening polymerization of L-lactide by $\text{Sn}(\text{Oct})_2$ -catalysis without further purification steps. All polymerizations were carried out in bulk within 3 h at 120 °C by addition of a 10 Vol%-solution of $\text{Sn}(\text{Oct})_2$ in toluene (present for transfer of the catalyst). The preparation of the PLLA multi-arm star polymers is feasible in a one-pot process by a combination of both steps without prior work-up of the precursor, which renders the material interesting for large scale production.

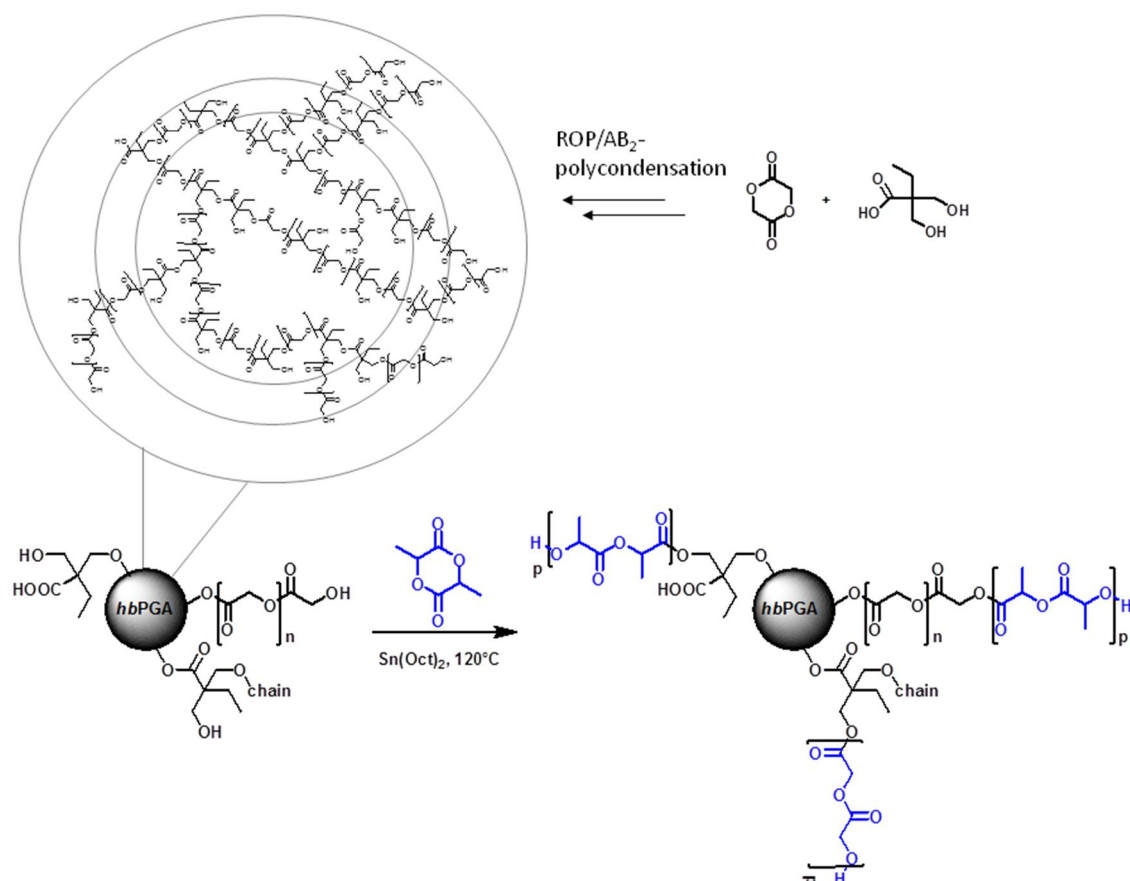


Figure 1. Synthesis of PLLA multi-arm stars based on a hyperbranched PGA copolymer core via a grafting-from approach.

By varying the monomer/initiator ratio a number of PLLA stars with different average PLLA chain length were obtained. With increasing lactide content, the hydrophilicity decreased and as a consequence PLLA stars with molecular weights > 2000 g/mol were insoluble in DMSO. As it is shown in Table 1, the polydispersities (PDI) of the prepared star polymers are in the range of 1.26-2.17. These moderate values arise with regard to the non-monodisperse macroinitiator (PDI=2.33) obtained by a polycondensation reaction (Figure 2). Probability theories have shown a relation between the polydispersity index of star polymers and the polydispersity index of the arms, resulting in a reduced PDI for the star polymer after grafting a number of f polydisperse arms to a multifunctional core molecule.³⁴ This effect and the increase of molecular weight contribute to the reduced polydispersity of the obtained star copolymers. Comparison of the SEC traces of the PLLA stars with the hyperbranched macroinitiator evidently proves the absence of prepolymer after ROP of L-lactide.

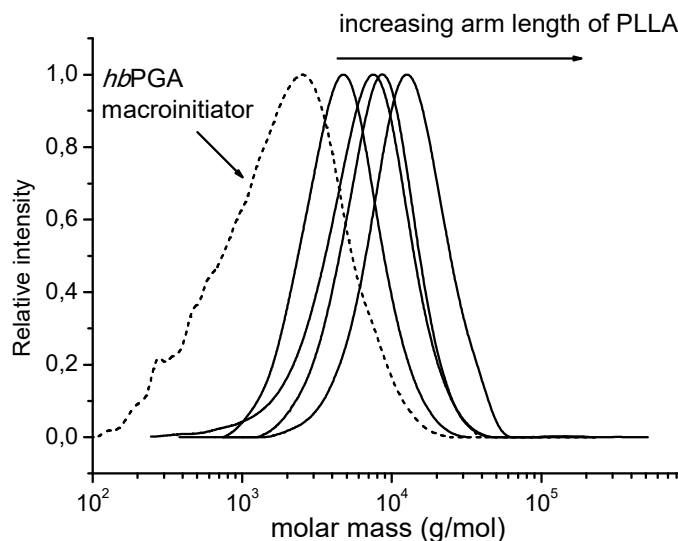


Figure 2. SEC traces (DMF, RI) of the PLLA multi-arm star copolymers obtained by a grafting-from approach based on $hbPGA_{0.6}$ (60 mol% PGA, DB=0.43).

The chemical nature of the multiple hydroxyl end groups at the $hbPGA$ macroinitiator plays an important role in the further functionalization step. Preceding work in our group ascertained a considerable difference in the reactivity of primary and secondary hydroxyl groups in ring-opening multibranching polymerization (ROMBP) of lactide and 5-hydroxymethyl-1,4-dioxan-2-one (5HDON).⁷ The ROP of lactide is initiated first by the primary hydroxyl site of the 5HDON lactone, generating secondary hydroxyl termini. The ring-opening of 5HDON, which leads to new initiation sites, occurs mainly until the conversion of lactide is completed. In our case, the primary hydroxyl termini of the poly(glycolide)-based polyester polyol are considerably more reactive than the secondary hydroxyl groups formed upon ring-opening of the lactide monomer. This should lead to quantitative end group functionalization with PLLA chains.

Structural Investigation by 1D/2D NMR Analysis

The ¹H NMR spectrum of a multi-arm star copolymer in comparison with one of the hyperbranched PGA polymers is shown in Figure 3. Evidence for the successful linkage of the PLLA arms to the hyperbranched PGA core is obtained from the disappearance of the signals corresponding to the terminal glycolic acid units (CH_2OH_{GA} : 4.00 ppm; 4.10 ppm) and the free hydroxyl methylene protons of the bishydroxy acid (CH_2OH_{BHB} : 3.49 ppm). The signal assignment was confirmed by detailed 2D NMR spectroscopy and is consistent with our previous work.³³

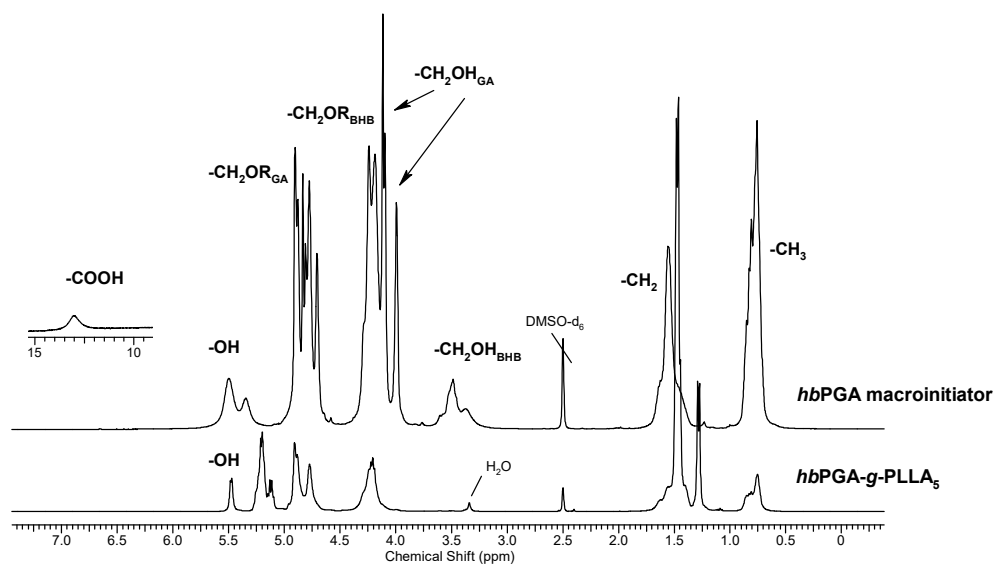


Figure 3. ^1H NMR analysis (400MHz, DMSO-d_6) of the polyol macroinitiator in comparison with the hbPGA-g-PLLA_5 star copolymer.

NMR studies also allowed for the determination of the molecular composition and the average PLLA arm length. Unfortunately, the signal of the terminal lactic acid unit is superimposed by the signals of esterified BHB hydroxymethylene protons in the ^1H NMR spectrum and therefore the average PLLA chain length had to be calculated out of the inverse gated-decoupling ^{13}C NMR spectrum. In Figure 4 ^1H NMR spectra of the star copolymer samples with different monomer composition are shown. As expected, the signal intensity of the hbPGA core decreases with increasing content of L-lactide. The NMR spectra measured in CDCl_3 show a characteristic splitting of the signal of the BHB methyl group (**A**) associated with the formation of only two different BHB units (focal dendritic (**Fd**) and dendritic (**D**) unit). The main resonances of the linear PGA units are in the range of 5.20 to 5.50 ppm (**F**). The signals of the lactide backbone (CH_{lin} , **E**) are well separated from the other lactide arm related signals **E'**, **B** and **B'**. In addition, the ^1H NMR spectrum measured in DMSO-d_6 (Figure 3) shows a signal due to the protons of the terminal hydroxyl group of the lactide arms at 5.50 ppm. This signal assignment was confirmed by an ^1H COSY NMR experiment (s. Supporting Information S2), relying on the cross correlation of the methyl (**B'**) or methine (**E'**) proton with the hydroxyl proton and by an ^1H , ^{13}C COSY NMR experiment (HMBC) (Figure 7) referring to the cross correlation of the carbonyl carbon (**K'**) with the hydroxyl proton.

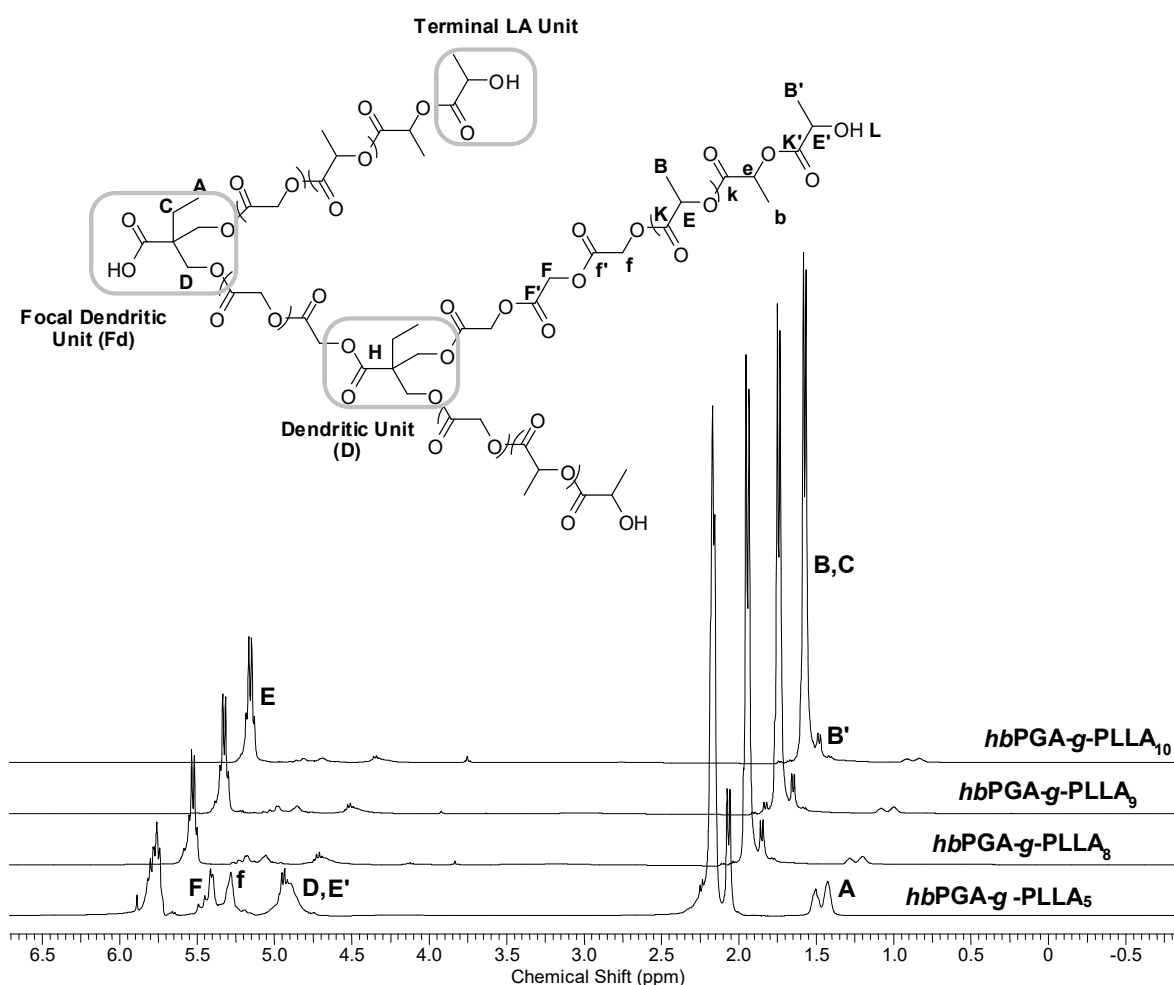


Figure 4. ^1H NMR analysis (400 MHz, CDCl_3) of the star block copolymers hbPGA-g-PLLA_x with increasing lactide to macroinitiator ratio (bottom to top; with x = average number of lactic acid units per PLLA arm).

Verification of the successful linkage of the PLLA arms with the hbPGA core is represented by the esterified glycolide end groups with lactide. Evidence for the attachment of the lactide arms is as well given by the ^{13}C NMR spectrum in Figure 5. The presence of only two BHB repeating units (**Fd**, **D**) underlines the successful conversion of the focal linear (**Fi**) and linear (**L**) BHB units. Special attention was paid to the disappearance of the terminal glycolic acid units with regard to the carbonyl carbons resonating at 172.16-173.16 ppm and the methylene carbons at 59.32 and 59.43 ppm.

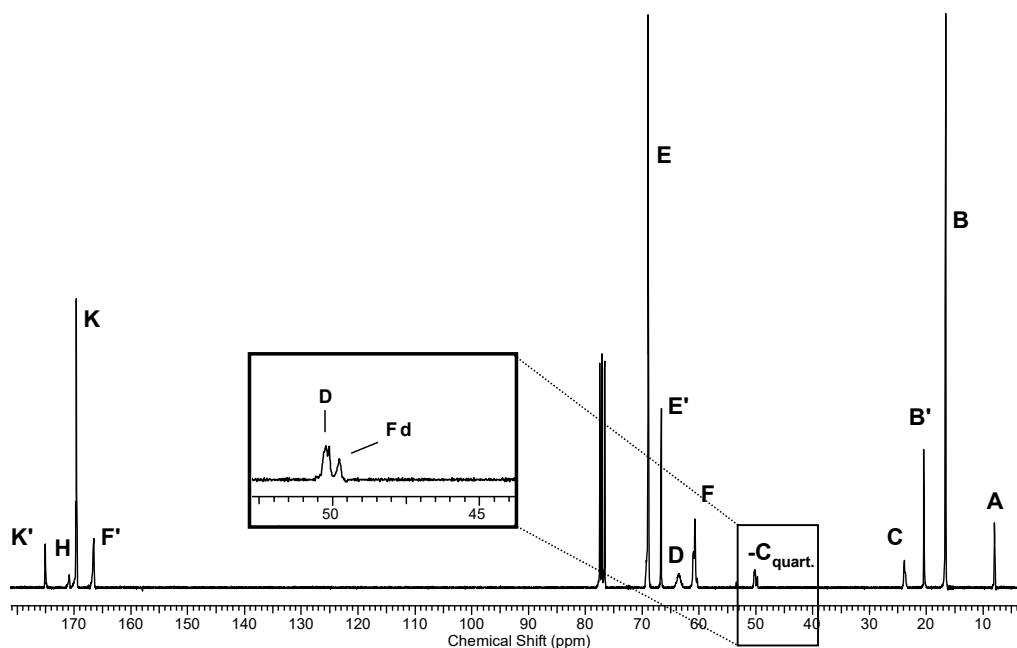


Figure 5. ^{13}C NMR spectrum (75 MHz, CDCl_3) of the synthesized *hbPGA-g-PLLA*₅ multi-arm star copolymer with zoom into the region of the quaternary carbons.

For the sequential synthesis of the PLLA stars it is essential that no transesterifications between the preformed PGA core and the lactide monomer occur during polymerization. Therefore 2D NMR spectroscopy experiments (HMBC) were performed to exclude such side reactions. Figure 6 shows a section of the heteronuclear multiple bonds coherence (HMBC) spectrum, with zoom into the region of the carbonyl carbons.

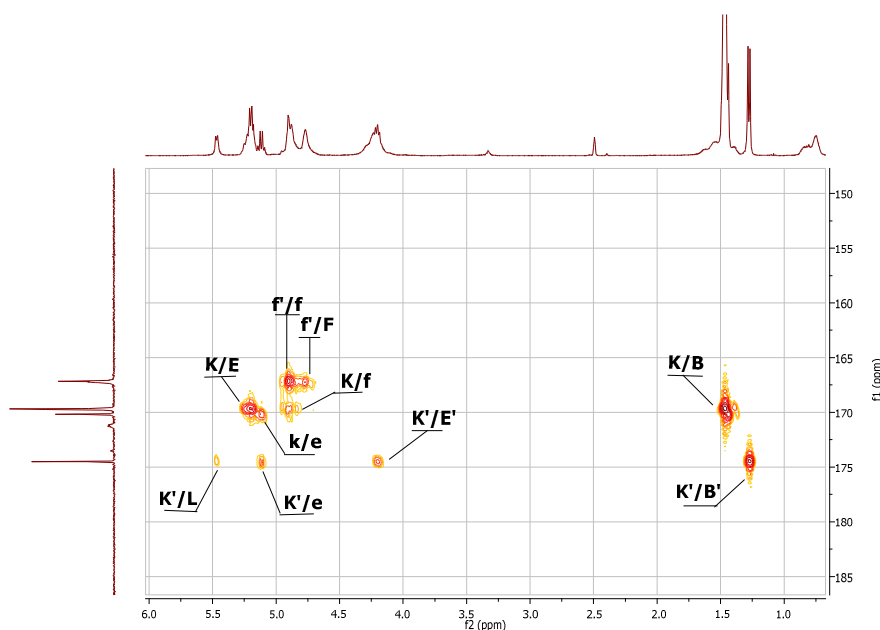


Figure 6. ^{13}C , ^1H -correlation: Zoom into HMBC NMR spectrum (full spectrum, see Supporting Information Figure S1) of *hbPGA-g-PLLA*₅ measured in DMSO-d_6 .

In case of transesterifications reactions (1) a cross correlation of the glycolide carbonyl carbon and the lactide methine protons should be observed (visualized in Figure 7). Instead, only the cross correlation (2) between the glycolide methylene protons and the lactide carbonyl carbon (**K/f**) is detectable, which confirms the attachment of PLLA to the hydroxyl-terminated PGA core (Figure 6). Furthermore, the ^{13}C NMR analysis gives distinct information of the sequence distribution of glycoyl and lactyl units as described in literature.³⁵ Especially the carbonyl carbon signals are very sensitive to sequence effects. After polymerization only the glycoyl-lactyl sequence is present whereas LLG, GLG, LGL and LGG sequences associated with random incorporation of the lactone monomers due to transesterification rearrangement are absent. In addition, the carbonyl carbon signals belonging to the GLL sequence can be clearly assigned (4.75 ppm).

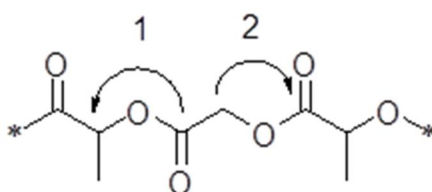


Figure 7. Visualisation and identification of sequence distribution with HMBC NMR analysis.

Table 1. Characterization of the *hbPGA-g-PLLA* multi-arm stars and the *hbPGA* copolymer core.

sample	M_n^a (g/mol)	M_w/M_n^a	T_g^b (°C)	T_m^b (°C)	ΔH_m (J/g)	LA units ^c
<i>hbPGA</i> _{0.6} ^d	1000	2.33	19.1	-	-	-
<i>hbPGA</i> _{0.6-g-PLLA} ₅	1500	2.17	29.8	-	-	5
<i>hbPGA</i> _{0.6-g-PLLA} ₈	4800	1.57	42.1	119.0	35.6	8
<i>hbPGA</i> _{0.6-g-PLLA} ₉	6500	1.36	49.0	126.5	44.7	9
<i>hbPGA</i> _{0.6-g-PLLA} ₁₀	10000	1.40	49.4	145.6	50.9	10

^a SEC: DMF as eluent, PS standard for calibration; ^b determined from the 2nd heating scan;

^c average number of L-lactide units per PLLA arm, calculated from inverse gated-decoupling ^{13}C NMR spectra; ^d hyperbranched PGA copolymer (60 mol% PGA, DB=0.43)

Thermal Properties

The thermal properties of the *hbPGA-g-PLLA* star copolymers have been investigated by DSC analysis. In Table 1 the results obtained from SEC and DSC analysis with respect to the average PLLA arm length are summarized. The *hbPGA* macroinitiator is an amorphous material, which exhibits a T_g at 19.1 °C. In contrast, the linear PLLA homopolymer possesses a T_g between 57-60 °C and a melting temperature (T_m) of 174-178 °C.³⁶ PLLA star copolymers with more than 5 lactic acids units per arm show a sharp melting point, which increases with increasing PLLA chain length. As expected, crystallization of the PLLA blocks is possible above a critical chain length. The glass transition temperature of the prepared multi-arm stars is lowered (29-49 °C) in comparison to linear PLLA, and an increase of the T_g with increasing PLLA arm length is observed (see Figure 8). This dependency is known as well for linear polymers. For all star copolymers an increase of the melting enthalpy (ΔH_m) with increasing PLLA chain length per arm is obtained. In contrast to the copolymers quenched from melt, all of the star copolymers precipitated from solution show a T_m in the first heating scan, indicating a lowered crystallization rate of the PLLA chains (see Figure 9). This observation emphasizes that the prior thermal treatment of the sample exerts a great influence on the material properties. In addition, the large number of end groups also has a great influence on the thermal behaviour of polymers, which was studied on the basis of PLLA stars with different number of hydroxyl termini.^{13,37} In the second heating run, the sample *hbPGA-g-PLLA*₁₀ shows the characteristic transition curves including the glass transition, the cold recrystallization and the melting. The phenomenon of two melting peaks results from the two different crystal structures (α/α') formed by PLLA. The α' structure is the thermodynamically less favoured structure.^{38,39} This observation might be due to the slow crystallization rate of the PLLA chains, which leads to an inhomogeneous crystallization upon quenching. In fact, the star topology with the hyperbranched PGA core contributes to a depressed melting point compared to the linear PLLA homopolymer. Due to the lowered crystallization rate the morphology of the star copolymers strongly depends on the prior thermal treatment of the sample ranging from amorphous to crystalline materials.

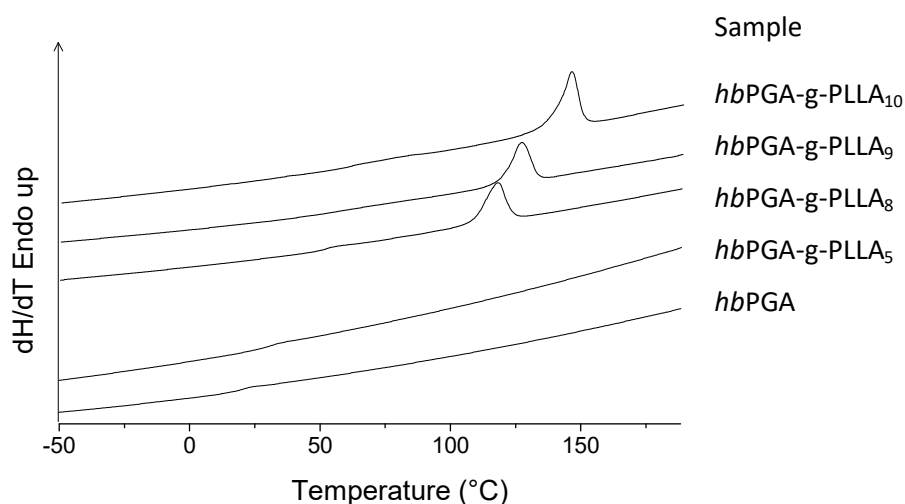


Figure 8. DSC heating traces of the PLLA multi-arm stars and the polyester polyol (*hbPGA*) obtained from the 1st heating scan with a heating rate of 40 °C/min.

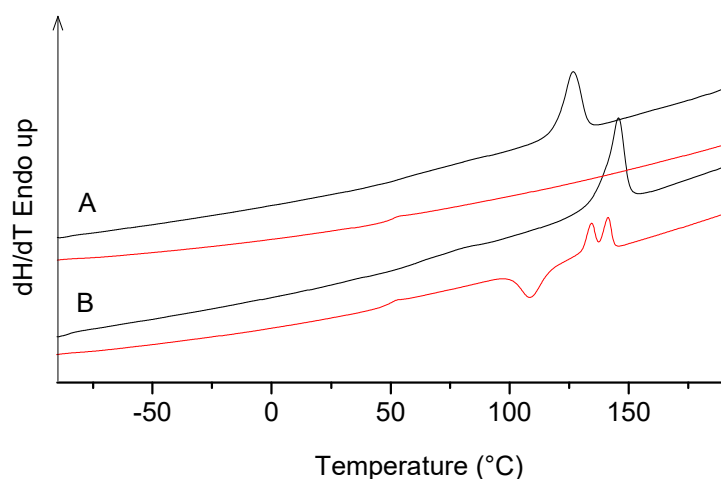


Figure 9. DSC heating curves of quenched (red colour) star copolymers from melt and those precipitated from solution, comparing the first and second heating run (red colour) with each other: (A) *hbPGA*_{0.6}-*g-PLLA*₉ and (B) *hbPGA*_{0.6}-*g-PLLA*₁₀

Solution Properties

The hydrodynamic radius (R_h) was determined by DLS measurements. SLS measurements were carried out at different scattering angles (25°-152°) and different concentrations (2-10 g/L) to determine the weight-average molecular weight (M_w) of the star copolymers. Hexafluoroisopropanol (HFIP) was chosen as a standard for the SLS measurements because of the low value of the refractive index increment (dn/dc) of PLA in THF and $CHCl_3$. Due to undesired aggregation, other possible solvents, as for example acetone or pyridine, were not used. Table 2 shows the hydrodynamic radii of the different multi-arm stars obtained by DLS measurements in HFIP. As expected, the size of the

particles increases with increasing PLLA arm length. In addition, a Zimm plot can be applied to macromolecular structures for the determination of M_w from SLS measurements by the angle and concentration dependency of $Kc/\Delta R_\theta$ with the following equation 1:^{40,41}

$$\frac{Kc}{\Delta R_\theta} = \frac{1}{M_w} \left[1 + \frac{q^2 R_g^2}{3} \right] + 2A_2c \quad (1)$$

with the optical parameter $K = 4\pi^2 n^2 (dn/dc)^2 / N_A \lambda^4$, the scattering vector for vertically polarized light $q = 4\pi n_0 \sin(\theta/2) / \lambda$, the refractive index of the liquid medium n , the Avogadro's constant N_A , the wave length of the laser λ and the excess Rayleigh ratio [$\Delta R_\theta = R_\theta(\text{solution}) - R_\theta(\text{solvent})$]. M_w is estimated by extrapolation of the concentration c and the angle θ to zero.

All obtained results for the star copolymers derived from SLS and DLS are summarized in Table 2. The SEC data for the stars (see Table 1) are based on a poly(styrene) (PS) standard and therefore are not comparable with the SLS data. In fact, it is known that conventional SEC has limited suitability to determine the molecular weight of star copolymers due to their more compact structure and therefore smaller hydrodynamic volume compared with linear copolymers. Hence, it is appropriate to determine the absolute M_w by SLS instead of SEC in order to gain information about the actual dimensions, regardless of the macromolecular architecture. SLS is known to have poor resolution for low molecular weight polymers; therefore no SLS and DLS data have been obtained for the macroinitiator and the star copolymer with the lowest molecular weight. Since we were not able to determine the radius of gyration (R_g) due to low resolution capacity; the calculation of the R_g/R_h ratio has not been possible, which would have been crucial to evidence the star topology.

Table 2. Hydrodynamic radius (R_h) and weight-average molecular weight (M_w) of *hbPGA-g-PLLA* star copolymers.

sample	R_h^a /nm (DLS)	M_w^b /g mol ⁻¹ (SLS)	M_w^c /g mol ⁻¹ (SEC)
<i>hbPGA-g-PLLA</i> ₅	n.d.	n.d.	3300
<i>hbPGA-g-PLLA</i> ₈	2.6	7570	7540
<i>hbPGA-g-PLLA</i> ₉	2.9	10,200	8840
<i>hbPGA-g-PLLA</i> ₁₀	3.1	12,200	14,000

^{a)}determined by DLS measurements at 23 °C in THF

^{b)}determined by SLS measurements at 23 °C in HFIP with dn/dc (mL/g)=0.162±0.0022

^{c)}determined from SEC analysis in DMF with PS standard calibration

Surprisingly, the weight average molecular weight, which has been determined by SLS measurements in HFIP ($M_{w,SLS}$) is similar to the values obtained from SEC analysis ($M_{w,SEC}$). The hydrodynamic radii (R_h) of the star copolymers, which have been determined by DLS in THF, are in the range of 2.6 to 3.1 nm, indicating the absence of aggregation and thus the suitability of the utilized solvent. Generally, star polymers obtain smaller radii in comparison to their linear analogues with identical molecular weight. The effect of the topology on the solution behaviour increases with increasing number of arms.⁴¹ In our case, the solution properties might be influenced both by the number of arms and the hyperbranched core. In further studies the behaviour of the intrinsic viscosity $[\eta]$ shall be examined to support the structural topology.

Conclusion

Poly(lactide) multi-arm stars have been synthesized in a grafting-from approach by $\text{Sn}(\text{Oct})_2$ -catalyzed ring-opening polymerization using a hyperbranched polyester polyol based on poly(glycolide) as a macroinitiator. Importantly, a detailed 1D/2D NMR analysis confirms a successful conversion of all hydroxyl groups and permits the identification of a single glycoyl-lactyl sequence, which excludes possible transesterifications during ROP of L-lactide. By varying the monomer/initiator ratio, polymers of various molecular weights were obtained in a controlled fashion. The glass temperature and the melting point were found to be lower in comparison with linear PLLA due to the influence of the inner hyperbranched PGA core on the crystallization tendency of the PLLA arms. In fact, the crystallization of the PLLA arms is effectively adjustable by the prior treatment of the samples. As expected, the DLS and SLS measurements revealed an increase of R_h and M_w with increasing PLLA block length. Due to the degradable PGA core and the biocompatible PLLA side chains these polyester star block copolymers possess promising potential for biomedical applications. Further current studies are focused on the effect of the PLA chain length on the degradation time of the star polymers. The aliphatic polyester structure might be useful for controlled release systems since a wide range of degradation rates should be achievable by simply adjusting the PGA/PLLA molar ratio.

Supporting Information

I. Additional 2D-NMR Data

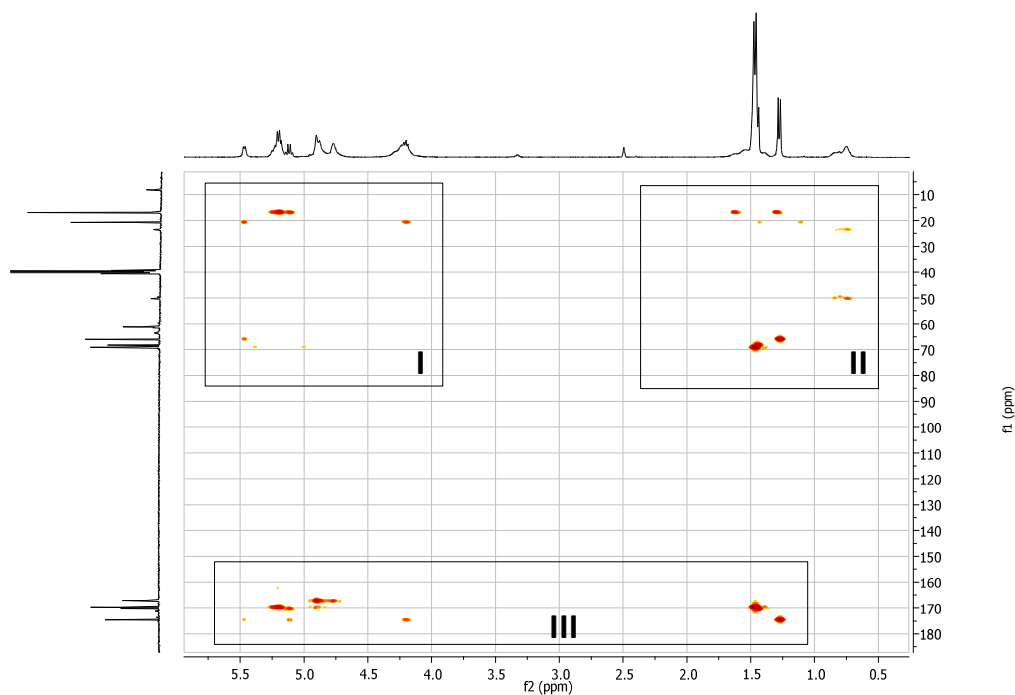


Figure S1. Complete HMBC (Heteronuclear Multiple Bond Coherence) spectrum (DMSO- d_6 , 400 MHz) of *hbPGA-g-PLLA*₅.

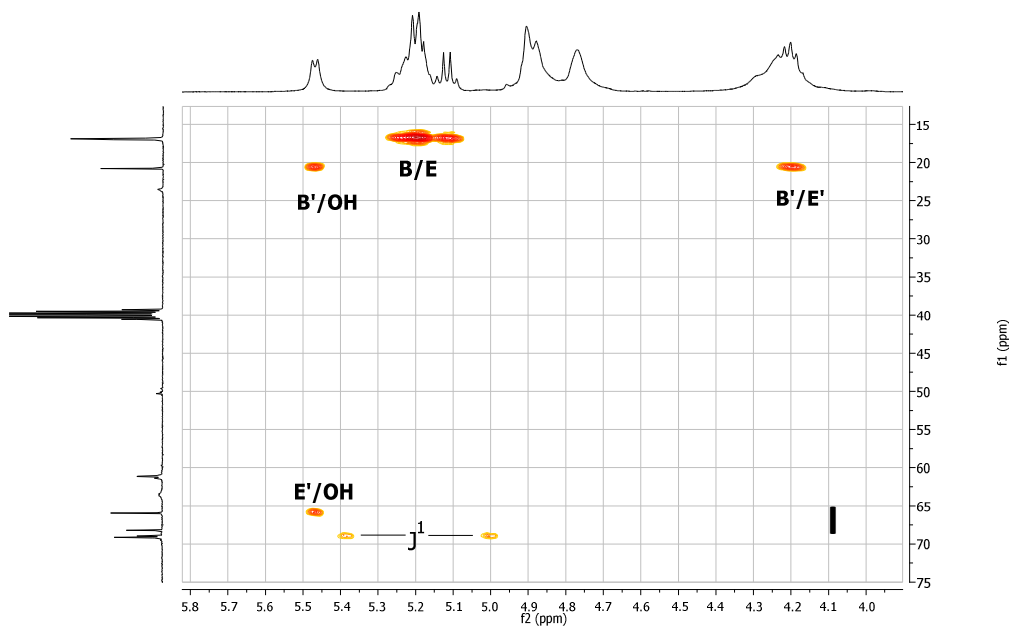


Figure S2. Zoom into section I of the HMBC spectrum (S1).

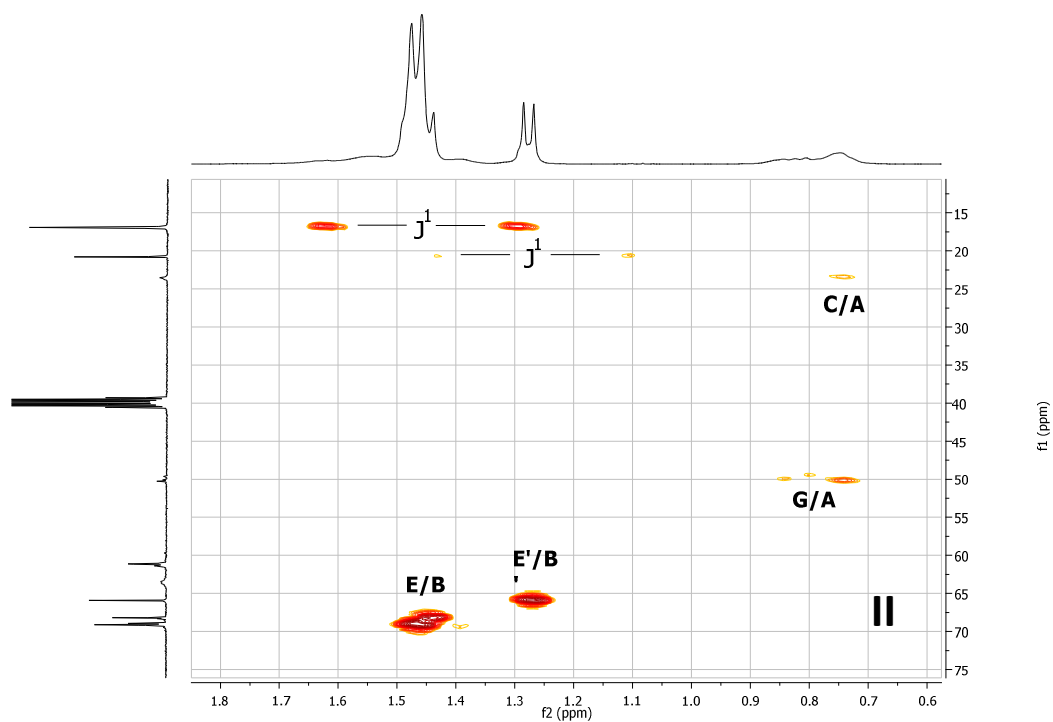


Figure S1.2. Zoom into section II of the HMBC spectrum (S1).

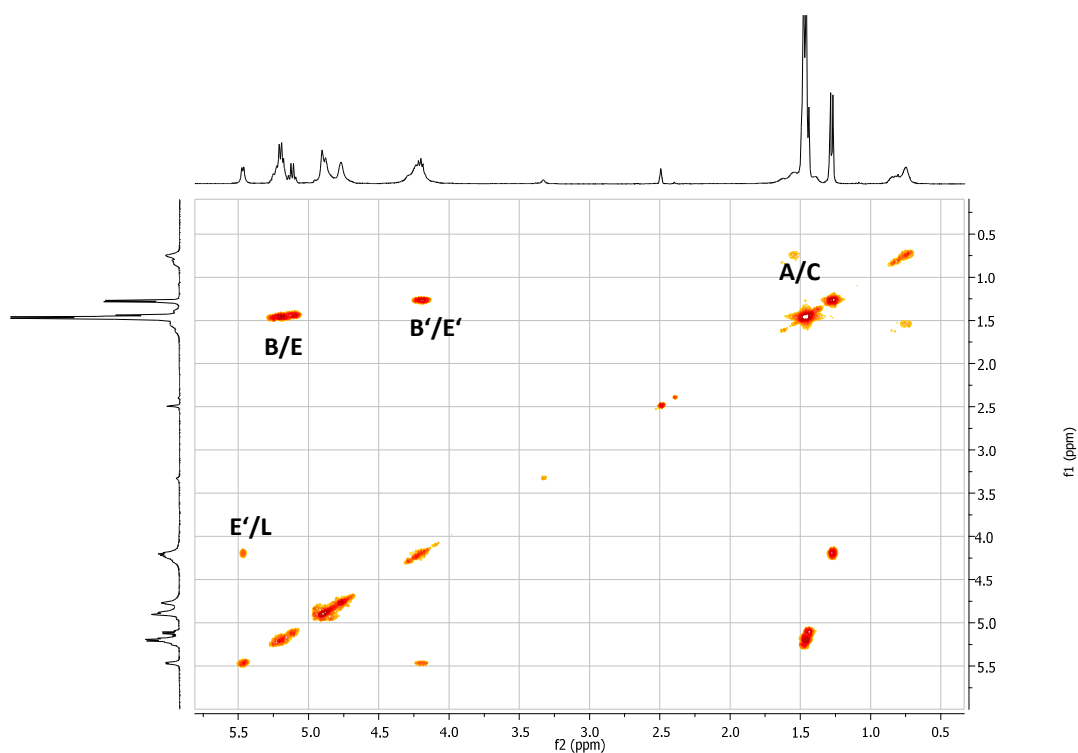


Figure S3. ¹H, ¹H COSY (Homocorrelation Spectroscopy) NMR spectrum (DMSO-d₆, 400 MHz) of *hbPGA-g-PLLA*₅.

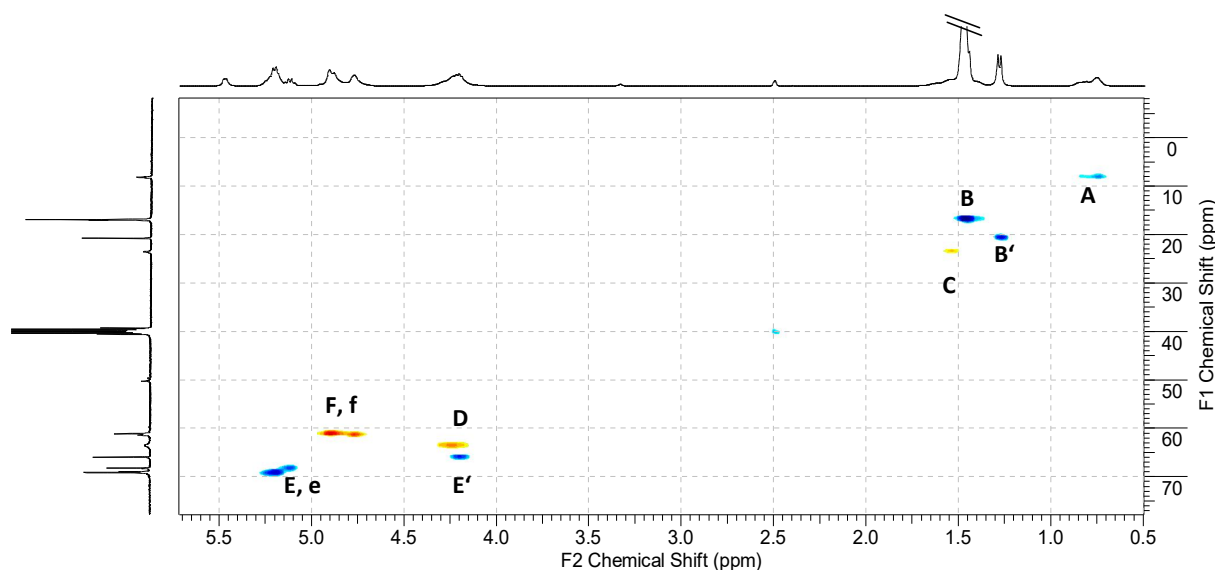


Figure S4. HSQC (Heteronuclear Single Quantum Coherence) NMR spectrum (DMSO- d_6 , 400 MHz) of *hbPGA-g-PLLA*₅ with additional distortionless enhancement by polarization transfer (DEPT) information (methyl/methine: blue; methylene: red)

References

1. Katoaka, K.; Harada, A.; Nagasaki, Y. *Advanced Drug Delivery Reviews* **2001**, *47*, 113-131.
2. Liechty, W.B.; Kryscio, D. R.; Slaughter, B. V.; Peppas, N. A. *Annu. Rev. Chem. Biomol. Eng.* **2010**, *1*, 149-173.
3. Tokiwa, Y.; Calabia, B. P. *Appl. Microbiol. Biotechnol.* **2006**, *72*, 244-251.
4. Dove, A. P. *Chem. Commun.* **2008**, *48*, 6446-6470.
5. Schömer, M.; Frey, H. *Macromol. Chem. Phys.* **2011**, *212*, 2478-2486.
6. Anderson, K. S.; Schreck, K. M.; Hillmyer, M. A. *Polymer Reviews* **2008**, *48*, 85-108.
7. Wolf, F. K.; Frey H. *Macromolecules* **2009**, *42*, 9443-9456.
8. Smet, M.; Gottschalk, C.; Frey, H. *Macromol. Chem. Phys.* **2005**, *206*, 2421-2428.
9. Skaria, S.; Smet, M.; Frey, Holger *Macromol. Rapid Commun.* **2002**, *23*, 292-296.
10. Choi, J.; Kwak, S.-J. *Macromolecules* **2003**, *36*, 8630-8637.
11. Žagar, E.; Žigon, M. *Progr. Polym. Sci.* **2010**, *36*, 53-88.
12. Xi, W.; Jiang, N.; Gan, Z. *Macromol. Biosci.* **2008**, *8*, 775-784.
13. Hao, Q.; Li, F.; Li, Q.; Li, Y.; Jia, L.; Yang, J.; Fang, Q.; Cao, A. *Biomacromol.* **2005**, *6*, 2236-2237.
14. Klok, H.-A.; Becker, S.; Schuch, F.; Pakula, T.; Müllen, K. *Macromol. Biosci.* **2003**, 729-741.
15. Cameron, D. J. A.; Shaver, M. P. *Chem. Soc. Rev.* **2011**, *40*, 1761-1776.
16. Li, Y.; Vollhand, C.; Kissel T. *Polymer* **1998**, *39*, 3087-3097.

17. Trollsås, M.; Hedrick, J. L. *J. Am. Chem. Soc.* **1998**, *120*, 4644-4651.
18. Voit, B. I.; Lederer, A. *Chem. Rev.* **2009**, *109*, 5924-5973.
19. Jikei, M.; Kakimoto, M.-a. *Prog. Polym. Sci.* **2001**, *26*, 1233-1285.
20. Gao, C.; Yan, D. *Prog. Polym. Sci.* **2004**, *29*, 183-275.
21. Hult, A.; Johansson, M.; Malmström, E. *Adv. Polym. Sci.* **1999**, *Vol. 143*, 1-34.
22. Jones, M.-C.; Leroux, J.-C. *Soft Matter* **2010**, *6*, 5850-5859.
23. Burgath, A.; Sunder, A.; Neuner, I.; Mülhaupt, R.; Frey, H. *Macromol. Chem. Phys.* **2000**, *201*, 792-797.
24. Wolf, F. K.; Fischer, A. M.; Frey, H. *Beilstein J. Org. Chem.* **2010**, *6*, No.67.
25. Chen, Y.; Shen, Z.; Barriau, E.; Kautz, H.; Frey, H. *Biomacromolecules* **2006**, *7*, 919-926.
26. Gottschalk, C.; Wolf, F. K.; Frey, H. *Macromol. Chem. Phys.* **2007**, *208*, 1657-1665.
27. Ternat, C.; Kreutzer, G.; Plummer, C. J. G.; Ngyen, T. Q.; Herrmann, A.; Ouali, L.; Sommer, H.; Fieber, W.; Velazco, M. I.; Klok, H.-A.; Månson, J.-A. E. *Macromol. Chem. Phys.* **2007**, *208*, 131-145.
28. Zhao, Y.-L.; Cai, Q.; Jiang, J.; Shuai, X.-T.; Bei, J.-Z.; Chen, C.-F.; Xi, F. *Polymer* **2002**, *43*, 5819-5825.
29. Adeli, M.; Haag, R. *J. Polym. Sci.: Part A: Polym. Chem.* **2006**, *44*, 5740-5749.
30. Arial, S.; Prabarahan, M.; Pilla, S.; Gong, S. *Int. J. Biol. Macromol.* **2009**, *44*, 346-352.
31. Hirao, A.; Yoo, H.-S. *Polymer Journal* **2011**, *43*, 2-17.
32. Nunez, E.; Ferrando, C.; Malmström, E.; Claesson, H.; Werner, P.-E.; Gedde, U. W. *Polymer* **2004**, *45*, 5251-5263.
33. Fischer, A. M.; Frey, H. *Macromolecules* **2010**, *43*, 8539-8548.
34. Gao, H. *Macromol. Rapid Commun.* **2012**, *33*, 722-734.
35. Kasperczyk, J. *Polymer* **1996**, *37*, 201-203.
36. Zhao, Y. L.; Chen, C. F.; Xi, F. *Polymer* **2005**, *48*, 5808-5819.
37. Donald, G. J. *Polym. Envir.* **2001**, *9*, 63-84.
38. Pan, P.; Zhu, B.; Kai, W.; Dong, T.; Innoe, Y. *Macromolecules* **2008**, *41*, 4296-4304.
39. Rathi, S.; Kalish, J. P.; Coughlin, E. B.; Hsu S. L. *Macromolecules* **2011**, *44*, 3410-3415
40. Yang, L.; Qi, X.; Liu, P.; El Ghzaoui, A.; Li, S. *Int. J. Pharm.* **2010**, *294*, 43-49.
41. Zimm, B. H.; *J. Chem. Phys.* **1948**, *16*, 1093-1099.
42. Burchard, W. *Adv. Polym. Sci.* **1999**, *143*, 114-194.

Chapter 3: Glycerol-Based Poly(glycolide) Copolymers

3.1 Poly(glycolide) Multi-Arm Star Polymers: Improved Solubility via Limited Arm Length

Florian K. Wolf, Anna M. Fischer and Holger Frey

Published in *Beilstein J. Org. Chem.* **2010**, *6*, No.67

Abstract

Due to low solubility of poly(glycolic acid) (PGA), its use is generally limited to random copolyesters with other hydroxy acids, such as lactic acid or applications that permit direct processing from the polymer melt. Insolubility is generally observed for PGA with a degree of polymerization exceeding 20. Here we present a strategy which allows for the preparation of PGA-based multi-arm structures, significantly exceeding the molecular weight of processible oligomeric linear PGA (<1000 g/mol). This was achieved by the use of a multifunctional hyperbranched polyglycerol (PG) macroinitiator and the tin(II)-ethylhexanoate-catalyzed ring-opening polymerization of glycolide in the melt. This strategy permits to combine high molecular weight with good molecular weight-control (up to 16.000 g/mol, PDI= 1.4-1.7), resulting in PGA multi-arm star block copolymers containing more than 90 weight % GA. The successful linkage of PGA arms and PG core via this core first/grafting-from strategy was confirmed by detailed NMR and SEC-characterization. Various PG/glycolide ratios were employed to vary the length of the PGA arms. Besides fluorinated solvents, the materials were soluble in DMF and DMSO up to an average arm length of 12 glycolic acid units. Reductions in T_g and melting temperature compared to the homopolymer PGA promise simplified processing conditions. These findings contribute to broadening the range of biomedical applications of PGA.

Keywords: Poly(glycolide), PGA, star polymer, block copolymer; hyperbranched; polyglycerol, polyester.

Introduction

Linear aliphatic polyesters such as poly(lactic acid) (PLA) and poly(ϵ -caprolactone)¹ are of great interest due to their biodegradability, biocompatibility and permeability for many drugs. In contrast, poly(glycolic acid) (PGA) is scarcely used because of its high degree of crystallinity and its insolubility in all common solvents. However, glycolic acid is widely employed in copolymers of varying composition with the abovementioned lactone comonomers.² For the PGA homopolymers, special processing techniques for the polymer melt are required and characterization is limited to solid-state techniques.³ In recent works, PLA and poly(ϵ -caprolactone)⁴ have been successfully used for the synthesis of numerous star⁵ and multi-arm star⁶ as well as (hyper)branched polymers.⁷ Although PGA-rich polymers exhibit a superior degradation rate in comparison to poly(lactide), star copolymers primarily composed of this building unit have hardly been described in literature.⁸ However, star copolymers, in a general sense, have attracted increasing interest for the fabrication of unimolecular micelles;⁹ in particular when they consist of a hydrophilic, hyperbranched (or dendritic) core and a hydrophobic corona.¹⁰ Their potential arises from their ability to encapsulate and release hydrophilic molecules slowly. Particularly, PEG/PLA-based copolymers have been intensely studied in this context.¹¹⁻¹³ Apart from this special application in solution, analogs of well-known linear polymers with star architectures exhibit significantly altered physical properties.^{14,15} This is often considered the primary motivation for the choice of this interesting polymer architecture.¹⁶

A suitable multifunctional core molecule is required to prepare multi-arm star polymers with core-shell characteristics. Apart from dendrimers,^{17,18} well-defined hyperbranched polymers¹⁹ fulfill this requirement and benefit from their accessibility via a facile one-step synthesis, which makes a tedious, generation-wise build-up ubiquitous. Besides poly(ethylene imine) (PEI),²⁰ hyperbranched polyglycerol²¹⁻²⁶ has proven to be a versatile and highly potent multifunctional core molecule.²⁷⁻²⁹ Derivatization and functionalization of the peripheral hydroxyl groups of this polyether polyol have afforded a number of carrier systems,³⁰⁻³⁴ matching the concept outlined above. In contrast to dendrimers, where functional groups are exclusively located at the surface, poly(glycerol) scaffolds also contain hydroxyl groups throughout the structure. At first glance this might be considered a disadvantage; however, this is in fact beneficial for the significantly hydrophilized core environment when core-shell topologies for encapsulation are desired.

Here we present a solvent-free synthetic strategy for multi-arm star block copolymers with a hyperbranched polyether core and PGA arms, systematically varying arm length. The combination of glycolide with a multifunctional initiator studied in this paper is of a rather fundamental nature. Our primary objective is to improve the solubility of PGA in standard organic solvents and thus facilitate characterization as well as processing, while keeping the overall glycolide weight fraction high. Multi-arm star copolymers³⁵ should permit the combination of short average chain length with high

molecular weight. Since the high number of functionalities of the core molecules is ideally translated into a matching number of arms with a respective chain end, end-group effects are expected to exert a significant influence on solubility and crystallization tendencies of the polymer.

Results and Discussion

The hyperbranched poly(glycerol)s (PGs) with multiple poly(glycolide) arms were prepared by a straightforward two-step approach as shown in Figure 1. In the first step, we polymerized glycidol anionically by the method described previously,¹⁹ using trimethylolpropane as a trifunctional initiator. The hydroxyl groups of PG were deprotonated to an extent of 10% before the slow addition of glycidol monomer was started. The subsequent polymerization proceeds via a ring-opening branching reaction where branching occurs due to a fast proton exchange equilibrium which is a well-known phenomenon in oxyanionic polymerizations.

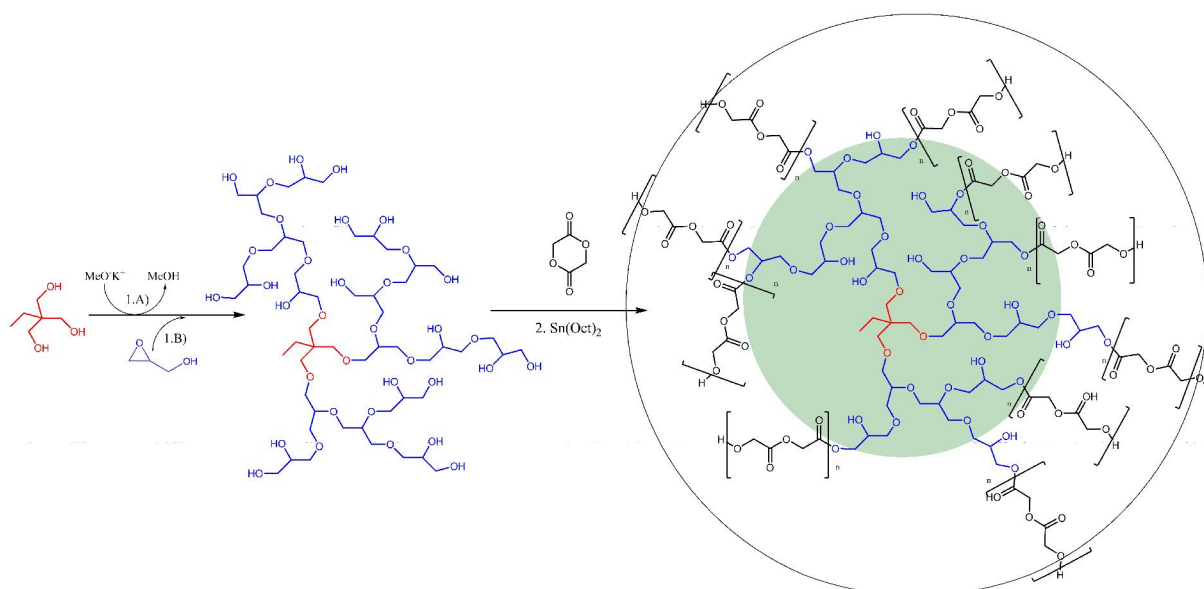


Figure 1. Synthetic route to *hb*-PG-*b*-PGA multi-arm star copolymers in a two step sequence. The well-established anionic ring-opening multibranching polymerization of glycidol is followed by the Sn(Oct)₂ mediated copolymerization of glycolide.

In the second step, the polyether-polyols were used as macroinitiators for the ring-opening polymerization of glycolide via Sn(Oct)₂ catalysis. All polymerization experiments were carried out in bulk (with a minimum of toluene present for transfer of the catalyst) at 120 °C for 24 h with systematic variation of the glycolide monomer/*hb*-PG-OH ratios. Since each glycidol unit leads to the formation of an additional end-group after ring-opening and attachment to the growing PG, the corresponding total number of primary and secondary hydroxyl groups of the polymer $n(\text{OH})$ is equal to the sum of the initiator functionality f and the degree of polymerization DP_n .

$$n(\text{OH}) = \text{DP}_n + f \quad (1)$$

By varying of the initiator/monomer ratio, two hyperbranched poly(glycerol) samples with different degrees of polymerization DP_n were obtained. Their theoretical number of initiating hydroxyl groups was calculated from the degree of polymerization which is available from ^1H NMR according to Equation 1. PG_{14} and PG_{38} thus offer an average of 17 and 41 potential initiating moieties for the grafting-from reaction with glycolide. It should be emphasized that according to Equation 1, the number of hydroxyl groups is independent of the degree of branching (DB). Typically, the poly(glycerol) macroinitiators possess primary as well as secondary $-\text{OH}$ groups, which likely show different reactivities in the initial reaction with glycolide. Since the accessibility of functional groups of PG is believed to play an important role in the properties of the resulting star block copolymer, the branched topology and the distribution of OH groups therein are key factors that will also be addressed in the following text. Careful drying of the PG cores under vacuum is a crucial step for the controlled synthesis of the multi-arm star polymers in order to avoid initiation by trace amounts of water, which leads to concurrent glycolide homopolymerization and thus an undesired mixture of linear and star-like PGAs. In order to prevent possible precipitation from solution, the polymerization was conducted in bulk without added solvent under $\text{Sn}(\text{Oct})_2$ catalysis with an average catalyst loading of 0.1 mol % of the glycolide feed. The mixed compounds yielded a homogeneous melt at 120 °C, fulfilling a prerequisite for an efficient grafting from approach. Under the reaction conditions employed and taking the high number of initiating groups into account, the conversion proceeds to high values within short reaction times. The polymers obtained show improved solubility properties compared to linear PGA and thus permit the use of common characterization methods such as NMR in $\text{DMSO}-d_6$ and SEC in DMF. This is largely attributed to the high end-group concentration in combination with a short average PGA chain length in the multi-arm structure.

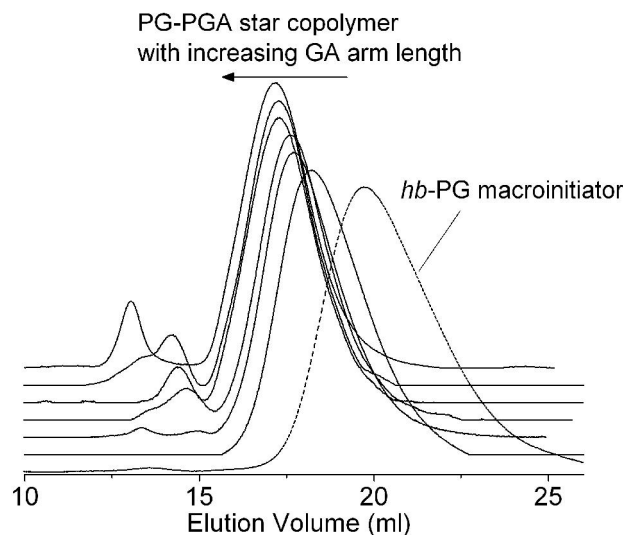


Figure 2. SEC elugrams of the obtained multi-arm star-block copolymers derived from PG₃₈. The grafting of poly(glycolide) on the poly(glycerol) macroinitiator is accompanied by a significant decrease in elution volume.

With increasing glycolide content, a second high-molecular weight distribution mode appears together with a gradual shift of the main distribution mode to lower elution volume (Figure 2) which is in line with expectations. These apparent impurities could be caused by compounds capable of co-initiation such as water or other hydroxyl functionalities. Table 1 illustrates the correlation between theoretical molecular weight and values obtained from SEC measurements via calibration with polyethylene glycol (PEG) standards. The obvious underestimation of the molecular weight by SEC is attributed to the peculiar spherical geometry of the multi-arm star copolymer and has also been observed with other star polymers. The polydispersities of the materials are in the range of 1.3–1.7 for the series of star polymers prepared, which is moderate. These values can be explained by the non-monodisperse multifunctional initiator (PDI: 1.9–2.0), although transesterification/ cyclization reactions during the synthesis cannot be completely excluded. A detailed account of the NMR studies aimed at determining the PGA arm length of the polymers is given in the following text. In this context, it should be emphasized that solubility in DMF and DMSO was generally limited to star polymers with targeted arm length of up to 12 glycolic acid units. Obviously, samples exceeding these values have not been characterized by SEC or NMR and are thus not listed in Table 1.

Table 1. Characterization data of the multi-arm star block copolymers originating from two different *hb*-PG macroinitiators from NMR and SEC.

sample	glycolide content (weight ratio)	Yield (%)	M_n (theor./NMR*)	M_n (GPC)	PDI (GPC)	average arm length (NMR)
PG ₁₄	0	-	1140*	1130	2.0	-
P(G ₁₄ GA ₄)	0.77	48	5000	5400	1.6	7
P(G ₁₄ GA ₈)	0.87	90	8800	6500	1.5	10.6
P(G ₁₄ GA ₁₂)	0.91	94	-	-	-	12.1
PG ₃₈	0	-	2900*	2450	1.9	-
P(G ₃₈ GA ₂)	0.62	45	7600	6300	1.7	3.9
P(G ₃₈ GA ₄)	0.76	72	12300	9300	1.5	5.6
P(G ₃₈ GA ₆)	0.83	88	17000	11000	1.4	7.2
P(G ₃₈ GA ₈)	0.87	83	21700	14300	1.5	8.6
P(G ₃₈ GA ₁₀)	0.89	92	26400	15600	1.4	9.5
P(G ₃₈ GA ₁₂)	0.91	93	31100	17000	1.3	9.8

The ¹H NMR spectra of multi-arm polymer samples with varying composition (based on PG₃₈) are shown in Figure 3. As expected, an increase in the glycolide feed results in an increase in the glycolide backbone signal at 4.91 ppm (**B**) and a relative decrease in signal intensity of the PG core. The resonances of the core are mainly distributed between 3.1 and 3.8 ppm (**e**). Special attention was paid to the terminal glycolic acid unit, since it enables the determination of the average chain length of the oligoglycolide arms. The respective signal can be found at 4.12 ppm and is thus well separated from the other glycolide arm-related signals **B**, **C**, **H** and **H'**.

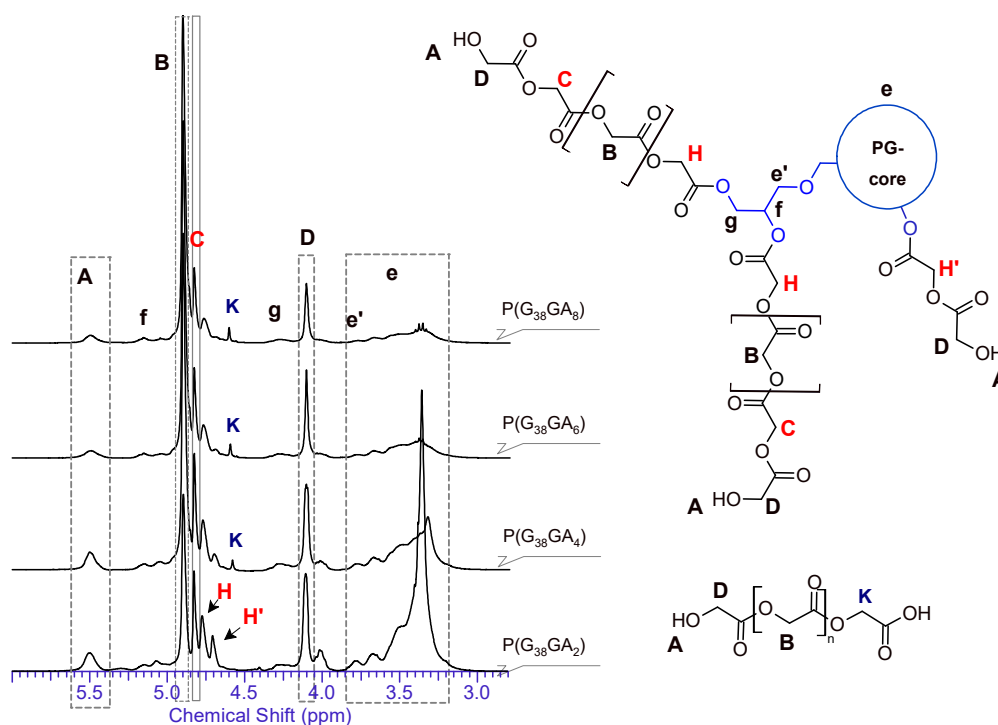


Figure 3. ^1H NMR analysis of the star-block copolymers with an increasing glycolide to poly(glycerol) ratio with PG_{38} as core molecule.

Furthermore, the signal denoted **A** at 5.5 ppm can be assigned to the terminal hydroxyl group of the arms. This important signal assignment was confirmed by an ^1H COSY NMR experiment (Figure 4), relying on the cross correlation of the methylene group **D** with the hydroxyl proton **A**. Verification of the assignment of methylene and methine protons of the esterified primary and secondary OH groups of the PG core is crucial, since they evidence the successful linkage of arms and core. Unequivocal proof of attachment is obtained from the cross correlation of the methine/methylene proton of the major initiating species, the terminal glycerol units of *hb*-PG. Clear cross correlations between esterified secondary PG-OH (methine proton) groups (**f**) and esterified primary PG-OH (methylene proton) units (**g**) as well as esterified secondary PG-OH methine (**f**)/primary ether (**e**) methylene protons can be observed. In the 2D NMR spectra of the star polymers, these protons have undergone a significant downfield shift (5.0–5.4 ppm), compared to the non-functionalized *hb*-PG-related signals, which are mainly found between 3.82 and 3.1 ppm. Although direct experimental proof could not be provided via 2D NMR, the signal denoted **C** at 4.84 ppm is assigned to the penultimate glycolic acid repeat unit. The first glycolic acid repeat unit, directly attached to the PG core, is represented by two different signals: **H** (4.78 ppm) or **H'** (4.72 ppm). While **H** corresponds to the first glycolic acid unit of a PGA chain, directly attached to the poly(glycerol) core, **H'** represents the special case of an α -unit of a glycolic acid dimer directly attached to the PG core (i.e. first and penultimate unit at the same time). Hence **H'** is predominantly observed for low glycolide fractions.

This signal assignment is consistent with literature data for PGA-co-poly(ϵ -caprolactone) copolymers,^{36,37} as well as PLLA-PG star block copolymers which have recently been developed by our group.²²

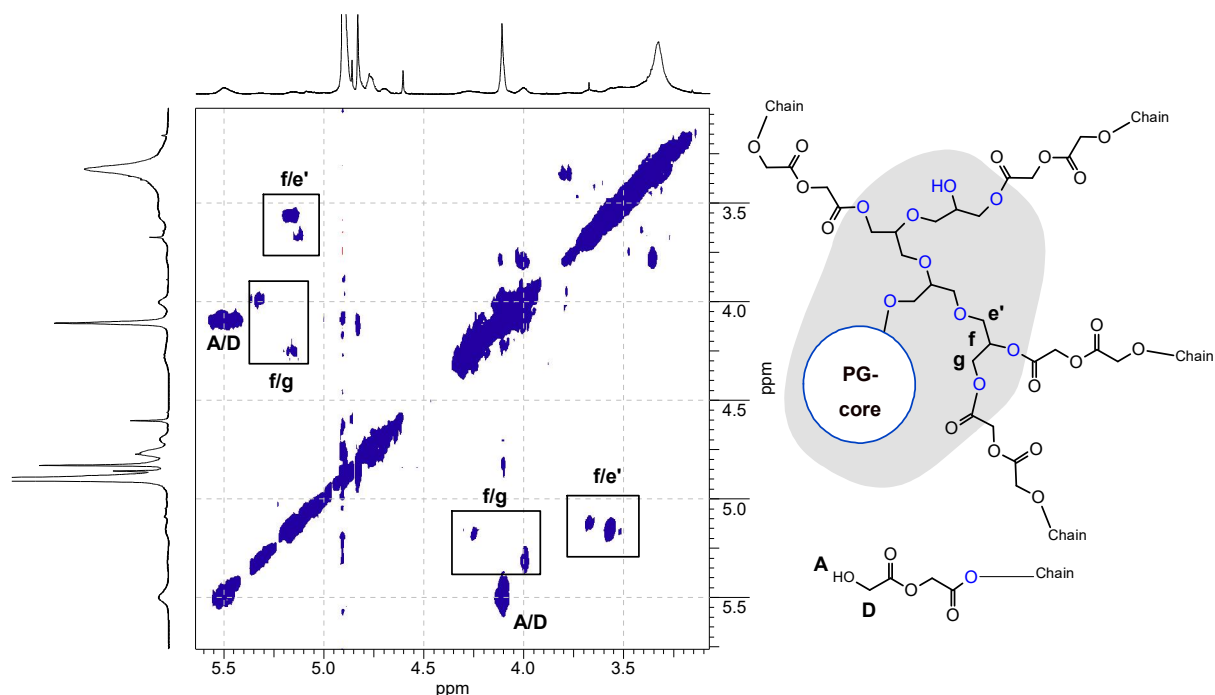


Figure 4. $^1\text{H},^1\text{H}$ -Correlation COSY NMR: This experiment visualizes correlations of terminal groups with their adjacent hydroxyl groups as well as correlations within esterified glycerol units (f/g & f/e'). The most pronounced cross correlation peak can be assigned to the terminal hydroxyl-methyl group of poly(glycolide) at 5.5/4.12 ppm (A/D).

The ^1H COSY NMR spectrum further suggests that the linear and terminal glycolic acid units do not suffer from signal superposition and can thus be evaluated for the determination of the average arm length, which was achieved by the comparison of end-group- and backbone-related signals (B and D). Although a precise signal-to-structure correlation is difficult to establish, differentiation between PG and poly(glycolide) signals was achieved, confirming successful grafting of poly(glycolide) onto the PG core. Even more important, it was confirmed that the majority of the hydroxyl groups of PG, particularly in the periphery of the core, was esterified.

An interesting correlation between the high-molecular-weight modes observed in SEC and the NMR spectra was found in the singlet, present at 4.61 ppm (K). According to literature data, this can be related to a carboxylic acid chain end of PGA homopolymer.³⁸ It can be observed for samples that exhibit an additional mode in SEC. This therefore supports the assumed formation of PGA homopolymer by co-initiation with water. Despite careful drying of the hygroscopic PG macroinitiator in vacuo, contamination with water could obviously not be fully eliminated. Since glycolide has been

used as received and not stored in vacuo or under an inert gas atmosphere, this is the most likely cause for the introduction of traces of moisture into the system.

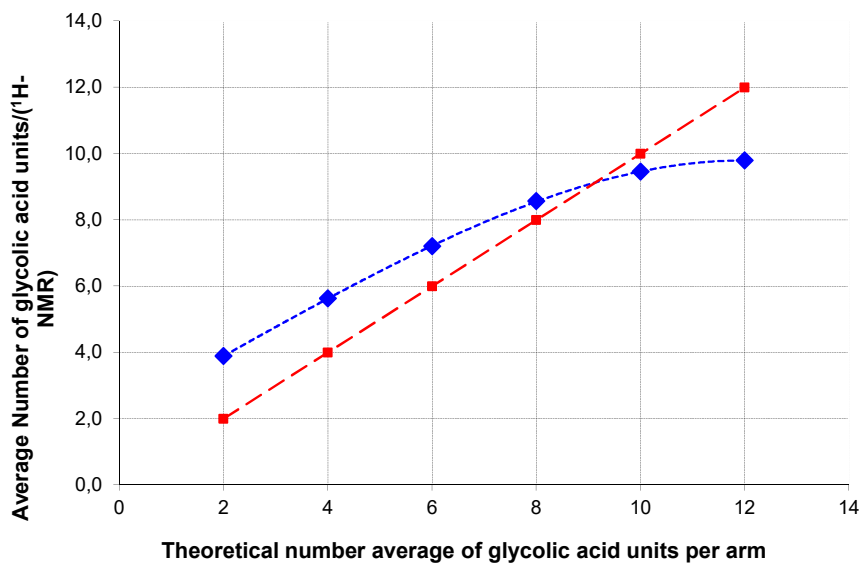


Figure 5. Comparison of average number of repeat units vs. the theoretical number based on the ratio of PG and glycolic acid. The dotted line represents the ideal case of matching numbers and was added as guide to the eyes.

The graph shown in Figure 5 relates the number of glycolic acid repeat units per arm, calculated from ¹H NMR for the series of PG38-derived star polymers. These values are compared with the theoretical number expected from the ratio of glycolide monomer to the sum of possible initiating sites in hb-PG. Indeed, an interesting trend can be observed. This trend is most likely influenced by two factors: 1.) For very low and moderate numbers of GA repeat units, the observed chain length of the glycolide stars exceeds theoretical expectations. This difference can be attributed to the difference in accessibility and nature (primary/secondary) of the hydroxyl groups of the hyperbranched PG core. A certain fraction of potential initiating sites suffers from a reduced reactivity towards the employed glycolide lactone monomer. Especially, the hydroxyl groups close to the core of the hyperbranched structure and/or those of a secondary nature are less active toward glycolide addition. The first ring-opening step of the glycolide lactone always generates/retains a primary hydroxyl group which is more reactive for the attachment of further glycolide monomers than the average PG-hydroxyl groups. Nevertheless, the observed yield of the precipitated star polymers (Table 1) was high enough to assume conversions exceeding 90% before the polymer melt congealed. In addition, ¹H NMR spectra of the samples showed no residual glycolide monomer with its distinct singlet signal at 5.06 ppm (in DMSO-d₆).

2.) With increasing arm length, the observed number of units drops below the theoretical value. As stated above, we assume that water was introduced via the glycolide monomer (indicated by signal K). Hence, co-initiation by trace amounts of water increases with increase in the glycolide/macroiinitiator ratio.

Since the effect discussed in the second postulate counteracts that in the first, we observe the described trend as an overestimation of the chain length rather than an underestimation. During the polymerization in the melt, continuous polymer melts with high viscosity are only observed for samples with a targeted average of up to 5–6 GA units. For longer arm lengths, the high mobility of the oligo-GA chains contributes to the consolidation of the melt via crystallization when reaching high conversion with a lack of molten glycolide monomer that can act as a plasticizer. This is supported by the results of the DSC measurements (Figure 6) of the star copolymers *hb*-PG₃₈-*b*-GA₄, *hb*-PG₃₈-*b*-GA₈ and *hb*-PG₃₈-*b*-GA₁₂ which confirm the variety of glycolide arm lengths achieved.

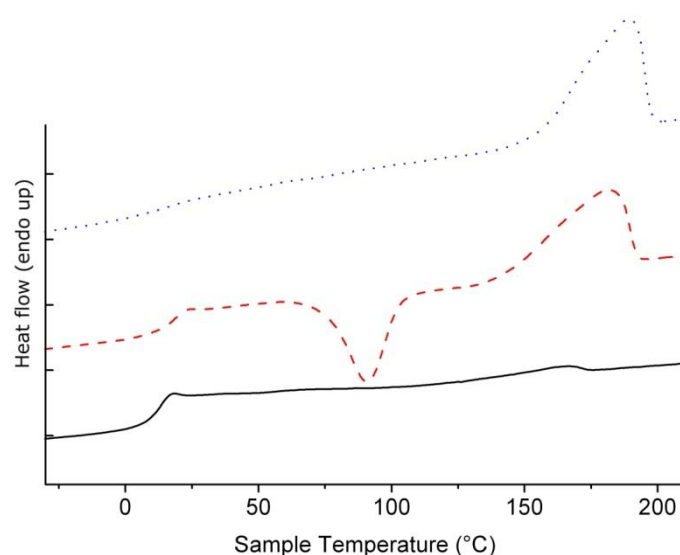


Figure 6. DSC-heating traces (second heating run at 20°C/min) for *hb*-PG₃₈-*b*-GA₄ (bottom); *hb*-PG₃₈-*b*-GA₈ (middle) and *hb*-PG₃₈-*b*-GA₁₂ (top), reflecting the increasing influence of poly(glycolide) chain length.

Table 2. Thermal properties of selected multi-arm star copolymers.

Samples	GA- units/arm(theor.)	. GA- units/arm (found)	T _g (°C)	ΔH _m (J/g)	T _m (°C)
P(G ₃₈ GA ₄)	4	5.6	10.13	3.1	161.4
P(G ₃₈ GA ₈)	8	8.6	15.44	57.6	180.7
P(G ₃₈ GA ₁₂)	12	9.8	17.5	59.9	189.5

Generally, the observed glass transition (T_g) of the glycolide arms for *hb*-PG₃₈-*b*-GA₂ and *hb*-PG₃₈-*b*-GA₄ is significantly depressed (10-18 °C) in comparison to literature data for PGA homopolymers (approximately 40–50 °C).³⁹ This reflects the influence of the flexible PG core. The T_g increased slightly with molecular weight, as it is also observed for most linear polymers. Both findings can be attributed to the low average number of repeating units per arm and are often observed for oligomers. This generally ensures increased chain mobility. As expected, this increased mobility enables efficient crystalline packing for a very short average chain length of 8.6 GA repeating units (for *hb*-PG₃₈-*b*-GA₈). Even for *hb*-PG₃₈-*b*-GA₄ with very low average PGA arm length a slight endothermic melting peak is visible in the DSC heating trace. The high crystallization tendency of the star block copolymers, despite the generally impeded crystallization due to the strongly branched PG core, is obvious from the data. An average chain length of less than 8-9 glycolic acid units is sufficient for a crystallization-induced vitrification of the polymer melt at 120 °C. The observed melting temperatures for star-shaped PGA range between 170 and 190 °C (Table 2) and are significantly depressed compared to PGA homopolymers of comparable molecular weight. This should allow polymer processing at lower temperatures which is, in particular, advantageous for such a thermolabile material.

Conclusion

This work presents the first synthesis of star block copolymers based on glycerol and glycolide. *Hb*-PG-*b*-PGA multi-arm star copolymers have been prepared via a core first approach, using hyperbranched poly(glycerol) with different hydroxyl functionalities as core molecules. The melt copolymerization with *hb*-PG as macroinitiator via Sn(Oct)₂ catalysis afforded well-defined complex polymer structures with predictable molecular weights. In contrast to their linear analogs of comparable molecular weight, the polymers exhibited superior solubility in organic solvents such as DMF and DMSO. This permitted detailed characterization via 1D and 2D NMR, SEC and DSC. It should be emphasized that the multi-arm star polymers presented possess molecular weights up to 31,000 g/mol and high glycolide weight content up to approximately 91 wt %. The short chain lengths of the oligoglycolic acid chains along with the increased number of end-groups are expected to enhance hydrolytic degradability significantly, rendering the novel materials promising candidates for drug release applications.

Experimental Section

Instrumentation

^1H NMR spectra were recorded at 300 MHz on a Bruker AC 300. The spectra were measured in DMSO-d_6 and the chemical shifts are referenced to residual solvent signals. (^1H proton NMR signal: 2.50 ppm). 2D-NMR experiments were performed on a Bruker Avance-II-400 (400 MHz) equipped with an inverse multinuclear 5mm probe head and a z-gradient coil. Standard pulse sequences for gs-COSY, and gs-NOESY experiments were used. The refocusing delays for the inverse hetero-correlations were set to 3.45 and 62.5 ms, corresponding to $^1J_{\text{C,H}} = 145$ Hz and $^nJ_{\text{C,H}} = 8$ Hz, respectively.

For SEC measurements in DMF (containing 1 g/L of lithium bromide as an additive), an Agilent 1100 series was used as an integrated instrument, including a PSS Gral column ($10^4/10^4/10^2$ Å porosity) and RI detector. Calibration was achieved with poly(ethylene glycol) standards provided by Polymer Standards Service (PSS)/Germany. Differential scanning calorimetry (DSC) measurements were carried out on a Perkin-Elmer 7 Series Thermal Analysis System with auto sampler in the temperature range of -40 to 230 °C at a heating rate of 20 K/min. The melting points of indium ($T_m = 156.6$ °C) and Millipore water ($T_m = 0$ °C) were used for calibration.

Reagents.

Diglyme (99%) and glycidol (Sigma Aldrich) were purified by vacuum distillation over CaH_2 directly prior to use. Tetrahydrofuran (THF) was refluxed with sodium/benzophenone before distillation. Glycolide was purchased from Purac®/Gorinchem (Netherlands) and used as received. Tin(II)-2-ethylhexanoate ($\text{Sn}(\text{Oct})_2$), 97% was obtained from Acros and used as received.

The synthesis of *hb*-PG was conducted as described in previous publications, using the slow monomer addition technique.^{21,25,26}

“Grafting from” polymerization of glycolide with hyperbranched polyglycerol-polyol as a macroinitiator. In a typical experiment, exemplified for the synthesis of star-block copolymers *hb*-PG₃₈-*b*-GA₆ 0.530 g *hb*-PG₃₈ (0.181 mmol/7.33 mmol of primary and secondary hydroxyl groups, according to equation 1) were placed in a flask immersed in an oil bath at 120 °C and evacuated for at least 20 minutes. 2.55 g (22.0 mmol) of glycolide were charged to the flask, which was re-immersed into the oil bath. 75 µl of a 10% solution of $\text{Sn}(\text{Oct})_2$ (= 0.022 mmol) were injected to the homogenous melt. The mixture was stirred vigorously under N_2 atmosphere for 24 h. After cooling down, the mixture was dissolved in hexafluoroisopropanol, and precipitated in excess diethyl ether. The precipitation/purification process was executed twice to yield pure polymer. The product was isolated by filtration and dried in vacuum at room temperature for 24 h to yield a white powder in all

cases, except for the copolymer with an average targeted GA amount of 2 units per arm (P(G₃₈GA₂)), which gave a viscous, non transparent, white oil.

Acknowledgement. Florian Wolf acknowledges the IMPRS (International Max Planck-Research School) of the Max Planck Society for continuous support. The authors thank Heinz Kolshorn for his valuable help with the detailed NMR characterization of the materials. H. F. acknowledges valuable support from the Fonds der Chemischen Industrie as well as from the SFB 625.

References

1. Sanda, F.; Sanada, H.; Shibasaki, Y.; Endo, T. *Macromolecules* **2002**, *35*, 680-683. doi:10.1021/ma011341f
2. Li, Y.; Kissel, Th. *Polymer* **1998**, *39*, 4421-4427. doi:10.1016/S0032-3861(97)10362-7
3. Sekine, S.; Yamauchi, K.; Aoki, A.; Asakura, T. *Polymer* **2009**, *50*, 6083-6090. doi:10.1016/j.polymer.2009.10.040
4. Lu, C.; Liu, L.; Guo, S.-R.; Zhang, Y.; Li, Z.; Gu, J. *Eur. Polym. J.* **2007**, *43*, 1857-1865. doi:10.1016/j.eurpolymj.2007.02.039
5. Buwalda, S. J.; Dijkstra, P. J.; Calucci, L.; Forte, C.; Feijen, J. *Biomacromolecules* **2010**, *11*, 224-232. doi:10.1021/bm901080d
6. Burgath, A.; Sunder, A.; Neuner, I.; Mülhaupt, R.; Frey, H. *Macromol. Chem. Phys.* **2000**, *201*, 792-797. doi:10.1002/(SICI)1521-3935(20000401)201:7<792::AID-MACP792>3.0.CO;2-K
7. Wolf, F. K.; Frey, H. *Macromolecules* **2009**, *42*, 9443-9456. doi:10.1021/ma9016746
8. Joziassse, C. A. P.; Grablowitz, H.; Pennings, A. J. *Macromol. Chem. Phys.* **2000**, *201*, 107-112. doi:10.1002/(SICI)1521-3935(20000101)201:1<107::AID-MACP107>3.0.CO;2-W
9. Satoh, T. *Soft Matter* **2009**, *5*, 1972-1982. doi:10.1039/b819748b
10. Jones, M.-C.; Gao, H.; Leroux, J.-C. *J. Controlled Release* **2008**, *132*, 208-215. doi:10.1016/j.jconrel.2008.05.006
11. Lemmouchi, Y.; Perry, M. C.; Amass, A. J.; Chakraborty, K.; Schacht, E. *J. Polym. Sci., Part A: Polym. Chem.* **2007**, *45*, 3966-3974. doi:10.1002/pola.22150
12. Jie, P.; Venkatraman, S. S.; Min, F.; Freddy, B. Y. C.; Huat, G. L. *J. Controlled Release* **2005**, *110*, 20-33. doi:10.1016/j.jconrel.2005.09.011
13. Lapienis, G. *Prog. Polym. Sci.* **2009**, *34*, 852-892. doi:10.1016/j.progpolymsci.2009.04.006
14. Finne, A.; Albertsson, A.-C. *Biomacromolecules* **2002**, *3*, 684-690. doi:10.1021/bm020009o
15. Tsuji, H.; Miyase, T.; Tezuka, Y.; Saha, S. K. *Biomacromolecules* **2005**, *6*, 244-254. doi:10.1021/bm049552q

16. Nagahama, K.; Shimizu, K.; Ouchi, T.; Ohya, Y. *React. Funct. Polym.* **2009**, *69*, 891-897. doi:10.1016/j.reactfunctpolym.2009.09.004
17. Zhao, Y.; Shuai, X.; Chen, C.; Xi, F. *Chem. Mater.* **2003**, *15*, 2836-2843. doi:10.1021/cm0210694
18. Zhao, Y.; Shuai, X.; Chen, C.; Xi, F. *Macromolecules* **2004**, *37*, 8854-8862. doi:10.1021/ma048303r
19. Wolf, F. K.; Frey, H. *Macromolecules* **2009**, *42*, 9443-9456. doi:10.1021/ma9016746
20. Cao, P.-F.; Xiang, R.; Liu, X.-Y.; Zhang, C.-X.; Cheng, F.; Chen, Y.J. *Polym. Sci., Part A: Polym. Chem.* **2009**, *47*, 5184-5193. doi:10.1002/pola.23568
21. Sunder, A.; Hanselmann, R.; Frey, H.; Mülhaupt, R. *Macromolecules* **1999**, *32*, 4240-4246. doi:10.1021/ma990090w
22. Sunder, A.; Frey, H.; Mülhaupt, R. *Macromol. Symp.* **2000**, *153*, 187-196. doi:10.1002/1521-3900(200003)153:1<187::AID-MASY187>3.0.CO;2-I
23. Sunder, A.; Mülhaupt, R.; Haag, R.; Frey, H. *Adv. Mater.* **2000**, *12*, 235-239. doi:10.1002/(SICI)1521-4095(200002)12:3<235::AID-ADMA235>3.0.CO;2-Y
24. Wilms, D.; Wurm, F.; Nieberle, J.; Böhm, P.; Kemmer-Jonas, U.; Frey, H. *Macromolecules* **2009**, *42*, 3230-3236. doi:10.1021/ma802701g
25. Wilms, D.; Stiriba, S.-E.; Frey, H. *Acc. Chem. Res.* **2010**, *43*, 129-141. doi:10.1021/ar900158p
26. Calderón, M.; Quadir, M. A.; Sharma, S. K.; Haag, R. *Adv. Mater.* **2010**, *22*, 190-218. doi:10.1002/adma.200902144
27. Knischka, R.; Lutz, P. J.; Sunder, A.; Mülhaupt, R.; Frey, H. *Macromolecules* **2000**, *33*, 315-320. doi:10.1021/ma991192p
28. Frey, H.; Haag, R. *Rev. Mol. Biotechnol.* **2002**, *90*, 257-267. doi:10.1016/S1389-0352(01)00063-0
29. Shen, Y.; Kuang, M.; Shen, Z.; Nieberle, J.; Duan, H.; Frey, H. *Angew. Chem., Int. Ed.* **2008**, *47*, 2227-2230. doi:10.1002/anie.200704572
30. Sunder, A.; Krämer, M.; Hanselmann, R.; Mülhaupt, R.; Frey, H. *Angew. Chem., Int. Ed.* **1999**, *38*, 3552-3555. doi:10.1002/(SICI)1521-3773(19991203)38:23<3552::AID ANIE3552>3.0.CO;2-G
31. Slagt, M. Q.; Stiriba, S.-E.; Klein Gebbink, R. J. M.; Kautz, H.; Frey, H.; van Koten, G. *Macromolecules* **2002**, *35*, 5734-5737. doi:10.1021/ma020094s
32. Stiriba, S.-E.; Kautz, H.; Frey, H. *J. Am. Chem. Soc.* **2002**, *124*, 9698-9699. doi:10.1021/ja026835m
33. Burakowska, E.; Quinn, J. R.; Zimmerman, S. C.; Haag, R. *J. Am. Chem. Soc.* **2009**, *131*, 10574-10580. doi:10.1021/ja902597h

34. Gottschalk, C.; Wolf, F.; Frey, H. *Macromol. Chem. Phys.* **2007**, *208*, 1657-1665.
doi:10.1002/macp.200700168
35. Chen, Y.; Shen, Z.; Barriau, E.; Kautz, H.; Frey, H. *Biomacromolecules* **2006**, *7*, 919-926.
doi:10.1021/bm050784e
36. Kasperczyk, J. *Macromol. Chem. Phys.* **1999**, *200*, 903-910. doi:10.1002/(SICI)1521-3935(19990401)200:4<903::AID-MACP903>3.0.CO;2-6
37. Dali, S.; Lefebvre, H.; El Gharbi, R.; Fradet, A. *e-Polym.* **2007**, No. 65.
38. Dali, S.; Lefebvre, H.; El Gharbi, R.; Fradet, A. *J. Polym. Sci., Part A: Polym. Chem.* **2006**, *44*, 3025-3035. doi:10.1002/pola.21405
39. Baker, G. L.; Vogel, E. B.; Smith, M. R., III. *Polym. Rev.* **2008**, *48*, 64-84.
doi:10.1080/15583720701834208

3.2 Synthesis of Branched Glycerol-Based Poly(glycolide) Copolymers via Ring-Opening Polymerization

Anna M. Fischer, Christoph Schüll and Holger Frey

Abstract

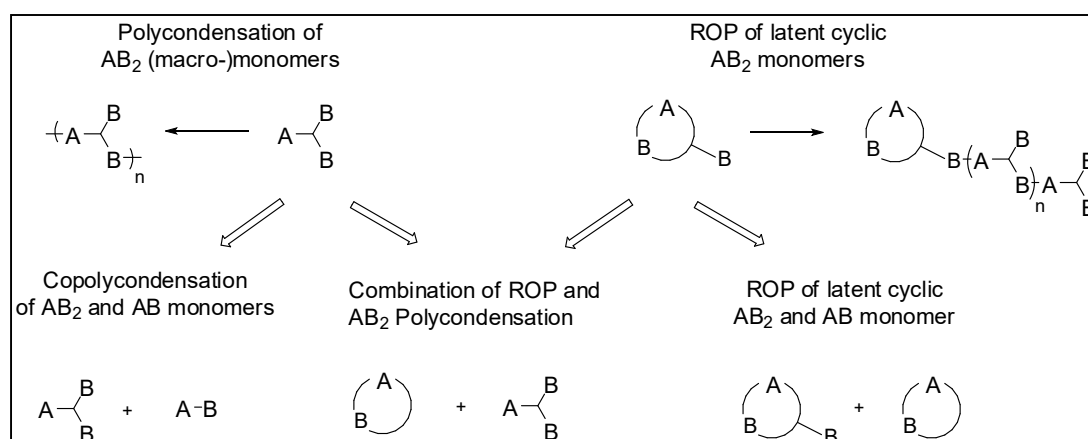
The Sn(Oct)₂-catalyzed synthesis of hyperbranched poly(glycolide) copolymers with glycerol branching points in the backbone via ring-opening multibranching copolymerization (ROMBP) of glycolide and 5HDON (5-hydroxymethyl-1,4-dioxan-2-one) is described. Using this strategy, well-defined soluble branched polyesters with molecular weights in the range of 1300 to 2000 g·mol⁻¹ and varying comonomer content (5HDON/glycolide=30:70-70:30) were obtained. 2D NMR spectroscopy, thermal analysis and MALDI-ToF mass spectrometry confirmed the successful incorporation of both monomers and the resulting branched structure. Multiple end group functionality offers the possibility for further post-polymerization modification, making these materials interesting for improved processing of PGA and potential applications ranging from novel polyurethane materials to biomedical targeting.

Introduction

In recent times, considerable attention has been paid to polyester-based materials produced from renewable resources because of their contribution in reducing the environmental impact.¹ In addition, limited fossil energy resources make non-degradable petroleum-based plastics less attractive. Both poly(lactic acid) (PLA) and poly(glycolic acid) (PGA) meet today's requirements of pharmaceutical and packaging industry and therefore represent widely used polymers in this area. Biocompatibility and biodegradability in vivo and in vitro render these materials highly attractive, especially in biomedical applications.^{2,3} Particularly glycolide is a favorable monomer for random copolymerization with other cyclic lactones to adjust degradation time by tuning the comonomer ratio. Despite its increased hydrophilic character and high tensile strength in comparison with PLA, PGA homopolymers have been scarcely utilized over time. This is based on three major key features: On the one hand PGA possesses a high melting temperature (210-230°C),⁴ which requires special processing techniques^{5,6} and characterization methods, e.g., solid state NMR spectroscopy,⁷ second, it shows insolubility in most common organic solvents, and third, it has a higher degradation rate⁸ in comparison with other polyesters.

Several methods may be pursued to facilitate handling of PGA: variation of the macromolecular architecture by copolymerization with other lactones,⁹⁻¹¹ limitation of the critical PGA chain length¹² or the introduction of branching points into the backbone.¹³ Since PGA possesses no side-chain functionalities at the backbone, the availability of reactive groups is highly desirable to tune the properties or for the attachment of relevant drugs. In the current work, the synthesis of branched, glycerol-based poly(glycolide) copolymers has been chosen to improve solubility via the introduction of branching points. Moreover, this concept also increases the number of end groups that are available for further functionalization.

There are three major pathways to synthesize hyperbranched polyesters based on AB₂ monomers (Scheme 1): First, polycondensation of AB₂ monomers,¹⁴ e.g., bishydroxy acids¹⁵ or self-designed AB₂ macromonomers;¹⁶ second, ring-opening polymerization (ROP) of latent AB₂ cyclic lactones¹⁷ and third, a combination of cyclic lactone ROP and AB₂-polycondensation.¹⁸ Within the first two strategies, one may distinguish between copolycondensation of AB and AB₂ monomers and the ROP of AB cyclic lactone and latent AB₂ monomers.¹⁹ Due to their branched structure and the high number of functionalities, branched polymers exhibit unique properties in comparison to their linear analogues.^{20,21} Usually, they exhibit low viscosities, low glass transition temperatures, and no entanglement.^{22,23} In contrast to perfectly branched dendrimers, randomly (hyper-)branched polymers are preferred for production on large scale due to their availability in sizable quantities mostly in a one-pot process.²⁴⁻²⁶



Scheme 1. Several synthesis strategies towards hyperbranched polyesters (with A=COOH groups and B=OH groups; in cyclic monomers after ring-opening).

In a recent work, we demonstrated the synthesis of hyperbranched poly(glycolide) copolymers using ROP and subsequent AB₂ polycondensation.¹³ However, this synthetic route requires harsh reaction conditions, i.e., reaction temperatures up to 170°C. This may lead to side reactions like transesterification, etherification²⁷ as well as broad molecular weight distributions ($M_w/M_n > 2$), well-

known for multifunctional step-growth polymerization. Therefore, in the current work we followed a route used by Wolf et al. which involves the inimer-promoted, ring-opening multibranching copolymerization (ROMBP) under mild reaction conditions.^{19a} Here, we wish to establish a new type of branched glycerol-based poly(glycolide) copolymer, utilizing a ring-opening copolymerization strategy to obtain macromolecules with an adjustable degree of branching and variable molecular weights. Glycerol is a side-product generated in large quantities in biodiesel and oleochemical industry. Downsizing the glutted markets worldwide via the conversion of glycerol into value-added products is an appreciated aim of current research.²⁸ Therefore, we focused on the Sn(Oct)₂-catalyzed ROMBP of glycolide with the latent cyclic AB₂ monomer 5-hydroxymethyl-1,4-dioxan-1-one (5HDON), a cyclic lactone with a pendant hydroxyl group obtained from glycerol. The kinetics of the branching reaction was studied via ¹H NMR spectroscopy and SEC analysis. One- and two-dimensional NMR spectrometry of the copolymers was performed to characterize the polymers in detail.

Experimental Section

Instrumentation. ¹H and ¹³C NMR spectra were recorded on a Bruker AC 300 (300 MHz, 75.5 MHz), a Bruker Avance-II 400 (400 MHz, 100.6 MHz) and a Bruker ARX 400 (400 MHz, 100.7 MHz) spectrometer. The chemical shifts were referenced internally to the solvent signal (¹H NMR (DMSO-d₆): 2.5 ppm; ¹³C NMR (DMSO-d₆): 39.52 ppm). FT-IR spectra were recorded on a Nicolet SDXC FT-IR spectrometer equipped with an ATR unit. Size exclusion chromatography (SEC) was carried out in DMF containing 0.25 g·L⁻¹ LiBr using an Agilent 1100 Series GPC Setup, including a HEMA column (10⁶/10⁵/10⁴ g·mol⁻¹), and RI as well as UV detectors. Calibration was carried out with polystyrene standards provided by Polymer Standards Service (PSS). Preparative SEC was carried out in DMF using a SEC setup with a Knauer HPLC pump K-501, an RI detector from Shodex RI-71 and a column (300x20 mm, MZ-Gelplus, 10μm) with 10³ Å porosity. Matrix-assisted laser desorption and ionization time-of-flight (MALDI-ToF) was performed on a Shimadzu AXIMA CFR MALDI-ToF mass spectrometer equipped with a nitrogen laser delivering 3 ns laser pulses at 377 nm. Dithranol (1,8-dihydroxy-9(10H)-anthracene, Aldrich 97%) was used as matrix while potassium triflate (Aldrich, 98%) was used as ionization agent. The samples were prepared from hexafluoroisopropanol solutions (1mg/0.1ml). The glass transition temperatures were measured by differential scanning calorimetry (DSC), using a Perkin Elmer 7 series thermal analysis system in the range of -100 to 200°C at heating rates of 10 and 20 K/min. The melting point of indium (156.6 °C) and of n-decane (-29.7 °C) were used for calibration.

Reagents. Glycolide was purchased from Purac®/Gorinchem (Netherlands), stored in a glove box and used as received. 5-Hydroxymethyl-1,4-dioxan-2-one (5HDON) was prepared according to literature

procedures and distilled prior to utilization.^{29,30} All reagents used were of analytical grade. Stannous-2-ethyl hexanoate ($\text{Sn}(\text{Oct})_2$, 97%) was obtained from Acros and used as received. All other chemicals were purchased from Sigma Aldrich or Acros, if not otherwise stated.

Synthesis

Procedure for the $\text{Sn}(\text{Oct})_2$ -catalyzed ring-opening polymerization of glycolide and 5HDON in bulk.

A Schlenk flask was charged with 5HDON in the quantities required and with a magnetic stir bar. The flask was closed with a rubber septum and transferred into the glove box, where stoichiometric amounts of glycolide were added. Outside the glove box, the flask was immersed into a preheated oil bath of 130°C. As soon as a homogenous melt was obtained, 0.1mol% $\text{Sn}(\text{Oct})_2$ (in 0.1ml toluene) were added by a syringe. The polymerization was conducted for 16 hours at 130 °C under argon atmosphere. Upon completion, the reaction mixture was dissolved in hexafluoroisopropanol (HFIP) and precipitated into methanol. After evaporation of the residual solvent, a glassy, solid polymer was obtained. ^1H NMR (400 MHz, DMSO-d_6): δ (ppm) 5.52 (br, OH), 5.37 (br, OH), 4.91-4.74 (PGA backbone CH_2OCO), 4.47-4.18 (5HDON backbone CH_2OCO , CH_2OR , CHO), 4.11-4.04 (terminal glycolic acid units CH_2OH), 3.91 (br, CH_D), 3.62 (br, CH_L), 3.49 (br, linear 5HDON units CH_2OH)

^{13}C NMR (300 MHz, DMSO-d_6): δ (ppm) 59.32-49.54 (terminal glycolic acid units; CH_2OH), 60.04-61.09 (PGA backbone CH_2OCO , B3), 62.04-63.50 (5HDON backbone A5/B5/C5), 64.66 (A3), 66.58-66.72 (B2/C2), 68.33-68.51 (A2), 68.82-69.05 (A4), 75.00-75.30 (CH_D), 78.14-78.53 (CH_L), 166.82-167.68 (PGA backbone COOR, A1), 169.66-170.29 (5HDON backbone COOR), 172.07-172.61 (terminal glycolic acid (GA) units OCOCH_2OH)

Synthesis of trifluoroacetate-functionalized copolyesters. A flask was charged with the respective copolyester sample and an excess of trifluoroacetic acid anhydride (TFA) was added under argon atmosphere. The mixture was stirred at room temperature for 3 hours until the glassy solid was completely dissolved. Residual TFA was removed by evaporation.

^1H NMR (400 MHz, DMSO-d_6): δ (ppm) 5.12-5.52 (CH_2OTf , GA), 4.97-4.77 (PGA backbone), 4.59-4.56 (CH_2OTf , 5HDON), 4.48-4.2 (5HDON backbone), 4.05 (CHCH_2OTf , 5HDON, CH_D2), 3.92 (CH_D1 , 5HDON)

Basic hydrolysis of the copolyesters in $\text{D}_2\text{O}/\text{NaOH}$ solution. In a flask with the appropriate copolyester sample, an excess of a 0.5 mM $\text{D}_2\text{O}/\text{NaOH}$ solution was added. The mixture was stirred at room temperature until the glassy solid was completely dissolved (30 min).

^1H NMR (400 MHz, D_2O): δ (ppm) 3.39 (s, a), 3.28 (s, b), 2.94 (m, c), 2.79 (m, CH)

Synthesis of phenylurethane-functionalized copolyesters. The sample $hbP(\text{GA}_{37}\text{CO-5HDON}_{63})$ was charged in a flask together with a magnetic stir bar and kept under argon atmosphere. The flask was immersed in a preheated oil bath (30°C) and an excess of phenyl isocyanate was added. The mixture was stirred overnight, quenched with HFIP and precipitated twice into methanol to yield a colorless powder.

FT-IR (ATR) $\tilde{\nu}$ [cm^{-1}]: 3325 (N-H), 2953; 1732 (C=O); 1600; 1537; 1500; 1427; 1188-1121 (C-O-C); 757-693

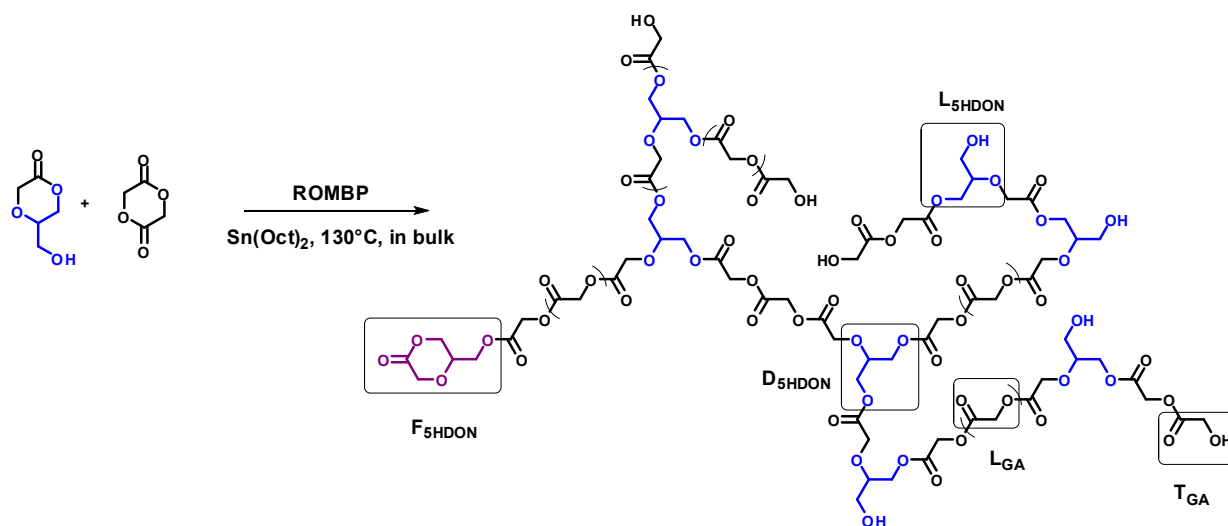
Results and Discussion

Synthesis and mechanism of ROMBP of glycolide and 5HDON. Generally, the ring-opening polymerization (ROP) of cyclic lactones is initiated via hydroxyl or amino groups in the presence of a catalyst, e.g., $\text{Sn}(\text{Oct})_2$ or 1,8-diazabicyclo[4.5.0]undec-7-ene (DBU).^{31,32} In contrast to other diesters (lactide, ϵ -caprolactone), the glycolide polymerization requires special reaction conditions due to the low solubility of monomer and polymer in common organic solvents.³³ In addition, the melt polymerization is challenging, as with increasing polymer chain length the melting temperature of the polymer increases. Furthermore, the polymer precipitates from the reaction mixture during polymerization due to lower polymerization temperatures in comparison with the polymers' melting point.⁶ Therefore, the $\text{Sn}(\text{Oct})_2$ -catalyzed ring-opening multibranching copolymerization (ROMBP) of glycolide and 5HDON was conducted in bulk at 130 °C to obtain a hyperbranched poly(glycolide) copolyester (*hbPGA*). The reaction temperature was kept at 130 °C to prevent precipitation when using higher glycolide contents and to avoid transesterification reactions, which arise at high reaction temperatures and long polymerization times.

$\text{Sn}(\text{Oct})_2$ was chosen as a catalyst, because it is well-known to catalyze the ROP of glycolide and other diesters efficiently via a coordination-insertion mechanism.³¹ Furthermore, $\text{Sn}(\text{Oct})_2$ is suitable for melt polymerizations of glycolide³⁴ and contributes to a homogenous melt, which is a prerequisite for an efficient ROP. The synthesis of *hbPGA* copolyesters requires a multifunctional lactone comonomer, 5-hydroxymethyl-1,4-dioxan-2-one (5HDON), which is based on glycerol and glycolic acid building blocks. The inimer 5HDON, functioning as initiator and monomer, bears one primary hydroxyl group, which can serve as an initiator for the copolymerization with glycolide. It is important to note that 5HDON was chosen as comonomer due to its primary hydroxyl group generated during ring-opening, ensuring efficient branching because of equal reactivity of all hydroxyl groups present during polymerization. 5HDON was freshly distilled prior to use, because of the tendency for autopolymerization, which generates terminal and linear subunits only, even after storage at low temperatures (Figure S1). 5HDON was prepared in a three-step synthesis according to literature procedures.^{29,30} The first step includes the synthesis of the glycerol benzylidene acetal. Then, the acetal is treated with bromo acetate and sodium hydride to generate the corresponding ether moiety. After acidic hydrolysis of the acetal moiety and removal of the benzaldehyde, low molecular weight polymers are obtained. Subsequent distillation of the oligomers gives the desired six-membered 5HDON via a back-biting mechanism (Scheme S1).

Rokicki et al.³⁰ reported that in contrast to the organobase 1,8-diazabicyclo[5.4.0]undec-7-ene (DBU), the tin catalyst suppresses the formation of terminal 5HDON units up to a certain time frame (< 24h).

The incorporation of one 5HDON terminal unit is negligible with respect to detailed spectroscopic analysis. After 24h, transesterification reactions occur and induce the formation of terminal 5HDON units. In order to limit the number of possible repeating units, the utilization of $\text{Sn}(\text{Oct})_2$ as a catalyst is favorable, especially with regard to ^1H NMR calculations



Scheme 2. Schematic illustration of the copolyester structure after ROMBP of glycolide and 5HDON with the incorporated subunits (dendritic (D), linear (L), terminal (T) and focal units).

Polymerization kinetics. Upon ring-opening of 5HDON, three different subunits arise (Scheme 2): focal (F), dendritic (D) and linear (L) units. To monitor the formation of dendritic units and the conversion of both monomers, time-dependent ^1H NMR measurements have been carried out. To this end, samples were collected from the melt at different times and the polymerization reaction was quenched by rapid cooling to -20°C . The aliquots were analyzed by ^1H NMR spectroscopy and SEC. In Figure 1 the development of the dendritic units in comparison to the linear 5HDON repeat units (D/L ratio) is plotted versus polymerization time. It should be mentioned, that the D/L ratio of 5HDON units cannot be correlated to the degree of branching (DB). To determine the DB value correctly, 5HDON as well as PGA repeat units have to be taken into account. The diagram shows a rapid increase for the D/L ratio of 5HDON units in the early stages of the polymerization, until equilibrium is reached. For high 5HDON/glycolide monomer ratios, the conversion of glycolide reaches completion faster than for low comonomer ratios (see Figure S2, S3), due to the lower reactivity of 5HDON compared to glycolide. In addition, one would assume that a higher initial 5HDON/glycolide ratio would result in a higher D/L ratio in the final polymer, which would be in correspondence with the assumption of a higher amount of branched repeat units for higher 5HDON content. Interestingly, this is not the case. At first, 5HDON is converted into focal 5HDON units via the

initiation of the ROP of glycolide. In the second step, if a sufficient amount of glycolide is present, the linear 5HDON units, formed via ROP of focal 5HDON units, are directly transferred into dendritic structures due to availability of an excess of glycolide monomer compared to 5HDON in the reaction system. This is in correspondence with the branching mechanism, which was recently described by our group.^{19a} In general, different reactivity of glycolide and 5HDON can be expected, due to the additional functional group in 5HDON and the availability of only one reaction site for ring-opening compared to glycolide. Still, after ring-opening only primary hydroxyl groups are formed for each monomer, leading to equal reactivity of all reactive sites during polymerization, in contrast to the formation of hyperbranched poly(lactide) by a related route.^{19a} We assume that due to the high reactivity of glycolide, the hydroxyl groups of unreacted 5HDON and those which are formed during ROP are consumed very fast. Therefore, lower glycolide content leads to a higher fraction of linear 5HDON units, and as a result the D/L ratio decreases for higher 5HDON/glycolide ratios. Since the calculation of the DB value must also include the linear PGA units, we may not transfer our observations to the final DB values. Upon approaching equilibrium of D/L 5HDON units, the SEC traces show no more shifting towards higher molecular weights. The shoulder arising at lower elution volumes might be due to transesterification reactions which most probably occur at longer reaction times.

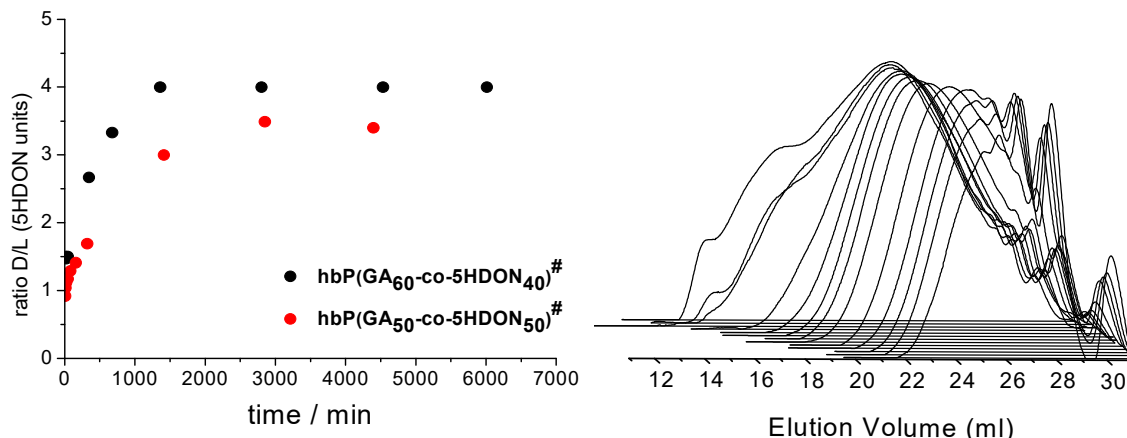


Figure 1. Left: Development of the D/L ratio of 5HDON units, calculated with time-dependent ^1H NMR measurements ($\#$ theoret. mol%); Right: the corresponding SEC traces (for $hbP(GA_{60}\text{-co-}5HDON_{40})$ (black dots), PS calibration standard, DMF as eluent).

Comparing the ^1H NMR spectra of the polymerization 5 min after initiation with the spectrum of 5HDON, we observe a new signal at 3.65 ppm, which arises with the formation of linear 5HDON units (Figure 2). Due to the signal overlap of monomer and polymer, a calculation of the D/L ratio is not possible before subtraction of the signals of residual monomer. Based on the conclusion (^{13}C NMR analysis) that no terminal 5HDON units arise during polymerization, the residual content of monomer

is given after subtraction of the signals of the linear methine protons (3.62 ppm) from the hydroxymethylene proton signals (3.49 ppm). The integral value of the dendritic methine signal is obtained after subtraction of the amount of monomer, calculated before. In Figure 2, the signals of the glycolic acid repeating units (4.70-4.91 ppm) may be clearly distinguished from those of residual glycolide monomer at 5.15 ppm. Furthermore, the signal at 4.95 ppm can be assigned to the hydroxyl protons of unconsumed 5HDON monomer. The given information enables to monitor the conversion of both monomers via ^1H NMR.

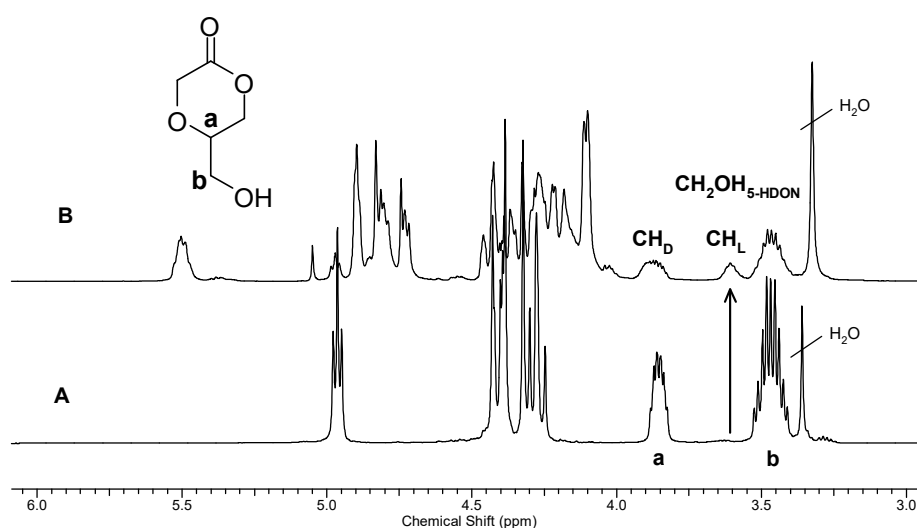


Figure 2. Comparison of the ^1H NMR spectra (400 MHz, $\text{DMSO}-d_6$) of (A) 5HDON and (B) copolymer (50:50 feed ratio) 5 min after initiation of the polymerization.

Structural characterization. All copolymerizations in this study were performed at 130°C in bulk for 16 hours to obtain almost complete conversion with systematic variation of the comonomer ratio in the presence of catalytic amounts of $\text{Sn}(\text{Oct})_2$. The structural elucidation is one major task to obtain information on the molar composition and the degree of branching (DB) of the resulting hyperbranched copolymers. Detailed NMR characterization of 5HDON model compounds and poly(lactide) copolymers, as recently described by our group,¹⁹ are a valuable support for the signal assignment. However, similar structural elements of the two comonomers and the sensitivity of GA methylene signals to the microstructure hamper the NMR analysis. A typical ^1H NMR spectrum of a branched glycerol-based PGA copolymer in $\text{DMSO}-d_6$ is shown in Figure 3. DMSO was chosen as a solvent for the NMR measurements because it ensures the solubility of the sample and has also been applied in NMR investigations of hyperbranched poly(5HDON)³⁰ and PGA.^{6,9,35} The characteristic signals for PGA backbone can be found in the range of 4.70 to 4.91 ppm (methylene group, assigned with $-\text{CH}_2\text{OR}_{\text{GA}}$). The terminal methylene groups of the PGA end group can be assigned at 4.05 to

4.10 ppm. Unfortunately, the methylene protons of the terminal PGA unit overlap with other 5HDON related signals. Thus, it is not possible to calculate the total conversion of the glycolide monomer during time-dependent ^1H NMR measurements. However, at high 5HDON/glycolide monomer ratios, faster glycolide conversion is observed in comparison to lower monomer ratios (see Supp. Inf., Figure S2, S3). This is in correspondence with the observation that more dendritic repeat units are formed at lower 5HDON/glycolide ratios and vice versa.

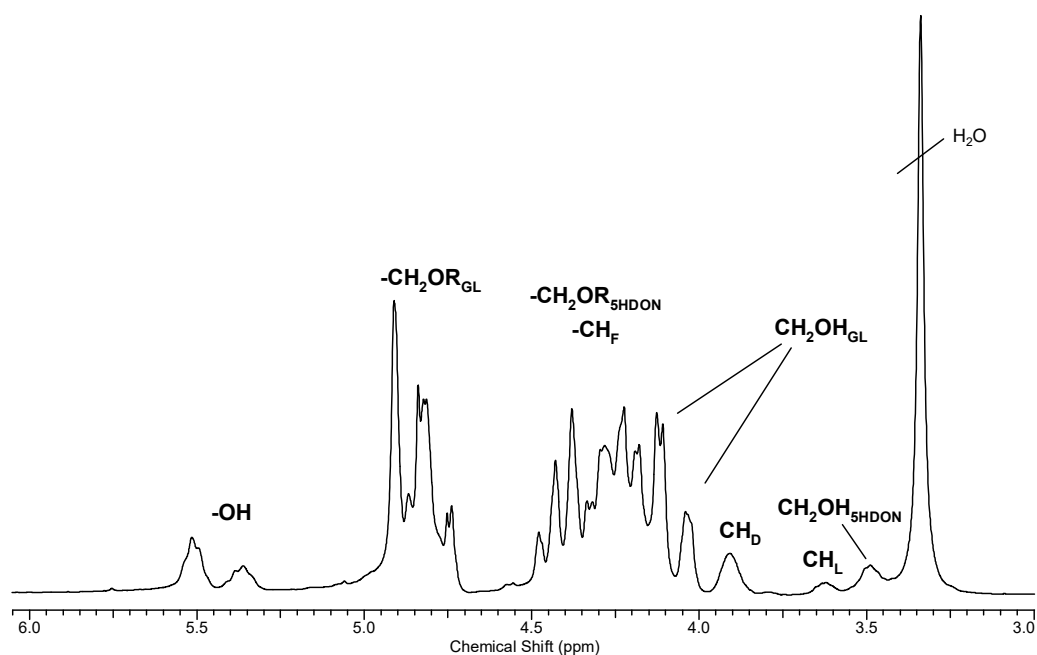


Figure 3. ^1H NMR spectrum (300 MHz, DMSO-d_6) of $hb\text{P}(\text{GA}_{65}\text{-co-5HDON}_{35})$.

The ^1H NMR spectra of copolymers with varying molar composition (see Supp. Inf., Figure S4) show an increase of the PGA backbone signal intensity at 4.91 ppm with increasing glycolide feed relative to other glycolide related signals. Within the signals of consumed 5HDON, one can differentiate between the etherified and esterified methylene protons which can be found in the region between 4.15-4.49 ppm. The identification of the 5HDON-related methine protons are of particular importance, because it reveals the different subunits and evidences successful branching. In order to differentiate the glycolide and 5HDON derived signals and to verify the structure assignment, 2D NMR analysis was performed. Figure 4 displays a typical HSQC (heteronuclear single quantum coherence) NMR spectrum of $hb(\text{PGA-co-5HDON})$ in DMSO-d_6 with additional coloured DEPT (distortionless enhancement polarization transfer) information. At first glance, three blue signals (A4, B4, C4) assigned to the 5HDON methine protons/carbons stem from the different subunits formed during ROP. A closer look in the region of 81 ppm verifies that no terminal 5HDON units are present. The hydroxyl groups of the terminal PGA units have been identified by $^1\text{H}, ^1\text{H}$ COSY NMR analysis (Figure S5, see Supp. Inf.) via the cross correlation of the methylene with the hydroxyl protons. The

HSQC NMR spectrum offers the possibility to clearly distinguish between PGA and 5HDON signals. Since the glycolide methylene and carbonyl carbons are sensitive to the microstructure, new signals arise due to the presence of 5HDON units. Additional HMBC (hetero multiple bond correlation) analysis evidences the formation of new methylene signals via the cross correlation of glycolide methylene protons with 5HDON related carbonyl carbon signals (Figure S6, see Supp. Info).

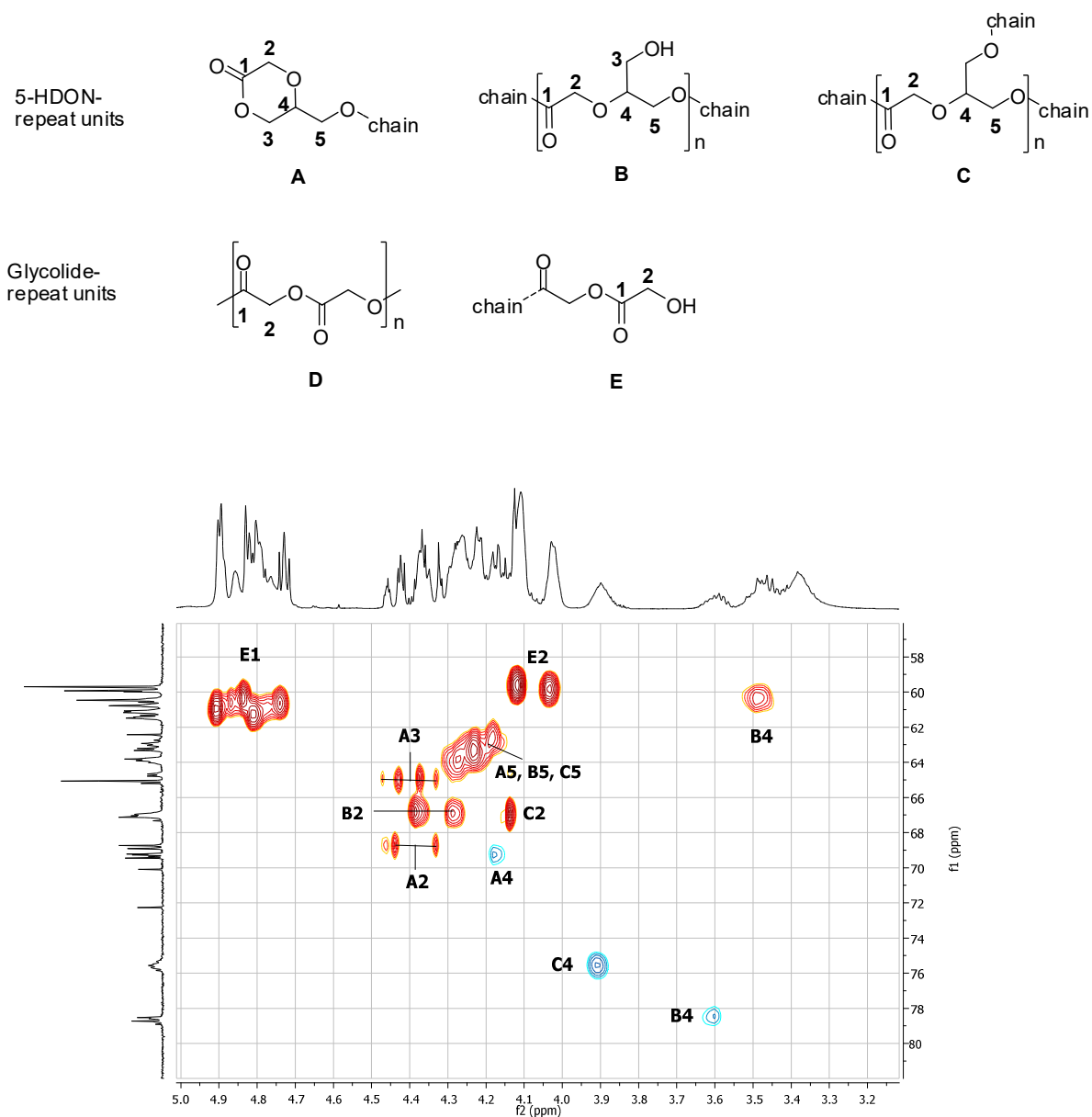


Figure 4. HSQC spectrum (400 MHz, DMSO-*d*₆) of *hbP*(GA₆₅-co-5HDON₃₅) with phase information given by coloration of cross peaks (red: methylene; blue: methine).

The molecular weight and the molecular weight distribution of the hyperbranched PGA copolymers were analyzed by SEC. In Figure 5, SEC traces of three different copolyesters are shown. In comparison with the SEC traces of a non purified sample, successful removal of unreacted monomers

and undesired oligomer side-products after precipitation in methanol is assured by the absence of former signals at lower retention times (see Supp. Inf., Figure S7).

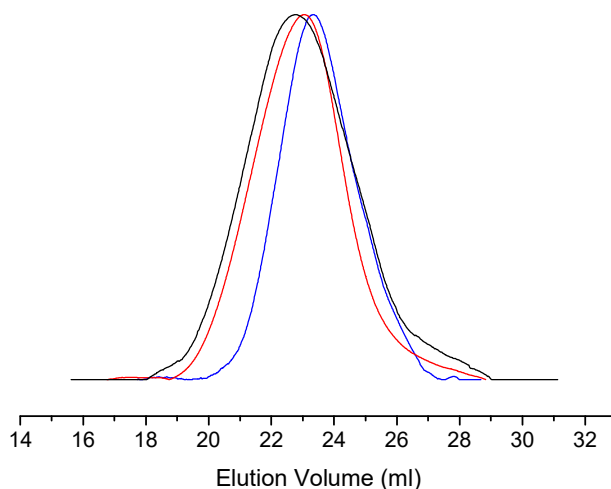


Figure 5. SEC traces (PS calibration standard, DMF as an eluent) of three branched glycerol-based PGA copolymers: *hbP*(GA₇₀-co-5HDON₃₀)(black); *hbP*(GA₆₄-co-5HDON₃₆) (red); *hbP*(GA₆₀-co-5HDON₄₀) (blue).

The polydispersities (M_w/M_n) of various copolyesters are in the range of 1.55 to 1.82, as expected for branched polymer architectures, synthesized by ROMBP.^{19a} The obtained values for the molecular weights, referenced to polystyrene (PS) standards, should be handled with care due to the different hydrodynamic volume of branched and linear macromolecules and the different chemical structure of PS compared to the polyesters. It is well-known that the molecular weight data for branched polymers determined via SEC using linear polymer standards is underestimated due to the lower hydrodynamic volume, which results in a higher retention time on the SEC column. As listed in Table 1, the molecular weights of *hbPGA* copolymers obtained by SEC are in the range of 1200 to 1800 g·mol⁻¹. The synthesized copolymers do not show a concise difference in the molecular weight with varying monomer feed ratio. However, the glycolide to 5HDON ratio, which ranges from 0.8 to 2.3 allows to adjust the average PGA chain length between the branching units (s. Figure 8). Due to insolubility of copolymers with a glycolide content > 70 mol%, higher molecular weights could not be obtained. Therefore, we assume that the copolymerization of glycolide and 5HDON leads to blocky incorporation of glycolic acid repeat units instead of a randomized copolyester structure. This results in insolubility of copolymers with higher glycolide content in common organic solvents, like DMSO or DMF.

Table 1. Characterization data of the synthesized copolymers of glycolide and 5HDON with different molar composition.

Sample	theo. feed ratio [mol%]	Calc. ^{a)} feed ratio [mol%]	Ratio GA/5HDON	M _n ^{b)} [g·mol ⁻¹]	M _w ^{b)} [g·mol ⁻¹]	M _w /M _n ^{b)}	DB ^{c)}	T _g ^{d)} [°C]
hbP(GA ₇₀ -co-5HDON ₃₀)	70:30	70:30	2.3	1300	3200	2.41	0.27	8.9
hbP(GA ₆₅ -co-5HDON ₃₅)	65:35	65:35	1.8	1700	3000	1.77	0.23	1.7
hbP(GA ₅₇ -co-5HDON ₄₃)	55:45	57:43	1.3	1800	3500	1.94	0.30	0.4
hbP(GA ₅₆ -co-5HDON ₄₄)	50:50	56:44	1.3	1400	3100	1.55	0.34	-8.2
hbP(GA ₄₅ -co-5HDON ₅₅)	40:60	45:55	0.8	2000	2100	1.51	0.32	-9.4
hbP(GA ₃₆ -co-5HDON ₆₄)	30:70	36:64	0.8	1200	2100	1.82	0.36	-16.3

^{a)}Feed ratio according to glycolide and 5HDON, determined via NMR after hydrolysis of the polymer in 0.5 mM D₂O/NaOH, ^{b)}determined via SEC in DMF with PS calibration standard, ^{c)} determined via ¹H NMR, ^{d)}determined by DSC (second heating scan, 10°C/min) with a heating rate of -50 to 50 °C, additional DSC data available in the Supp. Inf.

To calculate the molar repeat unit composition via ¹H NMR, the synthesized copolymers were hydrolyzed in basic milieu because of the overlap of 5HDON and glycolide signals, which impedes the integration of signal intensity for each single monomer. The composition was calculated according to equation 1:

$$\text{Glycolide [mol\%]} = \frac{\frac{\text{Integral } a}{2}}{\frac{\text{Integral } a}{2} + \text{Integral } b} \quad (1)$$

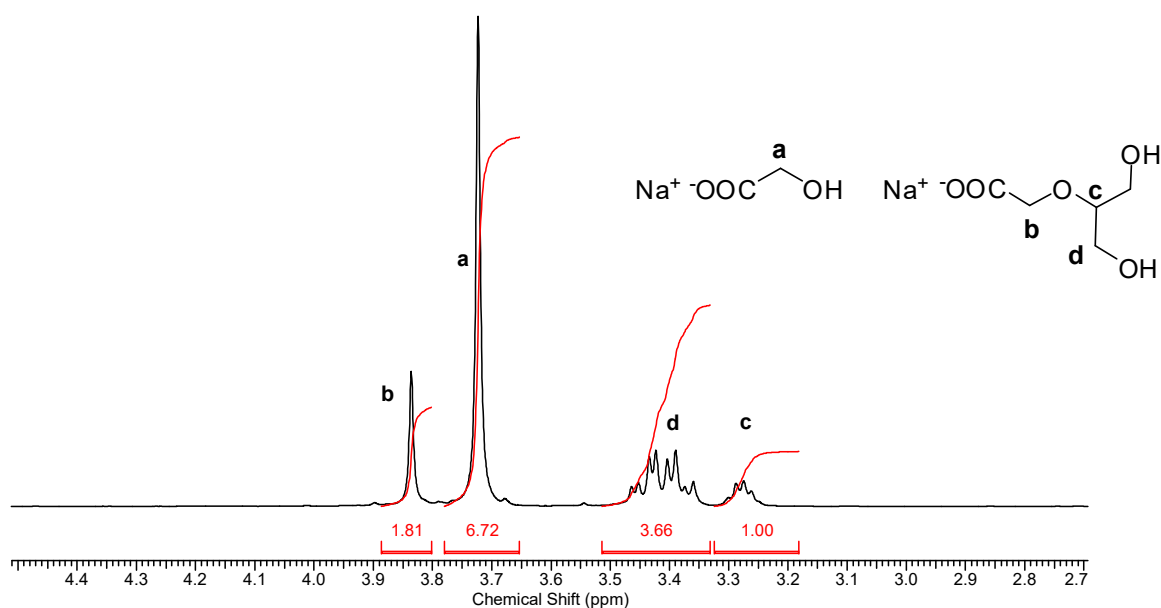


Figure 6. ^1H NMR (400 MHz, D_2O) after hydrolysis of $hbP(\text{GA}_{65}\text{-co-5HDON}_{35})$ in 0.5 mM NaOH/ D_2O solution.

Quantification of the degree of branching ($\text{DB} = 2\text{D}/(2\text{D} + \text{L}_{\text{CO}})$)³⁶⁻³⁸ has been accomplished by post-polymerization modification of the copolyesters with trifluoroacetic anhydride under mild conditions (Figure 7). Derivatization is necessary due to the signal overlap of relevant 5HDON and glycolide monomer signals. In this case, the resulting clearly distinguishable shift of the terminal glycolic acid units (4.04-4.11 ppm) to higher ppm values (5.12-5.52 ppm) allows differentiation between glycolide and 5HDON-related signals. Thereby, the dendritic (CH_{D1}) and linear (CH_{D2}) 5HDON units as well as the terminal (C) and linear (B) PGA units can be quantified directly by integration from the ^1H NMR spectrum. The quantity of focal 5HDON units was obtained indirectly from superimposed ^1H NMR signals. The degree of branching has been calculated by using the equation by Frey et al.³⁶

$$\text{Integral}(F_{5\text{HDON}}) = \frac{\text{Integral}(A) - [6 \times \text{Integral}(\text{CH}_{\text{D1}}) + 6 \times \text{Integral}(\text{CH}_{\text{D2}})]}{7} \quad (2)$$

$$\text{DB} = \frac{2\text{D}}{2\text{D} + \text{L}_{\text{CO}}} \text{ with } \text{L}_{\text{CO}} = \text{L}_{5\text{HDON}} + \text{F}_{5\text{HDON}} + \text{L}_{\text{GL}} \quad (3)$$

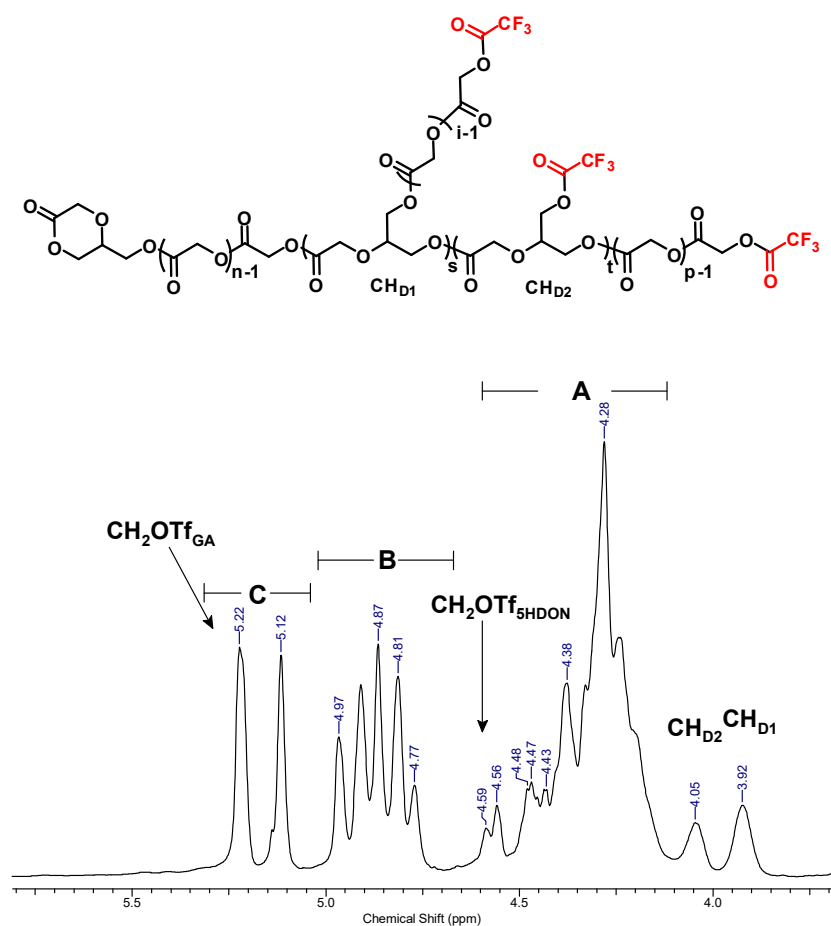


Figure 7. ^1H NMR spectrum (400 MHz, DMSO-d_6) of $hbP(\text{GA}_{60}\text{-co-5HDON}_{40})$ after esterification with trifluoroacetic anhydride.

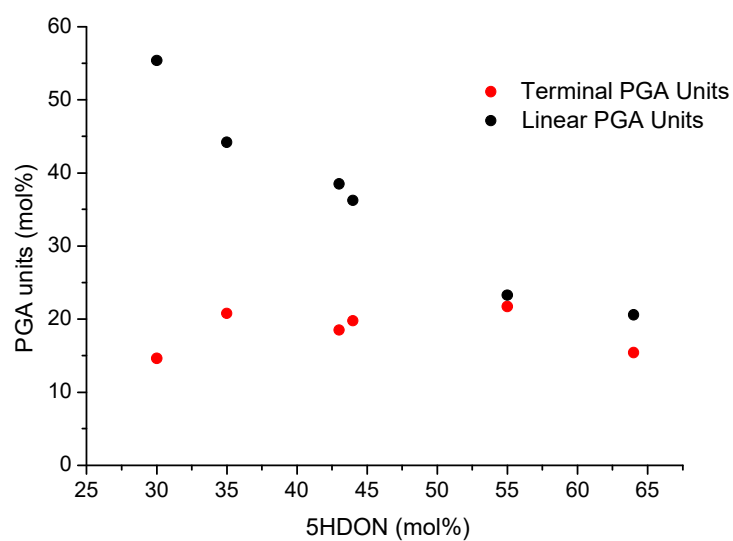


Figure 8. Correlation of the percentage of linear and terminal PGA units with the 5HDON molar content.

The calculated values for molar composition and DB are listed in Table 1. In Figure 8, the percentage of linear and terminal PGA units is plotted versus the 5HDON molar content for all copolymers. One can clearly observe a decrease of linear PGA repeat units with increasing 5HDON content. This is in agreement with the hypothesis that the PGA chain length between branching points is adjustable via the glycolide/5HDON ratio. The amount of terminal PGA units remains almost constant for varying 5HDON content.

Although, NMR characterization has already demonstrated the successful copolymerization of 5HDON and glycolide, MALDI-ToF mass spectrometry was expected to give evidence for the evidence of 5HDON homopolymer or PGA oligomer is present. Linear, high molecular weight PGA should be detectable due to its insolubility in the NMR solvent (DMSO- d_6) and precipitation of a white powder during polymerization. Instead, we obtain a colourless, glassy material. In previous publications of our group, the difficulty of mass spectrometry concerning polydisperse samples due to the mass discrimination effect was described. This problem can be overcome by separation of the polymer into more defined fractions with narrower molecular weight distribution < 2 .³⁹ In Figure 9, the SEC traces of the collected fractions obtained via preparative SEC in DMF are shown together with the SEC data.

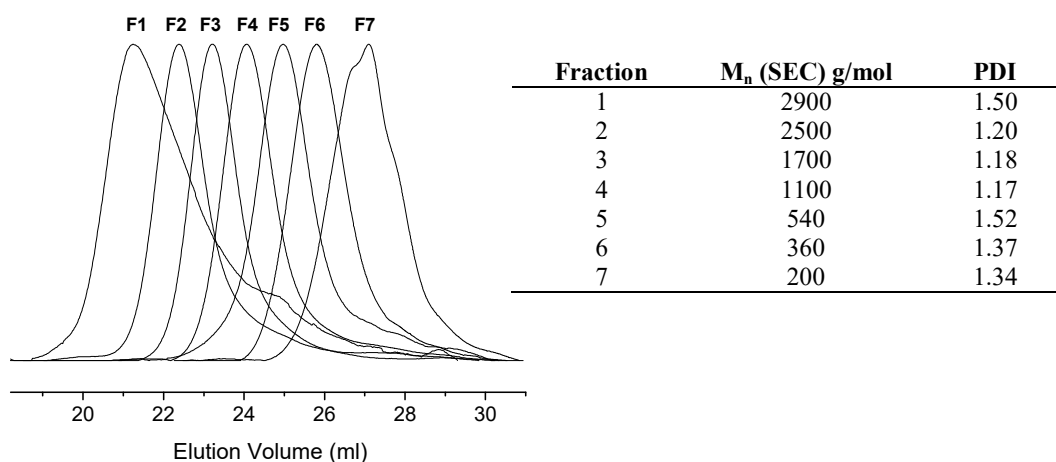


Figure 9. SEC traces (PS calibration standard, DMF as eluent) of the fractions (1-7) collected by preparative SEC of $hbP(GA_{60}\text{-co-}5\text{HDON}_{40})$ and additional SEC data.

Figure 10 exemplarily shows one MALDI-ToF spectrum of fraction 4 zooming into one region for detailed signal analysis. As it is shown, the different sub-distributions refer to different amounts of incorporated 5HDON. Hence, the incorporation of both monomers can be detected over the entire mass range. The observed signals show a mass difference of $16 \text{ g}\cdot\text{mol}^{-1}$, representing the mass difference of the repeating units (116 Da for glycolide and 132 Da for 5HDON). In addition, there are distributions present which show a mass increment of 58 Da referring to half of the mass of the

glycolide repeat units. In this case, transesterification reactions occurred during ROMBP under $\text{Sn}(\text{Oct})_2$ catalysis. As it has been already investigated by our group,⁴⁰ cyclization is a non-negligible side-reaction in the synthesis of hyperbranched polyesters. In the here presented case, cyclization is promoted by ring-opening of one single focal unit per copolymer via internal attack of a hydroxyl end group. Unfortunately, the cyclic and non-cyclic species cannot to be differentiated by their mass difference, because there is no release of a condensation product, e.g., water.

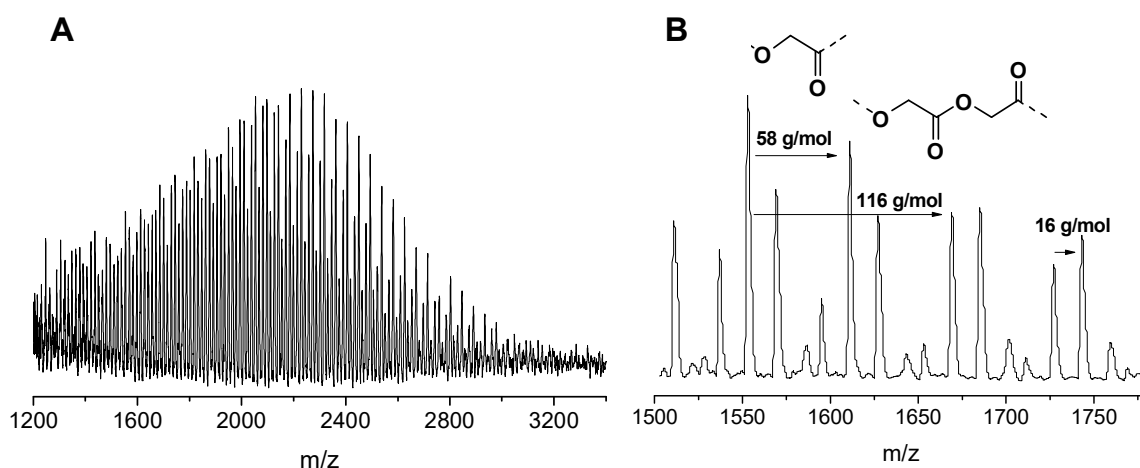


Figure 10. MALDI-ToF mass spectra of the collected fractions (A) fraction 4 and (B) with zoom into detail obtained from *hbP(GA₆₀-co-5HDON₄₀)*.

Thermal Properties. The thermal properties of the hyperbranched PGA copolyesters were investigated by DSC analysis to study the effect of the branched topology on the glass transition (T_g) and the melting temperature (T_m) upon increasing 5HDON content. The DSC thermograms have been obtained from the second heating run with a heating rate of $10^\circ\text{C}/\text{min}$. In general, a decrease of the glass temperature with increasing 5HDON molar content is observed in the range of 8.3 to -16.3°C . Both the dendritic units and the end groups have an influence on the polymers' ability to crystallize.⁴¹ In contrast to the branched glycerol-based PGA, linear PGA has a glass temperature of 30 - 35°C and a melting temperature of 210 - 230°C or 160 - 197°C for $9 \leq n \leq 13$ (with n =number of glycolic acid units).⁴ The effect of a depressed T_g due to the introduction of branching points into a polyester has been observed in our group for copolymers of L-lactide and 5HDON.^{19a} In the afore-mentioned work, a melting point of PLA is observed at DP_n exceeding 16. This is in agreement with the expectation that a critical PGA chain length between every branching point has to be reached at which crystallization of PGA is possible. Thus, the hyperbranched PGA copolymers can be obtained as amorphous materials despite the high melting point of PGA and its blocky incorporation into the backbone. This amorphous character is a major advantage of *hbPGA* compared to conventional PGA homopolymers with respect to processing in potential applications.

Functionalization of the hydroxyl end groups. The multiple end-functionalities render hyperbranched polymers attractive for further post-polymerization modifications compared to their structural linear analogues. Therefore, by addressing the abundant primary hydroxyl groups of *hbPGA*, offers the possibility for drug targeting, attachment of fluorescent dyes or for construction of complex polymer architectures, e.g., multi-arm stars with amphiphilic core-shell properties. To investigate the addressability of the end groups, phenylurethane-functionalization was accomplished by adding an excess of phenylisocyanate under mild conditions (at 40°C) to *hbPGA*. Especially polyester polyols are favourable compounds used in industry for reaction with diisocyanates to produce adhesives, foams and surface coatings. Both SEC and IR spectroscopy confirm the success of the functionalization reaction. Figure 11 shows the SEC traces of the sample before and after functionalization with phenylisocyanate. In contrast to the signal of the refractive index detector (RI), the UV-detector showed no signal prior to functionalization. After functionalization the molecular weight distribution remains unchanged (RI-signal) and the molar mass increases which confirms the multi-functionalization of each macromolecule. Additionally, the UV-detector shows a monomodal molecular weight distribution resulting from the selective and homogeneous introduction of aromatic phenylurethane groups. Before functionalization, IR analysis shows a broad O-H absorption at 3500 cm⁻¹ referring to the hydroxyl end groups of *hbPGA* and the hydroxyl groups of linear 5HDON units. After the transformation the signal intensity decreases and a new N-H related bond arises, which is shifted to lower wavenumber (3338 cm⁻¹). This gives evidence of a successful derivatization of the hydroxyl groups. Additional bonds, corresponding to aromatic (757-693 cm⁻¹) or amide vibrations (3325 cm⁻¹), underline the multivalent functionalization (Figure S9, Supp. Inf.). Because of the branched topology, some hydroxyl groups may not be converted into amides because of the sterically hindered accessibility of the end groups in the shielded inner part of the macromolecule.

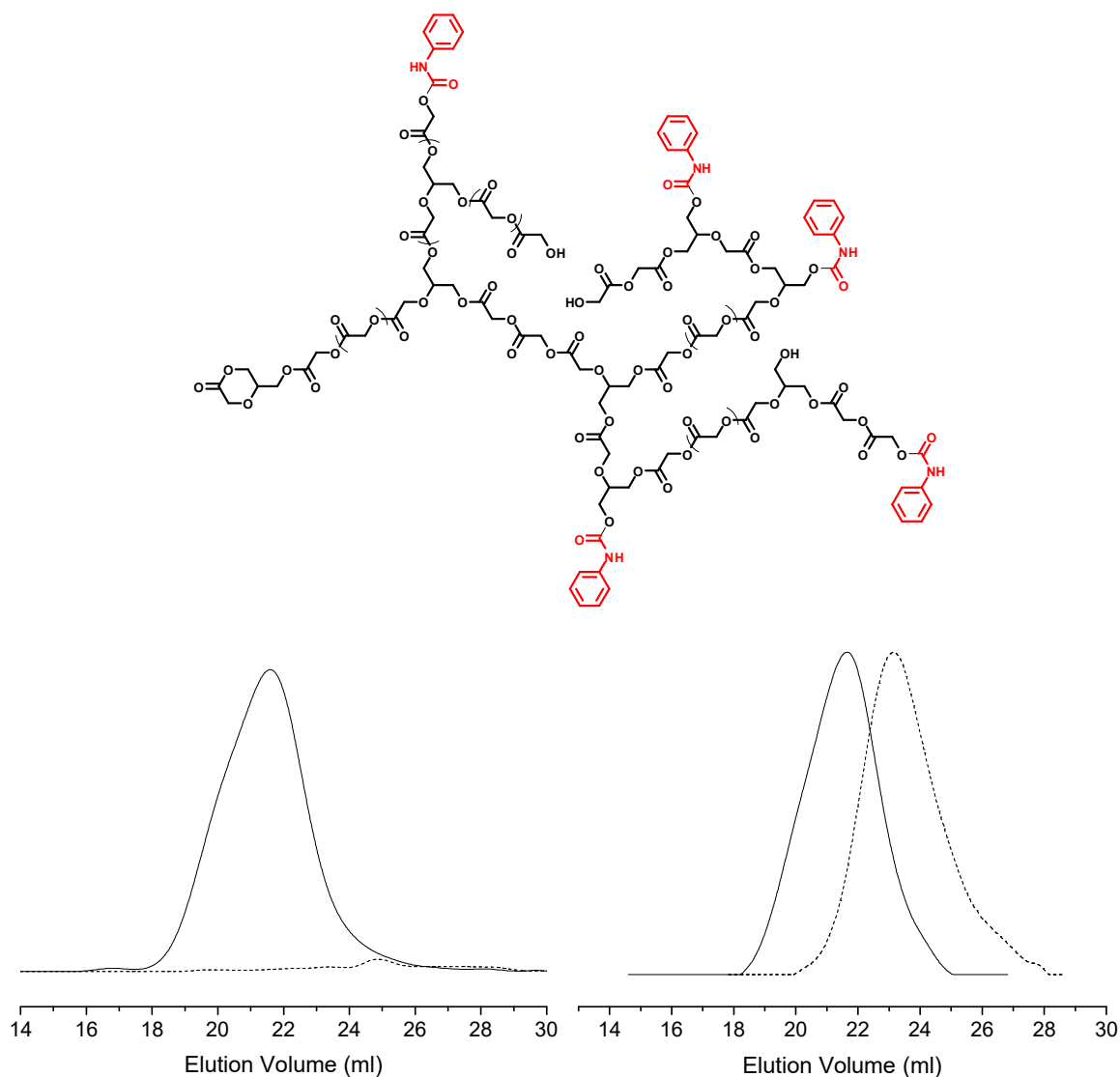


Figure 11. Left: SEC-UV traces; Right: SEC-RI traces before (---) and after (—) phenylurethane-functionalization of *hbP*(GA₆₄-co-5HDON₃₇) with phenylisocyanate (measured in DMF).

Conclusion

We described the synthesis of novel hyperbranched poly(glycolide) (*hbPGA*) copolymers with glycerol branching points via Sn(Oct)₂-catalyzed ring-opening multibranching polymerization of glycolide and the cyclic inimer 5HDON. The branching mechanism was investigated using kinetic ¹H NMR studies. A series of copolyesters with different molar composition (5HDON/glycolide=70:30-30:70) were analyzed with respect to thermal properties, comonomer incorporation and degree of branching. The incorporation of glycerol branching points suppresses crystallization of the PGA segments. With increasing 5HDON content a decrease of the glass transition temperatures is observed. The monomer to inimer ratio allows adjusting the PGA chain length between every branching point which leads to a limitation of the solubility at glycolide ratios exceeding 70% due to the structural analogy compared

to PGA homopolymers in the long linear segments between the branching points. In addition, the degree of branching in the range of 0.23-0.36, implies the formation of long-chain branched copolyesters via the so-called ROMBP.

It could be shown that the reaction mechanism defined by Wolf et al.^{19a} including the ROP of inimer-initiated PGA macromonomers is also applicable for the PGA-based comonomer system to overcome major drawbacks in the processing of PGA homopolymers. Interestingly, detailed ¹H NMR studies reveal the formation of a higher amount of dendritic repeat units for lower 5HDON/glycolide ratios due to the difference of the reactivity of both monomers. This strategy allows the incorporation of up to 70 mol% of glycolide. The suppression of PGA crystallization is ensured via the branched topology, which is highly advantageous with regard to solubility problems in processing and potential applications. In addition, the only building units, glycerol and glycolic acid, may guarantee a biocompatible material a fortiori after polymer degradation. The successful functionalization of the multiple end groups broadens the field of *hb*PGA applications, for example in polyurethane synthesis as polyester polyol component, with low PDIs for well-defined complex polymer architectures.

Supporting Information

I. Additional 1D/2D NMR spectra

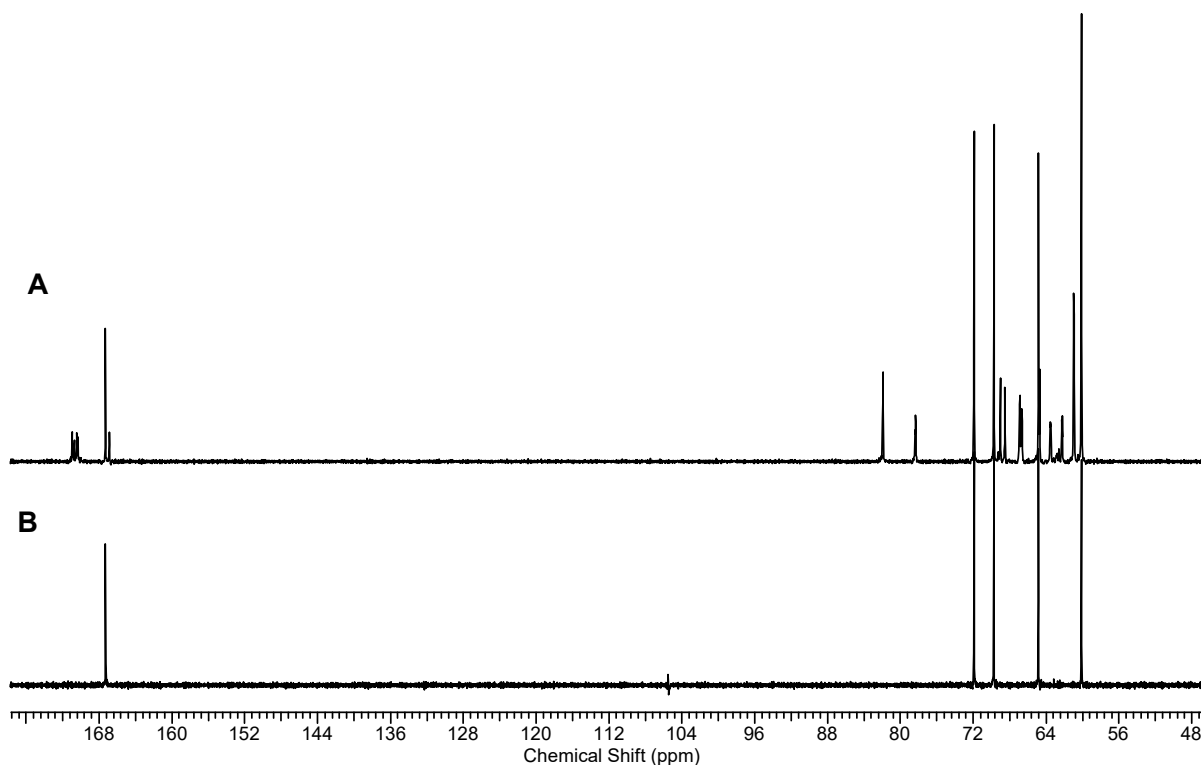
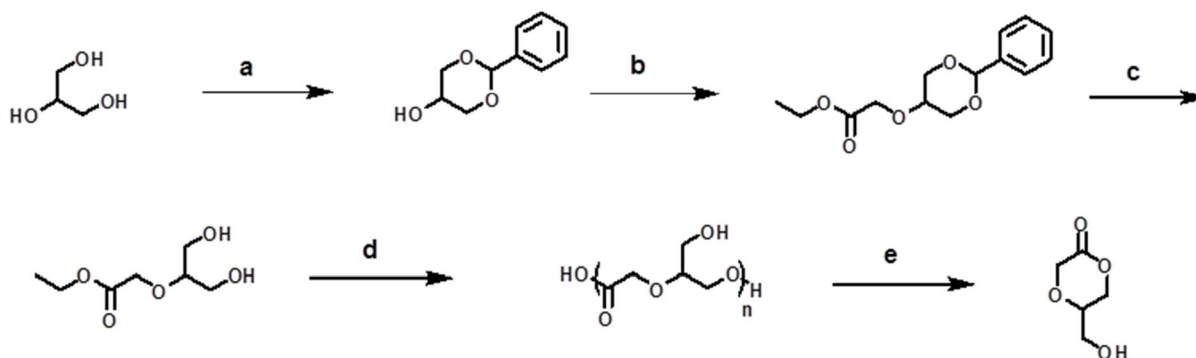


Figure S1. ^{13}C NMR spectra (75.5 MHz) of (A) 5HDON after 3 weeks storage and (B) freshly distilled 5HDON in DMSO-d_6 .



Scheme S1. Synthetic pathway to 5-hydroxymethyl-1,4-dioxan-2-one (5HDON)^{29,30}: (a) $\text{C}_6\text{H}_5\text{CHO}$, H_2SO_4 , benzene; (b) NaH , $\text{BrCH}_2\text{COOEt}$, toluene, rt; (c) 3% HCl (aq), EtOH , rt; (e) vacuum distillation 160°C , 2×10^{-2} mbar.

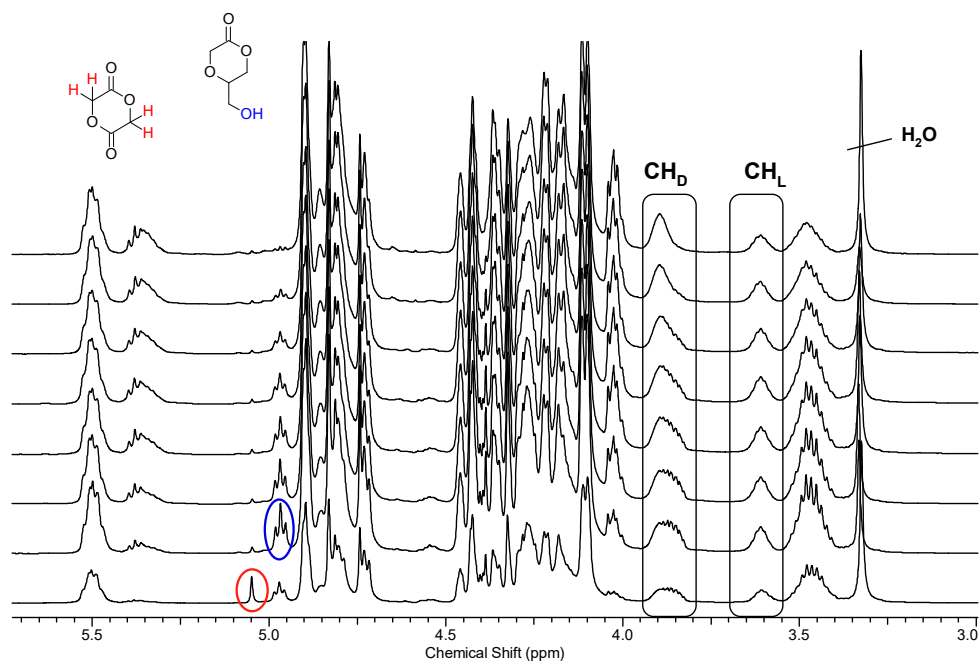


Figure S2. ^1H NMR spectra (400 MHz, DMSO-d_6) after different time intervals during $\text{Sn}(\text{Oct})_2$ -catalyzed ROMBP of glycolide and 5HDON (50:50 feed ratio; quenched by rapid cooling to -20°C) highlighting the linear and dendritic 5HDON methine proton signals (colour-coded) as well as residual monomer signals.

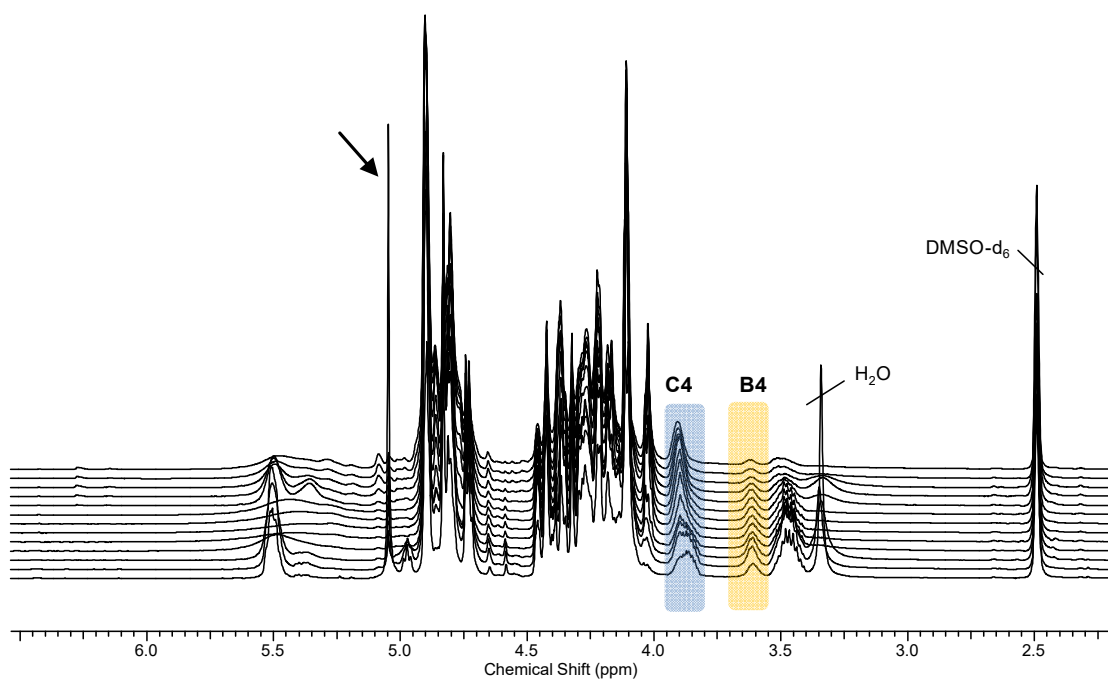
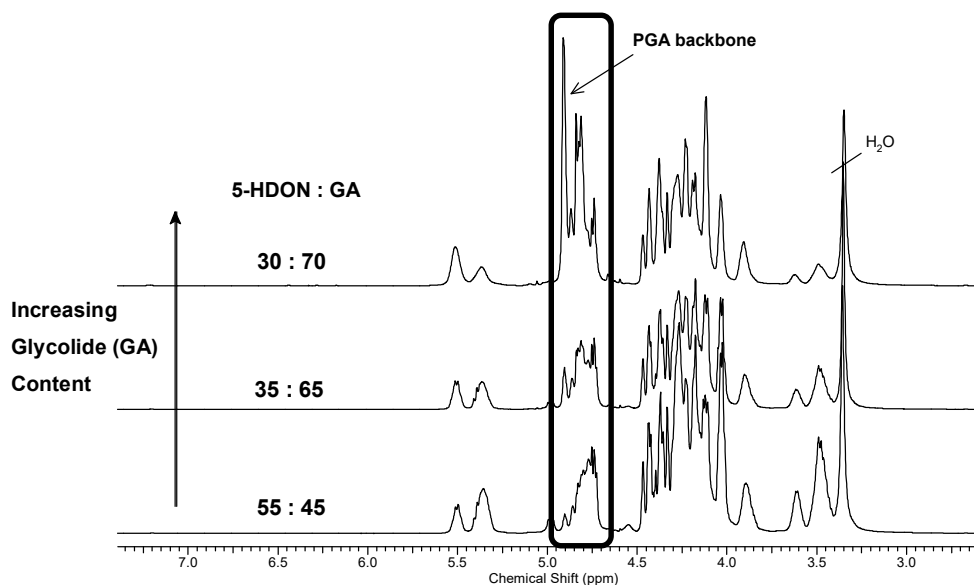


Figure S3. Time-dependent ^1H NMR measurements (400 MHz, DMSO-d_6) during $\text{Sn}(\text{Oct})_2$ -catalyzed ROMBP of glycolide and 5HDON (60:40 feed ratio; quenched by rapid cooling to -20°C).

Table S1. Time-dependent development of M_n and polydispersity index of the kinetic investigation (cf. Figure S3).

Time (min)	M_n (SEC) ^{a)} [g·mol ⁻¹]	M_p (SEC) ^{a)} [g·mol ⁻¹]	M_w/M_n ^{a)}
5	170	300	3.49
10	200	300	3.66
20	210	300	3.78
40	220	800	4.12
80	260	1200	4.53
160	330	1700	5.23
345	370	1900	5.58
676	390	2100	5.86
1359	450	2400	5.93
2801	600	2100	5.85
4533	700	2400	1.42
6012	670	2500	1.12
7482	890	2200	1.67

^{a)}determined by SEC analysis in DMF (PS calibration standard)

**Figure S4.** ¹H NMR spectra (400 MHz, DMSO-d₆) of copolymers with increasing glycolide/5HDON molar ratio.

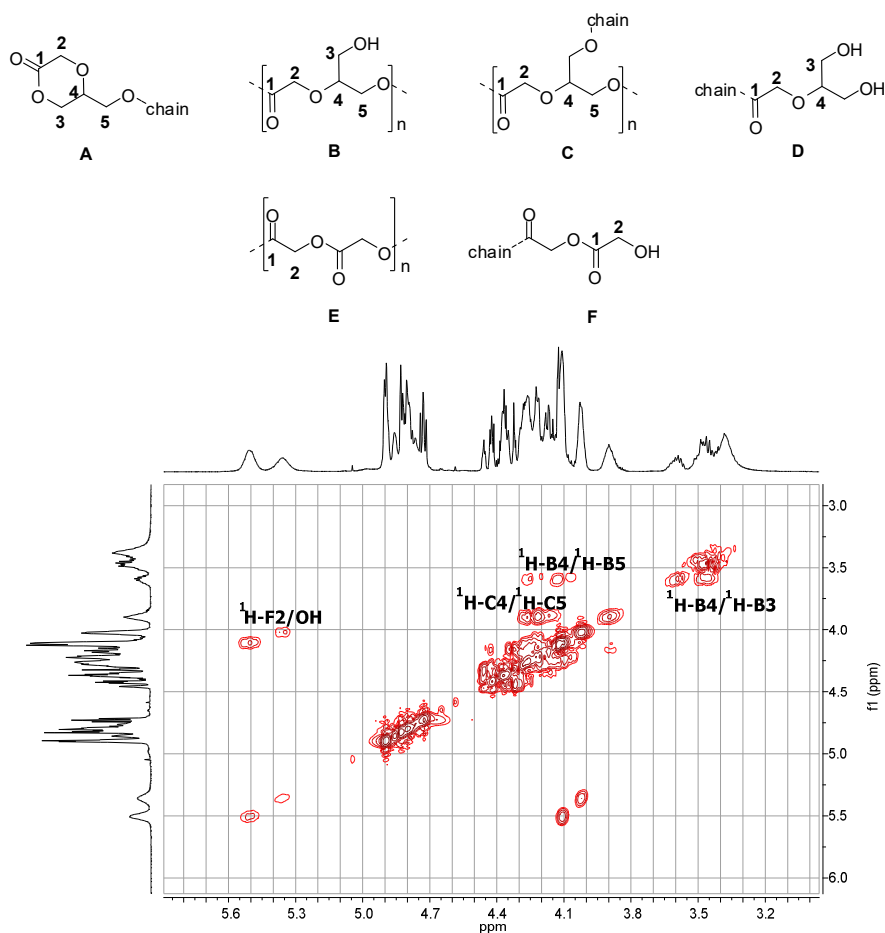


Figure S5. ^1H , ^1H COSY NMR (400 MHz, DMSO-d_6) of $hbP(\text{GA}_{65}\text{-co-5HDON}_{35})$ showing cross correlations over multiple bonds.

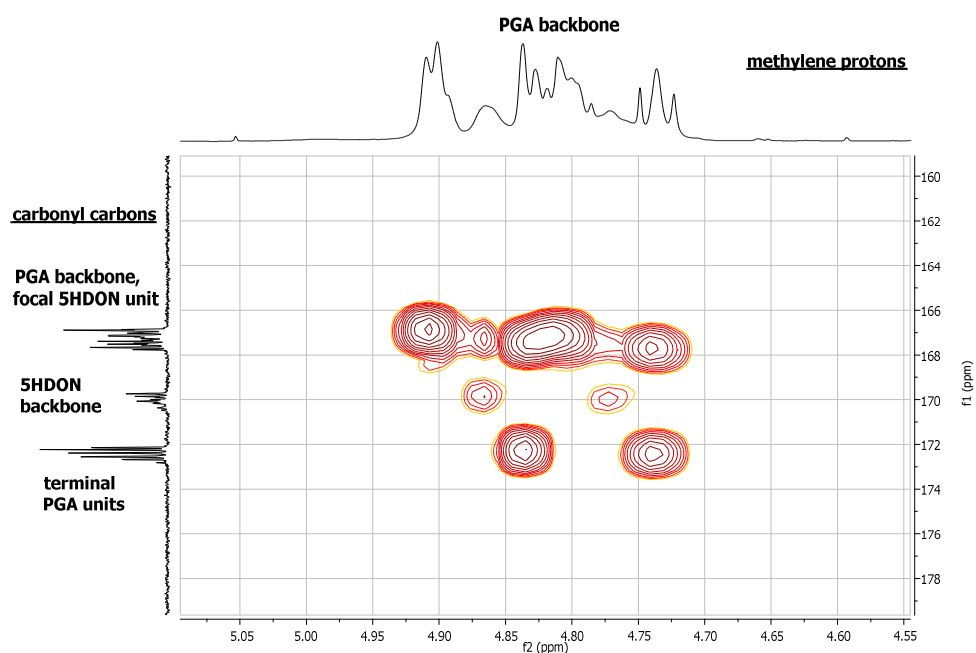


Figure S6. Section of HMBC (hetero multiple bond correlation) spectrum of $hbP(\text{GA}_{65}\text{-co-5HDON}_{35})$ showing ^1H , ^{13}C cross correlations over multiple bonds.

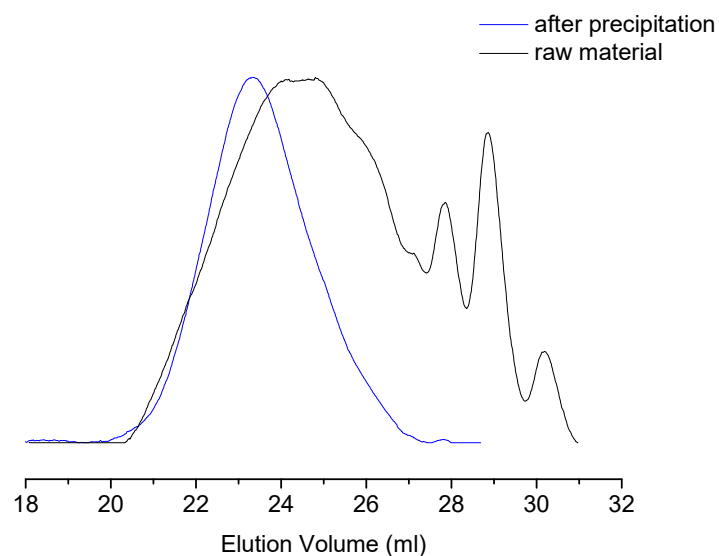


Figure S7. SEC traces of a polymer sample before (black line) and after (blue line) precipitation in methanol.

II. SEC and IR data after functionalization

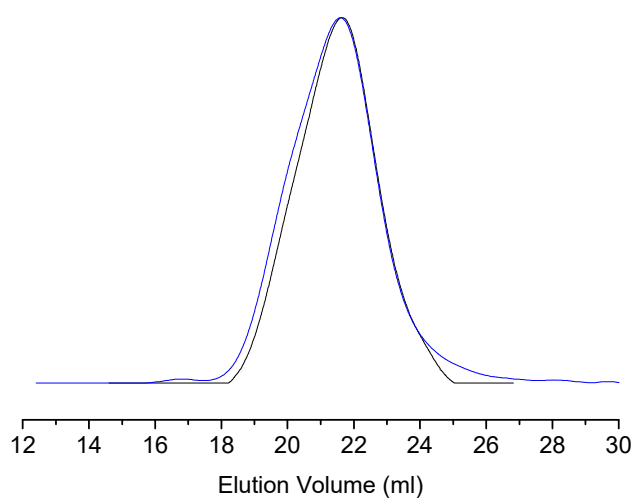


Figure S8. SEC traces of phenylurethane-functionalized $hbP(GA_{64}\text{-co-}5HDON_{37})$. Multifunctionalization over the entire mass range is shown by overlap of UV (blue line) and IR (black line) signals.

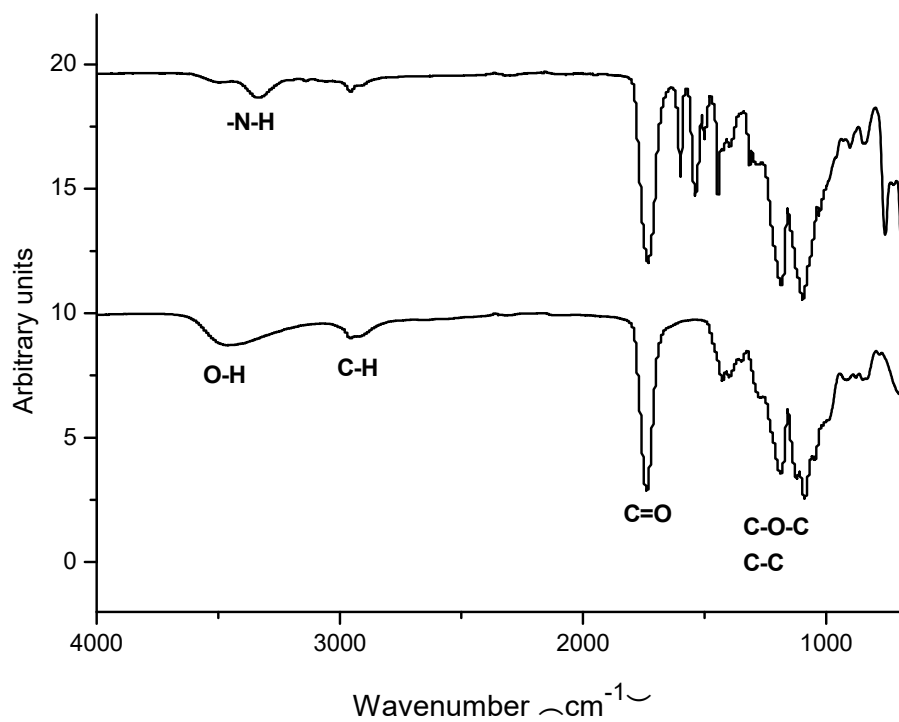


Figure S9. IR spectra before (bottom) and after (top) phenylurethane-functionalization of *hbP*(GA₆₄-co-5HDON₃₇).

III. Additional DSC Data

Table S3. DSC analysis in the range of -50 to 200 °C with a heating rate of 20 °C/min.

sample	T _g (°C)
<i>hbP</i> (GA ₇₀ -co-5HDON ₃₀)	8.4
<i>hbP</i> (GA ₆₅ -co-5HDON ₃₅)	1.1
<i>hbP</i> (GA ₅₇ -co-5HDON ₄₃)	-2.3
<i>hbP</i> (GA ₅₆ -co-5HDON ₄₄)	-9.2
<i>hbP</i> (GA ₄₅ -co-5HDON ₅₅)	-12.6
<i>hbP</i> (GA ₃₆ -co-5HDON ₆₄)	-23.0

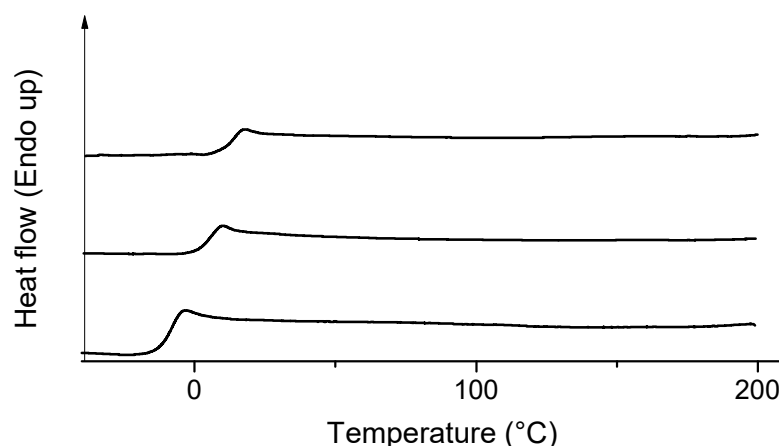


Figure S10. DSC heating traces (second heating scan with 20°C/min) for *hbP*(GA₄₅-co-5HDON₅₅) (bottom), *hbP*(GA₆₅-co-5HDON₃₅) (middle), *hbP*(GA₇₀-co-5HDON₃₀) (top) showing an increase of the glass temperature with increasing glycolide content.

References

1. Auras, R.; Harte B.; Selke, S. *Macromol. Biosci.* **2004**, *4*, 835-864.
2. Albertsson, A.-C.; Varma, I. K. *Biomacromolecules* **2003**, *4*, 1466-1486.
3. Middleton, J. C.; Tipton, A. J. *Biomaterials* **2000**, *21*, 2335-2346.
4. Andreas, F.; Sowada, R.; Scholz, J. *J. prakt. Chem.* **1962**, *18*, 141-149.
5. Sekine, S.; Yamauchi, K.; Aoki, A.; Asakura, T. *Polymer* **2009**, *50*, 6083-6090.
6. Dali, S.; Lefebvre, H.; El Gharbi, R.; Fradet, A. *J. Polym. Sci., Part A: Polym. Chem.* **2006**, *44*, 3025-3035.
7. Montes de Oca, H.; Ward, I. M.; Klein, P. G.; Ries, M. E.; Rose, J.; Farrar D. *Polymer* **2004**, *45*, 7261-7272.
8. Lendlein, A. *Chemie in unserer Zeit* **1999**, *5*, 279-295.
9. Kasperczyk, J. *Macromol. Chem. Phys.* **2009**, *200*, 903-910.
10. Zurita, R.; Puiggali, J.; Franco, L.; Rodríguez-Galán, A. *J. Polym. Sci.: Part A: Polym. Chem.* **2006**, *44*, 993-1013.
11. Rodríguez-Galán, A.; Franco, L.; Puiggali, J. *J. Polym. Sci.: Part A: Polym. Chem.* **2009**, *47*, 6758-6770.
12. (a) Wolf, F.K.; Fischer, A. M., Frey, H. *Beilstein J. Org. Chem.* **2010**, *6*, No.67; (b) Bááez, J. E.; Marcos-Fernández, Á. *Int. J. Polym. Anal. Charact.* **2011**, *16*, 269-276.
13. Fischer, A. M.; Frey, H. *Macromolecules* **2010**, *43*, 8539-8548.
14. Hawker, C. J.; Lee, R.; Fréchet J. M. *J. Am. Chem. Soc.* **1991**, *113*, 4583-4588.
15. Magnusson, H.; Malmström, E.; Hult, A. *Macromolecules* **2000**, *33*, 3099-3104.

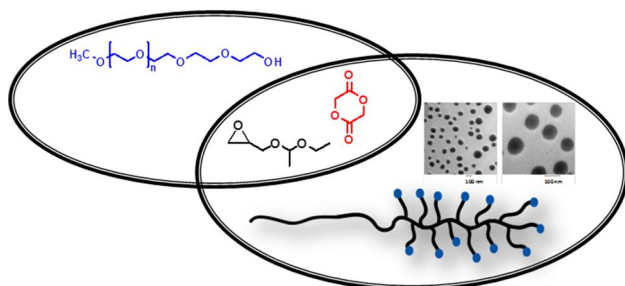
16. (a) Choi, J.; Kwak, S.-Y. *Macromolecules* **2003**, *36*, 8630; (b) Trollsås, M.; Hedrick, J. L. *Macromolecules* **1998**, *31* (13), 4390-4395.
17. (a) Trollsås, M.; Löwenhielm, P.; Lee, V. Y.; Möller, M.; Miller R. D.; Hedrick, J. L. *Macromolecules* **1999**, *32*, 9062-9066; (b) Liu, M.; Vladimirov, N.; Fréchet, J. M. *Macromolecules* **1999**, *32*, 6881-6884; (c) Yu, X.-H.; Feng, J.; Zhuo, R.-X. *Macromolecules* **2005**, *38*, 6244-6247.
18. (a) Smet, M.; Gottschalk, C.; Skaria, S.; Frey, H. *Macromol. Chem. Phys.* **2005**, *206*, 2421-2428; (b) Skaria, S.; Smet, M.; Frey, H. *Macromol. Rapid Commun.* **2002**, *23*, 292-296; (c) Fukuoka, T.; Habe, H.; Kitamoto, D.; Skakai, K. *J. Oleo. Sci.* **2011**, *60*, 369-373; (d) Rong-Xu, Z.; Lin, L.; Bin, W. *Polymer* **2012**, *53*, 719-727.
19. (a) Wolf, F. K.; Frey, H. *Macromolecules* **2009**, *42*, 9443-9456; (b) Pitet, L. M.; Hait, S. B.; Lanyk, T. J.; Knauss, D. M. *Macromolecules* **2007**, *40*, 2327; (c) Tasaka, F.; Ohya, Y.; Ouchi, T. *Macromol. Rapid Commun.* **2001**, *22*, 820-824.
20. Gao, C.; Yan, D. *Prog. Polym. Sci.* **2004**, *29*, 183-275.
21. Hult, A.; Johansson, M.; Malmström, E. *Adv. Polym. Sci.* **1999**, *143*, 1-34.
22. Žagar, E.; Žigon, M. *Prog. Polym. Sci.* **2011**, *36*, 53-88.
23. Jikei, M.; Kakimoto, M.-a. *Prog. Polym. Sci.* **2001**, *26*, 1233-1285.
24. Voit, B. I.; Lederer, A. *Chem. Rev.* **2009**, *109*, 5924-5973.
25. Wilms, D.; Stiriba, S.-E.; Frey, H. *Acc. Chem. Res.* **2010**, *43*, 129-141.
26. D. Yan, C. Gao, H. Frey "Hyperbranched Polymers: Syntheses, Properties and Applications", Eds.; **2011**, J. Wiley Publishers, New York and London.
27. Chikh, L.; Tessier, Fradet, A. *Polymer* **2007**, 1884-1892.
28. Fukuoka, T.; Habe, H.; Kitamoto, K.; Sakaki, K. *J. Oleo Sci.* **2011**, *60*, 369-373.
29. Brogini, G.; Zecchi, G. *Org. Prep. Proced. Int.* **1991**, *23*, 762-764.
30. Parzuchowski, P. G.; Grabowska, M.; Tryznowski, M.; Rokicki, G. *Macromolecules* **2006**, *39*, 7181-7186.
31. Dechy-Cabaret, O.; Martin-Vaca, B.; Bourissou D. *Chem. Rev.* **2004**, *104*, 6147-6176.
32. Kamber, N. E.; Jeong, W.; Waymouth, R. M.; Pratt, R. C.; Lohmeijer, B. G. G.; Hedrick J. L. *Chem. Rev.* **2007**, *107*, 5813-5840.
33. Quian, H.; Wohl, A. R.; Crow, J. T.; Macosko, C. W.; Hoye, T. R. *Macromolecules* **2011**, *44*, 7132-7140.
34. Nieuwenhuis, J. *Clin. Mater.* **1992**, *10*, 59-67.
35. Dali, S.; Lefebvre, H.; El Gharbi, R.; Fradet, A. *e-Polymers* **2007**, No. 65
36. Hölter, D.; Burgath, A.; Frey, H. *Acta Polym.* **1997**, *48*, 30-35.
37. Hölter, D.; Frey, H. *Acta Polym.* **1997**, *48*, 289-309.

38. Frey, H.; Hölter, D. *Acta Polym.* **1999**, *50*, 67-76.
39. Byrd, H. C. M.; McEwen, C. N. *Anal. Chem.* **2000**, *72*, 4568-4576.
40. Burgath, A.; Sunder A.; Frey, H. *Macromol. Chem. Phys.* **2000**, *201*, 782-791.
41. Stutz, H. J. *Polym. Sci. Part B: Polym. Phys.* **1995**, *33*, 333.

3.3 Poly(ethylene glycol)-*g*-Poly(glycolide) Copolymers: A Promising Polymer Surfactant for Microparticle Synthesis

Anna M. Fischer, Mathias Werre, Matthias Gabriel and Holger Frey

To be Submitted to *Biomacromolecules*



Keywords: polyester, polyglycolide, grafting, microparticle

Abstract

On the basis of well-defined poly(ethylene glycol)-block-poly(glycerol) (PEG-*b*-PG) precursors a series of biocompatible and partially degradable poly(glycolide) (PGA) graft copolymers with potential application as surfactants were synthesized. Oxyanionic ring-opening polymerization (ROP) of ethoxy ethyl glycidyl ether (EEGE), initiated via *m*-PEG (2000 and 5000 g mol⁻¹) yielded the linear block copolymer precursor PEG-*b*-PG after subsequent acetal cleavage. The obtained multifunctional macroinitiators with varying numbers of primary hydroxyl groups were used for Sn(Oct)₂-catalyzed ROP of glycolide. Solubility of the copolymers was ensured via limited PGA chain length and the molar content of glycolide was tailored via the number of initiating glycerol units. Since PGA homopolymers are well-known for their insolubility in common organic solvents, this approach permits a variation of molar composition without an increase of PGA chain length segments and at the same time guarantees high glycolide content (up to 62 wt%), while maintaining solubility. Well-defined graft copolymers of low polydispersity (PDI 1.08-1.20) and molecular weights in the range of 3900-10.800 g mol⁻¹ (SEC) were obtained. Complete incorporation of the initiators was evidenced by MALDI-ToF mass spectrometry and NMR analysis at all reaction stages. TEM images show micellar aggregation of the PGA graft copolymers in aqueous environment due to their amphiphilic character. This feature renders the copolymers interesting for biomedical applications, i.e., as emulsifier for the preparation of degradable polymer microspheres.

Introduction

Biodegradable polyesters, i.e., poly(lactide) (PLA), poly(lactide-co-glycolide) (PLGA), and poly(ϵ -caprolactone) (PCL), are currently used for a wide range of applications in the biomedical field such as implants,¹ drug delivery carriers² or scaffolds for tissue engineering.^{3,4} Poly(glycolide) (PGA) is the most simple poly(α -hydroxy acid) among the aliphatic polyesters. PGA captured the market of polymeric absorbable sutures in 1968/70 under the trade name Dexon.⁵ A series of PGA copolymers followed to enhance mechanical properties and decrease the degradation rate of the material. The pure homopolymer of glycolic acid is rarely utilized due to its high hydrolysis rate in comparison with other polyesters.⁶ Furthermore the synthesis and characterization of PGA is hampered due to its insolubility in common organic solvents and the high melting temperature (210-230°C) arising with a chain length >13 glycolic acid units.⁷ Therefore solid state techniques have been applied such as solid state NMR spectroscopy,⁸ melt rheology⁹ and X-ray diffractometry¹⁰ to characterize the insoluble material. Several synthetic strategies have been developed to tailor material properties of polymers such as copolymerization, introduction of a branched topology and blending.¹¹ A variety of PGA copolymers has been synthesized by ring-opening polymerization (ROP) of glycolide (comonomers: e.g., *p*-dioxanone, lactide, and ϵ -caprolactone)¹²⁻¹⁴ or polycondensation of glycolic acid (comonomers: i.e., 4-hydroxybutyric acid, and *p*-hydroxybenzoic acid).^{15,16} Copolymerization resulted in a depression of the melting point and depending on the amount of incorporated glycolide an amorphous material was obtained. In a recent work, our group established the successful synthesis of hyperbranched PGA via combined ROP/AB₂ polycondensation, which resulted in amorphous materials despite an incorporation of 82 mol% of glycolide.¹⁷ Another approach in optimizing solubility parameters is based on the synthesis of PGA multi-arm stars with hyperbranched poly(glycerol) core to obtain core-shell structures.¹⁸ The grafting of poly(glycolide) to the core was performed up to a glycolide weight fraction of 91 % with an average chain length of 12 glycolic acid units at the most. Zhang et al. prepared PEG-PGA diblock copolymers, using a PGA octamer, and studied the antitumor activity of the paclitaxel-conjugate against human cancer cells.¹⁹ The synthesis of brush-like PGA copolymers has been realized by grafting PGA oligomers onto a hydrophilic poly- α , β -[N-(2-hydroxyethyl)-L-aspartamide] (PHEA) backbone by ROP in the absence of any catalyst.²⁰ The obtained amphiphilic copolymers with different molar feed ratio were investigated with respect to degradation rate, encapsulation efficiency of prednisone acetate and drug release behaviour. Most of the presented copolymers exhibit low-molecular weight PGA blocks only. Amphiphilic poly(ethylene glycol)-based polyesters are one of the best established copolymers in drug delivery systems,²¹ and pharmaceutical applications have been reported in the form of micelles, microparticles and hydrogels.²²⁻²⁴ The polyester block representing the hydrophobic segment allows for controlled drug release²⁵ due to its degradability *in vivo*, and the hydrophilic PEG domain

guarantees water-solubility of the copolymer system.²⁶ Besides, PEG is a well-known biocompatible polymer which possesses low immunogenicity and antigenicity.^{27,28} Poly(ether-ester) structures based on linear and hyperbranched poly(glycerol) (PG), which also attract much interest in biomedical applications due to their biocompatibility and low toxicity,²⁹ have been synthesized via grafting of poly(lactide) or poly(ϵ -caprolactone) to obtain star-like topologies, brushes and dumbbell-like polymer architectures.³⁰⁻³² On the basis of these structures, degradation profiles and pH-dependent release were monitored that are relevant for drug delivery applications. In general, graft copolymers based on aliphatic polyesters are accessible in core-first or arm-first approaches.³³ The first strategy comprises the ROP of a cyclic lactone, initiated via a multifunctional core, which results in simultaneous chain growth, whereas the second strategy implies covalent coupling of preformed polymer arms to the core.

To the best of our knowledge, graft copolymers with a comb-like topology consisting of PGA side chains have not yet been investigated, although in recent years a variety of branched macromolecular architectures has been developed, including miktoarm stars, arborescent graft structures or linear-hyperbranched polymers, leading to a change in the crystalline order and rheological properties.³⁴

In the current work, amphiphilic PGA graft copolymers have been synthesized via Sn(Oct)₂-catalyzed ROP of glycolide on the basis of a multifunctional PEG-*b*-PG initiator. A facile approach gaining soluble PGA copolymers is presented, which allows for variation of the PGA molar content by increasing the number of PGA blocks instead of the block chain length. Since the Sn(Oct)₂-catalyzed ring-opening polymerization of glycolide is initiated by primary hydroxyl groups, the PEG chain has to provide at least one hydroxyl functionality to obtain a covalent linkage.³⁵ In order to introduce a higher amount of functionalities, block copolymers of PEG and linear poly(glycerol)³⁶ have been prepared, which allow for an increase of the PGA/PEG ratio despite limited PGA chain length via the increased number of glycerol units.

Furthermore, the aggregation behaviour in aqueous solution was investigated as well as the thermal properties with respect to the copolymer ratio adjusted. The introduction of the PEG block as the polar segment is furthermore expected to improve physical properties of PGA, to reduce local acidity upon PGA degradation, and broaden PGA application in the biomedical field.

Experimental Section

Instrumentation

^1H and ^{13}C NMR spectra were measured on a Bruker AC300, a Bruker AV400 and a Bruker ARX 400 spectrometer with the deuterated solvent as an internal standard (^1H (DMSO- d_6): 2.5 ppm, ^{13}C (DMSO- d_6): 39.52 ppm). FT-IR spectra were recorded on a Nicolet SDXC FT-IR spectrometer equipped with an ATR unit. Size exclusion chromatography (SEC) was carried out in DMF, containing 0.25 g L^{-1} LiBr using an Agilent 1100 Series GPC Setup, including a HEMA column ($10^6/10^5/10^4\text{ g}\cdot\text{mol}^{-1}$), and RI as well as UV detectors. Calibration was carried out with polystyrene standards provided from Polymer Standards Service. The thermal properties were investigated via differential scanning calorimetry (DSC), using a Perkin Elmer 7 series thermal analysis system, at a heating rate of 10 K min^{-1} in a temperature range of -100 to $250\text{ }^\circ\text{C}$. The data were taken from the second heating run. The DSC instrument was calibrated with the melting point of indium ($156.6\text{ }^\circ\text{C}$) and n-decane ($-29.7\text{ }^\circ\text{C}$). MALDI-ToF mass spectrometry was performed on a Shimadzu Axima CFR MALDI-ToF mass spectrometer equipped with a nitrogen laser delivering 3 ns laser pulses at 337 nm. Dithranol (1,8,9-trishydroxyanthracene, Aldrich 97%) was used as matrix for the PEG-b-PG-g-PGA copolymers, while potassium triflate (Aldrich, 98%) was used as an ionization agent. The samples were prepared from 1,1,1,3,3,3-hexafluoro-2-propanol (HFIP) solutions with a concentration of 10 g L^{-1} . Good results were obtained by mixing matrix solution (10 g L^{-1}), sample solution (10 g L^{-1}) and salt (0.1M) in a ratio of 10:10:1. $1\text{ }\mu\text{l}$ of this solution was deposited on a MALDI target to obtain a thin matrix/sample film, after evaporation of the solvent. α -Cyano-3-hydroxy cinnamic acid (CHCA) was used as a matrix for the PEG-b-PG copolymers ionized with potassium triflate. The samples were prepared from methanol solution with a concentration of 10 g L^{-1} (vide infra). Scanning electron microscopy was performed using a SEM Zeiss DSM 962 in SE-Modus. Samples were prepared by placing the PCL microspheres on an aluminum foil, drying overnight and sputter coating with gold prior to imaging (Sputter Coater S150P Edwards). Transmission electron microscopy was performed using a TEM FEI XM12 with an acceleration voltage of 120 kV. 10 mg of the graft copolymer were dissolved in 1 ml of DMSO and slowly 9 ml of distilled water were added. Dialysis of the micellar solution three times against 1 L of distilled water for 48h was performed with Cellu SepH1 membranes (Membrane Filtration Products, Inc.) with a molecular weight cut-off of 1000 g mol^{-1} . The micellar solution was drop-coated on a copper grid (1 mg ml^{-1}) and allowed to dry under vacuum for 4 hours at room temperature. Wide angle X-ray scattering measurements (WAXS) were performed using a Bruker AXS GADDS system equipped with a HighStar detector and a Cu $K\alpha$ source ($\lambda = 0,154\text{ nm}$).

Reagents

M-PEG-2000 and m-PEG-5000 were commercially available from Sigma Aldrich. Ethoxy ethyl glycidyl ether (EEGE) was prepared according to literature procedures,³⁷ dried over calcium hydride and

freshly distilled prior to use. Glycolide was purchased from Purac (Gorinchem, NL), stored in a glove box and used as received. Deuterated CDCl_3 and DMSO-d_6 were purchased from Deutero GmbH. All reagents and solvents were purchased from Acros or Sigma Aldrich and used as received, unless otherwise stated.

Synthesis of PEG-*b*-PEEGE Copolymers. The oxyanionic ring-opening polymerization of EEEG was carried out with two different PEG macroinitiators. M-PEG and 0.9 eq cesium monohydrate were placed in a Schlenk flask and dissolved in benzene. The mixture was stirred at 60 °C under argon atmosphere for 30 min and evacuated (at 10^{-3} mbar) over night to remove water azeotropic with benzene, forming the cesium alkoxide. Dry dioxane was transferred to the flask to dissolve the initiator salt. EEEG was cryo-transferred and syringed into the flask containing the initiator and dioxane. The mixture was heated to 90 °C and stirred for 12 hours under vacuum. Precipitation into diethyl ether yielded the pure copolymer (yield: ~90 %).

^1H NMR (400 MHz, DMSO-d_6): δ (ppm) 1.09 (t, CH_2CH_3), 1.17 (d, CH_3 -acetal), 3.24 (s, CH_3 -PEG), 3.30-3.70 (polyether backbone), 4.64 (br, acetal-H).

^{13}C NMR (100.15 MHz, DMSO-d_6): δ (ppm) 15.19 (OCH_2CH_3), 19.71 (CH_3 -acetal), 58.04 (CH_3), 60.15 (OCH_2CH_3), 64.62 (CHCH_2O), 68.93-71.55 (polyether backbone), 78.30 (CHCH_2O), 99.10-99.19 (CH -acetal).

Deprotection to PEG-*b*-PG Copolymers. The copolymer was dissolved in a 10 % solution of methanol and H_2O (9:1). A strong acidic ion exchange resin (Dowex W50) was added and the solution was refluxed over night. After filtration the solution was evaporated and precipitated in diethyl ether. (Yield: ~90%).

^1H NMR (400 MHz, DMSO-d_6): δ (ppm) 3.24 (s, CH_3), 3.29-3.68 (polyether backbone), 4.52 (br, OH).

^{13}C NMR (100.15 MHz, DMSO-d_6): δ (ppm) 58.07 (CH_3), 60.79-61.05 (CH_2OH), 63.10 (terminal PG unit, CH_2OH), 69.47-71.79 (polyether backbone), 79.90-80.13 (CH).

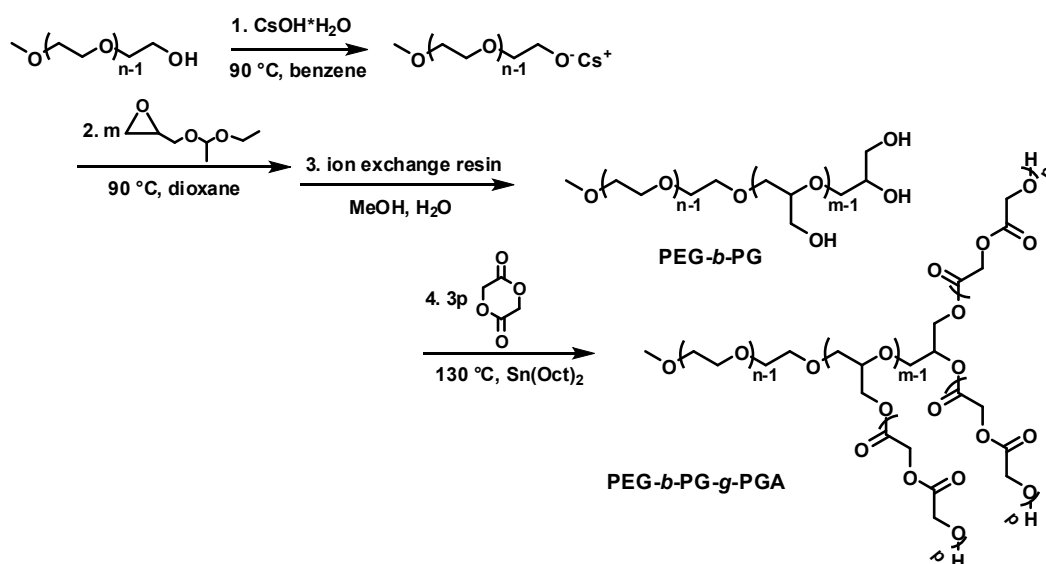
Synthesis of PEG-*b*-PG-*g*-PGA Copolymers. A schlenk flask was charged with PEG-*b*-PG macroinitiator and a stir bar. The flask was introduced into a glove box where glycolide was added in the quantities required. Outside the glove box the flask, kept under argon atmosphere, was placed in an oil bath preheated to 130 °C. As soon as a homogenous melt is obtained, 0.1 mol% tin octanoate were added via a syringe to initiate the ring-opening polymerization of glycolide. The reaction mixture was stirred for 1 hour at 130 °C and quenched upon cooling to room temperature. Precipitation once into ethyl acetate and second into diethyl ether yielded the pure graft copolymer.

^1H NMR (400 MHz, DMSO-d_6): δ (ppm) 3.23 (s, CH_3), 3.42-3.67 (polyether backbone), 4.01-4.13 (terminal PGA unit CH_2OH , esterified PG unit CH_2OR), 4.42 (br, esterified PG unit CH_2OR), 4.71-4.91 (PGA backbone), 5.53 (br, OH).

^{13}C NMR (75 MHz, DMSO- d_6): δ (ppm) 58.05 (CH_3), 59.30-59.92 (terminal PGA unit, CH_2OH), 60.01-61.06 (PGA backbone, CH_2COO), 64.25 (esterified PG unit, CH_2OR), 68.39 (terminal esterified PG unit, CH_2OR), 69.45-70.17 (polyether backbone), 71.31 ($\text{CH}_3\text{CH}_2\text{CH}_2\text{O}$), 76.52 (CH), 166.78-167.67 (PGA backbone, $\text{CH}_2\text{COOCH}_2$), 172.15-172.29 (terminal PGA unit, COOCH_2OH).

Results and Discussion

Synthesis of Amphiphilic PGA Graft Copolymers. Biocompatible and partially degradable PGA graft copolymers consisting of a linear PEG block and short PGA segments were prepared from linear poly(ethylene glycol)-*block*-poly(glycerol) (PEG-*b*-PG) precursor copolymers. The linear block copolymers were obtained via oxyanionic ring-opening polymerization of a protected glycidyl ether, ethoxy ethyl glycidyl ether (EEGE), initiated with monofunctional *m*-PEGs of different molecular weights. After removal of the protecting groups via acidic hydrolysis, the linear precursors can be used as macroinitiators for the $\text{Sn}(\text{Oct})_2$ -catalyzed ring-opening polymerization of glycolide (Scheme 1).



Scheme 1. Grafting-from approach to amphiphilic PEG-*b*-PG-*g*-PGA copolymers by oxyanionic ROP of EEGE, subsequent acetal cleavage and $\text{Sn}(\text{Oct})_2$ -catalyzed ROP of glycolide.

This synthesis protocol allows for the preparation of well-defined, amphiphilic PGA graft copolymers (PDI: 1.08-1.2), with molecular weights up to 10.800 g mol⁻¹ (SEC), which differ in their block chain length and molar composition. The multiple functionality of the PG block can be varied via the degree of polymerization to adjust the number of grafted arms. Two different commercially available *m*-PEG macroinitiators with molecular weights of 2000 and 5000 g mol⁻¹ and varied degree of polymerization of the PG block (listed in Table 1, 1-5) have been employed. The degree of polymerization and the introduced number of PG units, respectively, were determined via ^1H NMR

spectroscopy by integrating the methyl group of the initiator (3.24 ppm), and the acetal protecting groups of the comonomer (4.64 ppm), bearing in mind, that each EGE unit releases one primary hydroxyl function after deprotection. The copolymerization of the polyether polyols with glycolide allows for the incorporation of a higher glycolic acid (GA) molar content without increasing the PGA chain length. This is important because of the well-known insolubility of the linear PGA homopolymer at molecular weights exceeding 1000 g mol^{-1} in a broad range of common organic solvents and its high degree of crystallization, accompanied by a high melting point ($210\text{-}230^\circ\text{C}$).^{7,38} Suitable reaction conditions for the ROP of glycolide, which guarantee a homogenous reaction mixture, were found to be melt polymerizations at 130°C in the presence of catalytic amounts of tin octanoate ($\text{Sn}(\text{Oct})_2$). Due to the different solubility characteristics of monomer and polymer no suitable solvent has yet been identified for the ROP of glycolide. After 1 hour at 130°C the reaction was quenched by cooling to room temperature. The metal-coordination ROP of glycolide and lactide is well-known for its “living” character.³⁹ Therefore, the average PGA chain length, varying between 4 to 9 glycolic acid units per arm, was adjusted via the monomer/OH group ratio. This strategy permits the incorporation of 13 to 62 wt% PGA into the copolymer. In general, poly(glycolide) and PEG themselves are purified by precipitation into a non-common solvent (methanol for PGA, diethyl ether for PEG). Graft copolymers with high PEG content were soluble in methanol as well as the glycolide monomer. Precipitation into diethyl ether resulted in precipitation of both the monomer and the polymer. Therefore, precipitation in ethyl acetate was performed to ensure complete removal of residual glycolide monomer. Depending on the PEG/PGA ratio, the obtained graft copolymers were soluble in a broad range of solvents including methanol, water, dimethyl sulfoxide (DMSO) and dimethyl formamide (DMF), indicating the absence of precipitated PGA homopolymer. Hence, the PEG block contributes to an increase in solubility of the graft copolymer via its hydrophilic character and the PG block gives access to higher incorporation of PGA molar content with limited chain length. The PEG precursors (Table 1, 1-5) and the corresponding graft copolymers (Table 2, 1a-5d) have been characterized with respect to their molar composition, molecular weight and polydispersity (M_w/M_n) via NMR and SEC. Solubility tests and DSC characterization were employed to study the influence of the varying PEG/PGA block length on the copolymer properties.

Table 1. Characterization data of PEG-*b*-PG precursor copolymers.

Sample	M_n^a [g mol ⁻¹]	M_n^b [g mol ⁻¹]	PDI ^b	T_g^c [°C]	T_m^c [°C]
PEG ₁₁₄ - <i>b</i> -PG ₆ (1)	5500	4000	1.04	-	59.4
PEG ₁₁₄ - <i>b</i> -PG ₉ (2)	5700	4900	1.16	-	57.7
PEG ₄₅ - <i>b</i> -PG ₄ (3)	2300	2000	1.13	-	50.4
PEG ₄₅ - <i>b</i> -PG ₉ (4)	2700	2300	1.07	-35.3	49.3
PEG ₄₅ - <i>b</i> -PG ₁₂ (5)	2900	2500	1.07	-32.1	49.4

a) calculated via ¹H NMR spectroscopy before acetal cleavage; b) determined by SEC analysis in DMF with PEG standard calibration; c) DSC analysis in steps of 10 °C min⁻¹ (second heating run)

Table 2. Characterization data for amphiphilic PGA graft copolymers.

	PGA wt%	M_n^a [g/mol]	M_n^b [g/mol]	PDI ^b	T_g^c	T_m^c	ΔH	T_g^c	T_m^c	ΔH
					[°C]	[°C]	[J/g]	[°C]	[°C]	[J/g]
					PEG			PGA		
1a	13	6500	8700	1.11	-7.1	53.9	97.1	-	-	-
1b	28	7600	9000	1.13	-10	53.3	90.7	-	-	-
1c	32	8000	9700	1.09	-13	51.2	78.2	-	-	-
2a	19	7000	8500	1.18	-	53.9	88.3	-	-	-
2b	24	7500	9400	1.14	-4.4	52.1	75.8	-	172.8	9.2
2c	33	8500	10800	1.20	-6.3	51.3	57.1	-	178.5	30.5
3a	42	3900	4200	1.08	-31.0	39.5	55.2	-	-	-
3b	44	4060	4500	1.15	-24.7	39.6	46.2	-	174.5	6.0
3c	45	4100	5000	1.12	-22.1	40.6	24.9	-	178.4	37.8
4a	21	3400	3900	1.11	-10.2	41.69	65.5	-	-	-
4b	31	3900	5100	1.12	-27.6	-	-	-	-	-
4c	50	5300	6000	1.12	-26.4	-	-	43.0	-	-
4d	53	5700	6500	1.08	-28.5	-	-	42.3	171.8	19.9
5a	39	4700	4400	1.11	-30.6	-	-	31.9	-	-
5b	51	5800	5000	1.15	-24.2	-	-	-	-	-
5c	56	6500	7000	1.16	-20.8	-	-	42.3	-	-
5d	62	7600	8000	1.13	-26.1	-	-	42.9	179.6	19.1

a) calculated via ¹H NMR spectroscopy; b) determined by SEC analysis in DMF with PS standard calibration; c) DSC analysis in steps of 10 °C min⁻¹ (second heating run); d) DSC analysis (first heating scan)

¹H/¹³C NMR Analysis

As an example, the ¹H NMR spectra obtained after the consecutive steps in the synthesis of the amphiphilic PGA graft copolymers are shown in Figure 1. Subsequent to the release of the EEGE hydroxyl functions the characteristic signals, e.g., for the acetal proton at 4.64 ppm and methyl protons at 1.09 and 1.17 ppm disappear, and a new signal arises at 4.52 ppm corresponding to the protons of the hydroxyl groups. The successful removal of the protecting groups was also monitored by FT-IR spectroscopy. After acetal cleavage a broad band at 3410 cm⁻¹ is observed, which is characteristic for the emerging hydroxyl groups. After glycolide grafting the typical C=O band is observed at 1746 cm⁻¹ (Figure S5). Due to the similar structural elements of PEG and PG units, a broad signal for the poly(ether) backbone is obtained. The differentiation between both units is hampered especially after acetal cleavage due to the similarity of the poly(ether) structures. Nonetheless, the resonances that stem from the poly(glycolide) backbone are clearly distinguishable from the poly(ether) backbone (3.42-3.67 ppm). The ¹H NMR spectrum of the PGA graft copolymer shows several microstructure-related resonances between 4.71-4.91 ppm for the methylene protons of the PGA backbone, of which the signal at 4.91 ppm can be assigned to the in-chain PGA repeating units. Its signal intensity increases with increasing PGA/PEG feed ratios in reference with other PGA-related signals. The characteristic resonances for the hydroxymethylene protons of the terminal glycolic acid unit are observed at 4.11 ppm. The signal of the glycolic acid unit directly attached to the PG block is detected at 4.79 ppm. The esterified hydroxymethylene protons of the poly(glycerol) are shifted towards higher ppm values in comparison to the former resonances located in the region of the poly(ether) backbone. They are split due to the irregular stereocenter at the methine carbon, and they appear as singlet resonances at 4.3 ppm and at 4.11 ppm. Due to the signal overlap of esterified hydroxymethylene protons of the PG units and the terminal glycolic acid units, these signals cannot be used for the calculation of the PGA chain length per arm. However, the observed signal separation for the glycolic acid unit adjacent to the end group (4.84 ppm) compared to the in-chain methylene protons offers the possibility for the determination of the average PGA chain length and the number of end groups from the signal intensity ratio referenced to the methyl end group. In addition, the overall PGA content (wt%) was calculated from the PGA methylene signal intensity after subtraction of the esterified PG methylene protons from the terminal PGA units in reference to the methyl signal intensity. As expected, with lower PGA content fewer PG units were esterified and free hydroxymethylene protons remained, which was evident from the comparison with the number of terminal PGA units. All further calculations are based on the fact that PGA is fully attached to the precursor, since the ¹H NMR spectrum permits to exclude the formation of PGA homopolymer, since this side reaction may be identified by the occurrence of additional signals corresponding, i.e., to the carboxylic acid end group (4.61 ppm).⁴⁰ The accuracy of the signal assignment was confirmed via

two-dimensional NMR spectroscopy (^1H COSY; HSQC, Supporting Information, Figure S3, S4) supporting the successful synthesis of the desired graft copolymers.

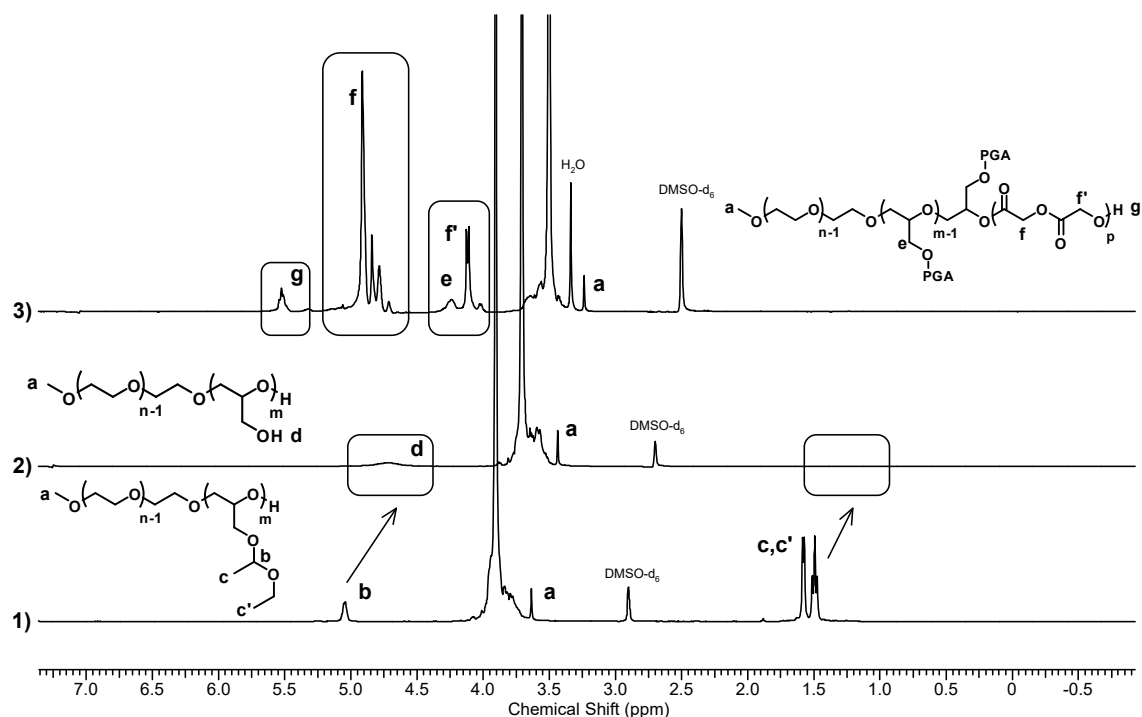


Figure 1. Comparison of ^1H NMR spectra of polymer sample **5c** obtained via $\text{Sn}(\text{Oct})_2$ -catalyzed ROP of glycolide (**3**) initiated with PEG-*b*-PG **5** (**2**) obtained after deprotection of the hydroxyl functions with strong acidic ion exchange resin.

The successful attachment of the PGA arms can be more precisely defined via ^{13}C NMR investigation, which allows for the identification and differentiation of esterified and non-esterified hydroxyl groups of the PG units. As presented in Figure 1, the ^{13}C NMR of the PEG-*b*-PG copolymer displays the typical resonances for the poly(ether) backbone between 69.45 and 70.17 ppm. We focused especially on the methine (79.90–80.13 ppm) and hydroxymethylene protons (60.79–61.05 ppm; 63.10 ppm) of the PG units, which can easily be identified according to their characteristic ^{13}C shifts. After poly(glycolide) grafting the successful linkage can be verified due to the formation of new signals upon esterification (see Figure 3, top spectrum).

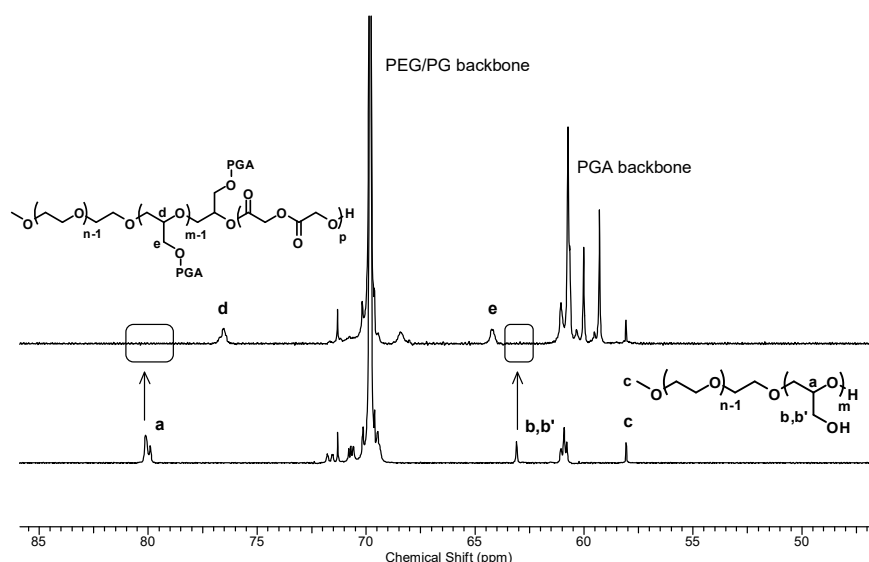


Figure 2. Comparison of ^{13}C NMR spectra (75.5 MHz, DMSO-d_6) of copolymer **3b** (top) after ROP of glycolide initiated with PEG-*b*-PG macroinitiator **3** (bottom); a full ^{13}C NMR spectrum is available in the Supp. Info. (Figure S2).

As it is shown in Figure 3, SEC analysis after each step confirms the successful synthesis of the precursor poly(ether)s and the complete deprotection of the hydroxyl functions which leads to a shift to higher elution volume. The final grafting of glycolide to the poly(ether) polyol is confirmed by an increase of the molecular weight. The molecular weight distributions after each step remain monomodal, and the final graft copolymers show narrow polydispersities in the range of 1.08-1.20. The calculated molecular weights determined via ^1H NMR measurements in DMSO-d_6 differ from the values obtained from SEC measurements in DMF (PS standards) as a consequence of the deviating hydrodynamic volume of branched polymer architectures in comparison to the linear standard.

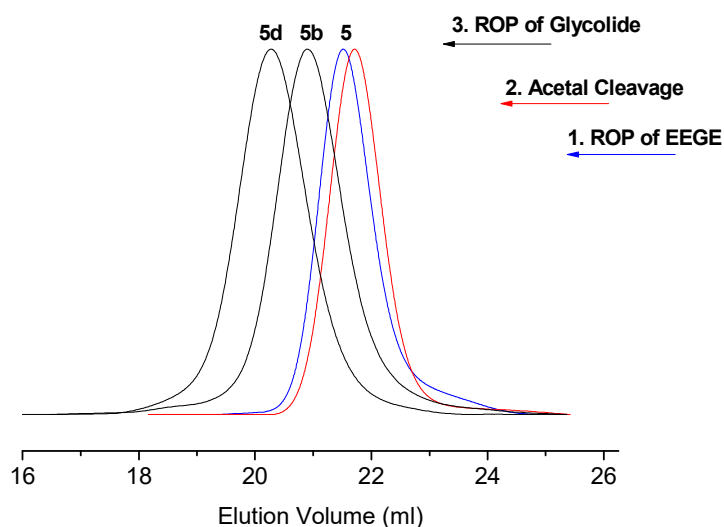


Figure 3. SEC traces after each step of synthesis of PGA graft copolymers (shifted to lower elution volume with higher molecular weight).

MALDI-ToF mass spectrometry characterization has been carried out to verify the accuracy of the synthesis and to enable precise end-group characterization. The respective measurements of the PEG-*b*-PG precursors support quantitative deprotection after acetal cleavage, showing two distribution modes with a constant mass difference corresponding to ethylene oxide (44 g mol^{-1}) and glycerol (74 g mol^{-1}) repeating units (Figure S6). It is important to note that no signals corresponding to the mass peak of non-functionalized poly(ethylene glycol) or residual PEG-*b*-PEEGE are present. The MALDI-ToF mass spectra of the final graft copolymers show a rather complex pattern typical for graft copolymers with varying PEG, PG and PGA block lengths (Figure S7). The additional mass increment of 116 g mol^{-1} reflects the molar mass of glycolide, whereas an odd number of incorporated glycolic acid units (GA molar mass: 58.1 g mol^{-1}) indicates transesterification reactions well-known for $\text{Sn}(\text{Oct})_2$ -catalyzed ROP.⁴¹

Thermal Behaviour

The thermal behaviour of the PGA graft copolymers has been investigated by DSC analysis with respect to the effect of the chain architecture and the influence of the increasing PGA content on the glass temperature (T_g), the melting point (T_m) and the degree of crystallization. The thermal properties play a key role for future applications in the biomedical field.

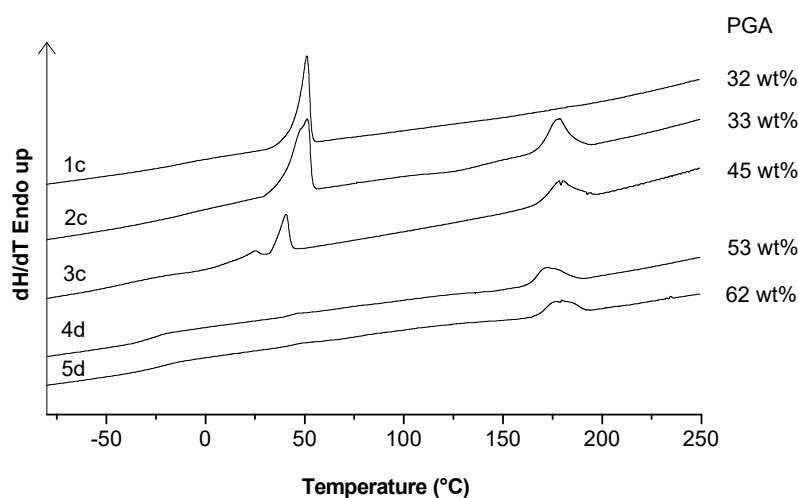


Figure 4. DSC heating curves (10 °C/min) after annealing for 15 h at 150 °C and subsequent cooling to room temperature (1 °C/min).

The obtained PEG-*b*-PG copolymers with PGA fractions up to 45 wt% show a rather constant glass transition between -32 and -35 °C and a melting point (T_m) in the range of 49 to 59 °C . The PEG homopolymer is a crystalline polymer with a T_m of 66 °C .⁴² With increasing PG block length the T_m of PEG is shifted to lower temperatures, whereas the T_g is increased. In contrast, the linear PGA homopolymer exhibits a T_g at about 30 - 45 °C and melts in the range of 210 - 230 °C , depending on

the chain length (PGA oligomers: 160-197°C ($9 \leq n \leq 13$, with n =glycolic acid units)).^{7,37} As expected, all graft copolymers comprising a long PEG chain (114 EO units) provide a sharp T_m of the PEG block that gradually decreases with increasing PGA block length. At the same time, the melting enthalpy is lowered, and an increase of T_g is detected. This observation may be tentatively attributed to miscibility of PEG and short PGA segments. For all graft copolymers exceeding a degree of polymerization of 8 glycolic acid units per arm a single T_m is detected in the range of 173 to 180 °C that stems from the PGA segments. With increasing arm length the melting enthalpy for this transition increases. In the case of shorter PEG blocks (45 EO units) the growing PGA content and chain length dominate the crystalline order, and the crystallization of the PEG segments is suppressed, which is evidenced from the disappearance of the melting point of PEG (see Figure 4). Clearly, the crystallization of PEG and PGA blocks is dependent on the relative length of the PGA and PEG chains. For PEG-*b*-PG with about 5000 g mol⁻¹, in which the PGA block lengths are short, the PEG segment dominates the crystalline order. This impedes a homogenous crystallization and thus a broad melting transition for the PGA segments is observed. For PEG-*b*-PG with about 2000 g mol⁻¹, in which the PGA content is 31-56 wt%, an amorphous material is obtained. All graft copolymers with short PEG blocks, show clear phase separation between the blocks, especially after annealing the samples. Hence two glass transition temperatures are detected, which are clearly assigned to PEG and PGA segments (4c-5d). Graft copolymers with PGA arms with a short chain length and low PEG content are obtained as amorphous materials (4a-c; 5a-d). The PGA chains are too short for crystallization, and the comb-like architecture disturbs the crystallization of PEG. As expected in this system, the prior thermal treatment exerts a significant influence on the degree of crystallization. After heating of the samples to 250 °C in the second run, which should erase the thermal history, either no melting point of PGA is present or a broad transition is slightly visible (s. Figure 5) in contrast to the previously studied precipitated samples (first heating run). This observation is due to the fast cooling rate applied (10 °C/min) by the cooling device, which leads to quenching of the structures. Annealing is a well-known strategy to improve the degree of crystallization and has a great effect on the crystalline morphology of crystalline-crystalline diblock copolymers.^{43,44} Yang et al.⁴⁵ studied PEG-*b*-PLA copolymers and they found that the precrystallization of PLLA affected the crystal orientation of PEG segments. Shin et al. observed PEG crystallization in the framework established by PLLA precrystallization.⁴⁶ The interplay between two crystalline blocks in crystalline-crystalline block copolymers is a topic of current research interest. In order, to assess the effect of annealing, we heated our samples to 150 °C for 15 hours and cooled to room temperature with a cooling rate of 1 °C min⁻¹ to give the PGA chains sufficient time for ordering. In this case, a sharp PGA melting peak can be detected in the first DSC heating scan, comparable with the peak obtained after precipitation. Hence, annealing is a promising way to enhance the degree of

crystallization. In fact, besides composition the prior thermal treatment is a major parameter for the sample morphology ranging from amorphous to semi-crystalline materials.

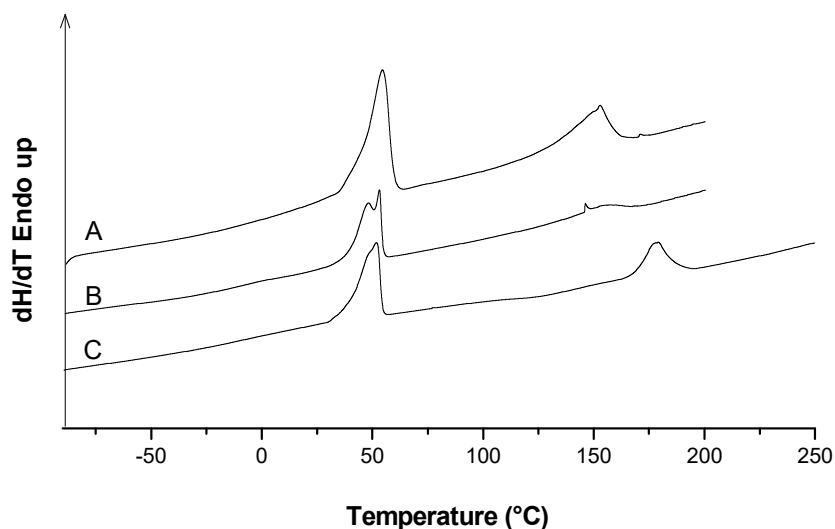


Figure 5. (A) First heating scan of sample **2c** precipitated from solution (T_m : 151.1 °C, ΔH_c : 27.2 J/g), (B) second heating scan of the previously molten sample **2c**, (C) first heating scan after annealing of sample **2c** (T_m : 178.5 °C, ΔH_c : 30.5 J/g).

Further wide-angle X-ray scattering (WAXS) measurements were performed to obtain detailed information on the structures of the materials. In Figure 6 the WAXS patterns are displayed for graft copolymers with varying molar composition. Linear PEG is known to exhibit two crystalline structures: one form has a helical conformation (monoclinic) and the other one has a planar-zigzag conformation (triclinic).^{47,48} In our X-ray powder diffraction studies, we observed two main diffraction peaks at $2\theta=19^\circ$ and $2\theta=23.1^\circ$ that correspond to the crystalline phase of the PEG block. The chain conformation of PGA is a planar-zigzag form arranged in a so-called sheet structure (orthorhombic).^{49,50} With increasing amount of glycolic acid units the characteristic reflections for the crystalline poly(glycolide) domains are observed at $2\theta=21.9^\circ$ and $2\theta=28.5^\circ$, which are in accordance with literature values.^{51,52} WAXS analysis reveals high crystallinity for PGA with decreasing PEG content and increasing PGA molar content. Hence the obtained graft copolymers with low PEG content are dominated by amorphous regions and the crystallization of PEG is suppressed which confirms the results of DSC measurements.

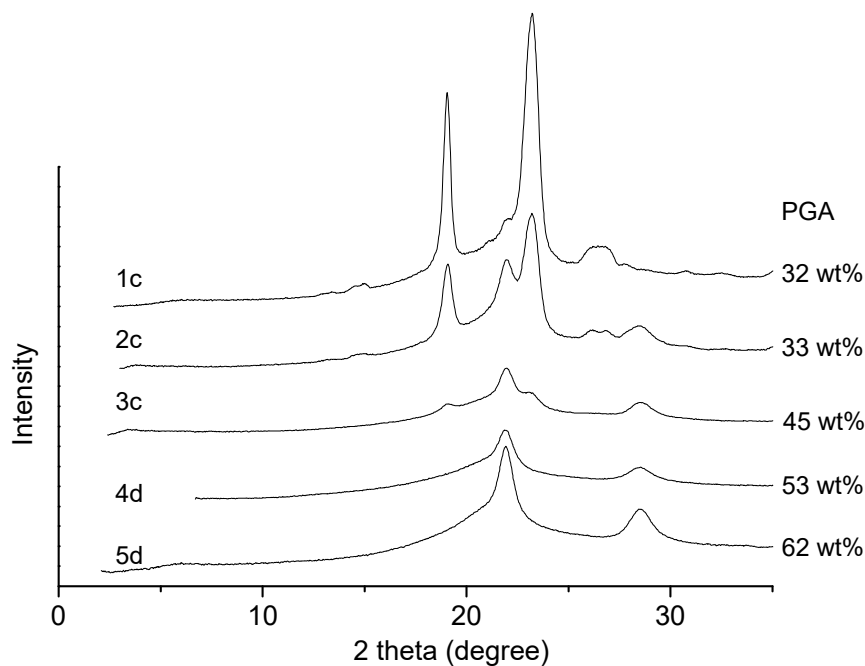


Figure 6. Wide-angle X-ray (WAXS) diffractograms of graft copolymers with different molar composition (in bulk, at room temperature).

Graft copolymers with high content of PEO and a rather small content of poly(glycolide) show water-solubility, as mentioned above. Amphiphilic biocompatible and degradable block copolymers currently attract considerable interest, since they are successfully applied as carrier systems for encapsulation and release of drugs due to their ability to form micelles in aqueous media.⁵³ Transmission electron microscopy (TEM) was performed to obtain information on the aggregation behaviour of the different PGA graft copolymers in solution by using the drop-cast method. The copolymers were initially dissolved in DMSO. Gradual elimination of the solvent was performed via dialysis against water to obtain the pure micelles. One drop of the aqueous solution ($c = 1 \text{ mg ml}^{-1}$) was deposited on a copper grid. After evaporation the samples were investigated by TEM. Representative images of PGA graft copolymers with different molar ratio are shown in Figure 7. As expected, graft copolymers with high hydrophilic to hydrophobic ratio showed spherical micellar aggregates. The diameter of the aggregates varied between 20-80 nm. We assume that the different sizes of the agglomerates depend on the content of the hydrophobic block and the molecular weight of the graft copolymers.

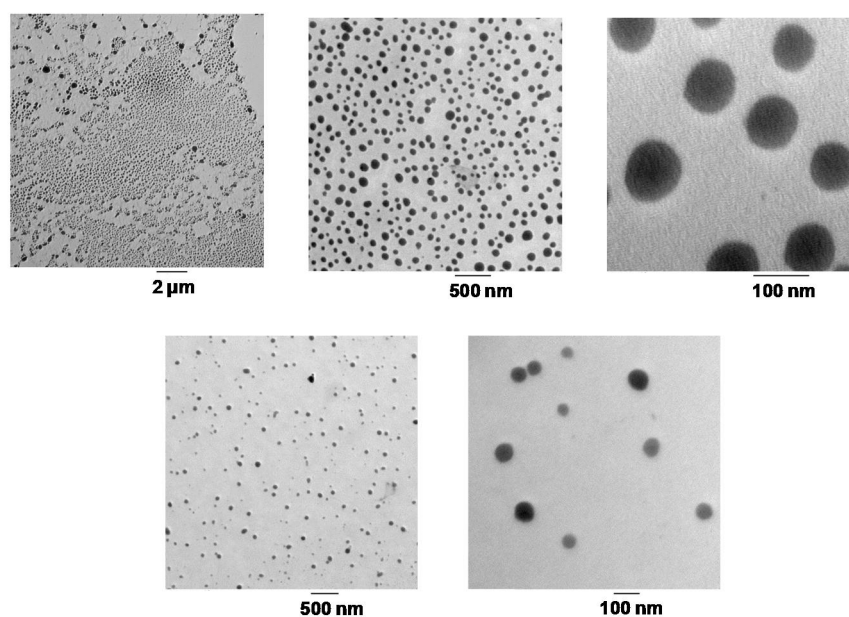


Figure 7. TEM images of graft copolymer **2a** (top) and **1a** (bottom) forming micellar aggregates with an average diameter of 50 to 80 nm.

Microparticle Preparation.

Taking advantage of the amphiphilic nature and the partial water solubility, PGA graft copolymers with PGA weight fractions up to 32 wt% can be applied for microsphere preparation. The basic requirement to develop microparticle delivery systems is the encapsulation of water-insoluble hydrophobic drugs which would be undeliverable in its pure form. Besides PLA and PLGA,⁵⁴ the research in microencapsulation involving poly(ϵ -caprolactone) (PCL) as injectable biodegradable polymer is well established.⁵⁵⁻⁵⁷ The fabrication of microparticles comprises various techniques, including modifications: (1) Emulsion-solvent extraction or evaporation, (2) Spray-drying, (3) Salting out/phase separation or (4) melting techniques.⁵¹ At present, mostly non-degradable polymers like poly(vinyl alcohol) (PVA), sodium dodecyl sulfate (SDS), or PEG-based materials, are used as surfactants in microparticle synthesis. Residual high molecular weight PVA may accumulate in the body and induce inflammatory response. To date, only diblock copolymers consisting of PEO and PLGA or PCL have been evaluated as stabilization agent for microparticle encapsulation.^{58,59} Our objective was to study the capability of the PGA graft copolymers as potential emulsifiers and stabilizers to prepare PCL microparticles by an emulsion-solvent evaporation process. To this end, a copolymer with high PEG content and short PGA chains was chosen to ensure water solubility (Table 2, 1c). By mixing of a 10 % PCL (10 kDa) solution (in dichloromethane) with distilled water (containing the graft copolymer in different concentrations (0.01-1.0 %) as a surfactant) with a homogenizer was obtained in a water-in-oil emulsion. The mixture was poured into an excess of a 0.5 % SDS solution and was stirred for 1 hour with a magnetic stirrer giving dichloromethane time to

evaporate. Spherical microparticles were obtained after centrifugation and have been redispersed in distilled water. This cleaning procedure was repeated twice to reduce residual free surfactant. Finally, the microspheres were drop-cast on an aluminum sheet and dried at room temperature. The PCL microparticles formed were studied by scanning electron microscopy (SEM). Representative images are presented in Figure 8, which display the formation of a mixture of spherical particles with different sizes and a diameter in the range of 10-100 μm . The influence of the hydrophilic/lipophilic ratio of the graft copolymers on the microsphere size is the impact of forthcoming studies.

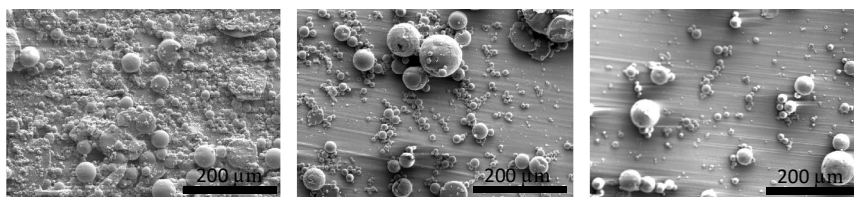


Figure 8. SEM images of PCL microparticles obtained by using copolymer **1c** as surfactant. From left to right: 1 % copolymer **1c** solution, 0.1 % copolymer **1c** solution, 0.01% copolymer **1c** solution.

Conclusion

A synthetic pathway to partially water-soluble poly(glycolic acid) (PGA) based graft copolymers containing one poly(ethylene glycol) block (PEG-*b*-PG) and a variable number of short poly(glycolide) chains has been developed. PEG-*b*-PG precursors have been used as macroinitiators for the ring-opening polymerization of glycolide to obtain well-defined copolymers with adjustable molecular weights in the range of 3900 to 10.800 g mol^{-1} . In order to increase the molar content of PGA, a different number of initiating glycerol units was introduced. This enabled the introduction up to 62 wt% of PGA into the copolymer via a “limited chain length approach” retaining solubility. The copolymers have been characterized with respect to their structure and material properties. 1D (^1H , ^{13}C) NMR measurements and 2D NMR techniques were employed to verify signal assignment and calculate the molar composition. Differential scanning calorimetry (DSC) and WAXS characterization demonstrated that the thermal behaviour is greatly influenced by the PGA/PEG ratio, the average block chain length and the increasing number of PGA side chains, but also by the thermal pre-treatment of the samples.

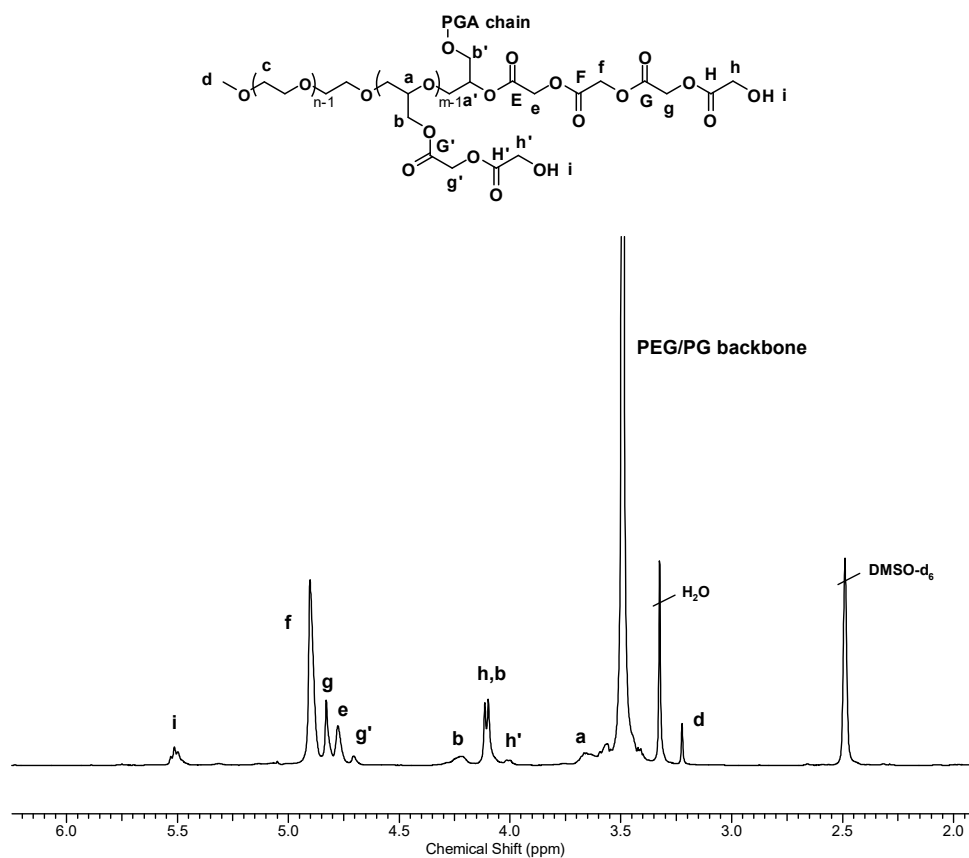
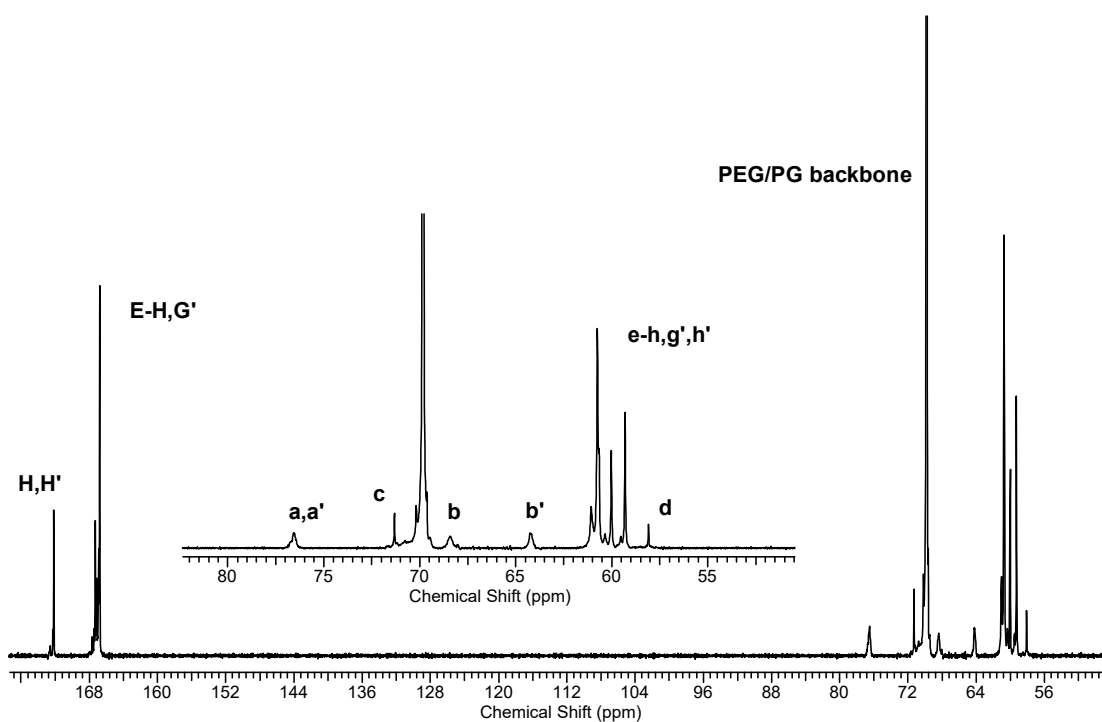
The linear PEG block ensures water-solubility, depending on the average chain length, enabling the formation of micellar aggregates in aqueous solution. The strategy applied to achieve solubility for PGA via limited PGA chain length is a promising route to a large variety of PEG/PGA compositions in the range of 13 to 62 wt% of PGA and provides an effective solution to overcome the well-known solubility problems related with linear PGA homopolymers. First studies dealing with microsphere preparation in emulsion have demonstrated that the linear-graft block copolymers are promising

candidates for interface stabilization. The versatile nature of amphiphilic poly(ester) structures and the multiple end groups render the novel materials interesting with respect to bioconjugation and drug delivery.

Acknowledgement. Dr. Stender is acknowledged for SEM measurements and Dr. M. Gabriel for support with the microparticle preparation. We are thankful for the WAXS measurements performed by Dr. D. Schollmeyer and R. Jung-Pothmann. Support in performing MALDI-ToF MS, SEC and DSC measurements by Dr. Elena Berger-Nicoletti, Monika Schmelzer and Maria Müller is acknowledged. M. W. is grateful to the Graduate School “Materials Science in Mainz” for valuable financial support.

Supporting Information

I. Additional 1D/2D NMR data

Figure S1. ¹H NMR (400 MHz, DMSO-d₆) of PGA graft copolymer **5c**.Figure S2. ¹³C NMR (100 MHz, DMSO-d₆) of PGA graft copolymer **3b**.

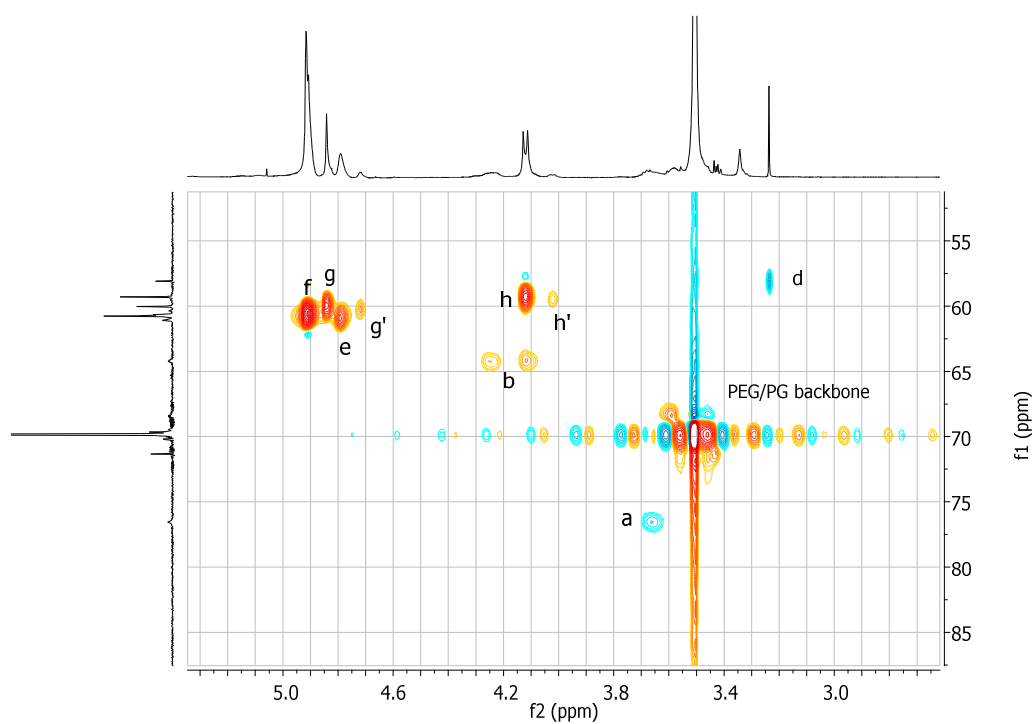


Figure S3. HSQC NMR spectrum of PGA graft copolymer **3b** with dept information (red: methylene, blue: methyl, methine).

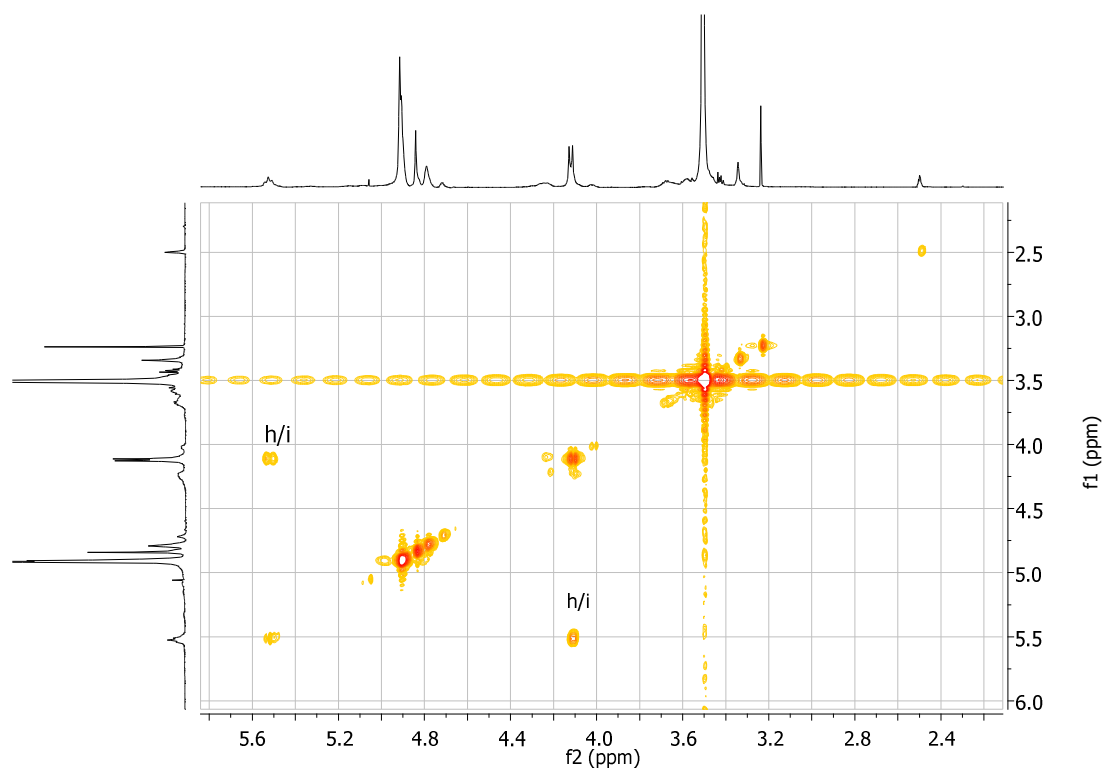


Figure S4. ^1H , ^1H COSY NMR spectrum of PGA graft copolymer **3b**.

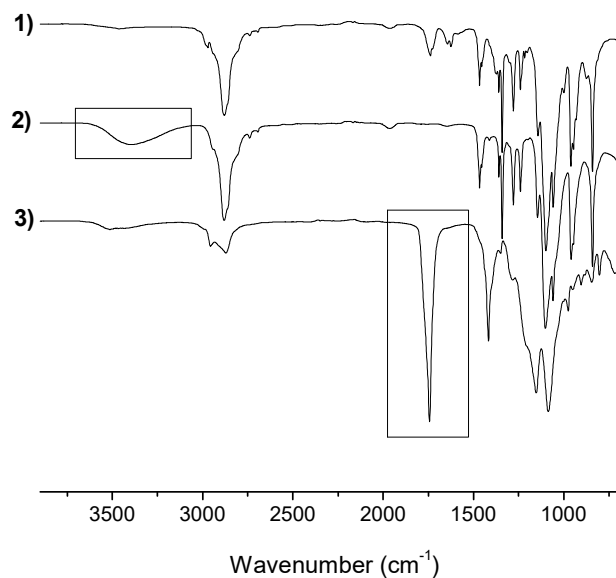


Figure S5. IR spectra (**5**, **5b**) after each step confirming the successful synthesis of PGA graft copolymers in a three-step protocol: (1) Oxyanionic ROP of EEGE, (2) acetal cleavage and (3) Sn(Oct)₂-catalyzed ROP of glycolide.

II. MALDI-ToF MS analysis

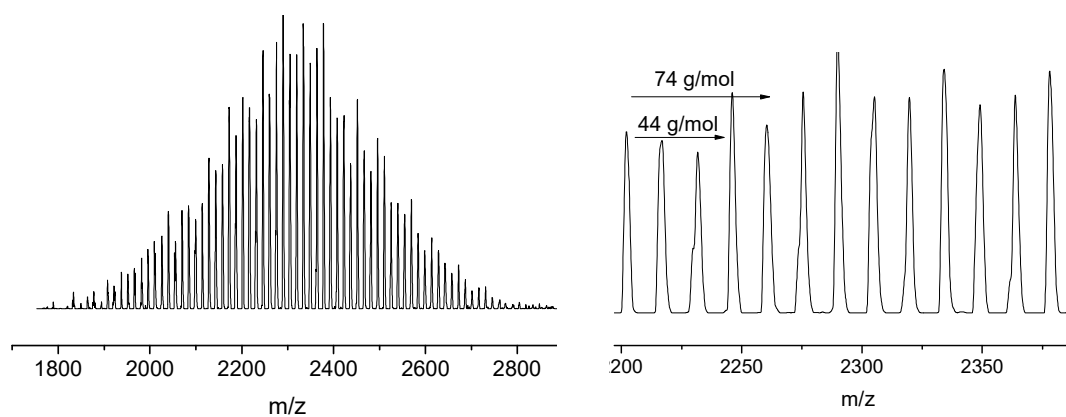


Figure S6. MALDI-ToF mass spectrum of **3** ionized with potassium as counterion.

Table S1. Representative mass peaks corresponding to Figure S6.

m/z	Formula
2202.2	CH ₃ O(CH ₂ CH ₂ O) ₄₅ (CH ₂ CHOCH ₂ OH) ₂ H K ⁺
2216.6	CH ₃ O(CH ₂ CH ₂ O) ₄₂ (CH ₂ CHOCH ₂ OH) ₄ H K ⁺
2231.8	CH ₃ O(CH ₂ CH ₂ O) ₄₄ (CH ₂ CHOCH ₂ OH) ₃ H K ⁺
2246.1	CH ₃ O(CH ₂ CH ₂ O) ₄₆ (CH ₂ CHOCH ₂ OH) ₂ H K ⁺
2275.7	CH ₃ O(CH ₂ CH ₂ O) ₄₅ (CH ₂ CHOCH ₂ OH) ₃ H K ⁺

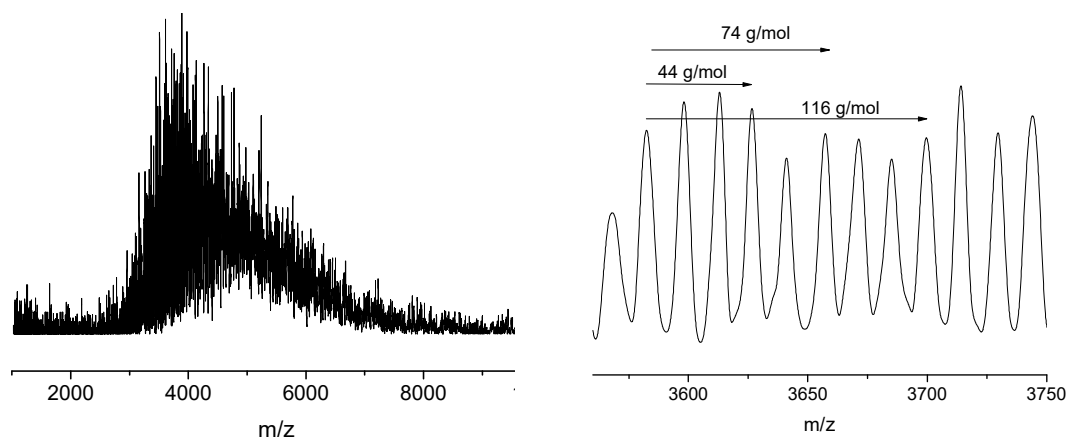


Figure S7. MALDI-ToF mass spectrum of **3b** ionized with potassium as counterion.

Table S2. Representative mass peaks corresponding to Figure S7.

m/z	Formula
3582.4	$\text{CH}_3\text{O}(\text{EO})_{44}(\text{G})_4(\text{GA})_{22}\text{H K}^+$
3598.1	$\text{CH}_3\text{O}(\text{EO})_{47}(\text{G})_4(\text{GA})_{20}\text{H K}^+$
3612.9	$\text{CH}_3\text{O}(\text{EO})_{46}(\text{G})_4(\text{GA})_{21}\text{H K}^+$
3626.6	$\text{CH}_3\text{O}(\text{EO})_{45}(\text{G})_4(\text{GA})_{22}\text{H K}^+$
3641.0	$\text{CH}_3\text{O}(\text{EO})_{44}(\text{G})_4(\text{GA})_{23}\text{H K}^+$
3699.7	$\text{CH}_3\text{O}(\text{EO})_{44}(\text{G})_4(\text{GA})_{24}\text{H K}^+$

References

- Middleton, J. C.; Tipton, A. J. *Biomaterials* **2000**, *21*, 2335-2346.
- Meng, F.; Zhong, Z.; Feijen, J. *Biomacromolecules* **2009**, *10*, 197-209.
- Tessmar, J. K; Göpferich, A. M. *Adv. Drug Delivery Rev.* **2007**, *59*, 274-291.
- Albertsson, A.-C.; Varma, I. K. *Biomacromolecules* **2003**, *4*, 1466-1486.
- Pillai, C. K. S.; Sharma, C. P. *J. Biomater. Appl.* **2010**, *25*, 291-366.
- Lendlein, A. *Chem. unserer Zeit* **1999**, *5*, 279-295.
- Andreas, F.; Sowada, R.; Scholz, J. *J. prakt. Chem.* **1962**, *18*, 141-149.
- Montes de Oca, H.; Ward, I. M.; Klein, P. G.; Ries, M. E.; Rose, J.; Farrar, D. *Polymer* **2004**, *45*, 7261-7272.
- Gautier, E.; Fuertes, P.; Cassagnau, P.; Pascault, J.-P.; Fleury, E. *J. Polym. Sci.: Part A: Polym. Chem.* **2008**, *47*, 1440-1449.
- Montes de Oca, H.; Ward, I. M. *Polymer* **2006**, *47*, 7070-7077.

11. Dickers, K. J.; Huatan, H.; Cameron, R. E. *J. Appl. Polym. Sci.* **2003**, *89*, 2937-2939.
12. Rodríguez-Galán, Franco, L.; Puiggali, J. *J. Polym. Sci.: Part A: Polym. Chem.* **2009**, *47*, 6758-6770.
13. Kasperczyk, J. *Polymer* **1996**, *37*, 201-203
14. Kricheldorf, H. R.; Mang, T.; Jonté, J. M. *Macromolecules* **1984**, *10*, 2173-2181.
15. Jin, X.; Carfacna, C.; Nicolais, L.; Lanzetta, R. *J. Polym. Sci.: Part A: Polym. Chem.* **1994**, *32*, 3115-3122.
16. Martínez-Palau, M.; Franco, L.; Puiggali, J. *J. Polym. Sci.: Part B: Polym. Phys.* **2008**, *46*, 121-133.
17. Fischer, A. M.; Frey, H. *Macromolecules* **2010**, *43*, 8539-8548.
18. Wolf, F. K.; Fischer, A. M.; Frey H. *Beilstein J. Org. Chem.* **2010**, *6*, No.67.
19. Zhang, L.; Fu, J.; Xia, Z.; Wu, P.; Zhang, X. *J. Appl. Polym. Sci.* **2011**, *122*, 758-766.
20. Peng, T.; Su, J.; Lin, G.; Cheng, S.-X.; Zhuo, R.-X. *Colloid Polym. Sci.* **2006**, *284*, 834-842.
21. Torchilin, P. V. *J. Controlled Release* **2001**, *73*, 137-172.
22. Letchford, K.; Burt, H. *Eur. J. Pharm. Biopharm.* **2007**, *65*, 259-269.
23. Kumar, N.; Ravikumar, M. N. V.; Domb, A. J. *Adv. Drug Delivery Rev.* **2001**, *53*, 23-44.
24. Joo, M. K.; Park, M. H.; Choi, B. G.; Jeong, B. *J. Mater. Chem.* **2009**, *19*, 5891-5905.
25. Onaca, O.; Enea, R.; Hughes, D. W.; Meier, W. *Macromol. Biosci.* **2009**, *9*, 129-139.
26. Dingels, C.; Schömer, M.; Frey, H. *Chem. unserer Zeit* **2011**, *45*, 338-349.
27. Zalipsky, S. *Adv. Drug Delivery Rev.* **1995**, *16*, 157-182.
28. Roberts, M. J.; Bentley, M. D.; Harris, J. M. *Adv. Drug Delivery Rev.* **2002**, *54*, 459-476.
29. (a) Kainthan, R. K.; Brooks, D. E. *Biomaterials* **2007**, *28*, 4779-4787; (b) Kainthan, R. K.; Hester, S. R.; Levin, E.; Devine, D. V.; Brooks, D. E. *Biomaterials* **2007**, *28*, 4581-4590; (c) Kainthan, R. K.; Janzen, J.; Levin, E.; Devine, D. V.; Brooks, D. E. *Biomacromolecules* **2006**, *7*, 703-709.
30. Hans, M.; Mourran, A.; Henke, A.; Keul, H.; Moeller, M. *Macromolecules* **2009**, *42*, 1031-1036.
31. Hans, M.; Keul, H.; Moeller, M. *Biomacromolecules* **2008**, *9*, 2954-2962.
32. Wang, J.; Kim, M. H.; Kang, D. E.; Suh, H.; Kim, I. *J. Polym. Sci.: Part A: Polym. Chem.* **2012**; DOI: 10.1002/pola.26040.
33. Donald J. A. Cameron and Michael P. Shaver *Chem. Soc. Rev.* **2011**, *40*, 1761-1776.
34. Wurm, F.; Frey, H. *Prog. Polym. Sci.* **2011**, *36*, 1-52.
35. Dechy-Cabaret, O.; Martin-Vaca, B.; Bourissou, D. *Chem. Rev.* **2004**, *104*, 6147-6176.
36. (a) Taton, D.; Le Borgne, A.; Sepulchre, M.; Spassky, N. *Macromol. Chem. Phys.* **1994**, *195*, 139-148; (b) Keul, H.; Möller, M. *J. Polym. Sci.: Part A: Polym. Chem.* **2009**, *47*, 3209-3231.
37. Fitton, A. O.; Hill, J.; Jane, D. E.; Millar, R. *Synthesis* 1987, 1140-1142.

38. Cohn, D.; Younes, H.; Marom, G. *Polymer* **1987**, *28*, 2018-2022.
39. Dechy-Cabaret, O.; Martin-Vaca, B.; Bourissou, D. *Chem. Rev.* **2004**, *104*, 6147-6176.
40. Dali, S.; Lefebvre, H.; El Gharbi, R.; Fradet, A. *J. Polym. Sci.: Part A: Polym. Chem.* **2006**, *44*, 3025-3035.
41. De Jong, S. J.; van Dijk-Wolthuis, W. N. E.; Kettenes-van den Bosch, J. J.; Schuyl, P. J. W.; Hennink, W. E. *Macromolecules* **1998**, *31*, 6397-6402.
42. Mandelkern, L. *Chem. Rev.* **1956**, *56*, 903-958.
43. Yang, J.; Liang, Y.; Luo, J.; Zhao, C.; Han, C. C. *Macromolecules* **2012**, doi: 10.1021/ma202505f.
44. Zhu, L.; Cheng, S. Z. D.; Calhoun, B. H.; Ge, Q.; Quirk, R. P.; Thomas, E. L.; Hsiao, B. S.; Yeh, F.; Lotz, B. *J. Am. Chem. Soc.* **2000**, *122*, 5957-5967.
45. Yang, J.; Zhao, T.; Zhou, Y.; Liu, L.; Li, G.; Zhou, E.; Chen, X. *Macromolecules* **2007**, *40*, 2791-2797.
46. Shin, D.; Shin, K.; Aamer, K. A.; Tew, G. N.; Russell, T. P.; Lee, J. H.; Jho, J. Y. *Macromolecules* **2005**, *38*, 104-109.
47. Takahashi, Y.; Sumita, I.; Tadokoro, H. *J. Polym. Sci.: Polym. Phys. Ed.* **1973**, *11*, 2113-2122.
48. Takahashi, Y.; Tadokoro, H. *Macromolecules* **1973**, *6*, 672-675.
49. Chatani, Y.; Suehiro, K.; Okita, Y.; Tadokoro, H.; Chujo, K. *Makromol. Chem.* **1968**, *113*, 215-229.
50. Marega, C.; Marigo, A.; Zannetti, R.; Paganetto, G. *Eur. Polym. J.* **1992**, *28*, 1485-1486.
51. Kim, S. Y.; Shin, K. I.; Lee, M. Y. *Biomaterials* **1999**, *20*, 1033-1042.
52. Montes de Oca, H.; Ward, I. M. *Polymer* **2006**, *47*, 7070-7077.
53. Adams, M. L.; Lavasanifar, A.; Kwon, G. S. *J. Pharm. Sci.* **2003**, *92*, 1343-1355.
54. Wischke, C.; Schwendeman, S. P. *Int. J. Pharm.* **2008**, *364*, 298-327.
55. Pérez, M. H.; Zinuttia, C.; Lamprecht, A.; Ubrich, N.; Astier, A.; Hoffman, M.; Bodmeier, R.; Maincent, P. *J. Controlled Release* **2000**, *65*, 429-438.
56. Youan, B. B. C.; Benoit, M.-A.; Baras, B.; Gillard, J. *J. Microencapsulation* **1999**, *16*, 587-599.
57. Chen, D. R.; Bei, J. Z.; Wang, S. G. *Polym. Degrad. Stab.* **2000**, *67*, 455-459.
58. Diab, R.; Hamoudeh, M.; Boyron, O.; Elaissari, A.; Fessi, H. *Drug Dev. Ind. Pharm.* **2010**, *36*, 456-469.
59. Bouillot, P.; Babak, V.; Dellacherie, E. *Pharm. Res.* **1999**, *16*, 148-154.

Chapter 4: Novel Copolymers Based on Poly(lactide)

4.1 Block Copolymers Based on Poly(lactide) and Poly(dimethylsiloxane): Strongly Segregated Systems

Paul Böhm, Anna M. Fischer, Marcin Makowski, Jochen S. Gutmann, Michael Kappl and Holger Frey

Abstract

AB- and ABA-type block copolymers consisting of poly(dimethylsiloxane) and poly(lactide) segments have been developed. The synthesis was carried out using hydroxyl end-functionalized poly(dimethylsiloxane)s, prepared via anionic or cationic ring-opening polymerization (ROP), as a macroinitiator for the ring-opening polymerization of the dilactide. Block-length ratios were calculated from ^1H NMR and were in the range of 1:9 to 9:1 (PDMS:PLLA) and molecular weights between 1.000 and 36.000 g/mol were synthesized, obtaining PDIs of 1.2 to 1.3. Thermal properties were analyzed by DSC measurements and the bulk structure and surface morphology of the different polymers was investigated by use of AFM and TEM analysis. Both PLLA- and PDLA-based block copolymers have been prepared and were demonstrated to form stereocomplexes. Materials derived from stereocomplexation of the poly(lactide) blocks offer potential for application in the field of thermoplastic silicone elastomers.

Introduction

During the last decade, there is an extensively growing interest in poly(lactide)s (PLA), especially for packaging purposes. Compared to common commodity plastics they owe some important advantages, as they are based on renewable resources and thus environmentally friendly while providing the same performance as commonly used polymers like for example poly(ethylene). Poly(lactide) is biodegradable, possesses good barrier properties and adapts well in the biological environment.¹⁻³ However, there are still some PLA features that need to be improved with respect to their application, especially its thermal stability and mechanical properties. Also with regard to processing steps like extrusion, a reduction of the high brittleness of poly(lactide) would be beneficial. An enhancement of the thermal stability of PLA can be achieved by stereocomplexation between poly(L-lactide) and poly(D-lactide), which leads to a significant increase of its melting point.⁴⁻⁸ Moreover, the stereocomplexation of PLA can be used to form or stabilize molecular assemblies, which is of special importance with regard to PLA-containing block copolymers. The use of PLA

stereocomplexation to stabilize certain morphologies has been demonstrated in several examples.⁹⁻
¹² Moreover, block copolymerization can also be used to enhance the properties of poly(lactide).¹³⁻¹⁸
In the current work we aim at a facile synthetic route towards block copolymers combining poly(lactide) and poly(dimethylsiloxane). The properties of silicones, especially poly(dimethylsiloxane)s are strikingly different from those of poly(lactide). This is particularly true with regard to the thermal behavior. Because of the high flexibility of the silicon-oxygen backbone, the glass transition temperature of poly(siloxane)s is lower than -100°C, which represents the lowest value of all known polymers. Therefore, the high flexibility and low viscosity of silicones is retained even at very low temperatures.¹⁹⁻²² Besides, silicones exhibit a set of unique properties that distinguishes them from almost any other polymer with organic backbone.²³⁻²⁶ They show extraordinarily high gas permeability, they are stable against atmospheric oxygen and UV-light and bioinert. This is the reason why silicones are of great importance and have gained an enormous market share in polymer industry. Consequently, silicones are especially qualified to soften polylactides, while additionally providing a set of beneficial properties that complement the features of the resulting material.

The different properties of poly(dimethylsiloxane)s (PDMS) and poly(L-lactide)s (PLLA) motivated us to generate a series of AB- and ABA-type block copolymers comprising these polymers. Very recently, Hillmyer et al. reported on the photolithographic application of PLLA-*b*-PDMS-*b*-PLLA ABA-type block copolymers synthesized by using a commercially available, bifunctional PDMS macroinitiator for the ring-opening polymerization of lactide.²⁷ Admittedly, the combination of these two polymers is extraordinarily interesting from several points of view, at which a precise investigation of the influence of different block length ratios on the properties of the resulting copolymers is required. Therefore we synthesized mono- and difunctional PDMS chains of several block lengths, investigating AB- as well as ABA-type block copolymer structures. The synthetic routes are shown in Figure 1 and 2. Polymers were characterized by ¹H NMR spectroscopy, and the molecular weights distributions were determined via size exclusion chromatography (SEC). The thermal properties of the di- and triblock copolymers were characterized by differential scanning calorimetry (DSC) measurements. Small-angle X-ray scattering (SAXS) as well as atomic force microscopy (AFM) were used to examine the bulk- and surface morphology of the material. Furthermore, the stereocomplexation between PDLA-*block*-PDMS-*block*-PDLA and PLLA-*block*-PDMS-*block*-PLLA was studied by DSC analysis.

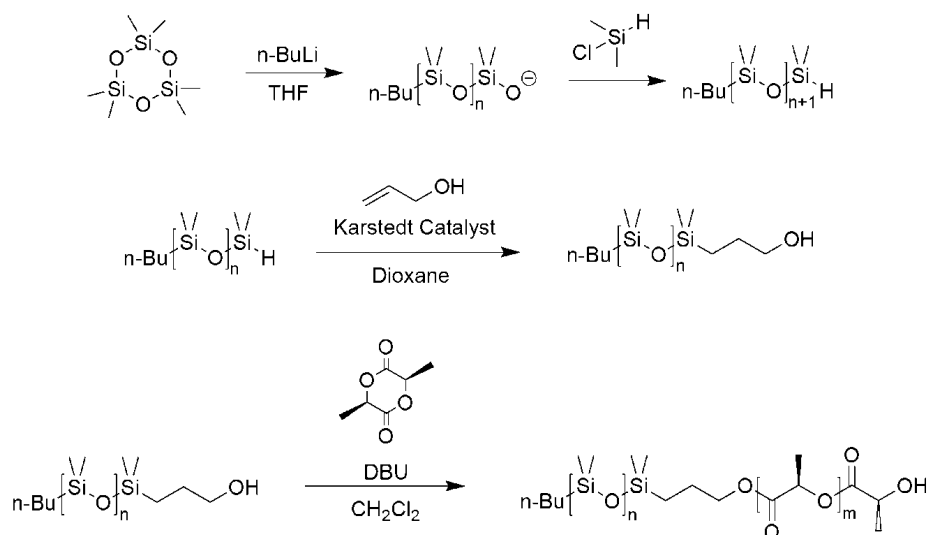


Figure 1. Synthesis of PDMS-*b*-PLLA diblock copolymers.

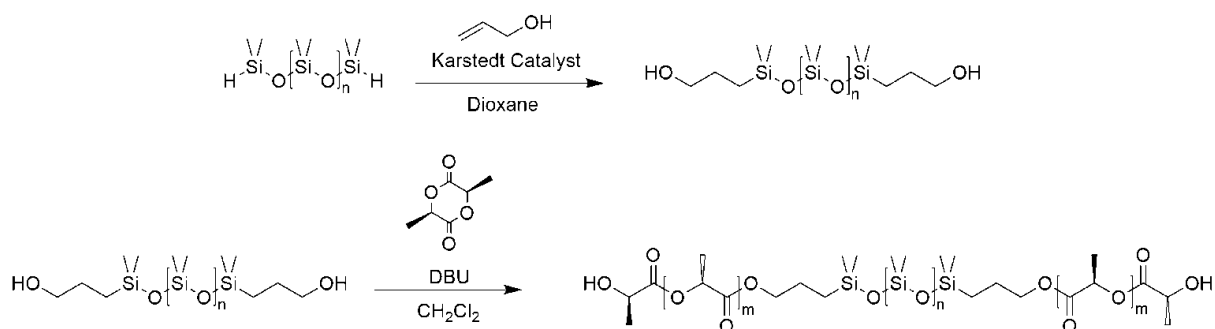


Figure 2. Synthesis of PLLA-*b*-PDMS-*b*-PLLA diblock copolymers.

Experimental Section

Reagents. All reagents and solvents were purchased from Acros Organics or Sigma-Aldrich and used without further purification unless otherwise stated. 1,8-Diaza-bicyclo[5.4.0]undec-7-ene (DBU) was purified by stirring with CaH_2 and subsequent distillation under Argon atmosphere and was stored at low temperatures for a maximum of one week prior to use. L-Lactide was purchased from Purac (Groningen, Netherlands), recrystallized twice from toluene and stored under vacuum prior to use. Hexamethylcyclotrisiloxane (D3) and octamethylcyclotetrasiloxane (D4) were purified by stirring with CaH_2 and freshly distilled before use. Dimethylsilylchloride and tetramethyldisiloxane were freshly distilled before use. Amberlite IRA 743 ion exchange resin was dried under reduced pressure at 60°C . Acid treated bentonite “Tonsil Optimum 210 FF” was purchased from Sued-Chemie and used as received.

Instrumentation. ^1H NMR spectra (300 MHz) were recorded using a Bruker AC 300. All spectra were referenced internally to residual proton signals of the deuterated solvent. For SEC measurements in chloroform, a setup consisting of a Waters 717 plus autosampler, a TSP Spectra Series P 100 pump, three PSS-SDV-5 μl -columns with 100, 1 000, and 10 000 Å pore diameter, respectively, a UV (275 nm), and an RI detector was used. Calibration was carried out using poly(styrene) standards provided by Polymer Standards Service (PSS). DSC curves were recorded on a Perkin Elmer DSC 7 and a Perkin Elmer Thermal Analysis Controller TAC 7/DX. Samples were measured in the range of -100 to 200°C with a heating and cooling rate of 20 or 10 K/min, respectively.

AFM images were taken in dynamic mode, using a Dimension 3100 from Veeco Instruments, CA, equipped with Olympus OMCL-AC240TS cantilevers suitable for soft materials imaging. Polymers were dissolved in methylene chloride and spin coated on a silicon wafer. Before spin coating, the silicon wafers were cleaned in an ultrasonic bath using ethanol and acetone and dried with nitrogen. After spin coating some of the samples were heated to 160°C for at least one hour to allow rearrangement of the polymer chains. Images were taken from droplets that formed during the dewetting process caused by heating the sample. Transmission Electron Micrographs were taken on a Philips EM-420, equipped with a slow-scan CCD camera and a LaB_6 cathode, operating at an acceleration voltage of 120 kV.

Synthetic Procedures.

Mono hydride-terminated PDMS by anionic ring-opening polymerization of D3. Hexamethylcyclotrisiloxane (D3) was cryo-transferred into a 100 ml Schlenk flask equipped with a stirring bar. The flask was purged with argon and sealed with a rubber septum. D3 was dissolved in anhydrous THF, which was added via syringe. Polymerization was started by adding the respective amount of *n*-butyllithium (1.6M solution in hexane). After 2 hours of stirring at ambient temperature, the reaction was quenched by a 1.5 fold excess (with respect to the amount of initiator) of chlorodimethylsilane, and the solution was stirred for another 30 minutes. Subsequently, water was added and the polymer was extracted by threefold extraction with pentane. The combined organic layers were dried over anhydrous MgSO_4 and the solvent removed under reduced pressure. After drying under high vacuum the polymer was obtained in 95% yield. ^1H NMR (CDCl_3 , 300 MHz) δ (ppm): 4.71 (s, 1H, SiH), 1.33 (br, 4H, $\text{CH}_3\text{CH}_2\text{CH}_2\text{CH}_2$), 0.89 (t, 3H, $\text{CH}_3\text{CH}_2\text{CH}_2$), 0.53 (SiCH₂), 0.07 (br, SiCH₃, backbone).

Double hydride-terminated PDMS by cationic ring-opening polymerization of D4. D4 was distilled into a Schlenk flask equipped with a stirring bar. While the flask was purged with argon, 0.02 weight% of acid-treated bentonite was added and the flask sealed with a rubber septum. A respective amount of tetramethyldisiloxane was then added via syringe and the mixture was heated

to 60°C. After an appropriate amount of time, the reaction was cooled to room-temperature. The polymer was dissolved in chloroform and filtered to remove the bentonite catalyst. The polymer was obtained by removing the solvent under reduced pressure and drying the polymer under high vacuum to yield double hydride-terminated PDMS in 85% yield. ^1H NMR (CDCl_3 , 300 MHz) δ (ppm): 4.71 (s, 2H, SiH), 0.07 (br, SiCH₃, backbone).

Hydrosilylation with hydride-terminated poly(dimethylsiloxane)s. A 100 ml Schlenk flask, equipped with a stirring bar and sealed with a rubber septum was put under argon atmosphere and the polymer together with a 1.3 fold excess of allyl alcohol were added and dissolved in anhydrous dioxane. The mixture was heated to 70°C and two drops of Karstedt's catalyst were added via syringe. After 8 hours, the reaction was cooled to room-temperature, the solvent removed under reduced pressure and residual allyl alcohol was disposed by distillation. To remove platinum, the obtained polymer was again dissolved in dioxane, Amberlite ion exchange resin was added and the stirring mixture was heated under reflux for two days. Subsequently, the ion exchange resin together with the adsorbed platinum was filtered off and the pure polymer was obtained by removing the solvent under reduced pressure. Yield: 98%. ^1H NMR (CDCl_3 , 300 MHz) δ (ppm): 3.58 (br, 4H, CH₂OH), 1.58 (br, 4H, CH₂CH₂OH), 0.52 (br, 4H, SiCH₂), 0.07 (br, SiCH₃, backbone).

Ring-opening polymerization of lactide. In a 100 ml Schlenk flask equipped with a stirring bar, the homo- or bishydroxy-functionalized PDMS macroinitiator together with the respective amount of lactide were dissolved in anhydrous methylene chloride (5 ml CH₂Cl₂/g lactide). The polymerization was started by adding 1 mol% of DBU (with respect to the amount of lactide) via syringe. After 20 minutes of stirring at ambient temperature, the reaction was quenched by addition of 1.3 mol% of benzoic acid (with respect to the amount of DBU), dissolved in methylene chloride. The reaction mixture was washed with water three times, the combined layers dried over anhydrous MgSO₄ and the solvent removed under reduced pressure to yield the block copolymer in 90 % yield. ^1H NMR (CDCl_3 , 300 MHz) δ (ppm): 5.16 (q, CH(CH₃), poly(lactide) chain) 4.36 (q, 2H, HOCH(CH₃)), 4.09 (br, 4H, CH₂CH₂O), 1.59 (d, CH(CH₃), poly(lactide) chain), 1.32 (br, 4H, SiCH₂CH₂), 0.89 (br, 3H, CH₂CH₂CH₃), 0.54 (br, 4H, SiCH₂), 0.07 (br, SiCH₃, poly(dimethylsiloxane) chain)

Stereocomplexation of PLLA and PDLA chains. Stereocomplexation between PLLA and PDLA blocks of two block copolymers was induced following the method of Ikada et al.²⁷ Both polymers were dissolved in methylene chloride to obtain a concentration of 1 g/ml. The two solutions were mixed dropwise under vigorous stirring at a 1:1 volume ratio. The mixed solution was cast on a flat glass slide, allowing the solvent to slowly evaporate for about 5 days. The resulting films were then dried in vacuo for 24 hours.

Results and Discussion

Anionic ring-opening polymerization of hexamethylcyclotrisiloxane. In order to synthesize PDMS with a silicon-bound hydrogen atom at only one end of the polymer chain, termination of the anionic ring-opening polymerization of hexamethylcyclotrisiloxane was carried out with chlorodimethylsilane. A 1.6 molar solution of *n*-butyllithium in hexane was used to initiate the polymerization. Due to its high ring strain, polymerization of the D3 monomer proceeds fast even at ambient temperature. Although polymerization time depends on the designated chain length, full conversion was achieved after 2 hours at most. The molecular weight of the obtained polymers was analyzed by SEC and additionally calculated from ^1H NMR spectroscopic data, correlating the integral values of the initiator and the methyl groups of the PDMS backbone. The values obtained by both methods are in good agreement at least for smaller chains. Nevertheless, the discrepancy between these two values becomes larger with growing size of the PDMS chain. (See Supporting Information for a Table of the SEC and ^1H NMR data of some of the PDMS macroinitiators). Molecular weight distributions of the polymers obtained are in the range of 1.1 – 1.3. The SEC curve of a PDMS macroinitiator is shown in Figure 3.

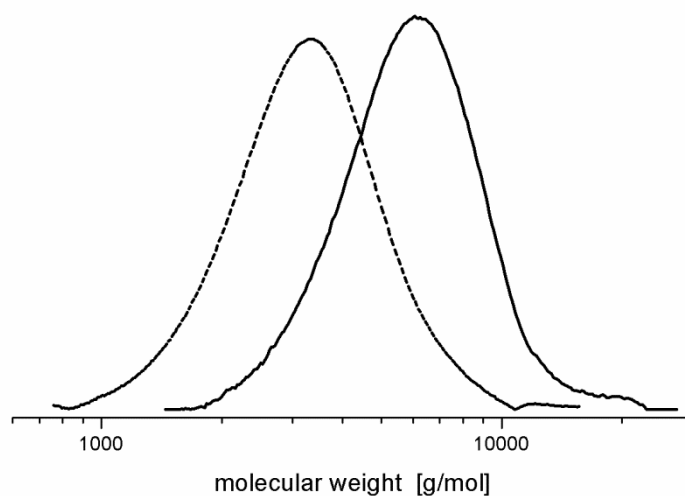


Figure 3. SEC (PS standard, eluent: chloroform) diagrams of hydroxyalkyl-terminated PDMS macroinitiator (---) and PDMS-*b*-PLLA (—).

Cationic ring-opening polymerization of octamethylcyclotetrasiloxane (D4). Cationic ring-opening polymerization of the D4 monomer was carried out to obtain bifunctional poly(dimethylsiloxane)s. Therefore we took advantage of a method developed in 2007 by Chen et al. in which acid treated bentonite is used as a catalyst.²⁹

Bentonite is a special kind of bleaching earth that is actually used for discoloration of oils or textiles.

Bentonite is made of montmorillonite, an aluminumhydrosilicate in which some of the silicon atoms are replaced by iron(III) and some of the aluminum atoms are replaced by magnesium. This leads to negatively charged metal layers between the oxygen atoms that stabilize the montmorillonite structure. This charge can be neutralized by any kind of cation located between the anionic layers. The fact, that these neutralized cations can be replaced easily, makes bentonite something like a natural cation exchange resin. Although the mechanism of this kind of polymerization is not definitively cleared to date, it is proposed that initiation takes place by adsorption of the cyclic monomer on the surface of the heterogeneous catalyst followed by ring-opening through a free proton located inside the montmorillonite. Subsequently, polymerization proceeds by electrophilic attack of the silicon cation on another cyclic monomer. Termination occurs when the growing chain attacks a molecule of the terminating agent tetramethyldisiloxane, leading to silicon-bounded hydrogen at each end of the polymer chain. The use of acid treated bentonite thus provides a facile route to obtain bifunctional poly(siloxane)s of narrow molecular weight distribution over a broad size range.

The synthesized polymers were characterized by ^1H NMR spectroscopy and SEC and show molecular weight distributions around 1.3 to 1.4. However, full conversion could not be accomplished and a certain amount of residual monomer had to be removed under vacuum at high temperature even after a polymerization time of several days. Due to the fact that back- and end biting processes become more and more dominant with longer reaction times, leading to broader molecular weight distributions and a higher amount of low-molecular weight species, we optimized polymerization times between 8 and 20 hours, depending on the chain length of the desired polymer. ^1H NMR spectroscopic data of the obtained polymer can be found in the supporting information.

Hydrosilylation of allyl alcohol with mono- and bifunctional poly(dimethylsiloxane)s.

Hydrosilylation reaction with allyl alcohol was carried out in order to accomplish hydroxyalkyl-functionalities at one or accordingly both ends of the poly(siloxane). Dioxane was chosen as solvent to properly dissolve the hydrophobic PDMS macroinitiator as well as the more hydrophilic allyl alcohol. A platinum-divinyltetramethyldisiloxane complex (Karstedt catalyst) was used to catalyze the hydrosilylation reaction. The reaction process was followed by IR spectroscopy, observing the gradual disappearance of the stretching vibration of the Si-H bond at about 2150 cm^{-1} . According to these results, hydrosilylations were carried out for 3 hours to ensure full conversion. Complete conversion could easily be proven by ^1H NMR spectroscopy, showing that neither a peak of silicon-bounded hydrogen of the PDMS chain nor olefinic protons of the allyl alcohol are left in the spectrum. A 1.3 fold excess of the olefinic compound was used in all hydrosilylation reactions. This point is crucial because unreacted PDMS chains would retain as macromolecular impurities which

can hardly be removed after polymerization of the lactide block. It is important to note that despite the fact that nucleophilic substitution of the silicon-bounded hydrogen by hydroxyl groups is a well-known side reaction in hydrosilylation of alcohols; no alkoxy-substituted silicon could be found in the ^{29}Si NMR spectra of the product.³⁰

Ring-opening polymerization of lactide from PDMS macroinitiators. The hydroxyalkyl-functionalized poly(dimethylsiloxane)s were used as macroinitiators for the ring-opening polymerization of the cyclic lactide monomer to obtain the desired poly(lactide)- poly(dimethylsiloxane) copolymers. A base-catalyzed mechanism was conducted for the lactide polymerization, using the well-known catalyst DBU, which works superb for ring-opening lactide polymerization on a laboratory scale. DBU-catalyzed lactide polymerization features an optimal balance of fast polymerization kinetics and well-controlled polymerization. Although all polymerizations were carried out at room temperature, the reaction time did not exceed 20 minutes. The degree of polymerization could be controlled by adjusting a suitable monomer/initiator ratio. Due to the size distribution of the PDMS macroinitiator it was difficult to target a precise chain-length of the PLLA block. For initiators of smaller molecular weight (< 4000 g/mol), the exact value was calculated from the signal integrals in the ^1H NMR spectrum, but because of growing impreciseness in the proportion of the different peak integrals, the M_n determined by SEC was used as a measure for the molecular weight of the hydroxyalkyl-terminated PDMS. Nevertheless, molecular weight distributions of the resulting block copolymers appeared considerably narrow after addition of the poly(lactide) block. In some cases, especially regarding the polymers composed of initiators of higher molecular weight, PDIs of the block copolymers were even smaller than that of the initiating PDMS. Certainly, it has to be taken into account that in case of the ABA-type triblocks, no information about the homogeneity of the size of the two PDMS-flanking PLLA blocks was available. Molecular weight of the AB- and ABA-type block copolymers was determined by SEC, but could also be calculated by ^1H NMR spectroscopy. For this purpose, signal integral of the methin proton of the PLLA end group was compared to the integral of the methin protons within the PLLA chain to calculate the length of the PLLA block, whereas the ratio between the integrals of the butyl-initiator and the methyl groups of the PDMS chain was used to determine the PDMS block length. Figure 4 shows the ^1H NMR spectrum of a PDMS-*b*-PLLA copolymer.

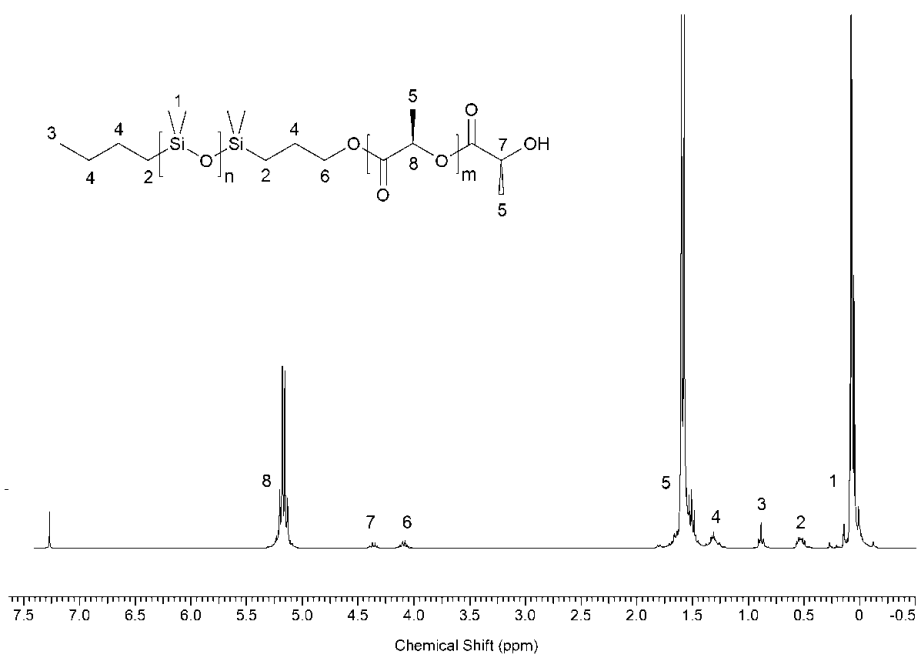


Figure 4. ^1H NMR spectrum (300MHz, CDCl_3) of PDMS-*b*-PLLA.

An overview of the block copolymers that were synthesized during this work is given in Table 1 and Table 2.

Table 1. Molecular weights of PDMS-*b*-PLLA diblock copolymers

PDMS block (g/mol)*	PLLA block (g/mol)*	M_n (g/mol) [†]	M_w (g/mol) [†]	PDI
1400	4600	8600	11600	1.15
1300	2500	7900	10400	1.31
3000	3200	5000	6000	1.19
4100	5100	6500	8200	1.27
1000	8700	7100	9100	1.28
3800	1400	3900	4900	1.28
8400	2800	6200	8000	1.29
10900	1700	6000	7900	1.30
700	600	1800	2400	1.30

*calculated from ^1H NMR spectrum (CDCl_3 , 300 MHz)

[†]SEC data, polystyrene standard, eluent: chloroform

Table 2. Molecular weights of PLLA-*b*-PDMS-*b*-PLLA triblock copolymers.

PDMS block (g/mol)*	PLA block (g/mol)* (per side)	M _n (g/mol) [†]	M _w (g/mol) [†]	PDI
9000	8300	20200	25000	1.24
2800	3200	9600	12900	1.34
3500	3300	9100	12000	1.30
6800	1500	10900	15200	1.40
26400	4900	36400	55300	1.64

*calculated from ¹H NMR spectrum (CDCl₃, 300MHz)

[†]SEC data, polystyrene standard, eluent: chloroform

The size of the PDMS block was varied between 1000 and 20,000 g/mol and the molecular weight of the PLLA chains is in the range between 1000 and 9000 g/mol. However, determining the exact size of the polymer becomes more difficult with increasing chain lengths. This is due to the fact that, as already mentioned above, calculations based on the correlation of the different peak integrals is only reliable up to a certain polymer size. Additionally, poly(styrene) standards were used to calibrate the SEC instrument, which somehow led to a systematic underestimation of the molecular weights of the samples. Nevertheless, the values of the molecular weight determined by SEC and ¹H NMR spectroscopy are in good agreement at least for the smaller polymers.

Thermal Properties of the Block Copolymers. Differential scanning calorimetry (DSC) was used to investigate the thermal properties of the synthesized block copolymers and the extent to which the phase transitions of the several blocks depend on the polymers' composition. Poly(dimethylsiloxane) homopolymers usually exhibit a very low glass transition temperature of about -125°C and a melting point of approximately 40°C. Depending on their chain-length, poly(L-lactide) homopolymers show a glass transition at 38 – 56 °C and a melting point between 135 and 170 °C. The respective values of the analyzed poly(dimethylsiloxane)-poly(lactide) block copolymers show only a slight dependency on the presence of the other block. Admittedly, the fact that these values are visible in the DSC experiment indicates that within the bulk structure of these polymers, the distinct blocks are arranged in separate domains, which explains the fact that they only slightly influence each other with regard to glass transition, crystallization and melting temperature. Nevertheless, a certain dependence of the polymer composition on the crystallization temperature of the PDMS block was observed. Table 3 depicts the results of the DSC measurements of some of the synthesized polymers. In case of the AB-like PDMS-*b*-PLLA block copolymers, crystallization of the PDMS block seems to be facilitated by an increasing length of the PLLA block. This is most probably due to a “fixation” of the

actually very flexible PDMS chains by crystalline PLLA segments that ease crystallization of the PDMS block. The contrary effect occurred regarding the glass transition of the PLLA block of the diblock copolymers. The highly flexible PDMS chains seem to impede the transition of the PLLA chain into the glassy state, leading to a decrease of the PLLA glass transition temperature with an increasing length of the PDMS block. However, there was no effect of the block length ratios on the melting point of the PLLA block which varied between 135 and 145 °C without showing any kind of systematic dependence. It should also be noted that some block copolymers showed neither a crystallization- nor a melting point of the PDMS block, an effect that is well-known for PDMS-containing block copolymers.³¹ Basically the same tendencies are visible in case of the ABA triblock copolymers, whereas the PDMS block tends to be much less affected by the PLLA block than vice versa. There are rather small differences in the crystallization temperature of the PDMS block, while the PLLA glass transition temperature is perceptibly decreasing with an increasing PDMS block length. This indicates an effect that becomes arbitrative in the process of stereocomplexation of the PLLA blocks of these copolymers which will be discussed further down, namely that the high flexibility of the PDMS chain significantly disturbs an accurate high order orientation of the system at least in some cases.

Table 3. DSC data of AB- and ABA-type block copolymers.

PDMS content (wt.%)	T _c (PDMS) (°C)	T _g (PLLA) (°C)	T _m (PLLA) (°C)	ΔH _m [J/g]
AB diblock copolymers				
23	-59.1	73.4	143.4	40.97
26	-60.9	66.3	141.3	34.35
33	-73.7	59.5	140.1	35.49
44	-74.4	33.4	150.8	21.50
50	-75.4	23.7	141.5	15.47
ABA triblock copolymers				
50	-76.6	67.1	135.5	16.72
52	-73.4	53.8	134.8	23.70
82	-54.3	46.4	110.14	22.83

Stereocomplexation. Hetero stereocomplexation of poly(lactide) was used to non-covalently crosslink the triblock copolymers. In order to achieve this, the same PDMS macroinitiator was used to carry out ring-opening polymerization of the L-lactide monomer to yield PLLA-*b*-PDMS-*b*-PLLA and for polymerization of D-lactide, which leads to PDLA-*b*-PDMS-*b*-PDLA. Fortunately, we managed to obtain two block copolymers of almost the same length of PLLA/PDLA blocks, so that stereochemistry

of the lactide units is the only difference between them. It is well-known that poly(lactide)s of different contrary stereochemistry have the ability to form complexes that exhibit high thermal stability and are stable even under harsh conditions. Nevertheless, formation of such stereocomplexes can be crucial if the poly(lactide) chain is part of a di-, tri-, or multiblock copolymer because specific orientation and aggregation usually deriving from incompatibility of the different blocks often hinders free accessibility of the poly(lactide). In order to induce stereocomplexation, solutions of both polymers are rapidly mixed and the solvent is slowly evaporated at room temperature to assure a slow and thorough aggregation process. Differential scanning calorimetry was used to trace stereocomplexation. The complexes formed between PDLA and PLLA chains exhibit a melting point of about 210°C, whereas poly(lactide) melts at about 140°C. Successful stereocomplexation can thus be proven by an increase of the poly(lactide) melting point. Figure 5 shows the DSC curves of a PLLA containing triblock copolymer before and after stereocomplexation with its respective D-lactide analogon.

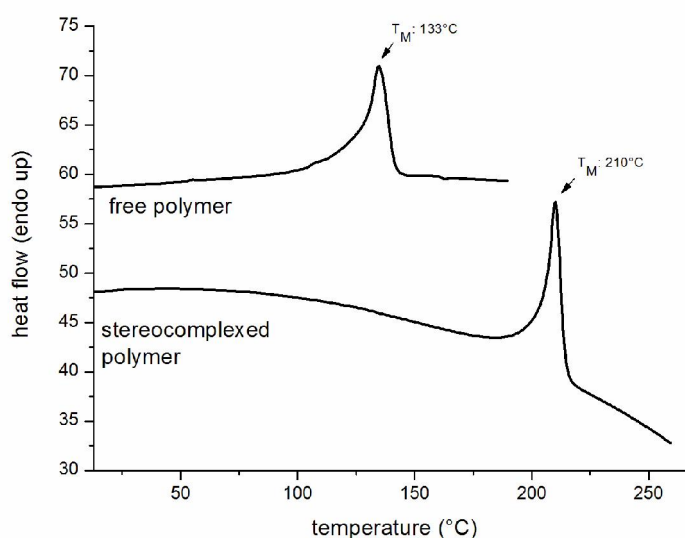


Figure 5. Melting points of PLLA45-b-PDMS47-b-PLLA45 before and after stereocomplexation, determined by DSC (heating rate: 20K/min).

Although we suspected flexible, elastomeric features because of the high PDMS content of the material, mechanical properties of the samples were poor with regard to softness and plasticity. In fact, the obtained materials were hard and brittle instead of showing elastomeric properties. We assume that the reason for this is the high entanglement of the central PDMS chain, which significantly lowers the mobility within the flexible PDMS domains of the network and thus impedes a softening effect of the poly(siloxane) block on the material. Nevertheless, it could be shown that

stereocomplexation works with the triblock copolymers, leading to an extensive increase in the melting point of the poly(lactide) domain.

Atomic Force Microscopy (AFM). To further analyze the structural orientation of the block copolymer, AFM images were taken from samples spin coated on silicon wafers. Without further treatment, none of the polymers showed any significant structural organization either on topography or on the phase image. Thus, samples were then heated to 160°C for at least one hour in order to allow reorganization of the material on the silicon surface. According to the results of the SAXS measurements, this treatment led to formation of organized morphologies. Lamellar patterns were observed for ABA- as well as AB-type block copolymers on topography and phase image, again proving that annealing the material above the PLLA melting point is essential for the formation of structural organization of those polymers. Phase and topography images of one diblock and one triblock copolymer are shown in Figure 7 and 8. We analyzed the images of one diblock and one triblock copolymer, namely PDMS₅₁-*b*-PLLA₁₉ and PLLA₄₄-*b*-PDMS₃₈-*b*-PLLA₄₄ by power spectral density function to determine the average distance between the distinct lamella. For the diblock copolymer shown in Figure 7 the distance was estimated to 18.90 nm, in case of the triblock, the same processing afforded a value of 22.07 nm. The correlations between molecular weight and lamellar thickness are in good agreement with the theories of microphase separated structures developed by Meier, Helfand, Semenov and Kawasaki, stating that $D \sim M^a$, with an exponent of 0.66 or close to 0.66.¹⁸ These calculated distances are reasonable compared to the block lengths that were calculated from the degree of polymerization and an estimated monomer length of 0.29 nm for PDMS and 0.37 nm for PLLA, taking into account that there has to be a certain overlap of the adjacent chains of the same block. Therefore, the calculated values of chain length of 21.76 nm for PDMS₅₁-*b*-PLLA₁₉ and 44.32 nm for PLLA₄₄-*b*-PDMS₃₈-*b*-PLLA₄₄ are higher than those determined by the spectral density function. Figure 9 depicts the model that is suggested for the lamellar orientation of the polymer chains. For the ABA-type triblock copolymer, comparison of the theoretical and the calculated values of chain length suggests that the region of overlapping chain ends is 11.12 nm on each side, which corresponds to 30 lactide units. However, for the diblock copolymer, the overall overlap is only 2.86 nm in length. In that case, the existing data does not give information about the ratio of the overlapping lengths on the PDMS and the PLLA end of the chain.

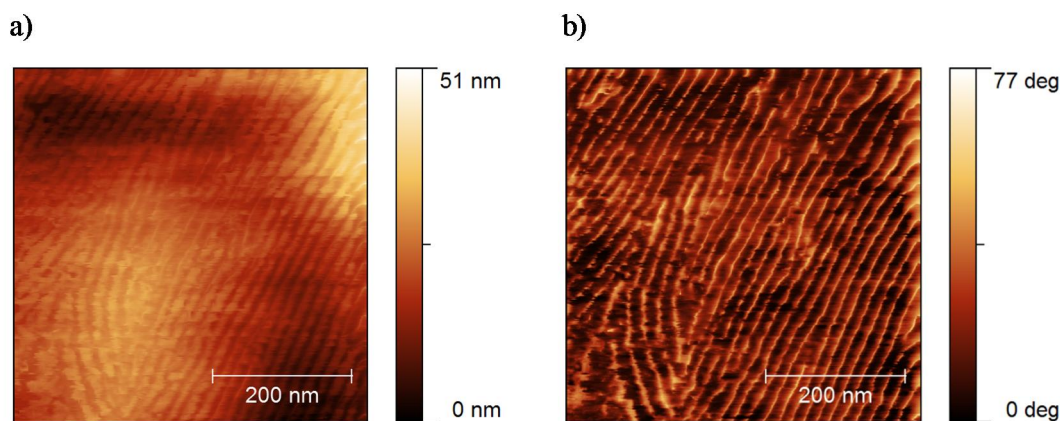


Figure 7. Topography (a) and phase images (b) of PDMS₅₁-*b*-PLLA₁₉ with periodicity of lamellar structure with an interval of 18.90 nm. The bright area on the phase image corresponds to softer parts of the polymer structure.

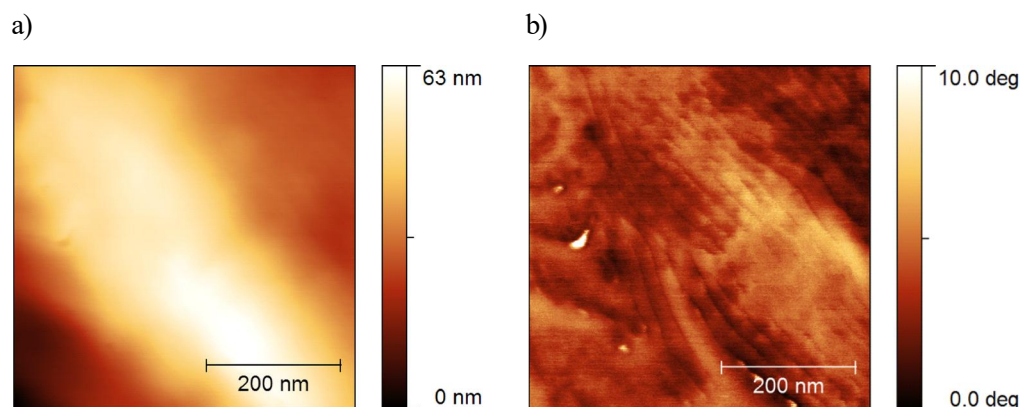


Figure 8. Topography (a) and phase images (b) of PLLA₄₄-*b*-PDMS₃₈-*b*-PLLA₄₄ with periodicity of lamellar structure with an interval of 22.07 nm. The bright area on the phase image corresponds to softer parts of the polymer structure.

Conclusion

We developed a novel kind of AB- and ABA-type block copolymer consisting of poly(dimethylsiloxane) and poly(lactide) segments. The synthetic pathway contained the controlled cationic or anionic ring-opening polymerization of cyclosiloxanes to obtain previously mono- and difunctional PDMS precursors. These were used as macroinitiators for the ring-opening polymerization of lactide, yielding diblock or triblock copolymers with narrow molecular weight distributions. AFM images revealed strong phase separation of the poly(siloxane) and poly(lactide) domains, resulting in a lamellar patterned structure of the material. We took advantage of the lamellar ordering by inducing stereocomplexation of the poly(lactide) blocks in order to stabilize the patterned structure. The

material thus consists of alternating soft PDMS segments and hard segments of stereocomplexed poly(lactide). As the PDMS segments are extremely flexible and the hard domains can be deformed when heated over their melting point of about 210°C, this material represents a structure that can be suitable for applications in the field of thermoplastic elastomers. The addition of the flexible PDMS segments leads to significant softening compared to pure PLA, which is a significant advantage with regard to the processing of the material.

Supporting Information

I. Further characterization data: SEC, ^1H NMR, and DSC

Table S1. Size and molecular weight distributions of mono- and difunctional PDMS macroinitiators
SEC data, PS standard, eluent: chloroform.

M_n (g/mol)	M_w (g/mol)	PDI	M_n (g/mol)	M_w (g/mol)	PDI
monofunctional			difunctional		
800	1000	1.16	2900	4300	1.49
1000	1200	1.25	3900	5400	1.39
3100	4400	1.40	7100	11200	1.57
4000	5400	1.36	9400	13300	1.41
4300	5800	1.36	24000	39000	1.63
10000	13400	1.33			

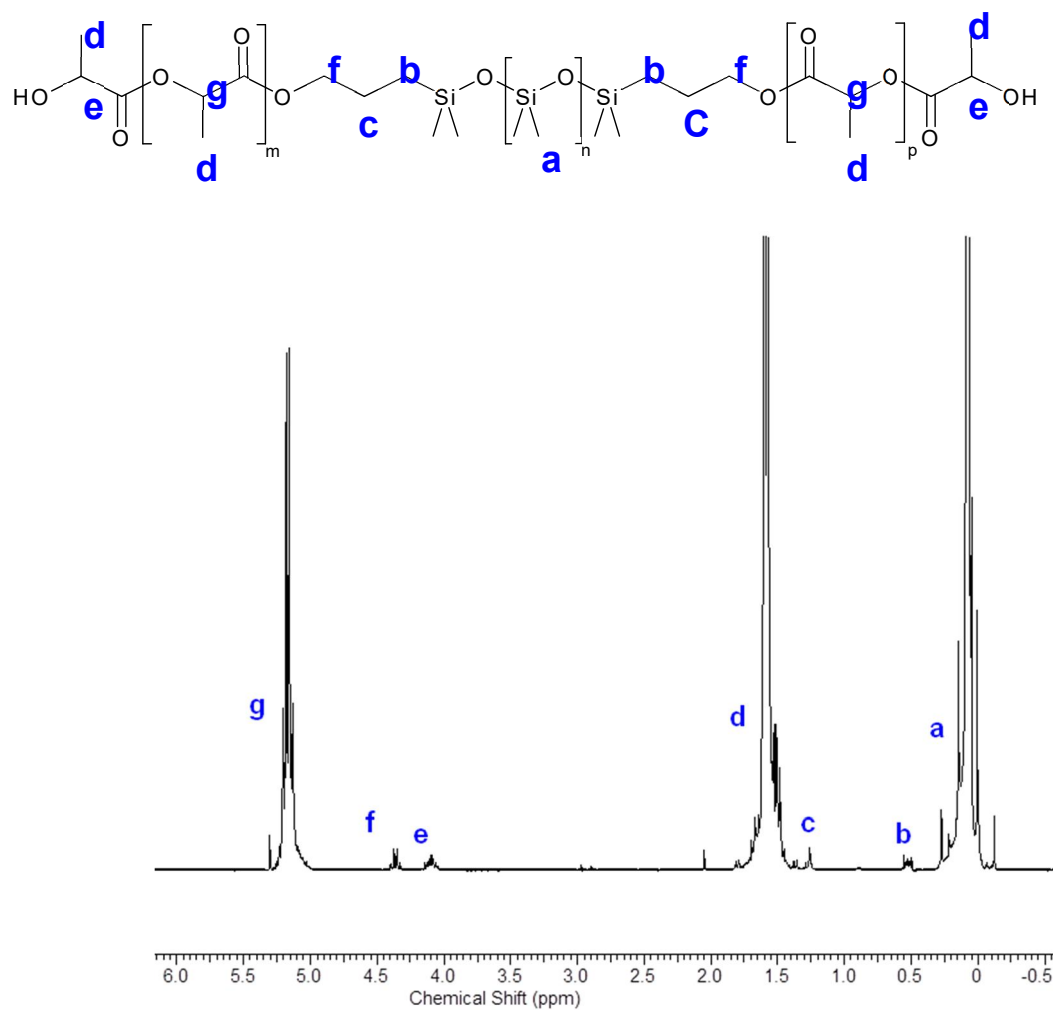


Figure S1. Structure and ^1H NMR spectrum (300MHz, CDCl_3) of PLA-*b*-PDMS-*b*-PLA triblock copolymer. Peaks are assigned by letters a-g.

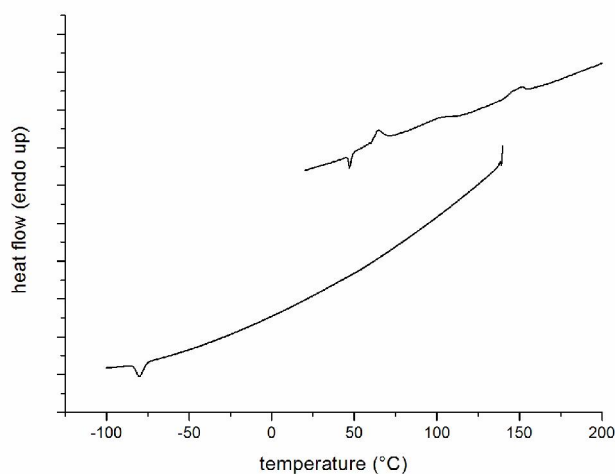


Figure S2. DSC diagram of $\text{PLA}_{xx}\text{-}b\text{-PDMS}_{378}\text{-}b\text{-PLA}_{xx}$, showing PDMS crystallization at -80°C , PLA glass transition at 62°C and PLA melting point at 151°C . heating/cooling rate: 20K/min

References

1. Plackett, D.V.; Holm, V.K.; Johansen, P.; Ndoni, S.; Nielsen, P.V.; Sipilainen-Malm, T.; Södergård, A.; Verstichel, S. *Packag. Technol. Sci.* **2006**, *19*, 1
2. Frederiksen, C.S.; Haugaard, V.K.; Poll, L.; Becker, E.M. *Eur. Food Res. Technol.* **2003**, *217*, 61
3. Ahmed, J.; Varshney, S.K.; Zhang, J.X.; Ramaswamy, H.S. *J. Food. Eng.* **2009**, *93*, 308
4. Tsuji, H. *Macromol. Biosci.* **2005**, *5*, 569
5. Mincheva, R.; Raquez, J.M.; Lison, V.; Duquesne, E.; Talon, O.; Dubois, P.; *Macromol. Chem. Phys.* **2012**, *213(6)*, 643
7. Michell, R.M.; Muller, A.J.; Spasova, M.; Dubois, P.; Burattini, S.; Greenland, B.W.; Hamley, I.W.; Hermida-Merino, D.; Cheva, N.; Fahmi, A. *J. Polym. Sci. Pol. Phys.* **2011**, *49(19)*, 1397
8. Wu, X.H.; El-Ghzaoui, A.; Li, S.M. *Langmuir* **2011**, *27(13)*, 8000
9. Nouailhas, H.; El-Ghzaoui, A.; Li, S.M.; Coudane, J. *J. Appl. Polym. Sci.* **2011**, *122(3)*, 1599
10. Rodwogin, M.D.; Spanjers, C.S.; Leighton, C.; Hillmyer, M.A. *ACS NANO* **2010**, *4(2)*, 725
11. Frick, E.M.; Zalusky, A.S.; Hillmyer, M.A.; *Biomacromolecules* **2003**, *4*, 216
12. Wanamaker, C.L.; Bluemle, M.J.; Pitet, L.M.; O'Leary, L.E.; Tolman, W.B.; Hillmyer, M.A. *Biomacromolecules* **2009**, *10(10)*, 2904
13. Boudouris, B.W.; Frisbie, C.D.; Hillmyer, M.A. *Macromolecules* **2010**, *43*, 3566
14. Ou, X.; Cakmak, M. *Polymer* **2008**, *49*, 5344
15. Williams, C.K.; Hillmyer, M.A. *Polym. Rev.* **2008**, *48*, 1
16. Garlotta, D. *J. Polym. Env.* **2002**, *9*, 63
17. Ho, C.H.; Jang, G.W.; Lee, Y.D. *Polymer* **2002**, *51*, 1639

18. Ren, J.; Zhang, Z.H.; Feng, Y.; Li, J.B.; Yuan, W.Z. *J. Appl. Polym. Sci.* **2010**, *118*, 2650
19. Antunes, J.C.; Oliveira, J.M.; Reis, R.L.; Soria, J.M.; Gomez-Ribelles, J.L.; Mano, J.F. *J. Biomed. Mater. Res. A* **2010**, *94A*, 856
20. Mark, J.E. *Prog. Polym. Sci.* **2003**, *28*, 1205
21. Mark, J.E.; Allcock, H.R.; West, R. *Inorganic Polymers, 2nd ed.*; Oxford University Press. New York, **2004**
22. Brook, M. A. *Silicon in Organic, Organometallic and Polymer Chemistry*, Wiley Interscience, New York, **2000**
23. Mark, J.E. *Acc. Chem. Res.* **2004**, *37*, 946
24. Clarson, S.J.; Fitzgerald, J.J.; Owen, M.J.; Smith, S.D. *Silicones and Silicone-Modified Materials* ACS, Washington D.C., **2000**
25. Mark, J.E. *Physical Properties of Polymers Handbook*; Springer Verlag. New York, **1996**
26. Mark, J.E.; Odian, G. *Polymer Chemistry Course Manual*, ACS, Washington D.C., **1984**
27. Bates, F.S.; Fredrickson, G.H.; *Annu. Rev. Phys. Chem.* **1990**, *41*, 525
28. Tsuji, H.; Suong-Hyu, H.; Ikada, Y. *Macromolecules* **1991**, *24*, 5651
29. Chen, B.; Zhan, X.; Yi, L.; Chen, F. *Chin. J. Chem. Eng.* **2007**, *15(5)*, 661
30. Chung, D.W.; Kim, T.G. *J. Ind. Eng. Chem.* **2007**, *13(6)*, 979
31. Li, W.; Huang, B. *J. Polym. Sci. Part B: Polym. Phys.* **1992**, *30*, 727

4.2 Combining Polysulfides with Polyesters to Degradable Block Copolymers

Jasmin Preis, Anna M. Fischer, Ilja Tabujew, Nicola Tirelli and Holger Frey

Abstract

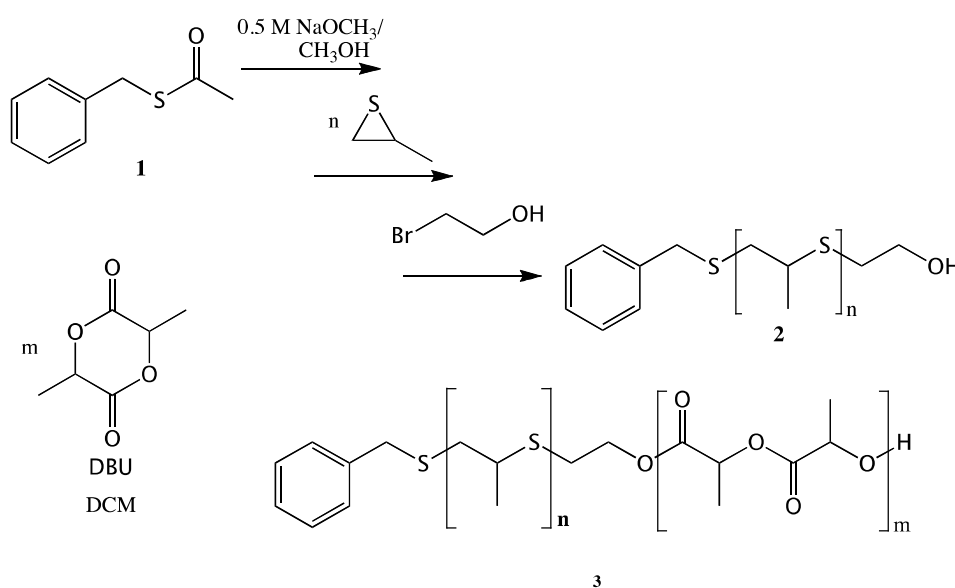
A new type of block copolymer composed of poly(propylene sulfide) and poly(lactide) was synthesized. Propylene sulfide was polymerized and terminated with 2-bromoethanol to gain a hydroxyl functionality at the end of the polysulfide backbone. Subsequently, L- or D-lactide was reacted via 1,8-diazabicyclo[5.4.0]undec-7-ene (DBU)-catalyzed ring-opening polymerization. The synthesized copolymers with different molar content of poly(lactide) were characterized with size exclusion chromatography (SEC), nuclear magnetic resonance spectroscopy (NMR) and differential scanning calorimetry (DSC). Furthermore the adhesion to gold was investigated. Both gold nanoparticles as well as flat gold substrates were coated with the sulfur-containing copolymer and analyzed via UV-Vis spectroscopy and atomic force microscopy (AFM).

Introduction

Poly(lactide) (PLA) is a biocompatible and biodegradable polymer.¹ It has been incorporated in various copolymers for example with poly(ϵ -caprolactone) (PCL)², poly(glycolide) (PGA)³, poly(ethylene glycol) (PEG)⁴, poly(allyl glycidyl ether) (PAGE)⁵ and poly(propylene oxide) (PPO)⁶. PLA copolymers have been successfully employed in numerous biomedical and pharmaceutical applications like in drug delivery systems and implants for bone fixation.¹

The sulfur-analog of PPO, poly(propylene sulfide) (PPS) has been used for copolymer structures, mostly in copolymers with PEG.⁷⁻⁹ The amphiphilic structures of these copolymers are well-characterized, for example with regard to the aggregation behavior in aqueous media, which leads to potential applications for drug delivery.¹⁰⁻¹² Furthermore, different architectures of these species were characterized via polarized light optical microscopy (POM) to investigate the hydration of polymer films.^{13,14} In addition, the attraction between sulfur and gold was used to coat surfaces with these poly(thioethers) and the adsorption of proteins has been explored.¹⁵⁻¹⁷ In a recent work the synthesis of triblock copolymers of PEG, PPS and poly(ethylene imine) (PEI) was reported.¹⁸ In all approaches mentioned, the copolymer structure is achieved by post-polymerization modification. The first strategy pursues the use of a polymer-based macroinitiator for the anionic ring-opening

polymerization of propylene sulfide. The second strategy uses a polymer-based end-capping reagent to terminate the living PPS chain. The combination of both methods leads to triblock copolymers. Here we describe a novel approach, wherein the living PPS chain is end-capped with 2-bromoethanol to introduce a hydroxyl functionality at the end of the polysulfide backbone, which can be addressed directly in the DBU-catalyzed polymerization of L- or D-lactide. To our knowledge, it is the first approach that uses PPS as a macroinitiator. This synthetic strategy leads to tailored copolymers with adjustable block length through the monomer to initiator ratio. The composition of PPS and PLA leads to sensitive copolymers under different conditions. In case of PLA the polymer is completely degradable under enzymatic and hydrolytic conditions¹⁹ through cleavage of the polyester backbone. In contrast, the sulfur atoms of the PPS polymer backbone are oxidation sensitive and have been oxidised to sulfoxides²⁰, which leads to hydrophilic materials properties. The former hydrophobic polymer is then enabled to swell in water. The synthesis route leading to PPS-*b*-PLA copolymers is shown in Scheme 1.



Scheme 1. Synthesis of the poly(propylene sulfide)-*block*-poly(lactide) copolymers in a two step protocol.

A protected thiol acted as an initiator for the anionic ring-opening polymerization of propylene sulfide, namely benzyl thioacetate **1**. As described elsewhere,⁸ the reaction is carried out in degassed THF under argon atmosphere with tributylphosphine as a reducing agent and an in-situ deprotection of the thioacetate in basic media. Subsequent to the polymerization, the termination reaction is performed in acetic acid and DBU buffered solution. The reaction between a thiol and an aliphatic bromo substituted alcohol has previously been described for small molecules under basic conditions and as termination reaction for poly(propylene sulfide) star polymers.^{21,22}

In the present work we achieved an end-capping yield of the polymers **2** exceeding 85 mol%, in most cases even exceeding 90 mol%. We used an excess of DBU before 2-bromoethanol was added. The end-capping yield was calculated via the ratio of the ^1H NMR signals of the methylene group next to the benzene ring of the initiator at 3.77 ppm and the methylene group of the terminating agent adjacent to the hydroxyl function at 3.52 ppm. The infrared (IR) spectra of the synthesized PPS polymers show an adsorption band at 3463 cm^{-1} , which is typical for a hydroxyl functionality. This result confirms the successful termination reaction of the polysulfide with 2-bromoethanol and thereby the introduction of a hydroxyl group at the end of the polymer. The polymers **2** have also been characterized with size exclusion chromatography (SEC). The polydispersity index (PDI) is below 1.25 for all samples, and, as expected for a controlled anionic ring-opening polymerization the mass distribution is monomodal and narrow. After purification of the first block, these polymers were used as PPS-based macroinitiators for the ROP of poly(lactide). In a second step L- or D-lactide was reacted in a DBU-catalyzed ring-opening polymerization in dichloromethane to synthesize the PPS-*b*-PLA copolymers **3**.²³

Table 1. Characterization data of poly(propylene sulfide)-*b*-poly(lactide) copolymers.

Copolymer	Initiator	Sample	DP PPS ⁱ / DP PLA ⁱ	PLA content [wt%]	M _n ⁱ NMR [g·mol ⁻¹]	M _n ⁱⁱ SEC [g·mol ⁻¹]	PDI ⁱⁱ	Yield [%]
3a	2e	PPS- <i>b</i> -PLLA	63/2	6	5150	4000	1.15	quan
3b	2e	PPS- <i>b</i> -PLLA	59/9	23	5850	4400	1.31	71
3c	2d	PPS- <i>b</i> -PDLA	49/10	28	5250	4900	1.19	67
3d	2a	PPS- <i>b</i> -PLLA	30/18	54	5000	5800	1.15	68
3e	2a	PPS- <i>b</i> -PLLA	31/31	66	6950	7400	1.20	55
3f	2a	PPS- <i>b</i> -PLLA	35/69	79	12700	10800	1.21	60

ⁱcalculated by ^1H NMR, ratio of the CH₂-signal of the initiator (benzyl group) and the PPS backbone signals, accordingly to the PLA backbone. ⁱⁱSEC with chloroform as eluent, calibrated with polystyrene standards.

Table 1 summarizes the results of the synthesis of PPS-PLA block copolymers **3**. The weight fraction of poly(lactide) was varied between 6 and 79 weight percent (wt%). The degree of polymerization (DP) has been calculated via ^1H NMR signal ratios of the methylene group next to the benzene ring of the initiator of the PPS block at 3.77 ppm and the signals of the PPS backbone at 2.95-2.77 ppm, 2.67-2.57 ppm plus 1.33-1.30 ppm and accordingly to the signals of the PLA backbone at 5.15 ppm and

1.54-1.44 ppm. The synthesis of the novel copolymers is conducted in a controlled fashion with PDIs below 1.35. Figure 1 shows as an example the SEC traces of one PPS- based macroinitiator and three PPS-*b*-PLLA copolymers. A clear shift between the trace of the macroinitiator and the different copolymer traces to shorter retention times is observed, which indicates successful diblock copolymer formation. In the IR spectra an intensive band is found at 1750 cm^{-1} , the band of the carbonyl group of an ester compound. This also confirms polyester formation. Further hints at the proposed structure are given by ^1H NMR spectroscopy. The proton signal of the CH_2 -group next to the hydroxyl function of the PPS-based macroinitiator is at 3.52 ppm. This signal is shifted to 4.26-4.36 ppm in the NMR spectra of the PPS-*b*-PLA copolymers. The shift occurs due to the ester formation, which clearly demonstrates initiation of the poly(lactide) block by the poly(propylene sulfide) macroinitiator.

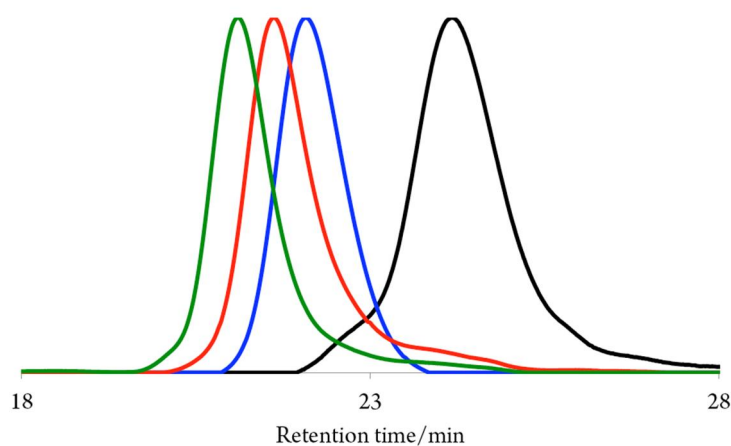


Figure 1. SEC traces (RI signal) in chloroform of the initiator (**2a**, black line) and three PPS-*b*-PLLA copolymers (**3d** blue line, **3e** red line, **3f** green line).

The thermal properties of the synthesized PPS-*b*-PLA copolymers **3** were investigated with differential scanning calorimetry. The results are summarized in Table 2. As a reference one PPS-macroinitiator is also noted. The glass transition temperature (T_g) of the PPS homopolymer is at -48°C , and with increasing PLA content of the copolymers the T_g of the PPS block increases to around -40°C . In the sample with the highest PLA content of 79 wt% the T_g of PPS is not observable anymore. This shows the influence of the less flexible poly(lactide) on the thermal behavior of the poly(propylene sulfide). The crystallization of the poly(lactide) block is first detectable with the copolymer **3b** with 23 wt% PLA. This structure shows a melting point (T_m) at 110°C . The T_m of PLA also increases with increasing poly(lactide) content up to 137°C , as expected. The melting point of PLLA with 100 % optical purity with 169°C is not achieved.²⁴ Furthermore the degree of crystallization of the poly(lactide) block has been calculated.^{25,26} The degree of crystallization rises with increasing PLA content.

Table 2. Thermal properties of the PPS-*b*-PLA copolymers.

Sample	PLA content [wt%]	T _g ⁱ [°C]	T _m [°C]	dH _m [J g ⁻¹]	χ _c ⁱⁱ [%]
2c	0	-48	-	-	-
3a	6	-42	-	-	-
3b	23	-41	104	4.5	1.11
3c	28	-40	111	7.8	2.34
3d	54	-38	120	14.2	8.25
3e	66	-41	124	10.4	7.39
3f	79	-	137	14.7	12.49

ⁱglass temperature PPS block; ⁱⁱdegree of crystallization^{25,26} of the PLA determined via

$$\chi_c = \frac{\Delta H_m}{\Delta H_m^\infty} \times f_w^{LA} \text{ with } \Delta H_m^\infty = 93 \text{ J g}^{-1}$$

The results are summarized in Table 2. As a reference one PPS-macroinitiator is also noted. The glass transition temperature (T_g) of the PPS homopolymer is at -48 °C, and with increasing PLA content of the copolymers the T_g of the PPS block increases to around -40 °C. In the sample with the highest PLA content of 79 wt% the T_g of PPS is not observable anymore. This shows the influence of the less flexible poly(lactide) on the thermal behavior of the poly(propylene sulfide). The crystallization of the poly(lactide) block is first detectable with the copolymer **3b** with 23 wt% PLA. This structure shows a melting point (T_m) at 110 °C. The T_m of PLA also increases with increasing poly(lactide) content up to 137 °C, as expected. The melting point of PLLA with 100 % optical purity with 169 °C is not achieved.²⁴ Furthermore the degree of crystallization of the poly(lactide) block has been calculated.^{25,26} The degree of crystallization rises with increasing PLA content.

The attraction between sulfur and gold can be used to coat poly(propylene sulfide) containing polymers to gold surfaces and gold nanoparticles. The adsorption of the PPS-*b*-PLA copolymers to bare template-stripped gold (TSG) substrates has been demonstrated to be successful. The static contact angle of a water droplet on the polymer coated surface with about 70° differs from the contact angle of the bare substrate with 88°, which is used as a reference. The reference sample has been equally processed, but was been dipped in dichloromethane instead of a polymer solution to exclude any influence by the used solvent.

The surface topography of the coated-gold substrates has been investigated via AFM measurements. Figure 2 shows AFM height and phase images of a polymer-coated gold support. The surface structure of the coated substrate is significantly different compared to the surface topology of the bare gold reference. The comparison of the phase contrast of the reference and the coated supports shows similar results. In addition, the root mean square (RMS) roughness of the height images was

calculated. The RMS roughness describes the standard deviation of the surface height and is a common value to determinate the roughness of a surface.²⁷ The RMS roughness ($1 \times 1 \mu\text{m}^2$) of the TSG amounted about 0.3 nm, which is used as reference. The values of the polymer-coated surfaces were slightly higher with 0.4 nm and 0.5 nm respectively, but it was in the range of the measurement error. Hence, it is assumed, that the copolymer recreated the relatively flat surface structure of the TSG. However, the gold surfaces were not in all cases completely covered by the PPS-*b*-PLA copolymers.

In a further approach the copolymers were employed for the surface modification of citrate-stabilized gold nanoparticles.²⁸ The aqueous gold nanoparticle solution was extracted with a polymer solution in dichloromethane. Figure 2 illustrates photographs of the different solutions before extraction and afterwards. The PPS macroinitiator **2c** acts as a reference (i.e. 0 wt% PLA) and the copolymers with 6 wt% (**3a**) and 23 wt% (**3b**) poly(lactide) content are shown. It is clearly observable that only the PPS homopolymer is capable of removing the red colored gold nanoparticles from the water phase. This observation was investigated with UV-Vis spectroscopy in more detail.

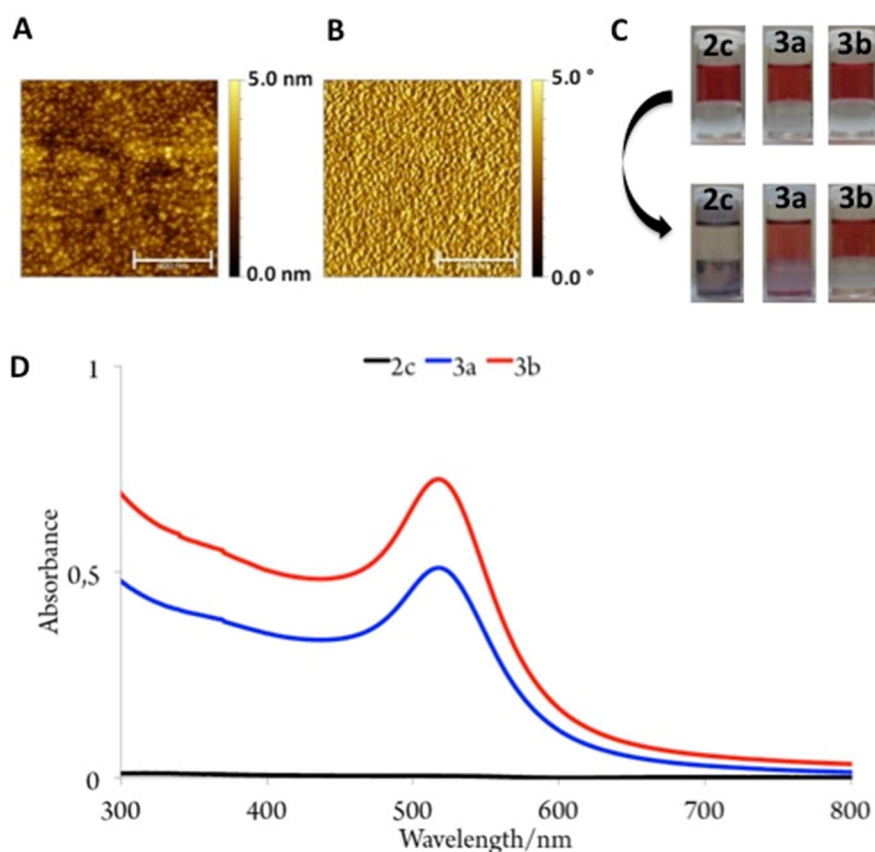


Figure 2. (A) AFM height image of copolymer **3d** on a gold substrate (scale bar 400 nm) (B) AFM phase image of copolymer **3d** on a gold substrate (scale bar 400 nm) (C) photographs of the gold nanoparticle extraction (D) UV-Vis adsorption of the aqueous solutions of gold nanoparticle extraction.

The results are shown in Figure 2 as well. In case of the macroinitiator no absorbance remains in the water phase, which means the gold nanoparticles are removed completely from the aqueous solution. The copolymer **3a** with a content of 6 wt% of PLA is capable of transferring a fraction of gold nanoparticles, indicated through the partially reduced absorbance of the water phase. All other copolymer samples with higher poly(lactide) content as 6 wt% are not able to bind to the gold nanoparticles and extract them from the aqueous solution. This suggests that the PLA block prevents the binding of the polysulfide block to gold nanoparticles. We tentatively ascribe this to shielding of the PPS block by PLA, considering that the sulfur atoms of the PPS cannot interact with the gold surface of the gold nanoparticles in the water phase.

In summary, the successful synthesis of hydroxyl-terminated poly(propylene sulfide) with narrow molecular mass distribution has been presented. In a second step the PPS was shown to act as a macroinitiator for the ring-opening polymerization of D- or L-lactide to form a novel type of copolymer in a controlled manner. The proposed structures of the samples were confirmed by NMR spectroscopy, DSC and IR spectroscopy. Furthermore the adsorption to gold substrates and gold nanoparticles was analyzed with AFM and UV-Vis spectroscopy. The adsorption of the copolymers from dichloromethane solutions to gold supports was demonstrated, as shown via static contact angle and AFM measurements. In case of the gold nanoparticles the adhesion of the PPS block was impeded by larger PLA blocks. For PPS-PLA block copolymers in dichloromethane with higher molar content than 6wt% poly(lactide) the binding to gold nanoparticles in aqueous solution is not viable.

Supporting Information. Experimental details, ^1H NMR and ^{13}C NMR spectra, IR spectra, UV-vis spectroscopy data, AFM height and phase images, data of the contact angle measurement. This material is available free of charge via the Internet at <http://pubs.acs.org>.

Notes

The authors declare no competing financial interest.

Acknowledgment. J. P. thanks Professor H. J. Butt, Dr. R. Berger and U. Rietzler of the Max Planck Institute for Polymer Research for the ability and support to use the AFM and Professor R. Zentel for the supply of the contact angle goniometer.

Supporting Information

Experimental Section

Materials and Instrumentation

All chemicals are commercially available from *Sigma-Aldrich Germany*, *Acros* or *Fluka* and were used as received, unless otherwise noted. Tetrahydrofuran (THF) was degassed via five cycles of freeze-pump-thaw. Dichloromethane (DCM) was stored over molecular sieve. 1,8-Diazabicyclo[5.4.0]undec-7-ene (DBU) was dried over calcium hydride and freshly distilled prior to use. The deuterated solvents (dimethyl sulfoxide- d_6 and chloroform- d) were purchased from *Deutero GmbH*. Benzyl thioacetate (**1**) was synthesized as described elsewhere.²⁹ Gold nanoparticles (20 nm) in aqueous solution were synthesized accordingly to the literature.³⁰ Flat gold substrates were produced via the template stripped gold method.³¹

The nuclear magnetic resonance spectra (NMR) were recorded on a *Bruker* spectrometer at a frequency of 300 MHz for the proton spectra and the carbon spectra were recorded at 75.5 MHz. All spectra were referred to an internal standard (the proton signal of the deuterated solvents). FT-IR spectra were recorded using a *Thermo Scientific* (Nicolet iS10) spectrometer. For the characterization of the substances only the typical and intensive bonds are given. The size exclusion chromatography (SEC) was performed in chloroform with 1 ml min⁻¹ on a set of three *PSS SDV* columns (10⁴/500/50 Å) connected to a RI and an UV detector as well as a *waters 717 plus* auto sampler and a *TSP Spectra Series P 100* pump. A polystyrene standard calibration was used. For the measurements of thermal properties a *Perkin Elmer* DSC 8500, calibrated with indium, in a temperature range from -95°C to 180°C and a heating rate of 10 K per minute was used. The UV-Vis spectra were measured on a *Jasco* V-630 Spectrophotometer at 20°C. The AFM measurements are carried out on a *Veeco NanoScope Dimension 3100* in tapping mode with silicon cantilevers with a resonance frequency of 300 kHz, a spring constant of 42 N m⁻¹ and a tip height of 11 µm. To collect the data nanoscope 5.31r1 and, to analyze the data, Gwyddion 2.25 was used. Static water contact angles were measured on a *data physics* OCA 20 with SCA 20 software. A droplet of deionized water was placed on the surface of the substrate and imaged via a video camera. The contact angle was calculated via software. This procedure was repeated 10 times on different positions of the substrate.

Synthesis of poly(propylene sulfide) with one terminal hydroxyl function (2)

In a typical experiment the reaction vessel was evacuated three times under high vacuum and purged again with argon. 5 ml of degassed THF were added to the reaction flask and benzyl thioacetate (**1**) in 1 ml THF was added. Then 5 equiv tributylphosphine (TBP) in 1 ml THF and 1.05 equiv sodium methoxide solution (0.5 M in methanol) in 1 ml of THF were introduced. After 5 minutes 10, 20, 30 or 40 equiv propylene sulfide in 1 ml THF were added and the reaction mixture

was stirred at room temperature for 45 minutes. The pH was adjusted using 1.1 equiv of acetic acid in 1 ml THF and 2.3 equiv DBU in 1 ml THF. 5 equiv of 2-bromoethanol in 1 ml THF were added and the reaction was stirred for 16 hours at room temperature. The solvent was removed at the rotary evaporator, the residue was redissolved in dichloromethane and extracted three times with water. The organic phase was dried over anhydrous sodium sulfate, filtrated and the solvent was completely removed. The viscous oil was extracted 3 times with methanol or petroleum ether and dried in vacuum.

FT-IR (on ATR crystal) [in cm^{-1}]: 3463, 2958, 2919, 2864, 1449, 1308, 1041, 1006, 734, 701. ^1H NMR (300 MHz, DMSO-d_6): δ (ppm) = 7.33-7.24 (m, $\text{C}_6\text{H}_5\text{-CH}_2\text{-}$); 3.77 (s, $\text{C}_6\text{H}_5\text{-CH}_2\text{-}$); 3.52 (t, $\text{-S-CH}_2\text{-CH}_2\text{-OH}$); 2.97-2.85 (broad, diastereotopic H of $\text{-CH}_2\text{-}$ PPS chain, -CH- PPS chain); 2.67-2.55 (broad, diastereotopic H of $\text{-CH}_2\text{-}$ PPS chain); 1.27-1.22 (broad, -CH_3 PPS chain). ^{13}C NMR (75.5 MHz, $\text{CHCl}_3\text{-d}$): δ (ppm) = 138.22, 128.96-127.18 ($\text{C}_6\text{H}_5\text{-CH}_2\text{-}$); 61.05 ($\text{-S-CH}_2\text{-CH}_2\text{-OH}$); 41.32-40.45 (-CH- PPS chain); 38.78-37.06 ($\text{-CH}_2\text{-}$ PPS chain); 34.16 ($\text{C}_6\text{H}_5\text{-CH}_2\text{-}$); 22.01-20.59 (-CH_3 PPS chain).

Table S1. Synthesized poly(propylene sulfide)s (PPS) with one terminal hydroxyl function.

Macroinitiator	DP PS ⁱ	M_n^i [g·mol ⁻¹]	M_n^{ii} [g·mol ⁻¹]	PDI ⁱⁱ	Yield [%]	End-capping ⁱⁱⁱ [mol%]
2a	25	2000	1400	1.15	45	90
2b	35	2800	1700	1.15	59	95
2c	39	3100	2500	1.21	30	85
2d	47	3700	2800	1.20	48	91
2e	48	3750	3300	1.24	48	100

ⁱcalculated by ^1H NMR, ratio of the CH_2 -signal of the initiator (benzyl group) and the PPS backbone signals. ⁱⁱSEC with chloroform as eluent, calibrated with polystyrene standards. ⁱⁱⁱRatio of the ^1H NMR signal of the CH_2 of the benzyl-group and the CH_2 -signal of the end-capping agent.

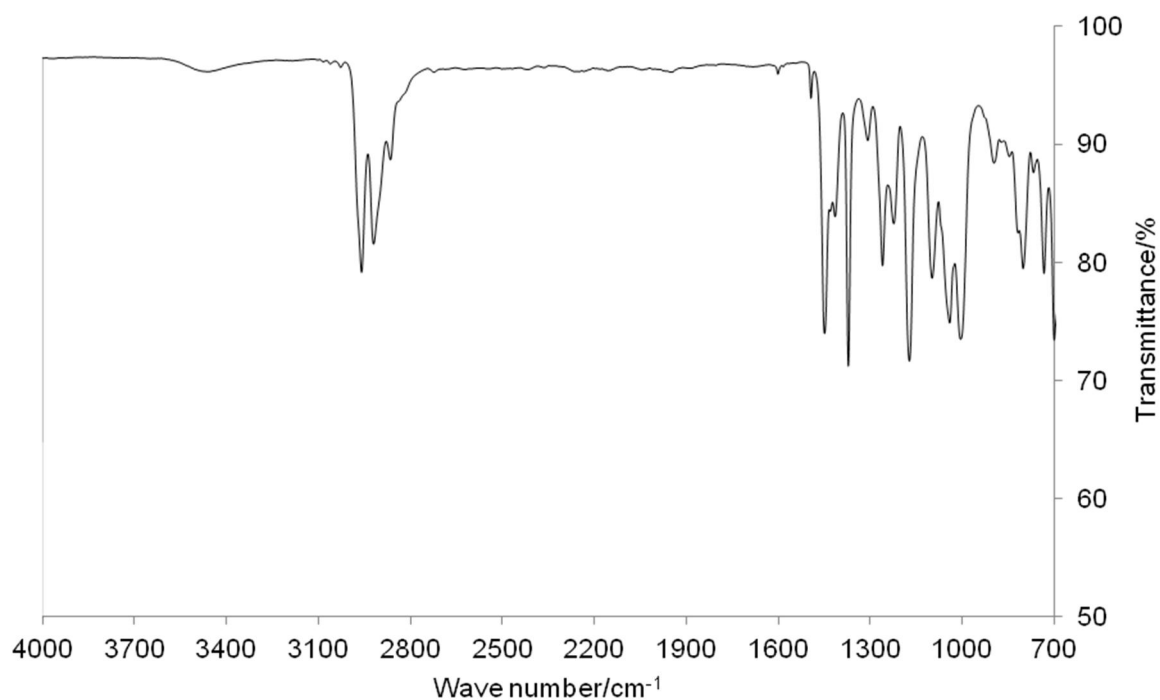


Figure S1. IR spectrum (film on ATR crystal) of PPS with one terminal hydroxyl function.

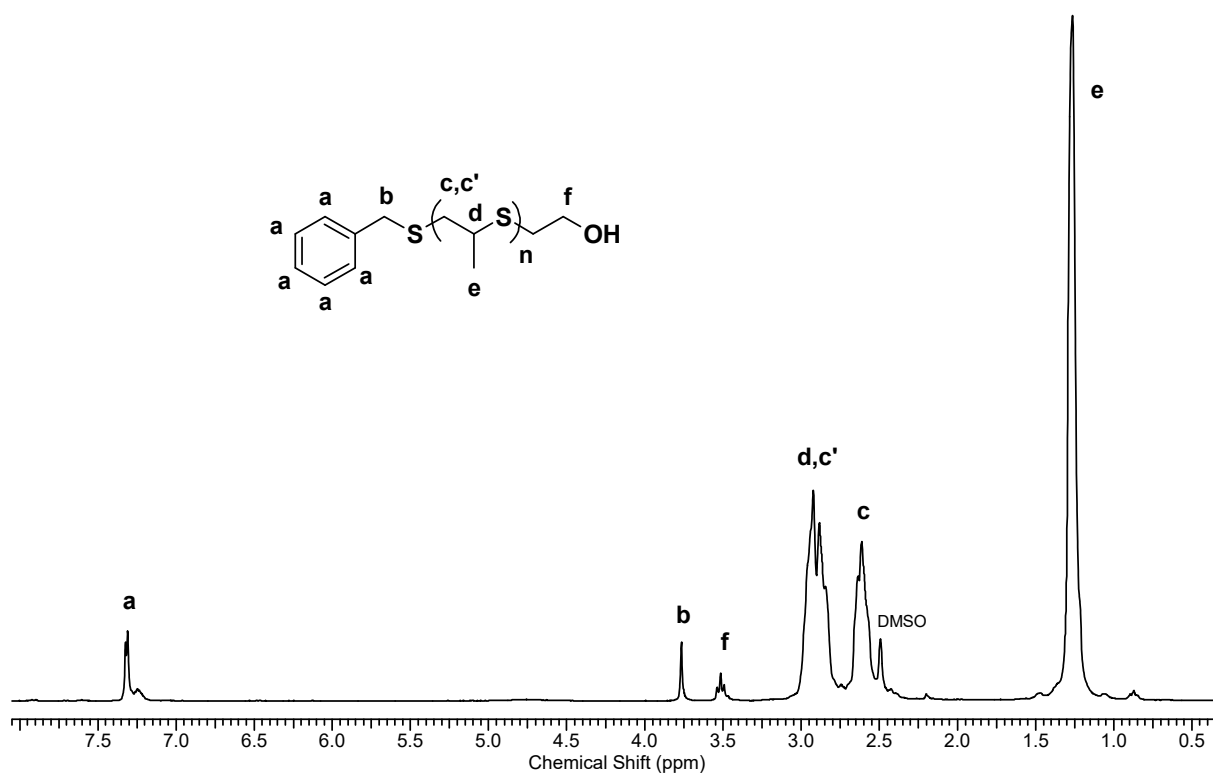


Figure S2. ¹H NMR (300MHz, DMSO-d₆) spectrum of PPS with one terminal hydroxyl function **2a**.

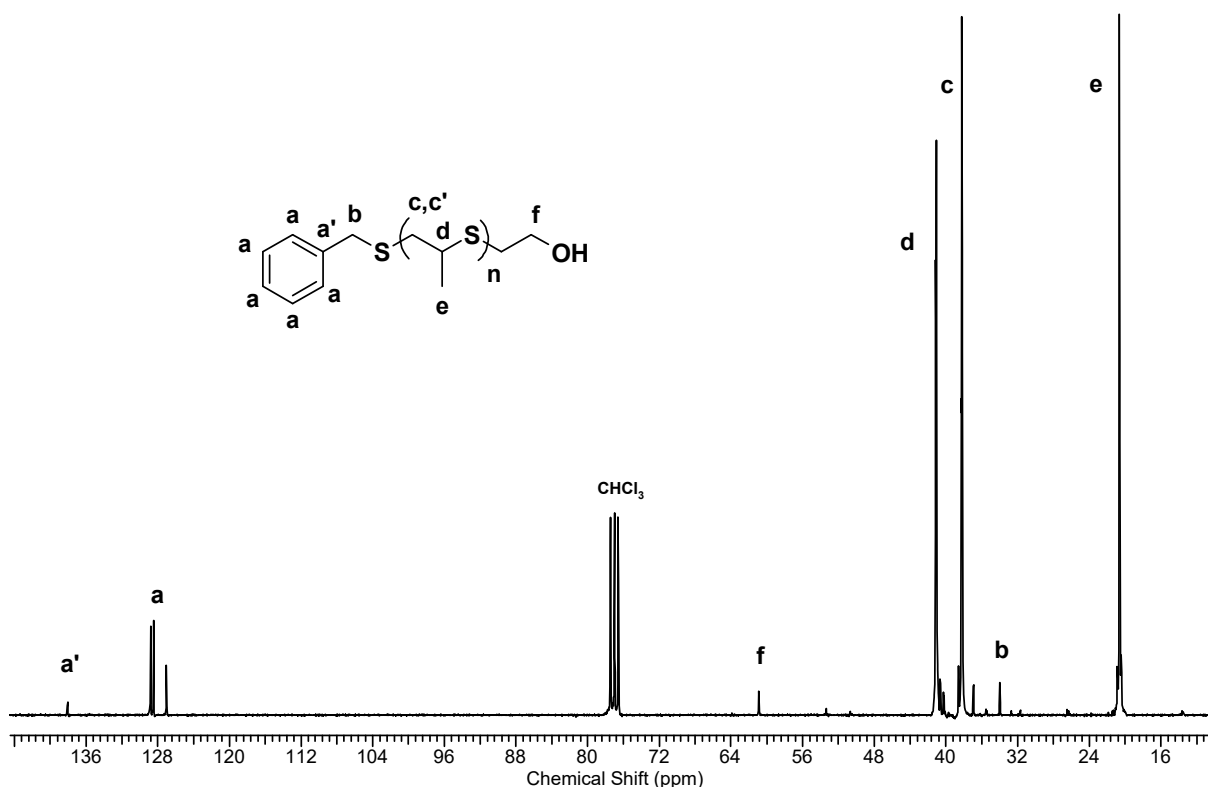


Figure S3. ^{13}C NMR (75.5 MHz, CHCl_3 -*d*) spectrum of a PPS with one terminal hydroxyl function.

Synthesis of poly(propylene sulfide)-*b*-poly(lactide) copolymers (PPS-*b*-PLA) (3)

Ring-opening polymerization of D- or L-lactide was performed in solution at room temperature with DBU as catalyst. A Schlenk flask equipped with a magnetic stirrer was charged with PPS initiator and transferred into a glove box, where various equiv D- or L-lactide were added. The flask was closed with a rubber septum and kept under argon atmosphere. Outside the glove box 2 ml dry dichloromethane were added to dissolve monomer and initiator. After the addition of DBU (monomer/catalyst=100/1) the polymerization was conducted at room temperature for 12 min. After completion, the reaction was quenched with benzoic acid (1.2 equiv according to DBU). The obtained block copolymer was precipitated into methanol or a mixture of ether and petroleum ether (1:1) (for copolymers with $<2000 \text{ g}\cdot\text{mol}^{-1}$ PLA chain length). The synthesized products were carefully dried in vacuum at room temperature.

FT-IR (on ATR crystal) [in cm^{-1}]: 2959, 1750, 1451, 1369, 1181, 1128, 1083, 1043, 734.

^1H NMR (300 MHz, CHCl_3 -*d*): δ (ppm) = 7.33-7.31 (m, C_6H_5 - CH_2 -); 5.15 (q, - CH - PLA chain); 4.36-4.26 (m, - S-CH_2 - CH_2 -O-PLA); 3.74 (s, C_6H_5 - CH_2 -); 2.95-2.77 (broad, diastereotopic H of - CH_2 - PPS chain, - CH - PPS chain); 2.67-2.57 (broad, diastereotopic H of - CH_2 - PPS chain); 1.54-1.44 (m, - CH_3 - PLA chain); 1.33-1.30 (broad, - CH_3 PPS chain).

^{13}C NMR (75.5 MHz, $\text{CHCl}_3\text{-d}$): δ (ppm) = 169.77 (-CO- PLA chain); 130.25, 129.10-127.34 ($\text{C}_6\text{H}_5\text{-CH}_2\text{-}$); 69.18-66.86 (-CH- PLA chain); 64.53 (-S- $\text{CH}_2\text{-CH}_2\text{-O-PLA}$); 41.45-40.98 (-CH- PPS chain); 38.95-37.22 (- $\text{CH}_2\text{-}$ PPS chain); 29.16 ($\text{C}_6\text{H}_5\text{-CH}_2\text{-}$); 20.70 (- CH_3 PPS chain); 17.21-16.74 (- $\text{CH}_3\text{-}$ PLA chain).

Table S2. Synthesized PPS-*b*-PLA copolymers.

Copolymer	Initiator	Sample	DP PPS ⁱ / DP PLA ⁱ	PLA content [wt%]	M_n^i NMR [g·mol ⁻¹]	M_n^{ii} SEC [g·mol ⁻¹]	PDI ⁱⁱ	Yield [%]
3a	2e	PPS- <i>b</i> -PLLA	63/2	6	5150	4000	1.15	quan
3b	2e	PPS- <i>b</i> -PLLA	59/9	23	5850	4400	1.31	71
3c	2d	PPS- <i>b</i> -PDLA	49/10	28	5250	4900	1.19	67
3d	2a	PPS- <i>b</i> -PLLA	30/18	54	5000	5800	1.15	68
3e	2a	PPS- <i>b</i> -PLLA	31/31	66	6950	7400	1.20	55
3f	2a	PPS- <i>b</i> -PLLA	35/69	79	12700	10800	1.21	60

ⁱcalculated by ^1H NMR, ratio of the CH_2 -signal of the initiator (benzyl group) and the PPS backbone signals and accordingly the PLA backbone. ⁱⁱSEC with chloroform as eluent, calibrated with polystyrene standards.

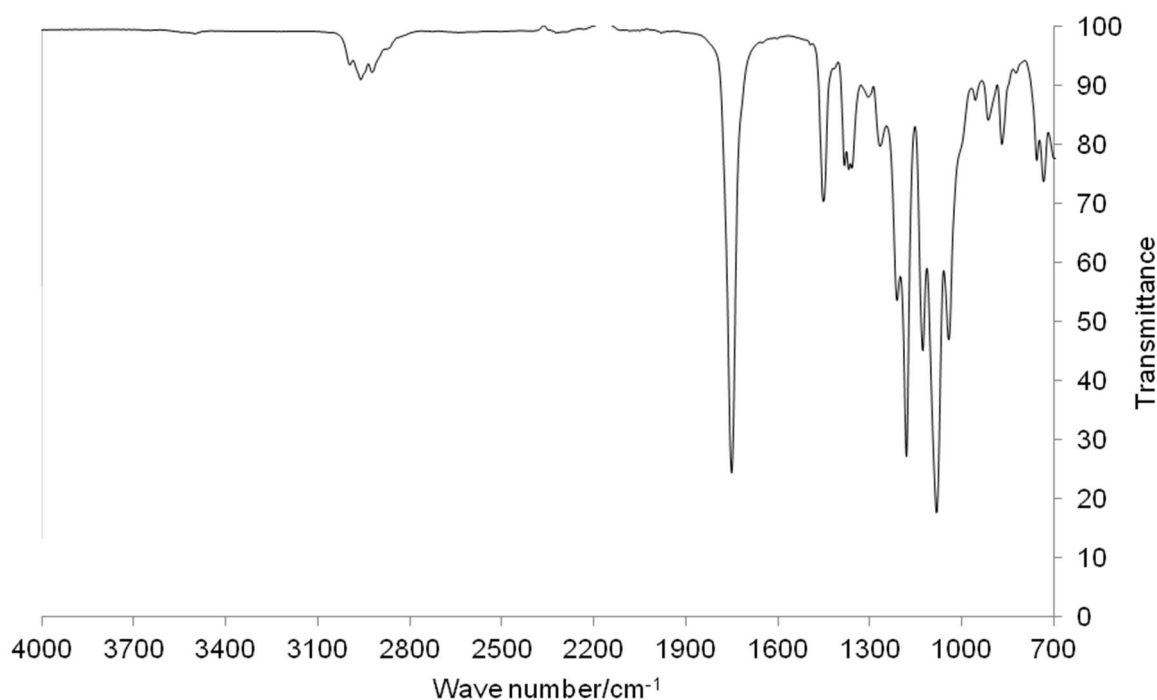


Figure S4. IR spectrum (film on ATR crystal) of PPS-*b*-PLLA.

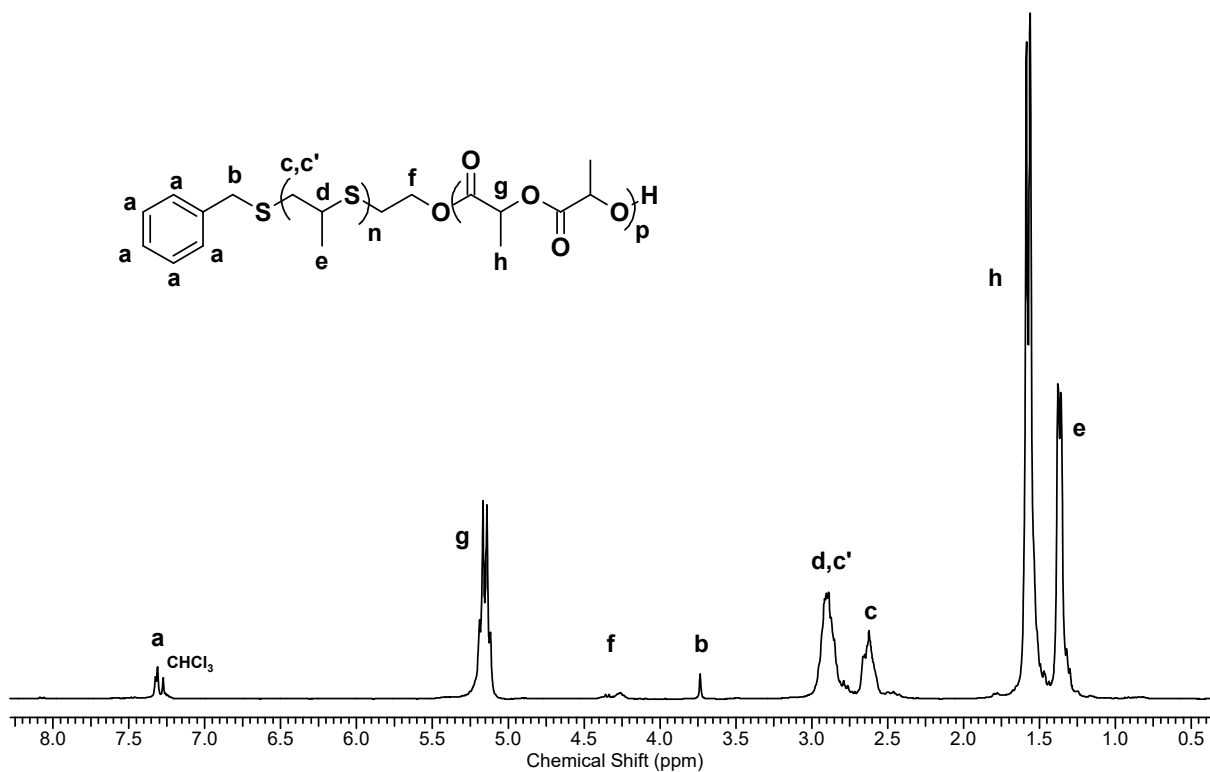


Figure S5. ¹H NMR (300MHz, CHCl₃-*d*) spectrum of PPS-*b*-PLLA.

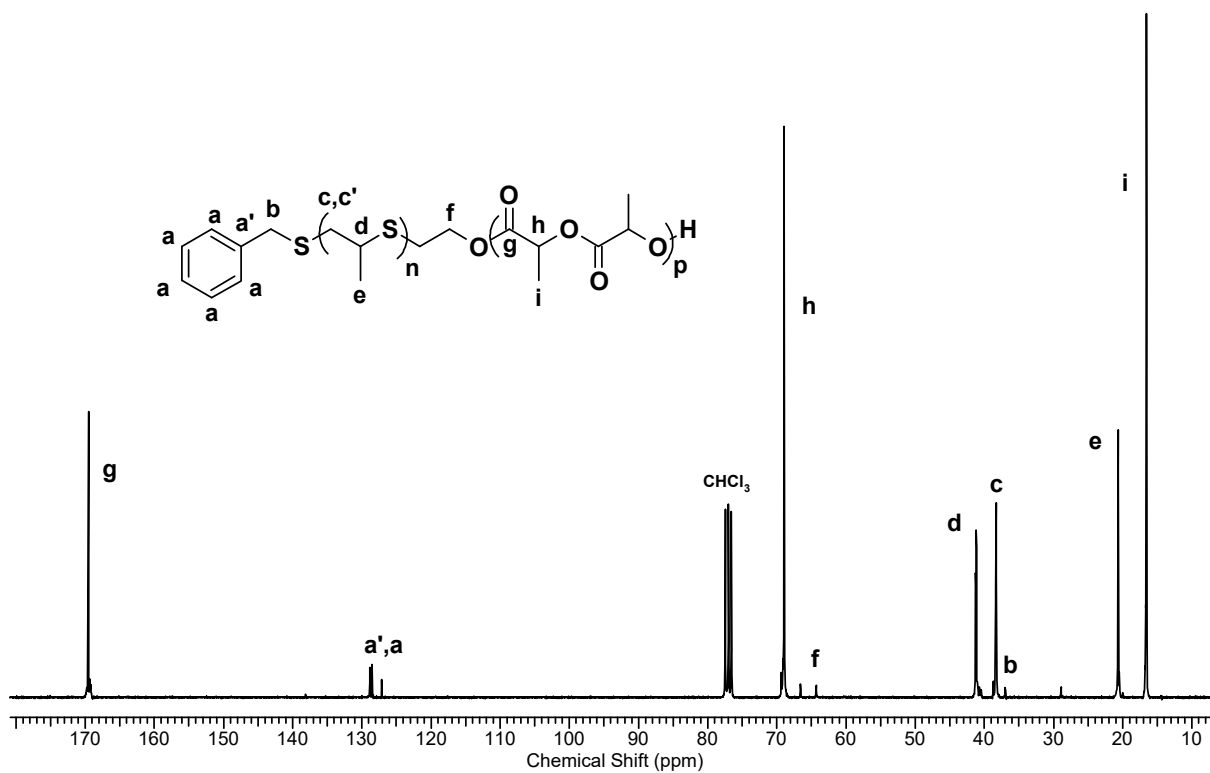


Figure S6. ¹³C NMR (75.5 MHz, CHCl₃-*d*) spectrum of PPS-*b*-PLLA.

Extraction of the gold nanoparticle solution

5 ml of the aqueous gold particle solution was extracted with 5 ml polymer solution ($1\text{mg}\cdot\text{ml}^{-1}$ in dichloromethane) via shaking at a frequency of 500 min^{-1} at room temperature for one hour. Immediately after this time the water phases were characterized using a UV-Vis spectrometer.

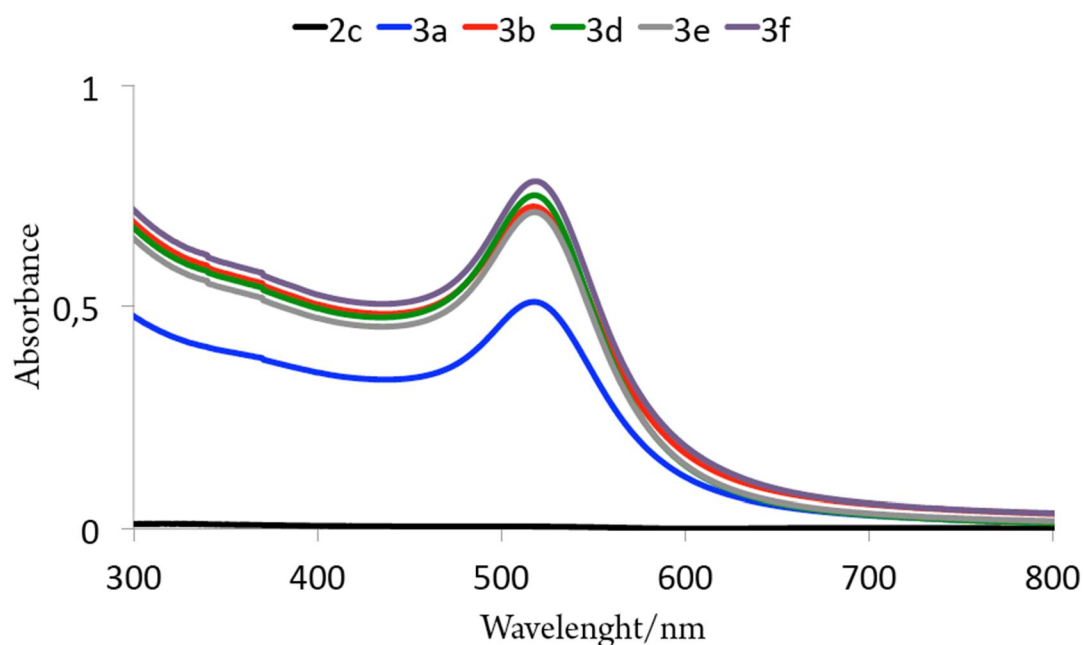


Figure S7. UV-Vis spectra of the aqueous solutions.

Adsorption of polymer to gold substrates

A gold substrate was dipped in 5 ml polymer solution ($1\text{mg}\cdot\text{ml}^{-1}$ in dichloromethane) for 15-30 minutes. The substrates were rinsed 10 times with dichloromethane, dried under argon stream and stored under argon atmosphere until the AFM and static contact angle measurements.

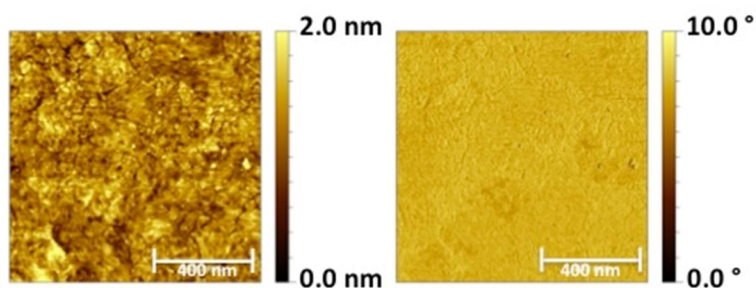


Figure S8. left: AFM height image of bare gold support; right: AFM phase image of bare gold support.

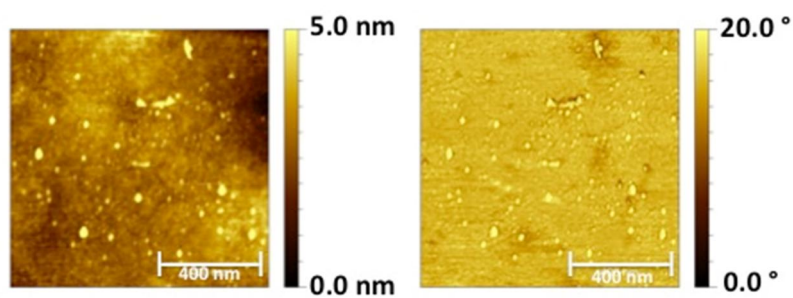


Figure S9. left: AFM height image of **3a**; right: AFM phase image of **3a**.

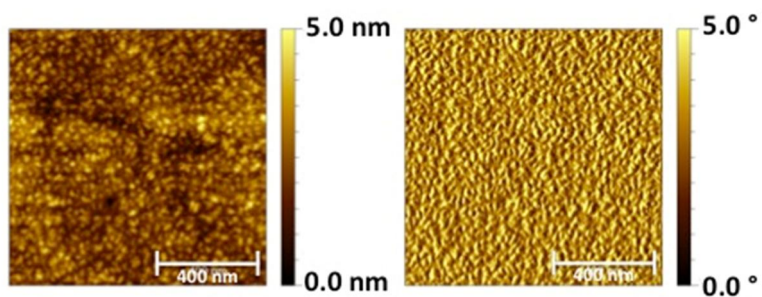


Figure S10. left: AFM height image of **3d**; right: AFM phase image of **3d**.

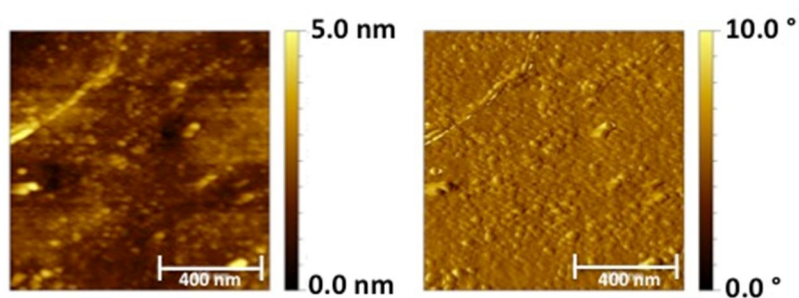


Figure S11. left: AFM height image of **3g**; right: AFM phase image of **3g**.

Table S3. Contact angle measurement.

Sample	Static contact angle [°]	RMS roughness (1 x 1 μm ²) [nm]
Bare gold substrate	88 ± 2	0.3 ± 0.1
3a	71 ± 3	0.4 ± 0.1
3d	72 ± 2	0.5 ± 0.1
3g	70 ± 2	0.4 ± 0.1

References

1. Oh, J. K.; *Soft Matter* **2011**, *7*, 5096-5108.
2. Darensbourg, D. J.; Karroonnirun, O.; *Macromolecules* **2011**, *43*, 8880-8886.
3. Kricheldorf, H. R.; Kreiser, I.; *Makromolekulare Chemie* **1987**, *188*, 1861-1873.
4. Zhu, K. J.; Xiangzhou, L.; Shilin, Y.; *J. Appl. Polym. Sci.* **1990**, *39*, 1-9.
5. Hu, Z.; Fan, X.; Wang, H.; Wang, J.; *Polymer* **2009**, *50*, 4175-4181.
6. Chisholm, M. H.; Navarro-Llobet, D.; *Macromolecules* **2001**, *34*, 8851-8857.
7. Napoli, A.; Tirelli, N.; Kilcher, G.; Hubbell, J. A.; *Macromolecules* **2001**, *34*, 8913-8917.
8. Wang, L.; Kilcher, G.; Tirelli, N.; *Macromol. Biosci.* **2007**, *7*, 987-998.
9. Domb, A.; Avny, Y.; *J. Appl. Polym. Sci.* **1984**, *29*, 2517-2528.
10. Cerritelli, S.; Fontana, A.; Velluto, D.; Adrian, M.; Dubochet, J.; De Maria, P.; Hubbell, J. A.; *Macromolecules* **2005**, *38*, 7845-7851.
11. Cerritelli, S.; O'Neil, C. P.; Velluto, D.; Fontana, A.; Adrian, M.; Dubochet, J.; Hubbell, J. A.; *Langmuir* **2009**, *25*, 11328-11335.
12. O'Neil, C. P.; van der Vlies, A. J.; Velluto, D.; Wandrey, C.; Demurtas, D.; Dubochet, J.; Hubbell, J. A.; *J. Controlled Release* **2009**, *137*, 146-151.
13. Napoli, A.; Tirelli, N.; Wehrli, E.; Hubbell, J. A.; *Langmuir* **2002**, *18*, 8324-8329.
14. Wang, L.; Hu, P.; Tirelli, N.; *Polymer* **2009**, *50*, 2863-2873.
15. Bearinger, J. P.; Stone, G.; Hiddessen, A. L.; Dugan, L. C.; Wu, L.; Hailey, P.; Conway, J. W.; Kuenzler, T.; Feller, L.; Cerritelli, S.; Hubbell, J. A.; *Langmuir* **2009**, *25*, 1238-1244.
16. Bearinger, J. P.; Terrettaz, S.; Michel, R.; Tirelli, N.; Vogel, H.; Textor, M.; Hubbell, J. A.; *Nat. Mater.* **2003**, *2*, 259-264.
17. Feller, L.; Bearinger, J. P.; Wu, L.; Hubbell, J. A.; Tosatti, S.; *Surf. Sci.* **2008**, *602*, 2305-2310.
18. Velluto, D.; Thomas, S. N.; Simeoni, E.; Schwartz, M. A.; Hubbell, J. A.; *Biomaterials* **2011**, *32*, 9839-9847.
19. Tokiwa, Y.; Calabia, B. P.; *Applied Microbiology and Biotechnology* **2006**, *72*, 244-251.
20. Vo, C. D.; Kilcher, G.; Tirelli, N.; *Macromol. Rapid Commun.* **2009**, *30*, 299-315.
21. Dzhabfarov, I. A.; Mamedbeili, E. G.; Kyazimova, T. G.; Gasanov, Kh. I.; Suleimanova, E. I.; *Russ. J. Appl. Chem.* **2010**, *5*, 854-857.
22. Nicol, E.; Bonnans-Plaisance, C.; Dony, P.; Levesque, G.; *Macromol. Chem. Phys.* **2001**, *202*, 2843.
23. Kamber, N. E.; Jeong, W.; Waymouth, R. M.; Pratt, R. C.; Lohmeijer, B. G. G.; Hedrick, J. L.; *Chem. Rev.* **2007**, *107*, 5813-5840.
24. Sarasua, J.-R.; Prud'homme, R. E.; Wisniewski, M.; Le Borgne, A.; Spassky, N.; *Macromolecules* **1998**, *31*, 3895-3905.

25. Rathi, S.; Kalish, J. P.; Coughlin, E. B.; Hsu, S. L.; *Macromolecules* **2011**, *44*, 3410-3415.
26. Wanamaker, C. L.; Tolman, W. B.; Hillmyer, M. A.; *Macromol. Symp.* **2009**, *283-284*, 130-138.
27. Gademawla, E. S.; Koura, M. M.; Maksoud, T. M. A.; Elewa, I. M.; Soliman, H. H.; *J. Mater. Process. Technol.* **2002**, *123*, 133.
28. Porta, F.; Speranza, G.; Krpetić, Ž.; Santo, V. D.; Francescato, P.; Scari, G.; *Mater. Sci. Eng. B* **2007**, *140*, 187-194.
29. Zheng, T.; Burkhart, M.; Richardson, D. E.; *Tetrahedron Lett.* **1999**, *40*, 603-606.
30. Porta, F.; Speranza, G.; Krpetić, Ž.; Dal Santo, V.; Francescato, P.; Scari, G.; *Mater. Sci. Eng. B* **2007**, *140*, 187-194.
31. Naumann, R.; Schiller, S. M.; Griess, F.; Grohe, B.; Hartmann, K. B.; Kärcher, I.; Köper, I.; Lübben, J.; Vasilev, K.; Knoll, W.; *Langmuir* **2003**, *19*, 5435-5443.

Chapter 5: Ongoing Projects

5.1 Thermorheological Properties of Hyperbranched Poly(glycolide) Copolymers

Carina Gillig, Anna M. Fischer, Christian Friedrich and Holger Frey

Introduction

Hyperbranched polymers represent a rapidly expanding field in macromolecular chemistry. The materials are obtained in a one-pot procedure^{1,2} in contrast to dendrimers, which require numerous protection and deprotection steps as well as exhaustive purification. Branched macromolecules are characterized by unique properties deviating from their linear analogues. These features include high surface functionality, low viscosity, low degree of crystallization (i.e., mostly amorphous materials) and improved solubility properties in comparison to the linear analogues.³ Since hyperbranched polyesters provide biodegradability and biocompatibility, they are suitable candidates for medical applications and for packaging purposes.⁴ A large number of published reports deal with studies on the commercially available hyperbranched polyester marketed under the trade name Boltorn®. The synthesis of this material proceeds via a pseudo one-pot polycondensation⁵ of 2,2-bis(hydroxymethyl)propionic acid (bis-MPA) together with ethoxylated pentaerythritol (PP50) as a core molecule. In contrast to monodisperse dendrimers, the former route yields polydisperse materials due to a series of side-reactions including cyclization, etherification and the formation of structures without core molecule.⁶

In recent years, considerable progress has been achieved in developing suitable applications for polyester polyols. The applications for hyperbranched polyesters and their derivatives include their utilization as a binder component in coating systems, as crosslinking agents, tougheners and chain extenders.⁷ In addition, they offer the possibility to covalently attach or physically entrap drugs to serve as transport vehicle in drug delivery.^{8,9} The suitability for a certain application depends on the polymers' mechanical and thermal properties and their chemical resistance. Furthermore, the raw material and the industrial process have to be profitable. The rheological behaviour of polymers represents a key feature for various fields of application. Rheological properties of dendritic molecules depend on different factors, such as molecular weight, degree of branching and molecular weight distribution. The degree of branching is determined by calculation of the amount of linear, dendritic, and terminal units. Using an equation postulated by Fréchet, the determination of DB is possible; however, a general equation according to Frey et al. is valid for a broad range of DB values and structures.^{10,11}

The rheological properties of hyperbranched (hb) polymers have only been investigated to a limited extent. One reason might be the lack of detailed understanding of the structure-property relationships. Comparison of different hb polymers with each other is commonly not possible due to their deviating material properties attributed to their high number of end functionalities with specific interactions. In the case of hb polyesters, the broad molecular mass distributions and the amount of side reactions during polycondensation indicate a complex multidistributed structure and impede reliable characterization.

A number of works deal with poly(bis-MPA) hb polyesters due to their availability on a commercial scale. For poly(bis-MPA) melts, Newtonian behaviour, shear-thinning and viscoelastic properties have been obtained, depending on the respective number of generations.⁶ The observed absence of entanglements is explained by the branched structure and generally appears for linear polymers below the critical molar mass (M_c). However, several recent studies indicated an entanglement for hyperbranched polymers with extremely high molecular weight.¹² Patil et al. obtained even higher M_c values for hb poly(ethylene) (PE) than for conventional linear PE.¹³

In this work, rheological and thermal properties of a series of hyperbranched poly(glycolide) (PGA) copolymers have been examined. The influence of the type of end groups with respect to hydrogen bonding, the degree of branching (DB) and the temperature on the rheological behaviour of these polyester polyols have also been studied. In chapter 2.1 the synthesis and characterization of these hyperbranched PGA copolymers combining ROP with AB_2 polycondensation has been summarized.¹⁴

Synthesis

The $Sn(Oct)_2$ -catalyzed ROP of glycolide has been initiated via 2,2-bis(hydroxymethyl)butyric acid (BHB, AB_2 branching monomer), resulting in bishydroxy acid-functional prepolymers which were subsequently reacted to yield amorphous polyester polyols. The branching AB_2 monomer can be incorporated either as a focal linear, linear, focal dendritic or dendritic subunit. The proposed mechanism is supported by the absence of terminal AB_2 units in the hyperbranched structures. The different incorporated units are distinguishable via the respective quaternary carbon atoms. Integration of the latter, using inverse-gated ^{13}C NMR, yields the percentage of every unit, which permits the calculation of the degree of branching (DB). All polymers were characterized by NMR spectroscopy and size exclusion chromatography (SEC). The DB is adjusted via increasing incorporation of the AB_2 branching unit. The data are summarized in Table 1.

Table 1. Characterization data of hb PGA copolymers.

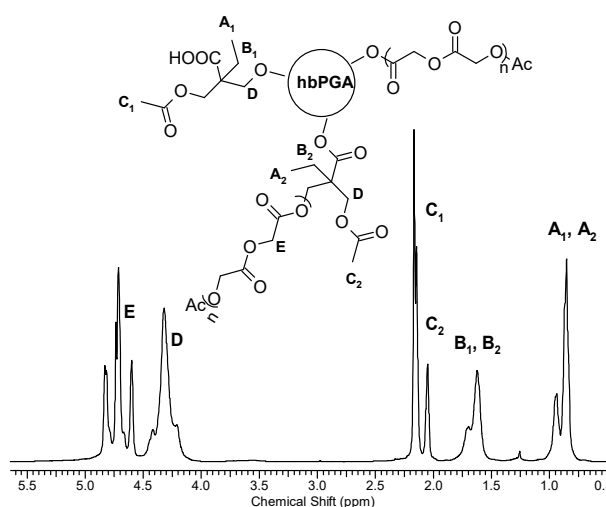
sample	G:BHB ^{a)} (mol%)	M _n ^{b)} (g/mol)	M _w /M _n ^{b)} (g/mol)	DB ^{a)}
PGAB76	76:24	950	3.30	0.28
PGAB71	71:29	1100	3.30	0.34
PGAB85	85:15	1200	2.36	0.21
PGAB55	55:45	1400	2.39	0.33
PGAB63	63:37	2500	2.37	0.38
PGAB51	51:49	3900	2.58	0.58

^{a)}calculated by ¹H NMR and inverse-gated ¹³C NMR;

^{b)}obtained from SEC analysis in DMF with 0.1% LiBr

Since hydrogen bonding might play a key role in the structure-property relationship of the hb polyesters, the hydroxyl groups of one sample (PGAB51) have been esterified with acetic anhydride in a polymer modification reaction to minimize end group interaction.

The success of this transformation has been confirmed by ¹H and ¹³C NMR analysis. The esterification of the hydroxyl groups is evidenced by the disappearance of the former hydroxymethylene protons (3.45-3.68 ppm) of the AB₂ monomer and the terminal glycolic acid units (4.00-4.11 ppm). The observed splitting of the methyl (0.85 ppm, 0.95 ppm) and methylene signals (1.62-1.70 ppm) is due to the deviating structural microenvironment, associated with dendritic and focal dendritic units (see Figure 1). ¹³C NMR analysis evidences successful derivatization, focusing on the different quaternary carbons of the hyperbranched structure (not shown here). In addition, the solubility is enhanced for a wide range of solvents, including chloroform and dichloromethane for example.


Figure 1. ¹H NMR spectrum (400 MHz, CDCl₃) of PGAB51 after esterification with acetic anhydride.

IR investigation evidences 100% conversion of the hydroxyl groups due to the absence of the O-H stretching band at wave numbers of $\sim 3500\text{ cm}^{-1}$ (Figure 2). Time-dependent IR measurements have also been performed to study hydrogen-bond interactions of the unprotected sample. By heating the sample up to $120\text{ }^{\circ}\text{C}$, the O-H stretching band is shifted to higher frequency (blue shift), indicating a weakening of hydrogen bonds, as reported in literature for poly(bis-MPA).¹⁵

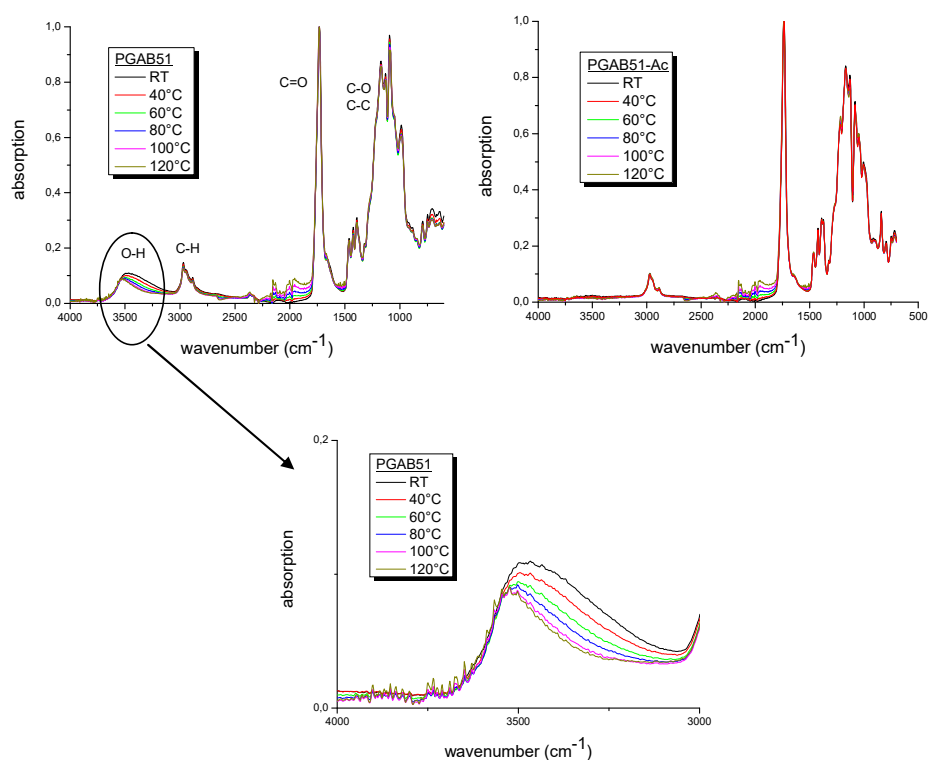


Figure 2. Temperature-dependent FT-IR measurements showing H-bond interactions of the unprotected sample PGAB51 (top left) and full conversion after derivatization (top right).

Thermal Properties

Investigation of rheological properties in melt implies thermal stability of the respective samples. In addition, thermal properties offer information about the temperature range applicable for rheological measurements. Thermal gravimetric analysis (TGA) has been performed to investigate the thermal decomposition of the prepared polyester polyols and their derivatives. All samples were measured under air atmosphere with a heating rate of 10 K/min . The degradation temperature has been determined from the onset of the mass loss curve. The thermal decomposition temperature for the series of hyperbranched PGA copolymers is in the range of $282\text{--}291\text{ }^{\circ}\text{C}$ (see Table 2). In contrast to linear PGA ($T_d=254\text{ }^{\circ}\text{C}$ for $50,000\text{ g/mol}$ PGA)¹⁶ the hyperbranched materials exhibit improved thermal stability. The thermal stability is further increased up to $328\text{ }^{\circ}\text{C}$ by derivatization of the end groups (Figure 3). In comparison, the thermal stability of hyperbranched poly(bis-MPA) is in the range

of 250-275 °C for PP50 and trimethylolpropane (TMP) as core molecules. Using 1,3,5-tris(2-hydroxyethyl)cyanuric acid (THECA) it is about 275-300 °C, thus depending on the respective core molecule. Further thermal properties of the prepared hyperbranched PGA copolymers have been investigated by differential scanning calorimetry (DSC, Table 2). Previous studies ascertained a suppression of the melting point as a consequence of the branched architecture that disturbs the formation of crystalline domains. The glass transition temperature is clearly shifted to lower temperatures (16.3 to 27.4 °C) in comparison with the linear homopolymer (PGA, T_g =35-50 °C).

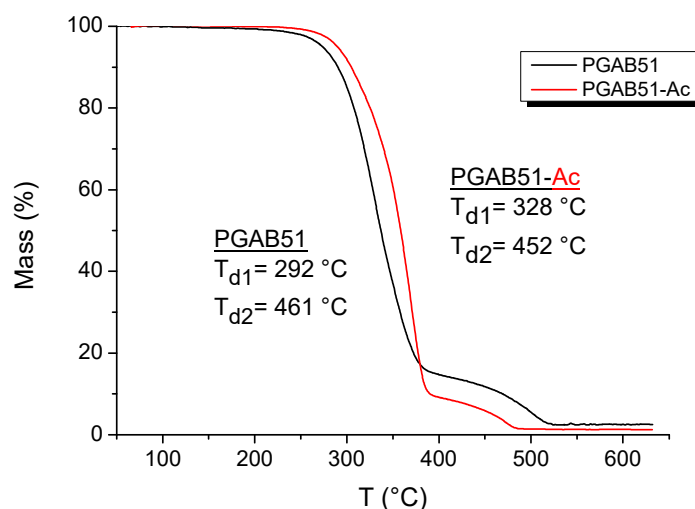


Figure 3. Thermo gravimetric analysis comparing PGAB51 and its derivative PGAB51-Ac.

Table 2. Thermal characterization of polyester polyols and the acetylated derivative.

sample	G:BHB ^{a)} (mol%)	T_g ^{b)} DSC (°C)	T_{d1} ^{c)} (°C)
PGAB76	76:24	22.2	291
PGAB71	71:29	22.9	282
PGAB85	85:15	27.4	287
PGAB55	55:45	21.8	289
PGAB63	63:37	24.9	288
PGAB51	51:49	16.3	292
PGAB51-Ac	49:51	6.3	328

^{a)}calculated from ^1H NMR; ^{b)} determined via DSC from the 2nd heating run (with 20K/min; 50-120 °C);

^{c)}determined via TGA from the onset (with 10K/min; 50-650 °C) under O_2 atmosphere

Rheology

Polymer melts are often characterized in a dynamic oscillatory shear experiment. The polymer melt is placed between two parallel plates, and upon shear the material response is measured. Typical measured parameters are the complex modulus G^* consisting of the storage component G' (real) being the elastic modulus, and the loss component G'' (imaginary) representing the viscous modulus of the system (equation 1). The rheological properties of a material are studied for different temperatures in a certain frequency range.

In Figure 4 the Booij-Palmen plot is displayed, a time-invariant illustration of the phase angle. For every isotherm the phase angle (δ) is plotted versus the complex modulus $|G^*|$ with

$$|G^*| = \sqrt{(G')^2 + (G'')^2} \quad (1)$$

$$\delta = \arctan(\tan\delta) \quad (2)$$

$$\tan\delta = \frac{G''}{G'} \quad (3)$$

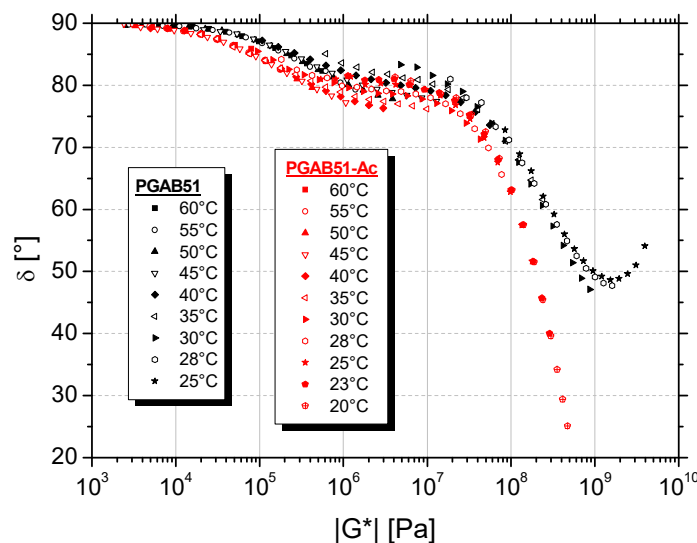


Figure 4. Booij-Palmen-Plot of unentangled PGAB51 and its acetylated derivative.

The phase angle reaches 90° for small values of the complex modulus $|G^*|$. The maximum at $\delta=90^\circ$ indicates the terminal flow region (highest temperature; lowest moduli), where the polymer behaves like a viscous fluid. With increasing $|G^*|$ and decreasing temperature the phase angle decreases, which is due to the transition to a glassy solid. While the time-temperature superposition (TTS) is fulfilled for the terminal regime and the glassy zone, at intermediate module ranges ($G^* \approx 10^6$ - 10^7 Pa); the phase angle reveals a breakdown of the time-temperature superposition principle, which has been previously reported for hyperbranched polymers.^{12,17} However, this behaviour has been

attributed to segmental relaxation or relaxation by H-bonds. The lack of a transition to the entangled regime is supported by $\delta > 45^\circ$ at $|G^*| \approx 10^5\text{-}10^7$ Pa and $G' < G''$ for the whole range between the terminal and the glassy zone. As expected, an entanglement has not been observed since the molecular weights of the hb PGA copolymers are below the critical entanglement molecular weight (for linear PGA homopolymer, $M_c = 11,000$ g/mol).¹⁸

The measured isotherms in the range of 60 °C to 25 °C have been shifted to a master curve (Figure 5) according to the time-temperature superposition (TTS) principle. The shift factors a_T were obtained by the horizontal shift (Figure 6) and fitted by the Williams-Landel Ferry (WLF) equation (4):

$$\log a_T = -\frac{c_1(T-T_0)}{c_2+T-T_0} \quad (4)$$

with the individual reference temperature T_0 , and the WLF fitting parameters c_1 and c_2 , which have been determined by the software IRIS Rheo Hub 2008.

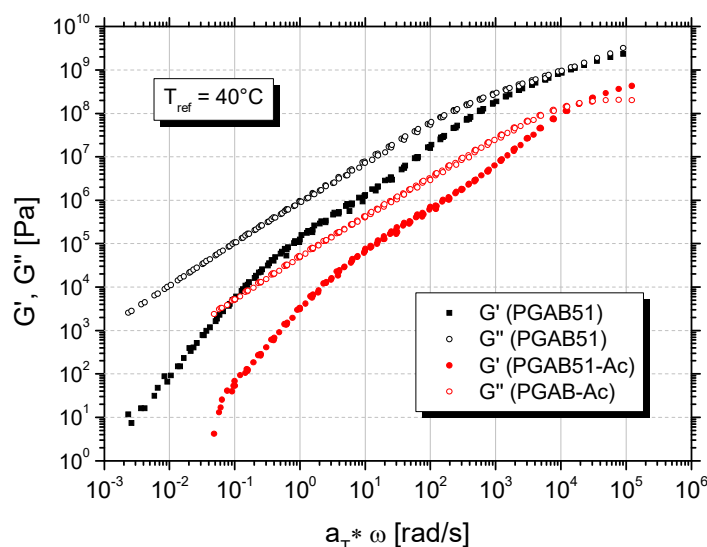


Figure 5. Master curve of PGAB51 and its derivative at $T_{ref}=313$ K, $b_T=1$.

In Figure 5 a full spectrum of rheological properties from the terminal at low frequencies to the glassy region at high frequencies is presented for a typical branched polymer sample and its derivative. The crossover at higher frequencies is representative for the dynamic glass transition of the samples. Similar behaviour was observed for copolymers of different comonomer composition and molecular weight.

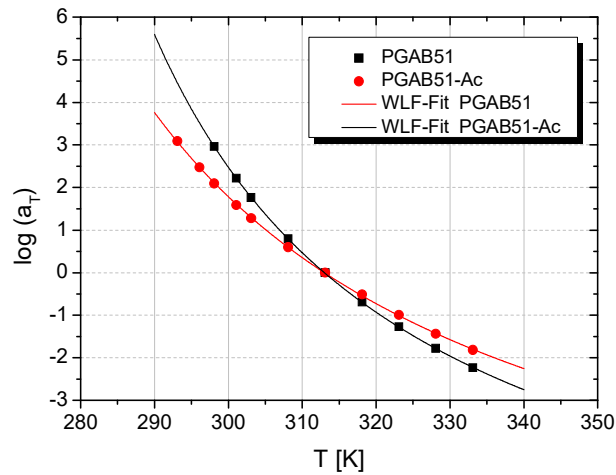


Figure 6. Shift factors a_T fitted by the WLF equation (Eq. 4) at $T_{\text{ref}}=313$ K for PGAB51 and its acetylated derivative.

Viscosity as a function of frequency is shown in Figure 7 for PGAB51 and its derivative. The viscosity in the Newtonian regime, the zero shear viscosity η_0 , was directly obtained by extrapolation of η' to low frequencies:

$$\eta_0(T_{\text{ref}}) = \lim_{\omega \rightarrow 0} \eta' = \lim_{\omega \rightarrow 0} \frac{G''}{\omega} \quad (5)$$

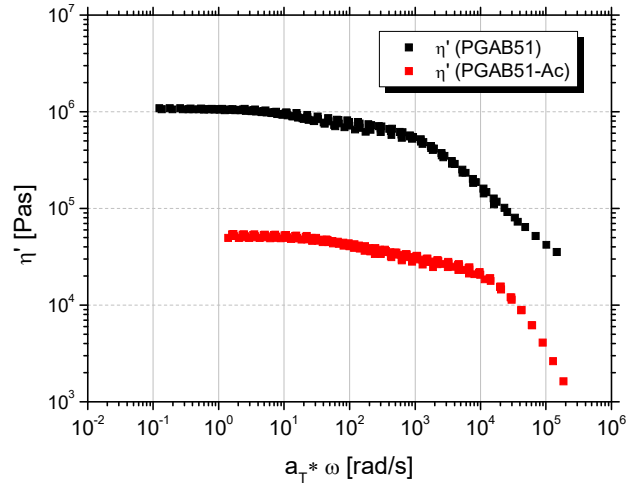


Figure 7. Determination of the zero shear viscosity η_0 of PGAB51 and its derivative at $T_{\text{ref}}=313$ K.

By extrapolation of η_0 to a value of 10^{12} Pas the rheological T_g can be calculated by the following equation (6):

$$\log a_T = \log \left(\frac{\eta_0(T_{\text{ref}})}{\eta_0(T_g)} \right) = - \frac{c_1(T_g - T_{\text{ref}})}{c_2 + T_g - T_{\text{ref}}} \quad (6)$$

In Figure 8 the rheological T_g and the DSC- T_g are plotted versus the content of glycolide for the whole series of hyperbranched PGA copolymers. In general, the plot shows a good agreement of both data.

The rheological T_g is slightly higher than the calorimetric T_g which might be due to the different techniques applied for determination. Interestingly, the T_g of the protected hyperbranched PGA copolymer (PGAB51-Ac) is 10 K lower as compared with the hydroxy-functional polyester sample. The lack of H-bond interaction increases the flexibility, resulting in a reduction of the T_g .^{19,20}

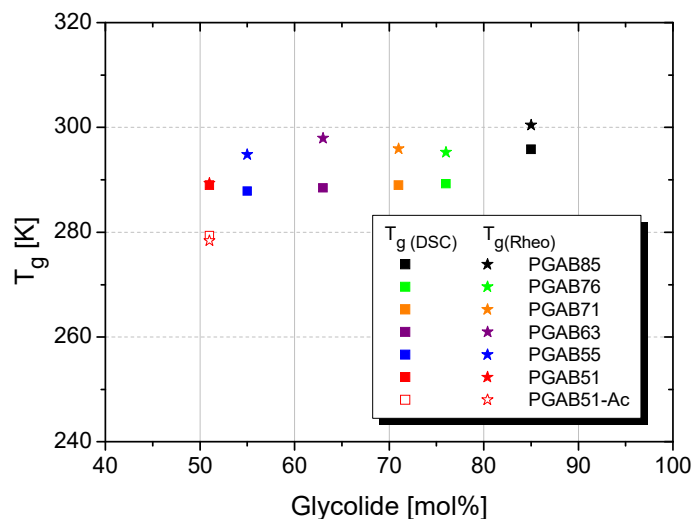


Figure 8. Comparison of the rheological T_g and the DSC- T_g for the whole series of hyperbranched PGA copolymers.

In Table 3 the thermo-rheological data for the series of hyperbranched PGA copolymers are presented.

Table 3. Thermo-rheological data for the series of hyperbranched PGA copolymers.

sample	G:BHB ^{a)} (mol%)	T_g ^{b)} DSC (K)	T_g ^{c)} Rheo (K)	T_{ref} ^{d)} (K)	C_1	C_2 ^{e)} (K)
PGAB76	76:24	295.2	289.2	310	8.23	50.87
PGAB71	71:29	295.9	289.0	310	7.27	47.02
PGAB85	85:15	300.4	295.8	313	9.21	50.66
PGAB55	55:45	294.8	287.8	310	9.03	56.29
PGAB63	63:37	297.9	288.4	313	7.85	55.43
PGAB51	51:49	289.3	288.9	313	8.86	59.78
PGAB51-Ac	49:51	279.3	278.4	313	8.52	75.17

^{a)} calculated from ^1H NMR; ^{b)} determined via DSC from the 2nd heating run (with 20K/min; 50-120 °C);

^{c)} T_g (rheo) in K: determined by equation (3); ^{d)} T_{ref} in K: reference temperature for the master curve;

^{e)} C_2 in K: determined from equation (2)

In order to compare all samples at an iso-free volume state, the viscosities were shifted to an equal distance to their rheological T_g . Since no absolute values of molar mass can be determined, no conclusions can be drawn about the dependency of the molar mass and the melt viscosity. Therefore, the zero shear viscosity is plotted as a function of the molar content of glycolide incorporated into the hyperbranched copolymer at $T_{ref}=T_g(\text{rheo})+50\text{K}$ (Figure 9). Clearly, the zero shear viscosity is not influenced by the amount of glycolide for the investigated copolymer composition. One may assume an increase of η_0 with increasing glycolide content, although this has to be verified by additional samples with high amounts of glycolide. The modification of the hydroxyl groups does not affect the zero shear viscosity, which might be due to the low molecular weight and low amount of hydroxyl groups in the respective polymer with low DB value.

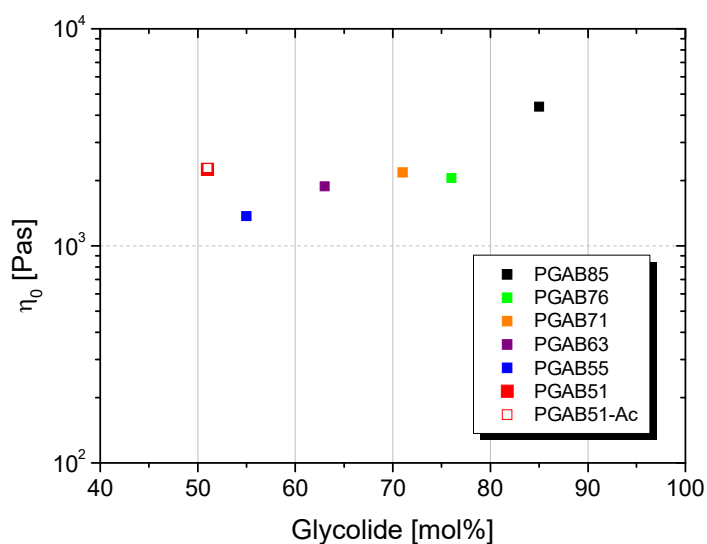


Figure 9. Molar composition dependency of zero shear viscosities at $T_{ref}=T_g(\text{rheo})+50\text{K}$.

Conclusion

In this work a series of hyperbranched PGA copolymers has been investigated with regard to thermal decomposition, H-bond interactions and thermo-rheological properties. The degree of branching (DB) has been adjusted by varying the amount of incorporated AB_2 monomer.

For the hyperbranched polyester polyols high thermal stability in the range of 282-291 °C has been observed in contrast to their linear analogue. The thermal stability could be increased by polymer modification of the hydroxyl end groups up to 328 °C. Temperature-dependent IR spectroscopy revealed the existence of H-bond network for the unprotected samples identified via the blue shift of the O-H stretching band at 3500 cm^{-1} for higher temperatures. For the protected samples a decrease of the glass temperature of 10 °C is observed in comparison with hydroxyl-functional copolymers.

Thermo-rheological measurements of protected and unprotected samples showed a break-down of the time-temperature superposition principle in the intermediate module range. This behaviour might be an effect of the hyperbranched structure and not of the hydrogen bonds, as it was observed for hydroxyl-functionalized as well as for modified copolymers.

The terminal relaxation scales with the temperature according to the WLF-law. Zero shear viscosities at $T_g(\text{rheo})+50\text{K}$ were compared and were almost independent of the molar content of glycolide. Due to the low molecular weight of the hyperbranched PGA copolymers no entanglements have been observed. In contrast to thermo-rheological studies on Boltorn®, we were able to cover a larger temperature and frequency range in our measurements, which provided us with detailed information on the material properties of hb PGA copolymers. The reproducibility of data ascertained an excellent thermo-mechanical stability of the obtained material.

Investigation of the time dependency of rheological parameters at different temperatures will be part of future studies, which gives information on the temperature-dependent mechanical stability of the copolymers over time.

References

1. Gao, C.; Yan, D. *Prog. Polym. Sci.* **2004**, *29*, 183-275.
2. Jikei, M.; Kakimoto, M.-A. *Prog. Polym. Sci.* **2001**, *26*, 1233-1285.
3. Voit, B. I.; Lederer, A. *Chem. Rev.* **2009**, *109*, 5924-5973.
4. Albertsson, A.-C.; Varma, I. K. *Biomacromolecules* **2003**, *4*, 1466-1486.
5. Malmström, E.; Johansson, M.; Hult, A. *Macromolecules* **1995**, *28*, 1698-1703.
6. Žagar, E.; Žigon, M. *Prog. Polym. Sci.* **2010**, *36*, 53-88.
7. Zhang, X. *Polym. Int.* **2011**, *60*, 153-166.
8. Kontoyianni, C.; Sideratou, Z.; Theodossiou, T.; Tziveleka, L.-A.; Tsiourvas, D.; Paleos, C.M. *Macromol. Biosci.* **2008**, *8*, 871-881.
9. Prabakaran, M.; Grailer, J. J.; Pilla, S.; Steeber, D. A.; Gong, S. Q.; *Macromol. Biosci.* **2009**, *9*, 515-524.
10. Hawker, C. J.; Fréchet, J. M. J. *J. Am. Chem. Soc.* **1991**, *113*, 4583-4588.
11. Hölter, D.; Burgath, A.; Frey, H. *Acta Polym.* **1997**, *48*, 30-35.
12. Tonhauser, C.; Wilms, D.; Korth, Y.; Frey, H.; Friedrich, C. *Macromol. Rapid Commun.* **2010**, *31*, 2127-2132.
13. Patil, R.; Colby, R. H.; Read, D. J.; Chen, G.; Guan, Z. *Macromolecules* **2005**, *38*, 10571-10579.
14. Fischer, A. M.; Frey, H. *Macromolecules* **2010**, *43*, 8539-8548.
15. Žagar, E.; Grdadolnik, J. *Journal of Molecular Structure* **2003**, *658*, 143-152.
16. Engelberg, I.; Kohn, J. *Biomaterials* **1991**, *12*, 292-304.

17. Dorgan, J. R.; Knauss, D. M.; Al-Muallem, H. A.; Huang, T. *Macromolecules* **2003**, *36*, 380-388.
18. Gautier, E.; Fuertes, P.; Cassagnau, P.; Pascault, J.-P.; Fleury, E. *J. Polym. Sci.: Part A: Polym. Chem.* **2009**, *47*, 1440-1449.
19. Foix, D.; Fernández-Francos, X.; Salla, J. M.; Serra, À.; Morancho, J. M.; Ramis, X. *Polym. Int.* **2011**, *60*, 389-397.
20. Schmaljohann, D.; Häußler, L.; Pötschke, P.; Voit, B. I.; Loontjens, T. J. A. *Macromol. Chem. Phys.* **2000**, *201*, 49-57.

5.2 Synthesis and Characterization of Functional P(HPMA)-block-P(DLLA) Copolymers as Surfactant for Miniemulsion Technique

Mirjam Clemens-Hemmelmann, Anna M. Fischer, Annette Kelsch, Holger Frey and Rudolf Zentel

Introduction

This study aims at the synthesis of biodegradable functional poly(N-(2-hydroxypropyl)-methacrylamide)-based block copolymers. Since the introduction of Ringsdorf's concept¹ in the 1970s, the work on polymeric drug conjugates has experienced tremendous progress.² The design and optimization of smart materials with specific targeting properties and controlled drug release upon pH-, thermal- or light-induced stimulus is a major concern in nanomedicine.^{3,4} Incorporation of a biologically active ligand is either achieved by covalent attachment to the polymer itself or physically driven by polymer-based micellar aggregation⁵ providing solubilisation of the hydrophobic drug and enhanced circulation time in the blood stream.

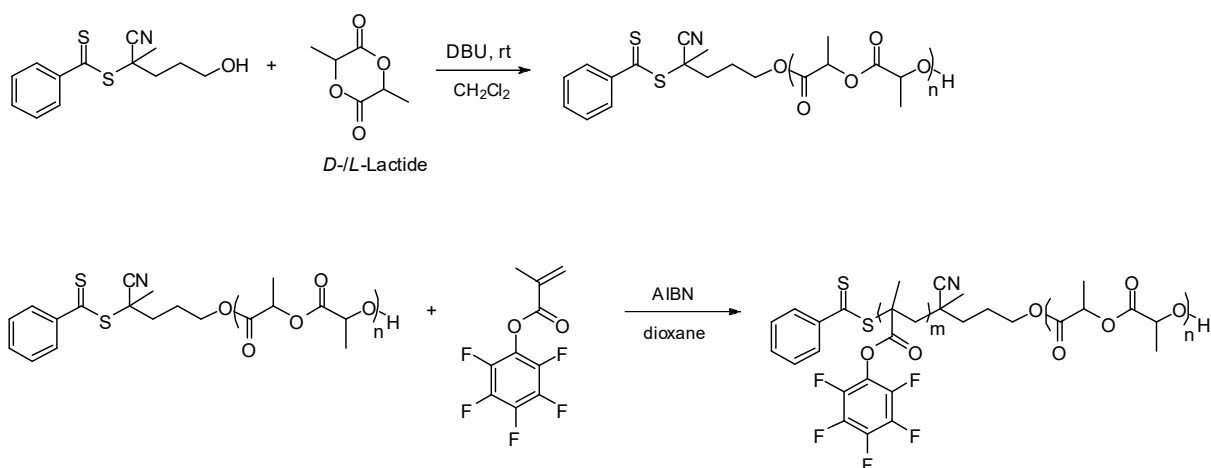
A plethora of poly(ethylene glycol)-based drug and protein conjugates have been established, which benefit from its hydrophilicity, non-toxicity as well as non-immunogenic properties.⁶⁻⁸ Another emerging field in this context are degradable diblock copolymers consisting of a biocompatible PEG block and degradable poly(lactide) (PLA)⁹ or poly(lactide-co-glycolide) (PLGA) blocks.¹⁰ Degradation of the poly(ester) segment leads to PEG fragments with molecular weights assuring renal elimination. One drawback of linear PEG is its lack of functionality, impeding targeting, except for the two terminal hydroxyl functions. Acrylate and acrylamide-based polymer conjugates provide a valuable alternative to PEG. Polymerization of reactive ester methacrylates provides access to versatile functionalities along the backbone and thus manifests the superiority of these systems compared with PEG. Controlled radical polymerizations, such as atom transfer radical polymerization (ATRP), reversible addition fragmentation chain transfer (RAFT) and nitrogen-mediated polymerization (NMP) allow for the synthesis of well-defined materials fulfilling the criteria for biomedical applications. In addition, radical polymerization permits the utilization of a wide range of functional monomers suitable under the respective synthesis conditions, in pronounced contrast to oxyanionic polymerization. Besides PEG, P(HPMA) is one of the best established biomedical polymers, which is also due to extensive studies by Duncan et al.¹¹ In clinical trials the biocompatibility of P(HPMA) has been approved, confirming its non-toxicity and non-immunogenic properties. These features render the material highly attractive for biomedical and pharmaceutical applications.

Recently, Barz et al. combined RAFT polymerization and ring-opening polymerization (ROP) strategies to obtain P(HPMA)-*b*-P(LLA) copolymers.¹² The synthesis was accomplished by DCC-mediated coupling of a hydroxyl-functional PLLA with a carboxyl-terminated RAFT chain transfer agent (CTA). In the next step, RAFT polymerization of pentafluorophenyl methacrylate (PFPMMA) was employed, using the preformed PLLA-based CTA precursor. This strategy yielded P(PFPMMA)-*b*-P(LLA) copolymers. The reactive pentafluorophenyl moieties allowed for selective derivatization of the respective diblock copolymers with fluorescent dyes. The micellization behaviour was investigated via fluorescence correlation spectroscopy (FCS), and toxicity tests confirmed the biocompatibility of the amphiphilic copolymers obtained. In ongoing studies, P(HPMA)-based diblock copolymers with poly(lactide) blocks of different stereochemistry have been investigated. Copolymerization of lactide stereoisomers yields materials with different thermal properties and different degradation profiles ranging from semi-crystalline (L-lactide > 75%) to amorphous polymers with increasing d-lactide content. Amorphous polymers are degraded faster than crystalline materials due to increased water penetration, especially into amorphous regions. On the basis of previous work, Barz et al.¹³ designed fluorescent-labeled P(HPMA)-based diblock copolymers and studied the difference of cellular uptake and drug formulations comparing P(HPMA)-*b*-P(LA) with different tacticity of the poly(lactide) block. Micellar aggregation of the amphiphilic polymer allowed encapsulation of paclitaxel, a useful drug in anticancer therapy. The atactic copolymer showed enhanced cellular uptake and drug encapsulation efficiency resulting in higher cytotoxicity compared with the isotactic analogue. In fact, these polymers represent high potential for pharmaceutical use. Nonetheless, the currently employed synthesis is not straight-forward, including demanding purification and low yield due to the multistep synthesis.

Synthesis

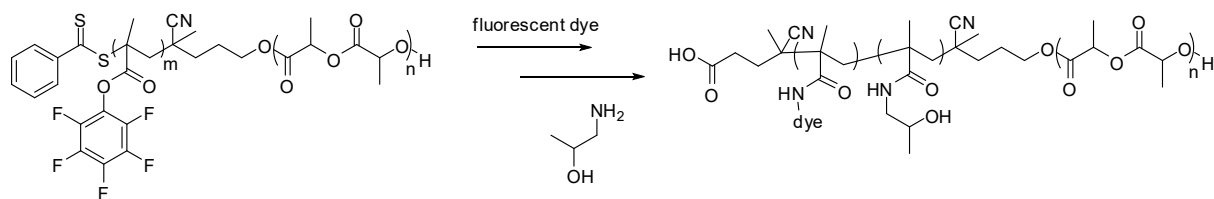
In this work, we present a shortened approach toward P(HPMA)-*b*-P(DLLA) diblock copolymers combining RAFT polymerization with organobase-catalyzed ROP. RAFT polymerization of reactive ester monomers permits the introduction of addressable functionalities for further attachment of drug and dye moieties. The molecular weight of the P(HPMA) block has been adjusted below the renal threshold to assure complete excretion (limit of renal clearance of HPMA copolymers $M_w < 40,000$ g/mol).¹⁴ Degradation of P(DLLA) proceeds via hydrolytic and enzymatic chain cleavage. The degradation product, lactic acid, is further metabolized via Krebs' cycle to water and carbon dioxide. The aim of this work is the synthesis of well-defined amphiphilic block copolymers suitable as surfactants, for instance for miniemulsion techniques. A prerequisite for the defined synthesis of poly(lactide) is the ROP in the presence of an alcoholic initiator.¹⁵ With these objectives in mind, a hydroxyl-functional RAFT chain transfer agent (CTA) has been synthesized, serving as a macroinitiator

in the subsequent ROP of L-/D-lactide catalyzed via 1,8-diazabicyclo[5.4.0]undec-7-ene (DBU). Subsequently, the PLA-based CTA has been used in the RAFT polymerization of pentafluorophenyl methacrylate, providing well-defined copolymers (Scheme 1). The main difference to the previously published strategy lies in the employment of a new CTA agent with a hydroxyl function, which permits direct ROP of lactide in a grafting-from approach. Hence, the DCC/DMAP mediated coupling step, which requires additional purification, is no longer required.



Scheme 1. Synthesis of P(PFPMA)-*b*-P(DLLA) by (1) DBU-catalyzed ROP of lactide, initiated via a hydroxyl-terminated CTA and (2) subsequent RAFT polymerization of PFMA using the PDLLA-based precursor as RAFT chain transfer agent.

The exchange of pentafluorophenyl groups against Oregon Green 488 cadaverine and 2-hydroxypropylamine yielded fluorescent-labeled amphiphilic P(HPMA)-*b*-P(DLLA) copolymers.



Scheme 2. Post-polymerization modification of P(PFPMA)-*b*-P(DLLA) via exchange of pentafluorophenyl ester groups with Oregon Green 488 cadaverine and 2-hydroxypropylamine.

The synthesis of the hydroxyl-functional RAFT chain transfer agent has been accomplished in 5 steps according to literature procedures with minor modifications.^{16,17}

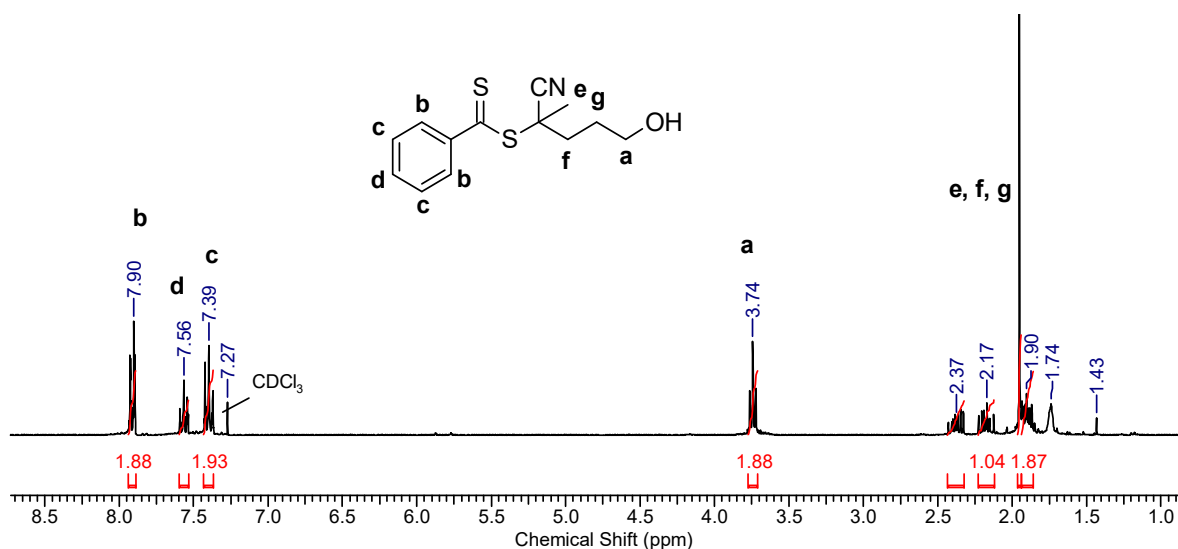


Figure 1. ¹H NMR (300 MHz, CDCl₃) of bifunctional RAFT chain transfer agent.

In view of the bifunctional initiator (CTA), two different routes appear viable for the synthesis of P(HPMA)-*b*-P(LA) copolymers: (1) synthesis of a PLA macroinitiator first, which is used subsequently in RAFT polymerization or (2) synthesis of a P(PFPMA) macroinitiator followed by ROP of lactide. However, starting with RAFT polymerization is not favorable due to possible transesterification rearrangements during ROP, involving the reactive pentafluorophenyl ester groups. Therefore, P(HPMA)-*b*-P(DLLA) copolymers have been synthesized in a 3 step protocol starting with the DBU-catalyzed ROP of lactide initiated via the above-mentioned hydroxyl-functional CTA. Addition of benzoic acid finally quenched the reaction after 15 min. The obtained copolymers have been investigated by ¹H NMR spectroscopy. After polymerization new signals appear that are caused by the poly(lactide) backbone at 5.14-5.20 ppm and a single terminal lactic acid unit at 4.35 ppm. The conversion of the CTA hydroxyl group is evidenced by a new signal at 4.23 ppm arising from esterification with P(DLLA). The ¹H NMR was used to calculate the average molecular weight in reference to the initiator signal c.

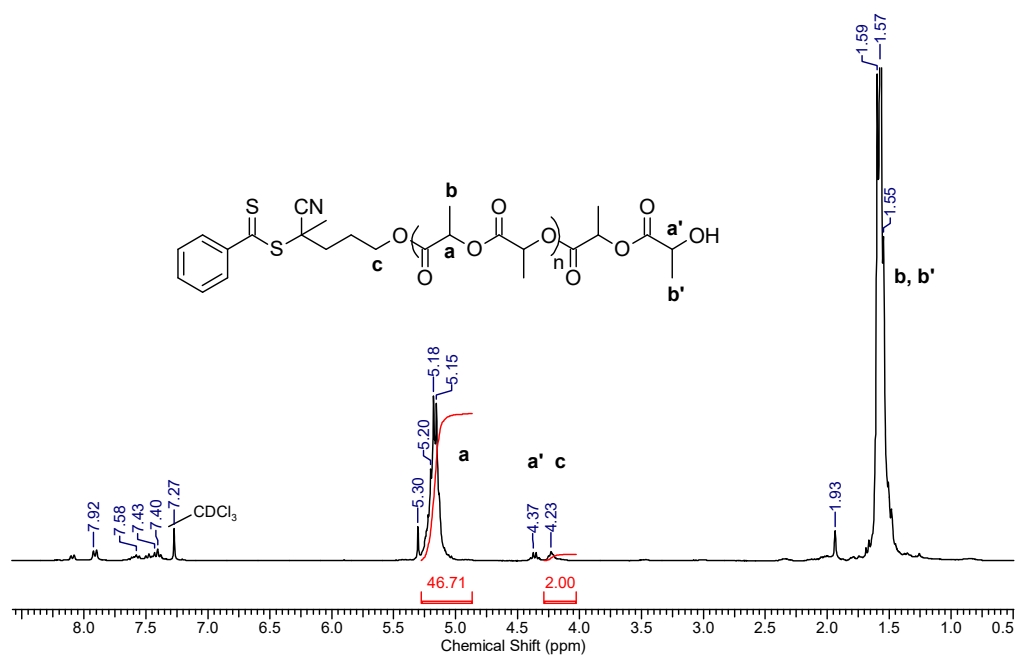


Figure 2. ^1H NMR (400 MHz, CDCl_3) of P(DLLA)-based CTA precursor (M_n : 3500 g/mol).

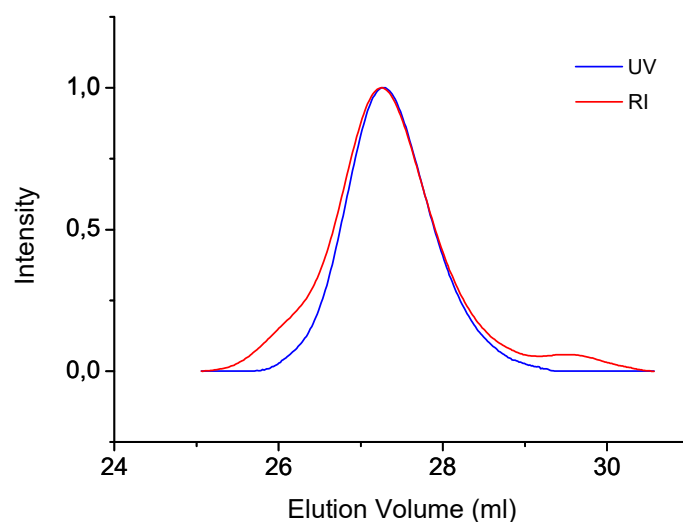


Figure 3. SEC elugram (in THF) of P(DLLA)-based CTA precursor with M_n : 4000 g/mol, M_w : 4600 g/mol PDI:1.13 obtained from the UV signal).

Purification of the PDLLA-based copolymer has been accomplished by precipitation into petrol ether/ether (50:50). SEC analysis confirmed the successful ROP initiated via the UV-absorbing chain transfer agent. Homopolymerization of lactide can be excluded, as seen from the overlay of UV and RI traces displayed in Figure 3.

Subsequent chain extension via AIBN-initiated RAFT polymerization of PFPMA afforded the desired diblock copolymers (^1H NMR, Figure 4). The polymerization has been performed according to procedures reported in literature.¹²

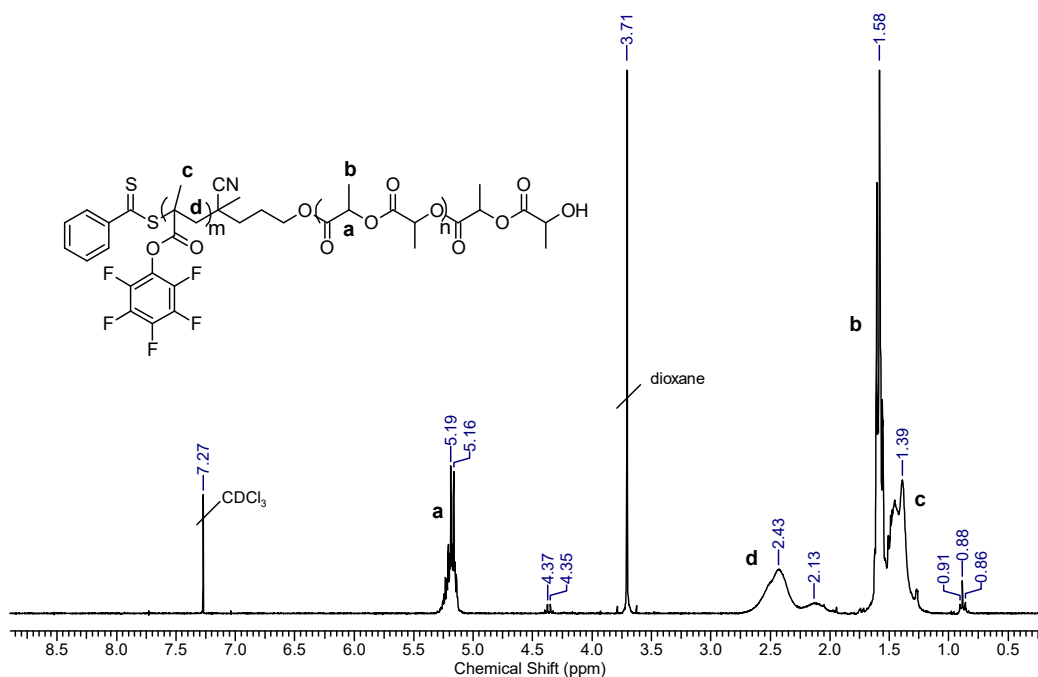


Figure 4. ^1H NMR (300 MHz, CDCl_3) of $\text{P(PFPMA)-}b\text{-P(DLLA)}$ after chain extension via RAFT polymerization.

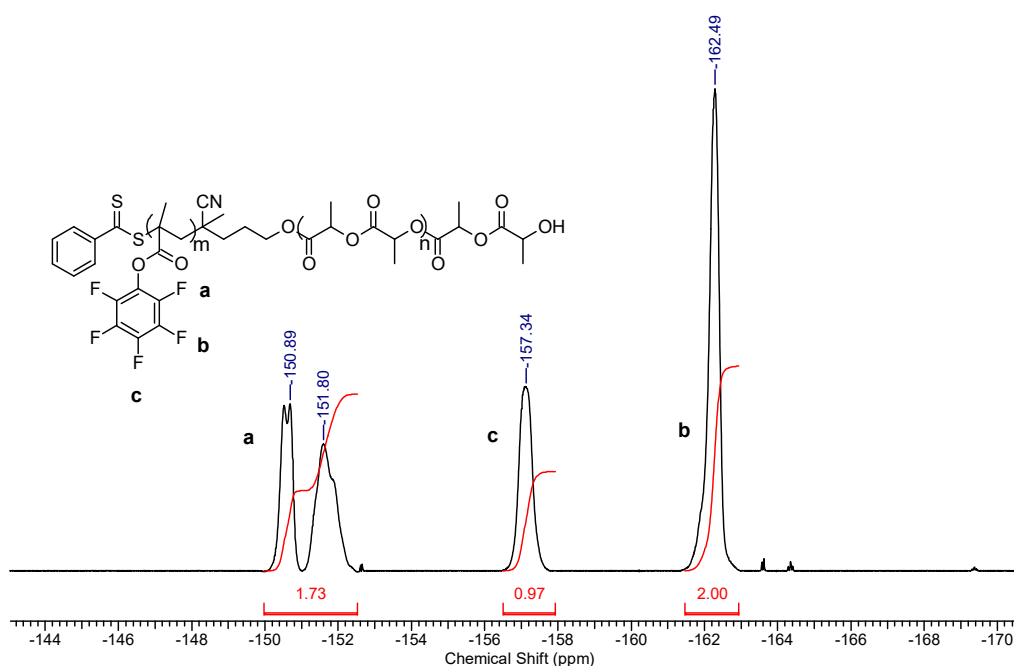


Figure 5. ^{19}F NMR (367.67 MHz) of $\text{P(PFPMA)-}b\text{-P(DLLA)}$ in CDCl_3 .

^{19}F NMR spectroscopy has been performed to confirm monomer conversion and to assure a uniform P(PFPMA) backbone, unaffected by cleavage of the reactive pentafluorophenyl groups (Figure 5), which is evidenced by the absence of additional signals associated with released pentafluorophenol. Raft polymerization of PFPMA afforded $\text{P(PFPMA)-}b\text{-P(DLLA)}$ copolymers with an average molecular weight of 35,000 g/mol and a moderate PDI of 1.18 estimated via SEC analysis.

The increase of molecular weight is evidenced by a shift of the elution volume to lower values in comparison with the PDLLA-based precursor. Monomodal SEC traces confirm controlled synthesis conditions without chain scission of the PDLLA block.

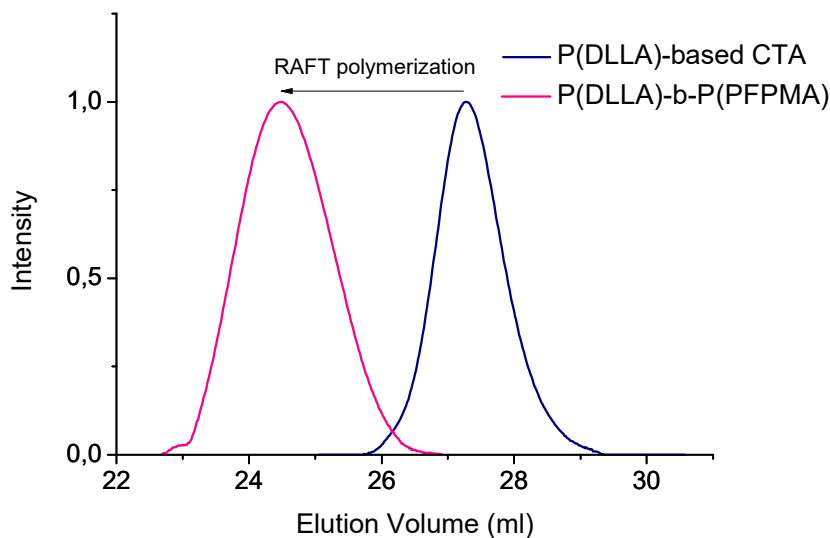


Figure 6. SEC elugram (in THF, UV signal, PMMA calibration) before and after chain extension with RAFT polymerization of PFPMA (P(DLLA)-*b*-P(PFPMA) with M_n :23,500, PDI:1.18).

In the next step, the terminal dithiobenzyl ester group has been converted into a carboxylic end group by a radical substitution reaction with 4,4'-azobis(4-cyanovaleric acid)¹⁸ to prevent possible disulfide formation and thiolactone cyclization. Subsequent exchange of the pentafluorophenyl ester groups with 2-hydroxypropylamine and Oregon Green 488 cadaverine resulted in a fluorescently labeled amphiphilic copolymer. The P(DLLA) to P(HPMA) block ratio before and after basic treatment remained constant, which evidences a successful post modification with the P(DLLA) block being unaffected by aminolysis. Integration of the signals corresponding to the P(DLLA) backbone (5.18-5.22 ppm, CH, b) referencing to the signals of the P(HPMA) (3.69 ppm, CH, a) yields a block ratio of 13:87 (PDLLA:HPMA) with an fluorescent dye content of 1% (see Figure 7). The completion upon transformation of P(PFPMA) into P(HPMA) is verified by ¹⁹F NMR. The obtained block copolymers were purified via preparative SEC (Sephadex G-25) to remove all side products.

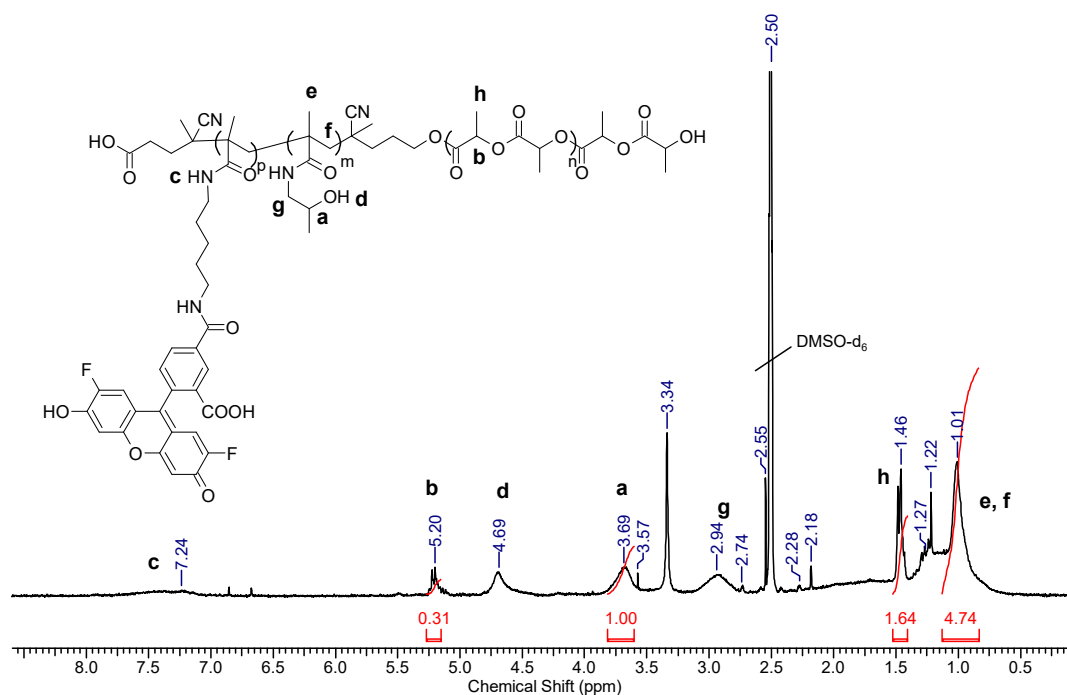


Figure 7. ^1H NMR (300 MHz, DMSO-d_6) of fluorescent-labeled $\text{P}(\text{HPMA})\text{-}b\text{-P}(\text{DLLA})$ after aminolysis.

The aim of this study has been the synthesis of smart materials with amphiphilic character labeled with a fluorescent tracer. The reactive ester approach yields reactive functionalities available for further derivatization with a drug useful in medical therapy. In recent studies¹² the biocompatibility of this material has been approved by *in vitro* cytotoxicity tests on HeLa cells, assuring non-toxicity of the $\text{P}(\text{HPMA})\text{-}b\text{-P}(\text{DLLA})$ copolymers.

Aiming at applications in drug delivery the prepared copolymers have been used as surfactant for microparticle synthesis via miniemulsion technique. In general, amphiphilic diblock copolymers represent an interesting class of polymer surfactants that are widely employed in industry for emulsion polymerization and as stabilizing agent for latex particle and flocculants.^{19,20} Using polymeric surfactants in emulsion polymerizations leads to an enhanced stabilization of the resulting microparticles due to anchoring of the surfactant directly at the particle surface by polarity driven aggregation. Surfactants like sodium dodecyl sulfate (SDS) tend to desorb under high shear rate resulting in flocculation of the targeted microparticles.²¹ The replacement of generally used emulsifiers, such as poly(vinyl alcohol) and SDS, is of major interest owing to their harmful consequences in the human body. The anionic surfactant SDS has been shown to influence the blood-brain barrier (BBB) permeability by interaction with major membrane components, which might have undesired effects on biochemical pathways.²²

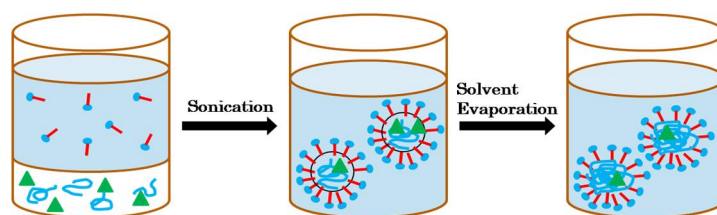


Figure 8. Procedure for microparticle preparation via miniemulsion technique.

The microspheres were prepared by an emulsion route in the absence of a low molecular weight surfactant. To this end, oil-in-water emulsions have been prepared with an aqueous phase containing 0.4 mg/ml of P(HPMA)-*b*-P(DLLA) copolymer as a surfactant and a dichloromethane solution of PDLLA (M_n : 3000 g/mol; 0.1g polymer/2.5g CH_2Cl_2) as an oil phase. The organic phase is emulsified in the aqueous solution via sonification to gain a stable emulsion of nanodroplets with homogeneously distributed PDLLA. The PDLLA microparticles with a diameter of 2-3 μm were fabricated by evaporation of dichloromethane from the emulsion and have been investigated by scanning electron microscopy (SEM) to gain information on size, particle size distribution and morphology.

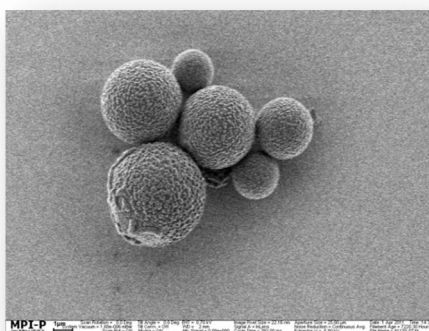


Figure 9. SEM image of microparticles obtained via miniemulsion technique.

Conclusions and future work

We have succeeded in developing a novel, optimized synthesis method toward well-defined amphiphilic poly(N-(2-hydroxypropyl)-methacrylamide)-*block*-poly(D,L-lactide) copolymers using a bifunctional initiator applicable in RAFT and ring-opening polymerization. Thus, the P(DLLA)-based CTA is obtained just by ROP without the requirement of additional coupling reactions. The following RAFT polymerization has been realized according to well-known literature procedures. Under controlled reaction conditions the labeling with a fluorescent dye has been accomplished, which can be used as tracer for *in vivo* studies of the distribution and accumulation of the synthesized nanomaterials. In addition, we were able to demonstrate the suitability of the prepared copolymers

in miniemulsion technique as particulate emulsifier. Further optimization of microparticle synthesis is required to reduce the particles' diameter and to obtain a homogenous distribution in particle size with regard to biomedical applications. In addition, investigation of the critical micelle concentration (CMC) and surface activity is crucial to gain more information of polymer specific surfactant properties.²³ Related studies are currently in progress.

References

1. Ringsdorf, H. J. *Polymer Sci. Symp.* **1975**, *51*, 135-153.
2. Vicent, M. J.; Duncan, R. *Adv. Drug Del. Rev.* **2009**, *61*, 1117-1120.
3. Duncan, R. *Nat. Rev. Cancer* **2006**, *6*, 668-701.
4. Meng, F.; Zhong, Z.; Feijen, J. *Biomacromolecules* **2009**, *10*, 197-209.
5. Torchilin, V. P. *Pharm. Res.* **2007**, *24*, 1-16.
6. Alconcel, S. N. S.; Baas, A. S.; Maynard, H. D.; *Polym. Chem.* **2011**, *2*, 1442-1448.
7. Otsuka, H.; Nagasaki, Y.; Kataoka, K. *Adv. Drug Del. Rev.* **2003**, *55*, 403-419.
8. Zalipsky, S. *Adv. Drug Del. Rev.* **1995**, *16*, 157-182.
9. Xiao, R. Z.; Zeng, Z. W.; Zhou, G. L.; Wang, J. J.; Li, F. Z.; Wang, A. M. *Int. J. Nanomed.* **2010**, *5*, 1057-1065.
10. Avgoustakis, K. *Current Drug Del.* **2004**, *1*, 321-333.
11. Vicent, M. J.; Duncan, R. *Adv. Drug Del. Rev.* **2010**, *62*, 272-282.
12. Barz, M.; Wolf, F. K.; Canal, F.; Koynov, K.; Vicent, M. J.; Frey, H.; Zentel, R. *Macromol. Rapid Commun.* **2010**, *31*, 1492-1500.
13. Barz, M.; Armiñán, A.; Canal, F.; Wolf, F. K.; Koynov, K.; Frey, H.; Zentel, R.; Vicent, M. J. *J. Controlled Release* **2012**; doi: 10.1016/j.jconrel.2012.05.024
14. Seymour, L. W.; Miyamoto, Y.; Maeda, H.; Brereton, M.; Strohalm, J.; Ulbrich, K.; Duncan, R. *Eur. J. Cancer* **1995**, *31*, 766-770.
15. Lohmeijer, B. G. G.; Pratt, R. C.; Leibfarth, F.; Logan, J. W.; Long, D. A.; Dove, A. P.; Nederberg, F.; Choi, J.; Wade, C.; Waymouth, R. M.; Hedrick, J. L. *Macromolecules* **2006**, *39*, 8574-8583.
16. Thang, S. H.; Chong, Y. K.; Mayadunne, R. T. A.; Moad, G.; Rizzardo, E. *Tetrahedron Letters* **1999**, *40*, 2435-2438.
17. Chong, Y. K.; Krstina, J.; Le, T. P. T.; Moad, G.; Postma, A.; Rizzardo, E.; Thang, S. H. *Macromolecules* **2003**, *36*, 2256-2272.
18. Perrier, S.; Takolpuckdee, P. Mars, C. A. *Macromolecules* **2005**, *38*, 2033.
19. Zhou, J.; Wang, L.; Ma, J. *Designed Monomers and Polymers* **2009**, *12*, 19-41.
20. Tadros, T. *Adv. Colloid Int. Sci.* **2009**, *147*, 281-299.
21. Guyot, A. *Macromol. Symp.* **2002**, *179*, 105-132.

22. Saija, A.; Princi, P.; Trombetta, D.; Lanza, M.; De Pasquale, A. *Exp. Brain Res.* **1997**, *115*, 546-551.
23. Halperin, A. *Polym. Rev.* **2006**, *46*, 173-214.

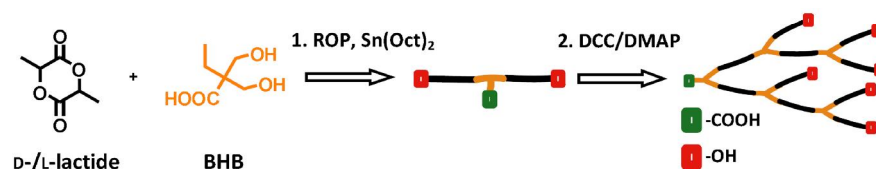
Appendix

A1. Long-Chain Branched Poly(lactide)s Based on Polycondensation of AB₂-type Macromonomers

Anna M. Fischer, Florian K. Wolf and Holger Frey

Published in *Macromol. Chem. Phys.* **2012**, doi: 10.1002/macp.201200082

In a two-step synthesis long-chain branched poly(lactide)s were obtained via polycondensation of AB₂-functional macromonomers. The preformed poly(lactide)-based macromonomers were synthesized by Sn(Oct)₂-catalyzed ring-opening polymerization. The spacing between the branching units was tuned by the variation of the lactide chain length.



Keywords: branched, macromonomers, poly(lactide), polymerization, polyester

Abstract

A series of long-chain branched poly(D-/L-lactide)s was synthesized in a two-step protocol by (1) ring-opening polymerization of lactide and (2) subsequent condensation of the preformed AB₂ macromonomers promoted by different coupling reagents. The linear AB₂ macromonomers were prepared by Sn(Oct)₂-catalyzed ROP of D- and L-lactide with 2,2-bis(hydroxymethyl)butyric acid (BHB) as an initiator. Optimization of the polymerization conditions allowed for the preparation of well-defined macromonomers ($M_w/M_n=1.09-1.30$) with adjustable molecular weights (760-7200 g mol⁻¹). The two-step approach of the synthesis comprised as well the coupling of these AB₂ macromonomers and hence allowed precise control over the lactide chain length between the branching units in contrast to a random polycondensation.

Introduction

Biocompatible, degradable polymer structures are of great importance, especially with respect to biomedical applications and packaging purposes. Polyesters, mainly poly(lactide) and poly(lactide-co-glycolide) are widely employed in medical applications, e.g., sutures^{1,2} and drug delivery systems.³⁻⁵ Although the number of groups focusing on poly(L-lactide) has increased in the last decades, this material still bears some disadvantages, e.g., a high degree of crystallization lowering the degradation rate. One strategy to tailor material properties and increase the functionality is the synthesis of more complex architectures such as star-shaped,⁶⁻⁸ branched and “dendrimer-like” polyesters. In recent years, hyperbranched polymers and dendrimers have attracted increasing interest, especially in biomedical and pharmaceutical applications.⁹

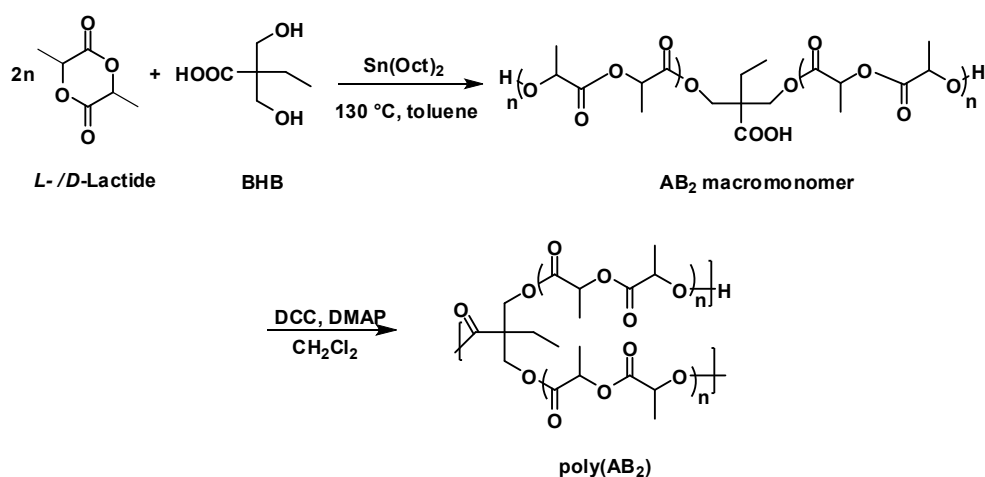
Because of their globular shape and the high number of end group functionality they exhibit unusual properties.^{10,11} Hedrick et al.¹² introduced the term “dendrimer-like star polymers”, referring to aliphatic polyesters synthesized by a divergent growth approach. Starting with a multifunctional core they generated a six-arm star polymer by ring-opening polymerization (ROP) of ϵ -caprolactone. The branching points were obtained by condensation reaction with a bishydroxy acid, followed by repetitive ROP. Hult and co-workers presented both dendritic and hyperbranched polyesters by polycondensation of 2,2-bis(hydroxymethyl)propionic acid (bis-MPA) together with a multifunctional core.^{13,14} To date, BoltornTM is the only commercially available aliphatic polyester prepared by a pseudo one-pot polycondensation of bis-MPA – an analogous procedure, to some extent comparable to the divergent growth approach for dendrimers.¹⁵ In contrast to perfectly branched dendrimers which require tedious multi-step synthesis, hyperbranched polymers are obtained from AB_n-type monomers in a one-pot synthesis. Extensive efforts are being made to prepare branched aliphatic polyesters in simple synthetic procedures, which are also applicable on industrial scale. Trollsås et al. reported the synthesis of hyperbranched poly(ϵ -caprolactone) by self-condensation of AB₂ macromonomers consisting of bis-MPA and ϵ -caprolactone using 4-(dimethylamino)pyridinium 4-toluenesulfonate (DPTS) and dicyclohexylcarbodiimide (DCC) as reagents.¹⁶ With an analogous synthetic approach Choi and Kwak synthesized branched poly(ϵ -caprolactone) by polycondensation with p-toluenesulfonic acid (p-TSA) under continuous water removal.¹⁷ Enzymatic and metal-catalyzed copolymerizations of ϵ -caprolactone and 2,2-bis(hydroxymethyl)butyric acid (BHB) by combination of ROP and polycondensation produced hyperbranched polymers without time-consuming synthesis, as reported by our group.^{18,19} Limiting factors in case of polycondensation are the increasing amount of the bishydroxy acid content and the removal of byproducts.

Various suitable procedures offer the possibility to prepare hyperbranched poly(ϵ -caprolactone) in a facile way. However, to the best of our knowledge the synthesis of branched poly(lactide) (PLA) is still hampered by different limitations.²⁰ At present, there are three different synthetic routes established

to produce PLA with a branched topology. One approach to obtain long-chain branched PLA is the $\text{Sn}(\text{Oct})_2$ -catalyzed ROP of lactide initiated with glycidol, as reported by Knauss et al.²¹ The PLA segments are separated by glycerol branching points. In a very recent approach, Zhao et al. copolymerized L-lactide with BHB as branching comonomer in the presence of a tertiary amine.²² Hyperbranched polyesters can also be prepared by the so-called “self-condensing cyclic ester polymerization”.²³ In an analogous approach our group synthesized (hyper)branched PLLA copolymers via ring-opening multibranching copolymerization (ROMBP) of L-lactide with a hydroxyl-functional lactone inimer called 5-HDON (5-hydroxymethyl-1,4-dioxan-2-one).²⁴ A further approach towards branched PLA was the copolycondensation of L-lactide with glyceric acid, obtained from glycerol in a bioprocess using acetic acid bacteria.²⁵

Tailoring the physical properties of poly(lactide)s (PLA) by variation of architecture, copolymerization and post-polymerization modifications allow optimization and thus specific applications. Apart from topological modification, the incorporation of functional groups is a key element in (bio-) polyester research to attach fluorescent dyes and relevant drugs. The introduction of a single or multiple pendent carboxylic acid groups in the middle of a PLA backbone without time-consuming protection and deprotection steps was demonstrated in an elegant work by Cooper and Storey.²⁶ Feijen and co-workers synthesized analogous polymers by $\text{Sn}(\text{Oct})_2$ -catalyzed ROP of ϵ -caprolactone and L-lactide with bis-MPA as initiator.²⁷ These polymers do not only offer the opportunity for post-polymerization modifications, but also fulfill the specifications as AB_2 macromonomers.

In the current paper we demonstrate an alternative route to branched PLA in a two-step approach involving the self-condensation of PLA-based AB_2 macromonomers (Scheme 1).



Scheme 1. Synthetic route to long-chain branched poly(D-/L-lactide)s by (1) $\text{Sn}(\text{Oct})_2$ -catalyzed ring-opening polymerization and subsequent (2) condensation with DCC/DMAP.

The suitability of different standard coupling agents was tested and evaluated with respect to the formation of branched poly(lactide)s. The branched macromolecules were obtained with a predetermined chain length between every branching point due to the predetermined poly(lactide) arm length of the AB₂ macromonomers, adjusted via the monomer to initiator ratio.

Experimental Section

Materials

D- and L-Lactide were purchased from Purac (Gorinchem, Netherlands), recrystallized twice from dry toluene and dried under vacuum at 40°C. 2,2-Bis(hydroxymethyl)butyric acid (BHB, 98%) was obtained from Sigma-Aldrich and used without further purification. Stannous 2-ethylhexanoate (Sn(Oct)₂) was purchased from Acros and used as received. 1,3-Dicyclohexylcarbodiimide (DCC) and 4-dimethylamino-pyridine (DMAP) were obtained from Sigma-Aldrich. Dichloromethane as solvent was dried over P₂O₅ and distilled under nitrogen- atmosphere. Toluene was dried over sodium, distilled under nitrogen atmosphere and stored over molecular sieve. Further solvents and reagents (1-ethyl-3-(3-dimethylaminopropyl)carbodiimide (EDC), hydroxybenzotriazole (HOBT), diisopropyl-azodicarboxylate (DIAD), triphenylphosphine (PPh₃)) were obtained from Sigma Aldrich and Acros and used as received, unless otherwise stated.

Instrumentation

Size exclusion chromatography (SEC) of the samples was carried out in THF (3 mg/ml) using a setup with a Waters 717 plus autosampler, a TSP Spectra Series P 100 pump including a set of three PSS-SDV 5A columns with 10², 10³ and 10⁴ Å porosity and a Wyatt Optilab DSP RI detector. All SEC traces were recorded using the signal of the RI detector. Poly(styrene) standards, provided by Polymer Standards Services (PSS, Mainz – Germany), were used for the internal calibration of the SEC system. Preparative SEC was performed in THF using a setup with a Knauer HPLC pump K-501, an RI detector from Shodex RI-71 and a column (300x20 mm, MZ-Gelplus, 10µm) with 10³ Å porosity. ¹H NMR spectra (300 and 400 MHz) and ¹³C NMR spectra (75 and 100 MHz) were obtained at 25 °C on a Bruker AC300 spectrometer or a Bruker ARX400 spectrometer. The spectra were measured in CDCl₃ and the chemical shifts were referred to the internal calibration of the solvents' residual peak. (¹H proton NMR signal: 7.24 ppm; ¹³C carbon NMR signal: 77.36 ppm). Deuterated chloroform-*d*₁ was purchased from Deutero GmbH, dried and stored over molecular sieve.

Differential scanning calorimetry (DSC) analyses were obtained using a Perkin Elmer 7 Series Thermal Analysis System with auto-sampler in the temperature range of -100°C and 200°C with heating rates of 20 K min⁻¹. The melting points of indium (T₀= 156.6 °C) and Millipore water (T₀= 0 °C) were used for calibration.

Matrix-assisted laser desorption and ionization time-of-flight mass spectrometry (MALDI-ToF MS) measurements were performed on a Shimadzu Axima CFR MALDI-ToF mass spectrometer equipped with a nitrogen laser delivering 3 ns laser pulses at 337 nm. Dithranol (1,8,9-trihydroxyanthracene, Aldrich 97%) was used as matrix, while potassium triflate (Aldrich, 98%) was used as ionization agent. The samples were prepared from THF solutions.

Optical rotation measurements were carried out at 23 °C on a Perkin Elmer Polarimeter 241 at two wave lengths (578 nm, 546 nm) equipped with an Hg lamp and extrapolated for $[\alpha]_D$.²⁸ The samples were prepared in THF as a solvent (0.01 g ml⁻¹).

Synthesis and Characterization

General Synthesis of AB₂ Macromonomers Based on Sn(Oct)₂-catalyzed ROP of D- and L-Lactide

The AB₂-type poly(lactide) prepolymers were synthesized via solution polymerization with 2,2-bis(hydroxymethyl)butyric acid (BHB) as initiator and Sn(Oct)₂ as catalyst. D-, L-Lactide (4 g, 0.028-mol in a molar ratio of 25:75) and BHB (1.04 g, 0.007 mol) were dissolved in dry toluene (1ml per g lactide) at 130 °C under argon atmosphere. The catalyst Sn(Oct)₂ (mol ratio, monomer to catalyst, M/cat=1000) was added to the clear reaction mixture as a 10 vol.% solution in toluene. After completion of the reaction, the viscous mixture was cooled to room temperature and diluted with 5-ml CHCl₃. The product was purified by precipitation into a cooled mixture (-10 °C) of ether/petroleum ether (50:50). After decantation of the solvent the solid product was dried *in vacuo* at 40 °C.

¹H NMR (400 MHz, CDCl₃-d₁, δ): 0.90 (t, 3H, CH₃), 1.43-1.65 (m, CH_{3 term/lin}, CH₂), 4.2-4.36 (CH_{term}, -CH₂OR), 5.15-5.25 (m, CH_{lin}); ¹³C NMR (75 MHz, CDCl₃-d₁, δ): 7.94 (CH₃), 16.58 (CH_{3 lin}), 20.37 (CH_{3 term}), 23.60 (CH₂), 49.71 (C_{quart.}), 63.24 (CH₂OR), 66.24 (CH_{term}), 68.89 (CH_{lin}), 169.50 (CO_{lin}), 173.90 (COOH), 175.00 (CO_{term}).

General Procedure for the Self-Condensation of AB_{2-x} Macromonomers

The respective AB₂ macromonomer and 0.14 eq DMAP were dissolved by stirring in dry dichloromethane (CH₂Cl₂) under argon atmosphere. 1.2 eq DCC, dissolved in dry CH₂Cl₂, were added dropwise to the clear solution. The mixture was allowed to react for 24 h, maintaining room temperature. After the reaction was completed, the resulting viscous solution was diluted with dichloromethane and the byproduct DCC-urea was filtered off. The organic layer was washed with a 10 wt.% solution of acetic acid, twice with distilled water, dried over MgSO₄ and evaporated *in vacuo*. The obtained product (a white solid) was further purified by dilution in CH₂Cl₂ and precipitating it twice in cold methanol or petroleum ether.

¹H NMR (300 MHz, CDCl₃-d₁, δ): 0.85 (CH₃), 1.4-1.65 (m, CH_{3 term/lin}, CH₂), 4.25-4.39 (CH_{term}, CH₂OR), 5.00-5.25 (m, CH_{lin}); ¹³C NMR (75 MHz, CDCl₃-d₁, δ): 7.96 (CH₃), 16.53-16.63 (CH_{3 lin}), 19.99-20.33

(CH₃_{term}), 23.90 (CH₂), 50.00 (C_q), 63.47 (br, CH₂OR), 66.61 (CH_{term}), 68.9-69.5 (CH_{lin}), 169.45-169.81 (CO_{lin}), 170.92 (COOR), 174.70-174.97 (CO_{term}).

Results and Discussion

Synthesis and Characterization of AB₂-x Macromonomers

The AB₂-type macromonomers (i.e., AB₂-5, -10,-20, -40 and -60) varying in the length of the poly(lactide) arms (theor. DP_n= 5, 10, 20, 40, 60) were successfully synthesized by Sn(Oct)₂-catalyzed ring-opening polymerization in solution with variable lactide-to-initiating BHB molar ratios.

The ¹H NMR spectra (Figure 1) were used to calculate the average number of lactide monomer units (DP_n) incorporated in the AB₂ macromonomers and the number average molecular weight (M_n). The DP_n was determined from the ratio of the integrated signal areas of the methine protons of the linear (m, 5.15 ppm, CH) and terminal (m, 4.3 ppm, CH, CH₂OR) lactide units to the methyl protons of 2,2-bis(hydroxymethyl)butyric acid (t, 0.9 ppm, CH₃). As it shown in Figure 1, the peak assigned to the repeating units (d, d'') is clearly separated from the resonance of the chain ends (d'), the integral intensity being accessible by subtraction of the hydroxyl methylene protons (c) of the initiator. This signal intensity is obtained from the initiator signal a. In addition, detailed ¹³C NMR characterization is of importance to verify the formation of new signals after self-condensation of the preformed oligomers in the next step (Figure S1). The single peak at 49.71 ppm, originating from the quaternary carbon, gives evidence that both hydroxyl groups are esterified and that no esterification of the carboxylic acid occurred.

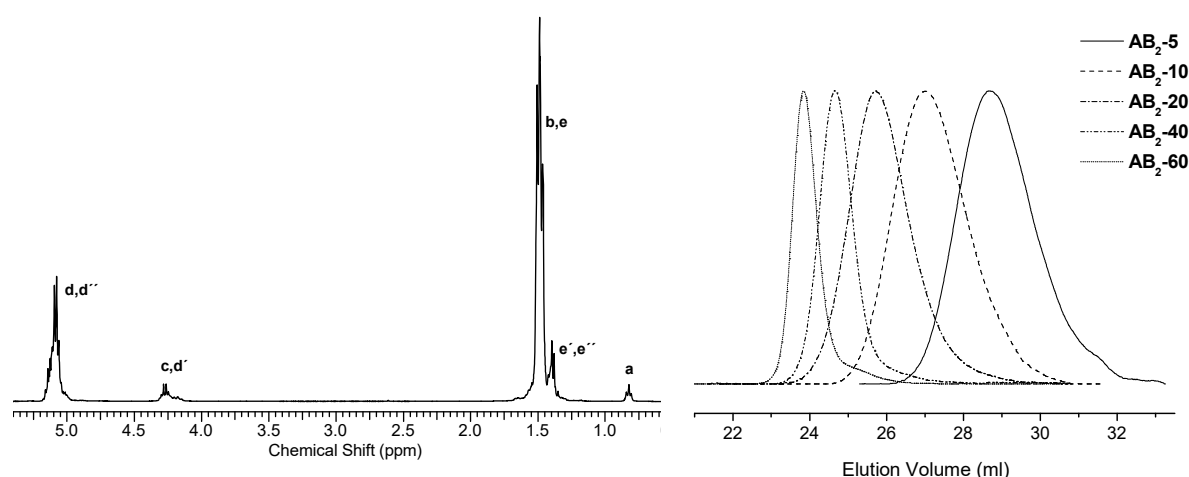


Figure 1. ¹H NMR spectrum (300 MHz) of AB₂-20 measured in CDCl₃ (left) and SEC elugrams (PS standard, THF) of linear AB₂ macromonomers (right).

The molecular weight distributions obtained from size exclusion (SEC) measurements are in the range of M_w/M_n= 1.09 to 1.30, as expected for this ROP with its living character. The resulting monomodal SEC traces are given in Figure 1. The discrepancy of the molecular weights obtained from

NMR and SEC can be explained by the deviating hydrodynamic radius compared to the poly(styrene) standard. Table 1 summarizes the results for the series of polymers prepared.

Table 1. Characterization data of linear AB₂ macromonomers.

Sample	Entr y M/I	M _n ^{a)} [g mol ⁻¹]	M _n ^{b)} [g mol ⁻¹]	M _w /M _n ^b	[α] _D ²³ [deg]	x _L ^{c)} [mol%]	T _g [°C]	Conversio n [%]
AB ₂ -5	5	760	900	1.30	-51.0	67.06	10.0	92
AB ₂ -10	10	1130	1700	1.28	-63.6	71.29	25.3	95
AB ₂ -20	20	2200	3600	1.22	-74.8	75.04	38.7	96
AB ₂ -40	40	4600	7200	1.09	-76.6	75.63	39.4	97
AB ₂ -60	60	7200	11400	1.10	-71.6	73.95	44.0	97

^{a)} determined by ¹H NMR; ^{b)} determined by SEC in THF vs polystyrene standards; ^{c)} x_L (molar content of L-lactide) determined by optical rotation $\frac{x_L}{100} = \frac{[\alpha]_D^{23} + [\alpha]_D^{23}(PLA\ 100)}{2 \cdot [\alpha]_D^{23}(PLA\ 100)}$ with $[\alpha]_D^{23}(PLA100) = -149.5^{\circ 30}$

In Figure 2 the MALDI-ToF mass spectrum of AB₂-60 is shown. The observed signals are composed of the molar mass of the initiator (BHB; 148.1 g mol⁻¹) and the repeating units (lactide, 144.1 g mol⁻¹), ionized as the respective potassium adducts. Species with 0 or more than 1 BHB unit were not detected.

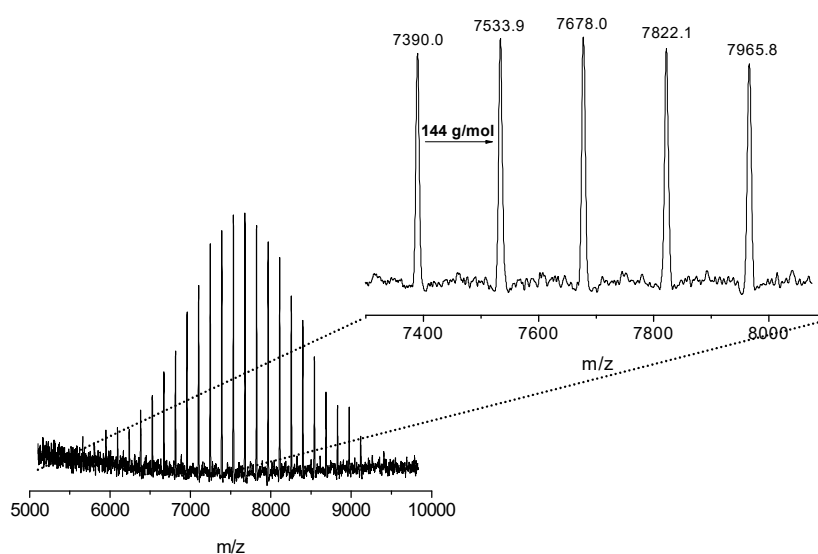


Figure 2. MALDI-ToF mass spectra of AB₂-60 with potassium as counterion.

The characterization data show that this polymerization yields predominantly linear species, as previously reported by Cooper and Storey.²⁶ The mass spectrum in Figure 2 shows a mass increment of 144.1 g mol^{-1} , which corresponds to the molar mass of one lactide repeat unit. The distribution curve of AB₂-40 (Figure S2) in contrast to AB₂-60 depicts a very low extent of polymer chains with an odd number of lactic acid units (LA, 72 g mol^{-1}), which are formed by transesterification reactions well-known for Sn(Oct)₂-catalyzed ROP.²⁹

Optical rotation measurements permitted the determination of the molar composition of the polymers with respect to the amount of D- and L-lactide. The specific rotation value ($[\alpha]_D^{23}$) of PLA₁₀₀ ($M_n/{}^1\text{H NMR}$: 4500 g mol^{-1}) was found to be -149.5° , which is in the range of values reported in literature (-149° to -156°).³⁰ The content of l-lactoyl units of the poly(D-/L-lactide)s was calculated from the specific rotation value compared with PLA₁₀₀.

The thermal properties of the AB₂ macromonomers were determined by DSC analysis (Figure S3). The glass transition temperature (T_g) detected in the second heating scan is in the range of 10 to 44°C , slightly decreased in contrast to that of pure PLLA ($57\text{--}60^\circ\text{C}$).³¹ The DSC curves show an increase of T_g with increasing number of lactide units. The low T_g according to the lower molecular weight poly(D-/L-lactide)s results from the higher contribution of hydroxyl chain ends, which has also been observed by Velthoen et al. for similar structures.²⁷ A melting temperature (T_m) was not detected for the AB₂ macromonomers because of the incorporation of stereochemical defects into PLLA. The introduction of d-units reduces the melting point, the rate and degree of crystallization.³² Incorporation of more than 15% of meso-lactide units suppresses crystallization, and an amorphous polymer is obtained, as reported by Fischer et al.³³ The same behaviour is observed for copolymers of L- and D-lactide. Tsuji and Ikada suggested, that for crystallization more than 76% L-lactide is needed.³⁴

A kinetic study was accomplished by time-dependent ${}^1\text{H NMR}$ and SEC measurements to optimize the polymerization conditions in terms of reaction time and catalyst concentration. This is especially desirable since reaction times that significantly exceed the time necessary to attune the monomer/polymer equilibrium concentrations are accompanied by undesired transesterification reactions. To cover a broad time range in the first experiments, samples were collected in logarithmically increasing intervals from the early state of the reaction until complete conversion. The reaction was quenched thermally by rapid cooling below room temperature. As it is shown in Figure 3, ${}^1\text{H NMR}$ spectra in CDCl_3 revealed a high conversion of ca. 99% after 160 min for polymers with an average molecular weight (M_n) of 4000 g mol^{-1} . The conversion was determined from the integral ratio of the methine protons of the monomer (q, CH, 5.03 ppm) and the polymer (q, CH_{lin}, 5.13 ppm; CH_{term}). Synthesis of poly(lactide)s with $M_n < 3000 \text{ g mol}^{-1}$ showed a lower conversion after

the same reaction time. In order to facilitate the quantitative evaluation of the polymerization kinetics via proton NMR, enantiomerically pure L-lactide was employed instead of the mixed isomers.

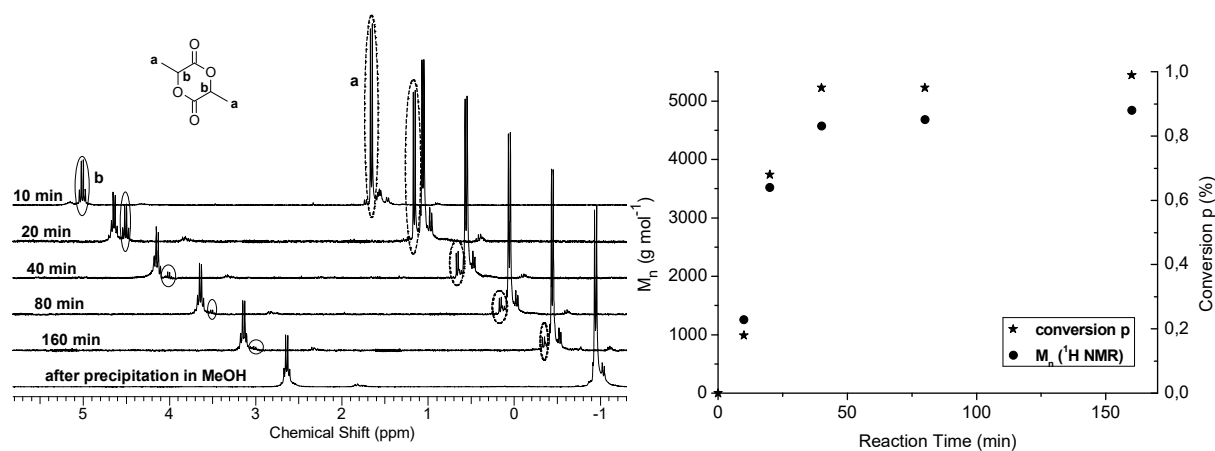


Figure 3. Left: Time-dependent ¹H NMR measurements in CDCl₃ (scale bar refers to the first ¹H NMR spectrum). Right: M_n , conversion p plotted versus reaction time; according to ROP of L-lactide with BHB as initiator.

This resulted in significantly smaller signal width and therefore improved signal separation between monomer and polymer. At low conversion, M_n increases linearly with conversion accompanied by an almost constant PDI (Table S1) which is characteristic for the “living” character of the coordination insertion polymerization. As reported in literature, transesterification competes with propagation when the monomer is nearly consumed. As a typical consequence of transesterification the molecular weight distribution becomes broader, and further intramolecular transesterification reactions lead to a decrease in M_n due to the formation of cyclic esters.³⁵

An optimization of the conversion was obtained by prolonging the reaction time. The improved reaction conditions were also accompanied by a small amount of transesterification, which was identified by MALDI-ToF measurements (Figure S2). Time-dependent ¹H NMR studies of the ring-opening polymerization revealed a significant reduction of the catalyst reactivity with increasing bishydroxy acid concentration.

Kinetic studies by Penczek et al. on lactide polymerization showed that the mechanism of the Sn(Oct)₂-catalyzed ROP includes the ligand dissociation from the metal complex as the corresponding acid.³⁶ In addition, Ryner et al.³⁷ observed a decrease of the polymerization rate by further addition of octanoic acid. This effect was explained by “a blocking of the coordination site or as a shift in the equilibrium between Sn(Oct)₂ and the Sn(Oct)₂-alkoxide species” and thus a deactivation of the

catalyst. Preliminary studies as well as the previous investigations by Ryner et al. indicated a strong effect of the carboxylic moiety of the BHB unit on the reaction rate of the polymerization.

Thus, an optimization of the AB₂ macromonomer synthesis was achieved via a ¹H NMR kinetic analysis providing greater synthetic control in terms of reaction time and conversion.

Figure 4 represents the results of the ¹H NMR study obtained from the comparison of ring-opening polymerizations of L-lactide with different amounts of 2,2-bis-(hydroxymethyl)butyric acid (BHB) maintaining the same catalyst concentration. After polymerization, the signals of the methine protons broaden, allowing calculations of conversion from the integrated intensities of the monomer (q, CH, 5.03 ppm) and the polymer methine signals (q, CH_{lin}, 5.15 ppm; CH_{term}).

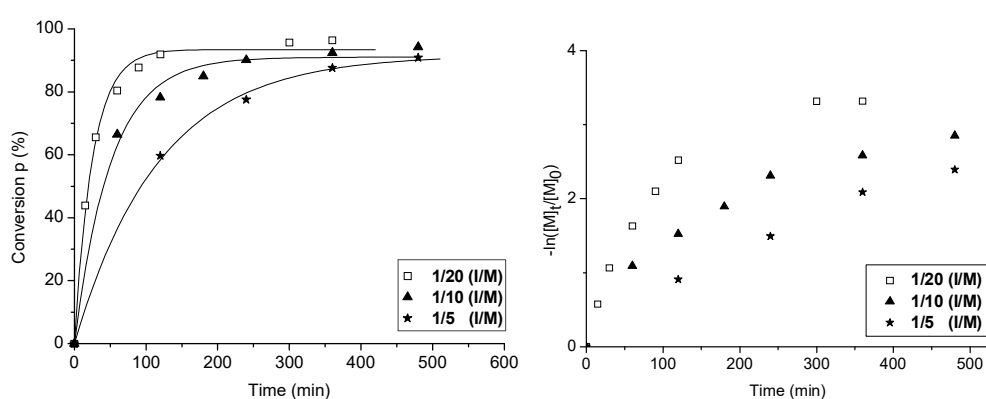


Figure 4. Conversion *p* (left) and kinetic data (right) for the solution polymerization of L-lactide with BHB as initiator, polymerization conditions: 130 °C, [monomer]/[catalyst]=1000, in toluene.

Ring-opening polymerizations of L-lactide typically follow first-order kinetics at low conversion,^{34,38} as shown in Equation 1:

$$-\ln([M]_t/[M]_0) = k_p[cat]_0 t \quad (1)$$

where k_p is the rate constant for propagation, $[cat]_0$ is the constant concentration of catalyst, $[M]_t$ is the monomer concentration at time t and $[M]_0$ is the initial monomer concentration. The equilibrium monomer concentration $[M]_{eq}$ was determined from the limiting conversion reached during polymerization. The polymerization/depolymerization equilibrium has to be taken into account, especially for the kinetics of lactide polymerization in bulk.³⁹ Our kinetic study reveals that an increasing amount of 2,2-bis(hydroxymethyl)butyric acid results in a decreased conversion and lower $k_p[cat]$ values. The data in Figure 4 show a linear dependence below 80% conversion, therefore the slopes of the plots were taken for the calculation of the $k_p[cat]$ values according to literature procedures.³⁸ The deviation from first-order kinetics at conversions >80% indicates a polymerization under equilibrium conditions. We assume that the observed behavior is probably caused by the

elevated reaction temperature. The calculated percentage of $[M]_{eq}$ shows an increase with increasing initiator concentration, which may support the influence of the bishydroxy acid on $\text{Sn}(\text{Oct})_2$ -catalyzed ROP. The $k_p[\text{cat}]$ values seem to depend also on the amount of carboxylic acid, with the polymerization of AB_2 -5 being the slowest, two times slower than AB_2 -10 and six times slower than the polymerization of AB_2 -20. The resulting $k_p[\text{cat}]$ and $[M]_{eq}$ values are given in the Supporting Information (Table S2). In a comparative study, the polymerization kinetics using 1,6-hexanediol (1,6-HD) as an initiator was examined to evaluate the influence of the carboxylic acid on the kinetic behavior maintaining the same catalyst concentration. The polymerization initiated via 1,6-HD resulted in faster polymerization rates (Figure S4).

Synthesis and Characterization of Long-Chain Branched Poly(AB_2 -x)

The obtained AB_2 macromonomers are appropriate building units for polycondensation with respect to their multiple hydroxyl end groups and the single carboxylic acid functionality in the polymeric backbone. In order to identify the best condensation conditions, four different esterification reagents have been tested to generate branched poly(lactide)s (listed in Figure 5). In consideration of the labile ester linkage we emphasized mild reaction conditions, avoiding high temperatures, strong bases and the use of strong acids. This was of special importance, since we were interested in preserving the well-defined structure of the macromonomer, which should allow precise control over the linear poly(lactide) segment length between two branching units in the final structure.

Figure 5 shows the different SEC elugrams after self-condensation of AB_2 macromonomers promoted by different esterification reagents. The reactions always took place in the presence of a solvent (CH_2Cl_2 , THF), a condensing agent (i.e., DCC, EDC) and a catalyst (i.e., DMAP, HOBT). The best results in terms of an increase in molecular weight (elution volume, SEC) were obtained with the well-established esterification agent 1,3-dicyclohexylcarbodiimide (DCC) and 4-dimethylaminopyridine (DMAP).

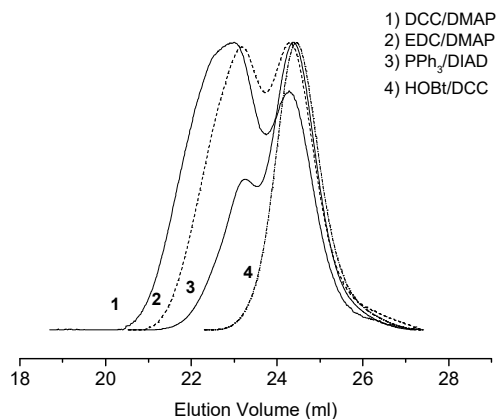


Figure 5. SEC elugrams after condensation of AB₂ macromonomer ($M_n=4000\text{ g}\cdot\text{mol}^{-1}$) via four different reaction routes.

In **Figure 6**, SEC elugrams show a significant shift of the elution volume towards higher molecular weights after the condensation of AB₂-10 and AB₂-20. Using the condensation polymerization, polymers with a broad molecular weight distribution ($M_w/M_n=1.94\text{-}2.24$) are formed, as expected. The small shoulder at lower elution volumes arising with the polycondensation reaction can be explained by the formation of macrocycles, which limit the conversion in an early state of reaction, as studied by MALDI-ToF mass spectrometry (vide infra).

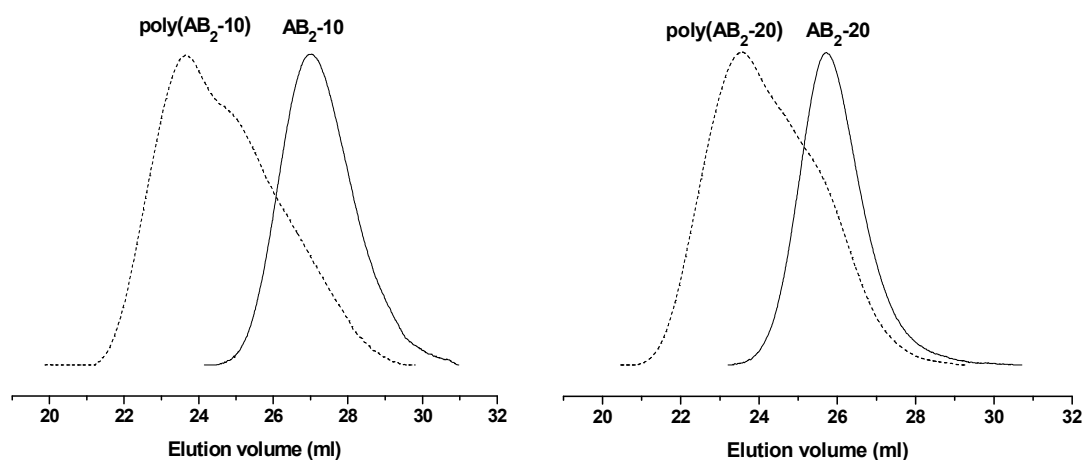


Figure 6. SEC elugrams (RI signal) before (AB₂-x) and after polycondensation (poly(AB₂-x)) of AB₂ macromonomers.

During condensation reactions of AB_n-type macromonomers, cyclization is always observed as a side reaction, limiting the amount of polycondensation and broadening the molecular weight distribution.^{40,41} The decrease in the reactivity of larger macromonomers (with $M_n=4600\text{ g mol}^{-1}$ and $M_n=7200\text{ g mol}^{-1}$) can be explained by a decrease in the concentration of functional end groups (Figure S6). In Table 2 the results of the polymer series are presented with respect to molecular weights and polydispersities. With decreasing length of the linear poly(lactide) segments, the conversion increased and the amount of cyclization was reduced. Nevertheless, the main polymeric species were of the non-cyclic form and the obtained branched poly(lactide)s showed a significant excess molecular weight in SEC compared to their linear precursors.

Table 2. Characterization of long-chain branched AB₂ macromonomers.

Sample	Entry macro-monomer	M _n (SEC) ^{a)} [g mol ⁻¹]	M _w /M _n ^{a)}	N _{AB₂} ^{b)}	M _n (NMR) ^{b)} [g mol ⁻¹]
poly(AB ₂ -5)	AB ₂ -5	2600	2.24	5.8	4300
poly(AB ₂ -10)	AB ₂ -10	5400	2.21	4.8	5400
poly(AB ₂ -20)	AB ₂ -20	7400	1.94	2.9	6400

^{a)} determined by SEC in THF vs polystyrene standards;

^{b)} determined by inverse gated ¹³C NMR analysis in CDCl₃

In contrast to SEC analysis which indicates a remarkable success in branching, the ¹H NMR spectra of the long-chain branched poly(lactide)s do not show a significant difference in comparison to the ¹H NMR of the AB₂ macromonomers. In the case of branching, one would expect a change in the ratio of the linear methine peaks and the terminal lactoyl residues in comparison to the prepolymers. Unfortunately, neither the terminal methine peaks nor the terminal methyl peaks are separated from other signals of the polymeric backbone in the proton NMR. Therefore inverse gated ¹³C NMR was used to determine the number of AB₂ units (N_{AB₂}) incorporated into the branched PLA in analogy to theoretical investigations used by Choi and Kwak.¹⁷ Using this approach the calculation of the theoretical M_n of the branched species is possible. The value of N_{AB₂} is determined on the basis of the branching theories by Flory⁴² and Stockmayer⁴³:

$$N_{AB_2} = \frac{m}{2 N_{LA} - m} \quad (2)$$

where m is denoted as the ratio of the integrated area of the repeating methine carbon units (CH lin; 68.8-69.5 ppm) to the integrated area of the methine carbon end groups (CH term; 66.61 ppm) of the branched poly(lactide)s. The number of lactide units incorporated into the AB₂ macromonomers, N_{LA}, was determined in a similar manner. With the value of N_{AB₂} the average molecular weight is obtained by Equation 3¹⁷:

$$M_n(\text{poly}(AB_2 - x)) = M_{n,NMR}(AB_2 - x) N_{AB_2} - M_w(H_2O) (N_{AB_2} - 1) \quad (3)$$

The characterization data obtained by NMR analysis are presented in Table 2. It is well-known from literature, that the M_n obtained by SEC for branched polymers is not comparable with the experimental data calculated from NMR spectroscopy. With branching, a decrease in the hydrodynamic volume occurs and a certain discrepancy from the polystyrene standard is observed. This explains the deviation in the average molecular weight of poly(AB₂-5) comparing the SEC and

^1H -NMR data. Additional evidence was gathered from ^{13}C NMR spectra. In the case of branching the formation of a new carbonyl carbon peak (CO) should be observed due to the condensation reaction. As it is highlighted in the ^{13}C NMR (Figure 7) a new carbonyl peak (170.94 ppm) is indeed identified, which is shifted to lower ppm. In addition, the shift of the quaternary carbon in the upper field (50.00-ppm) underlines the branching through the carboxylic acid group of BHB. This observation is in accordance with our previous studies concerning the different BHB units incorporated in the polymer backbone of hyperbranched poly(glycolide).⁴⁴ Due to low signal intensities, especially signals concerning the quaternary and carbonyl carbons, which show no proton coupling, are difficult to analyze. In fact, as the chemical environment barely changes, we do not expect new methine or methyl resonances.

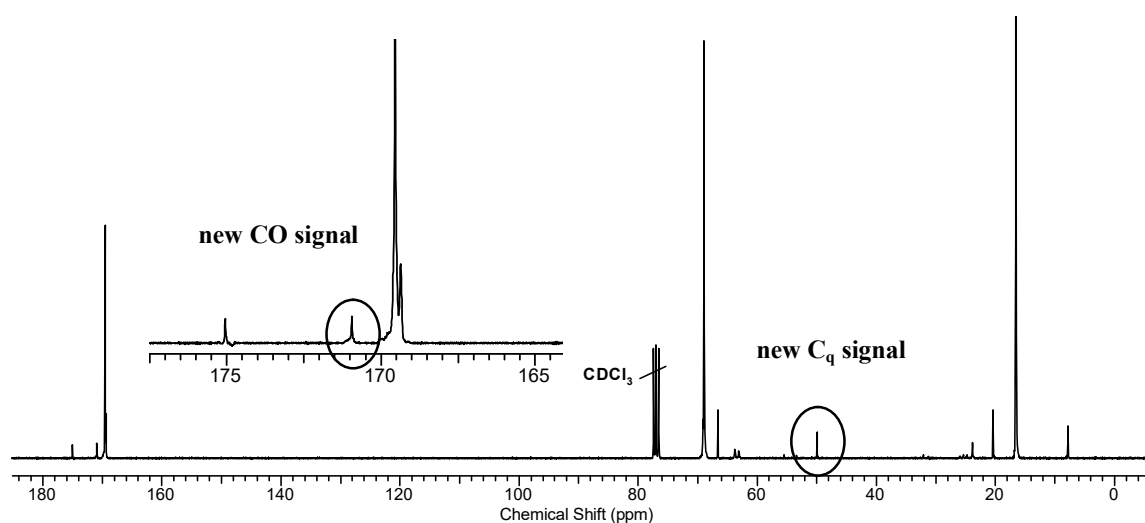


Figure 7. ^{13}C NMR spectrum (CDCl₃) of AB₂-10 after self-condensation.

MALDI-ToF MS provides important information according to the structural composition of the polymer molecules. It is well-known that polydisperse samples are difficult to analyze, since small macromolecules are favoured during ionization due to the mass discrimination effect.⁴⁵ Therefore, the objectivity of MALDI-ToF MS is limited, when the polydispersity of a polymer increases and significantly exceeds $M_w/M_n > 1.2$. To obtain insight into the distribution despite this problem, we fractionated the polydisperse samples of the branched polymers by preparative SEC in THF. The more defined fractions were reinjected in the SEC in order to determine their elution volume. Figure 8 shows the MALDI-ToF mass spectra and SEC elugrams of poly(AB₂-10) and its collected fractions.

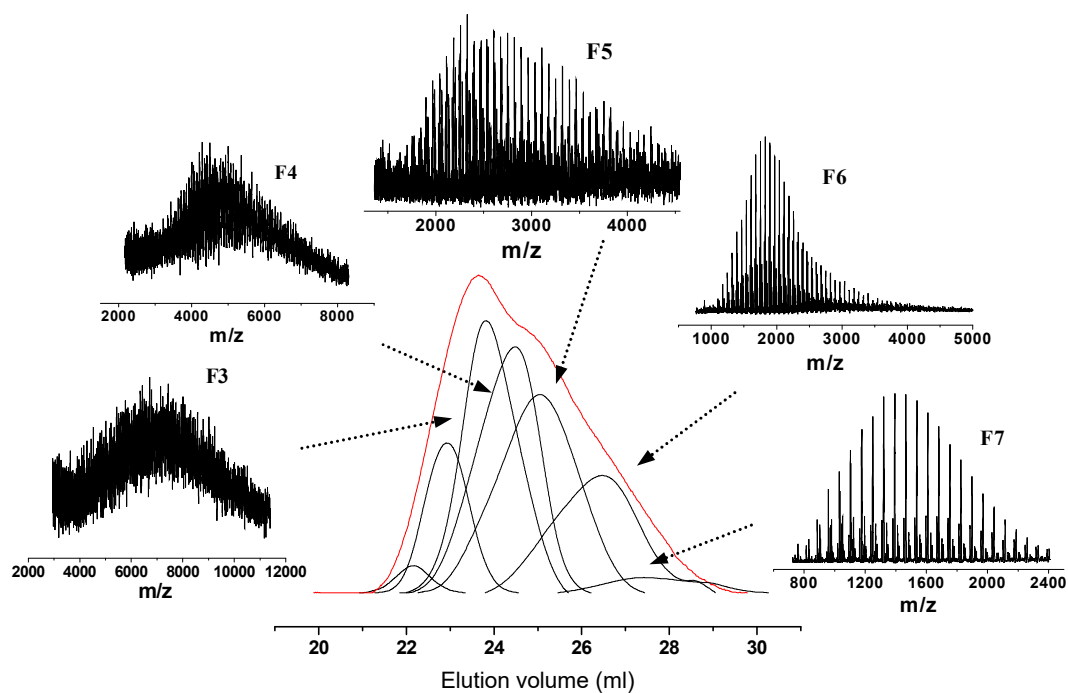


Figure 8. SEC elugrams of poly(AB_2 -10), fractions 1 to 7 collected by preparative SEC and MALDI-ToF MS spectra for F3 to F7 are displayed.

Unfortunately, the high molecular weight fractions 1 to 4 did not permit detailed signal assignment due to a lack of single mass signal resolution. Fractions 5 to 7 show several sub-distributions which reveal an incorporation of the AB_2 macromonomer over the entire detected mass range. Each of the sub-distributions is characterized by a different number of BHB units in contrast to one BHB molecule per AB_2 macromonomer, which evidences a successful condensation reaction. The mass difference of 18 g mol^{-1} compared to the main distribution indicates the formation of a single cycle per molecule by the self-condensation reaction of a focal and an end group of the same molecule. The odd number of lactic acid units refers again to transesterifications during $\text{Sn}(\text{Oct})_2$ -catalyzed ROP. In fact, different sub-distributions are obtained, which can be attributed to cyclization, to completely unreacted AB_2 macromonomer in a minor extent, and to a pronounced distribution emerging from the branched polymer with two or more BHB units. As expected, the last, lower molecular weight fractions contain a higher extent of cycles compared to the first collected fractions which represent the main condensation products (Figure S7-S9). Although the high number of sub-distributions present in the samples partially exceeds the resolution capacity of the MALDI-ToF MS instrument, detailed characterization analysis of the molecules with a higher extent of branching units is possible for instance for fraction 2 of poly(AB_2 -40) (Figure S8).

Conclusion

We have achieved the successful synthesis of long-chain branched poly(lactide)s via a facile two-step procedure involving (1) the Sn(Oct)₂-catalyzed ROP of lactide and (2) the self-condensation of AB₂ macromonomers under mild reaction conditions. The influence of the carboxylic acid on the polymerization rate was confirmed by ¹H NMR kinetic analysis, and suitable polymerization conditions were established by prolonging the reaction time. The ring-opening polymerization allows for the synthesis of macromonomers with controlled molecular weight by adjusting the monomer to initiator ratio.

The different lengths of the prepolymers have an influence on the success of the final polycondensation reaction, as shown by SEC and NMR analysis. The reaction route is limited to AB₂ macromonomers with a molecular weight < 4500 g mol⁻¹. The reactivity decreases with decreasing number of chain ends per unit volume. MALDI-ToF mass spectra and SEC elugrams showed a significantly higher molecular weight compared to the macromonomer, providing a convincing evidence of the successful coupling reaction and hence the formation of a branched structure. Detailed ¹³C NMR analysis confirmed the condensation reaction by the formation of new resonances, i.e. a new carbonyl ester peak. Our results show that the poly(lactide)-based macromonomers can be used for polycondensation without tedious protection and deprotection steps. High molecular weight branched PLAs are synthesized under mild reaction conditions preventing e.g., etherification as well as epimerization, which occur under acidic conditions used for polycondensation due to the harsh reaction conditions. In addition, the reacting functionalities of the AB₂-type prepolymers may exhibit lower sterical hindrance in comparison to generally used monomers, e.g., bis-MPA.¹⁴ The better accessibility may play a role in the success of branching. The synthesized structures are promising materials for drug release and transport of therapeutic agents. Future studies will focus on the biocompatibility of these polymers and their derivatization.

Acknowledgements. The authors thank Annika Hörberg and Ines Wollmer for technical assistance. Maria Müller is acknowledged for DSC measurements. We thank Monika Schmelzer for SEC measurements. A. M. Fischer is grateful for financial support of the International Max-Planck Research School for Polymer Materials, Mainz (IMPRS-PMS). H. Frey acknowledges financial support from the Fonds der Chemischen Industrie as well as the German Science Foundation (DFG).

Supporting Information

I. ^{13}C NMR analysis

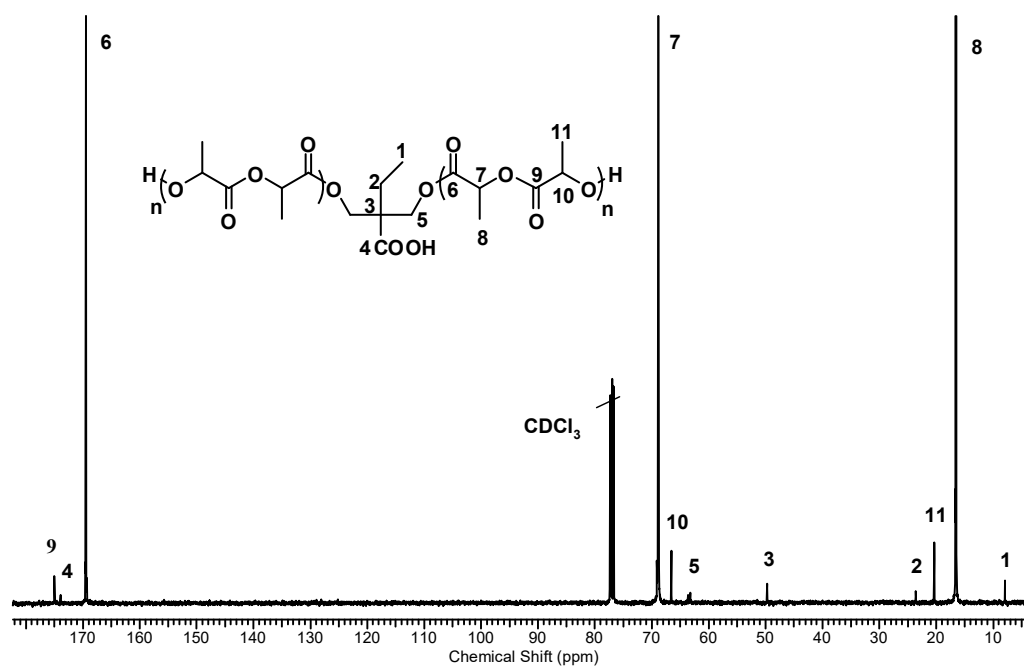


Figure S1. ^{13}C NMR spectrum (75 MHz) of AB₂-20 in CDCl₃.

II. MALDI-ToF mass spectrometry

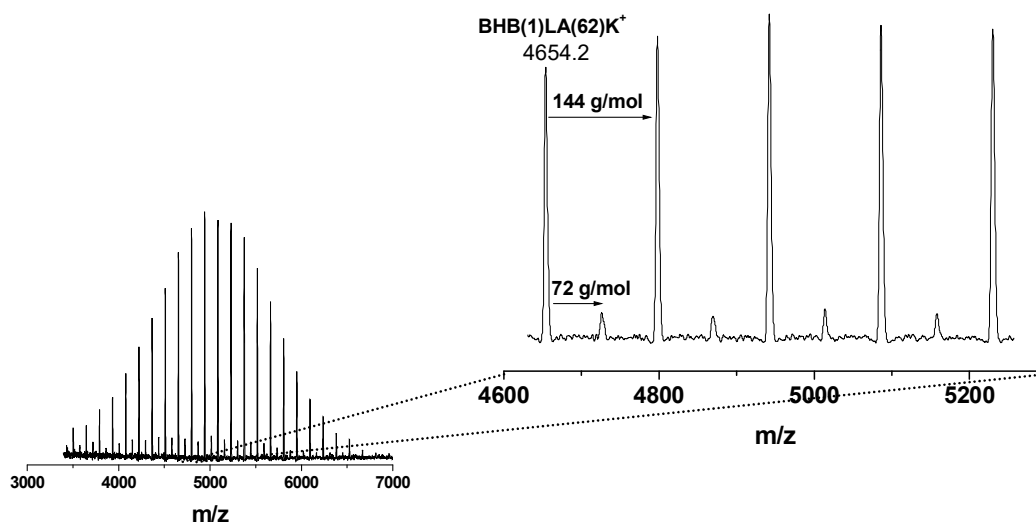


Figure S2. MALDI-ToF mass spectra of AB₂-40 with potassium as counterion.

III. DSC analysis

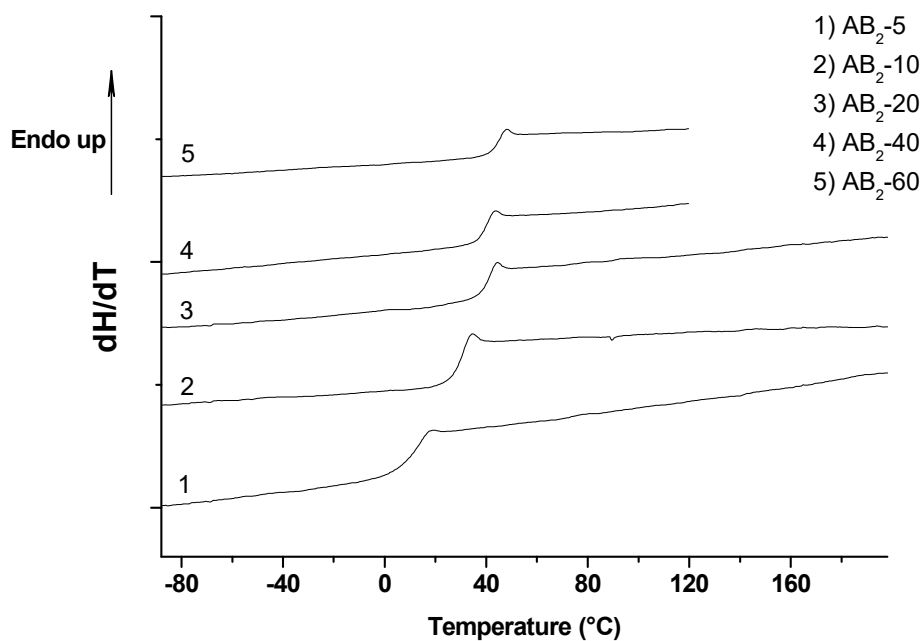


Figure S3. DSC curves of AB₂ macromonomers showing the second heating scan with a heating rate of 20K/min.

IV. Kinetic investigations

Table S1. SEC data for the kinetic investigation in Figure 3.

Time (min)	M _n (g·mol ⁻¹)	M _w /M _n
10	1900	1.16
20	5400	1.13
40	7000	1.15
80	7100	1.17
160	7500	1.15

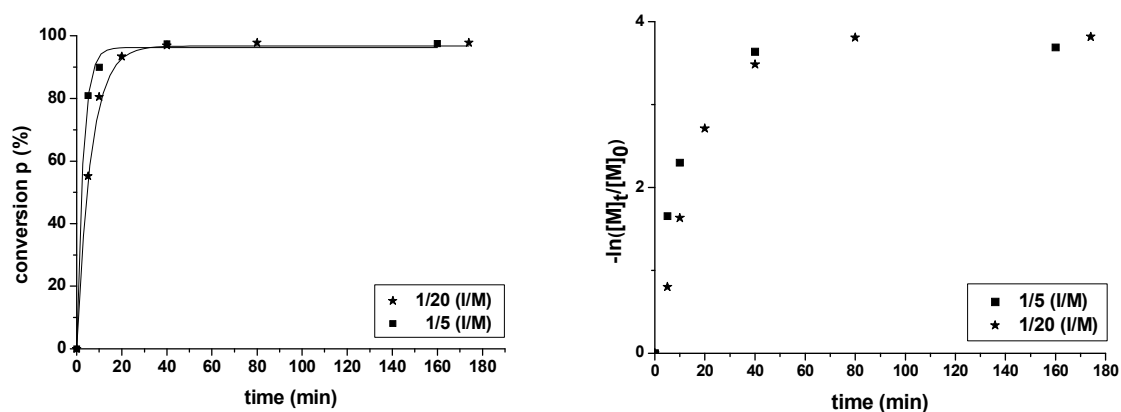


Figure S4. Conversion p (left) and kinetic data (right) for the solution polymerization of L-lactide with 1,6-hexanediol as initiator, polymerization conditions: 130 °C, [monomer]/[catalyst]=1000 in toluene.

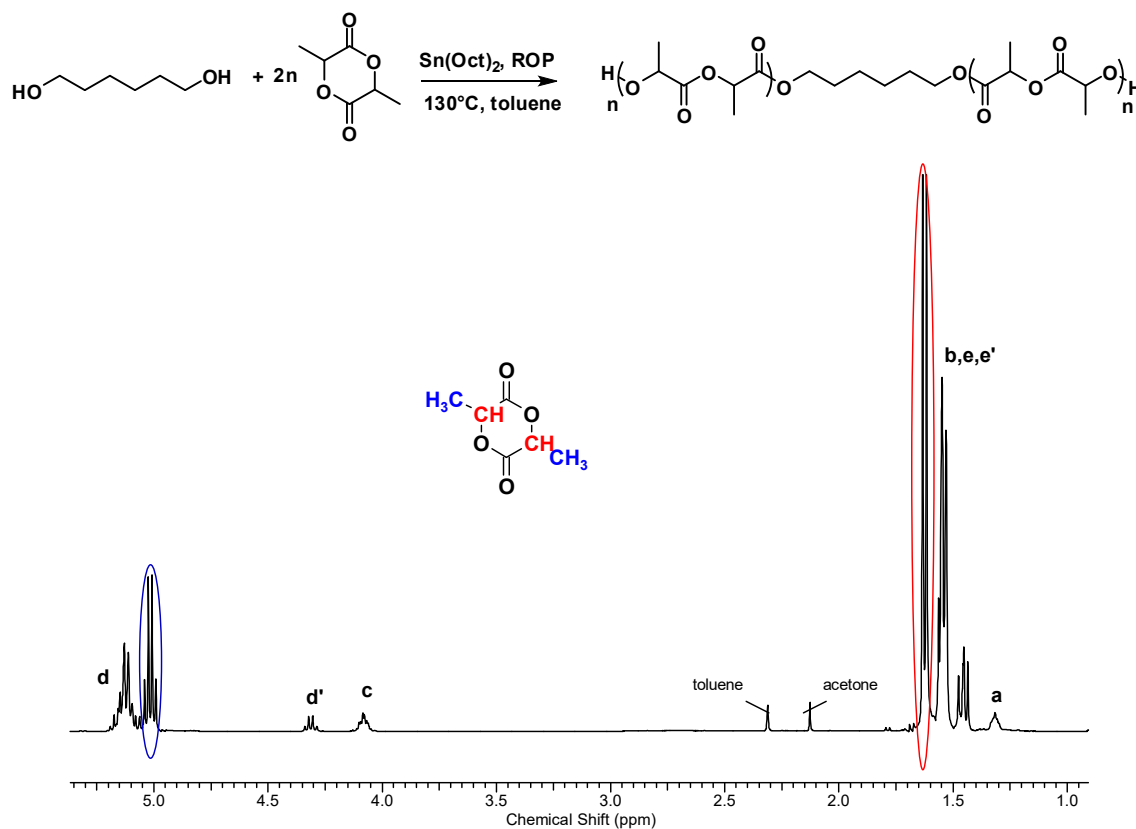
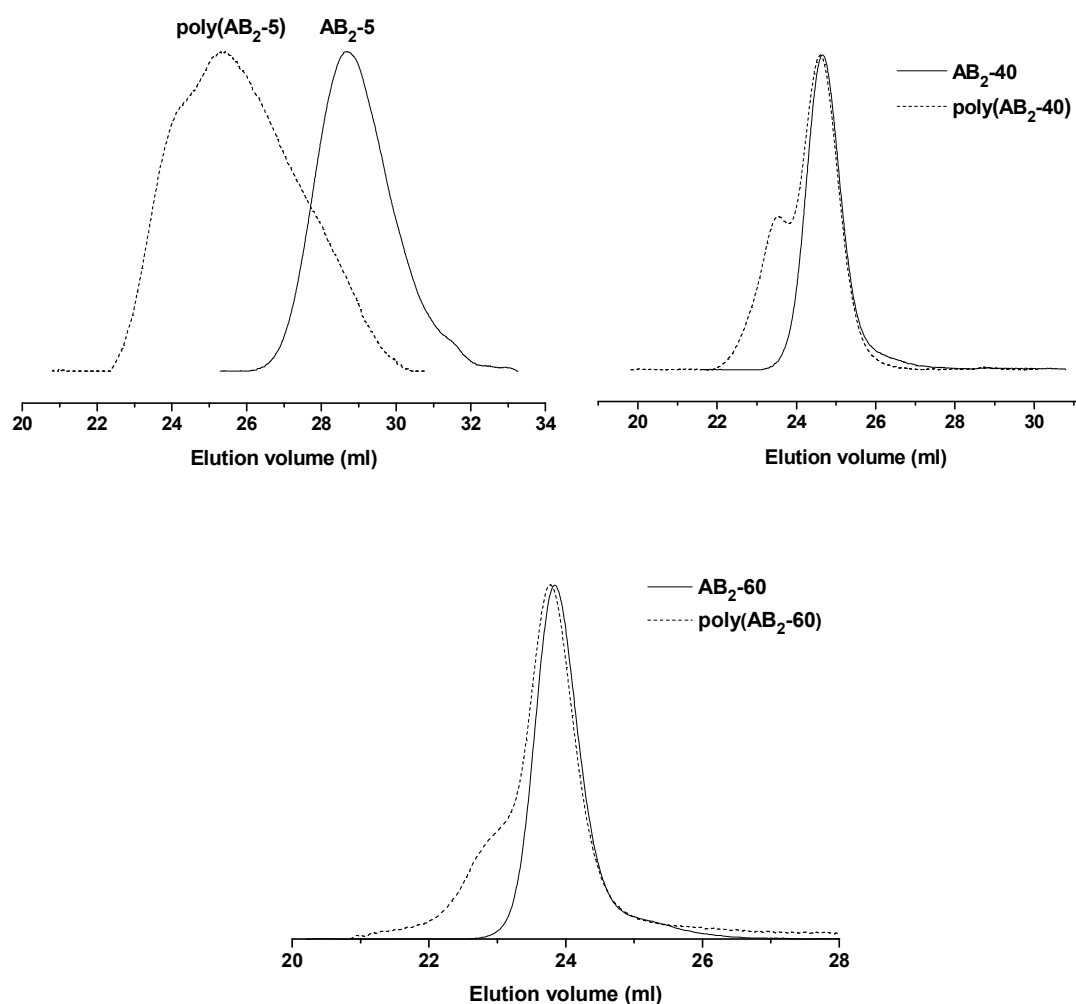


Figure S5. ^1H NMR (CDCl_3) after 5 min; solution polymerization of L-lactide with 1,6-hexanediol as initiator ($M/I=20$).

Table S2. Relative polymerization rates of L-lactide using BHB or 1,6-HD as initiator.

Initiator, entry M/I	[M] _{eq}	$k_p[\text{cat}]_0$ (min ⁻¹)
BHB, AB ₂ -5	8.28%	$0.0061 \pm 2.66 \cdot 10^{-4}$
BHB, AB ₂ -10	5.07%	$0.0138 \pm 1.57 \cdot 10^{-3}$
BHB, AB ₂ -20	3.60%	$0.0361 \pm 8.58 \cdot 10^{-4}$
1,6-HD, AB ₂ -5	2.50%	0.3308 ± 0
1,6-HD, AB ₂ -20	2.20%	$0.1620 \pm 8.48 \cdot 10^{-4}$

V. Size exclusion chromatography

**Figure S6.** SEC traces of AB₂-5, AB₂-40 and AB₂-60 before and after polycondensation.

VI. Investigation of MALDI-ToF mass spectra

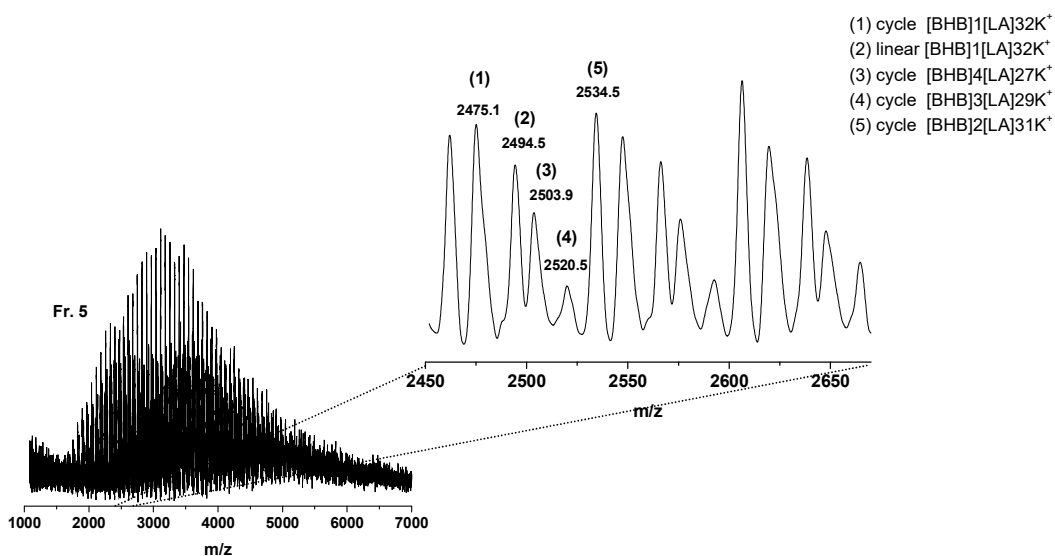


Figure S7. Detailed MALDI-ToF mass spectrum of poly(AB₂-10), fraction 5, measured with dithranol matrix and potassium as counterion.

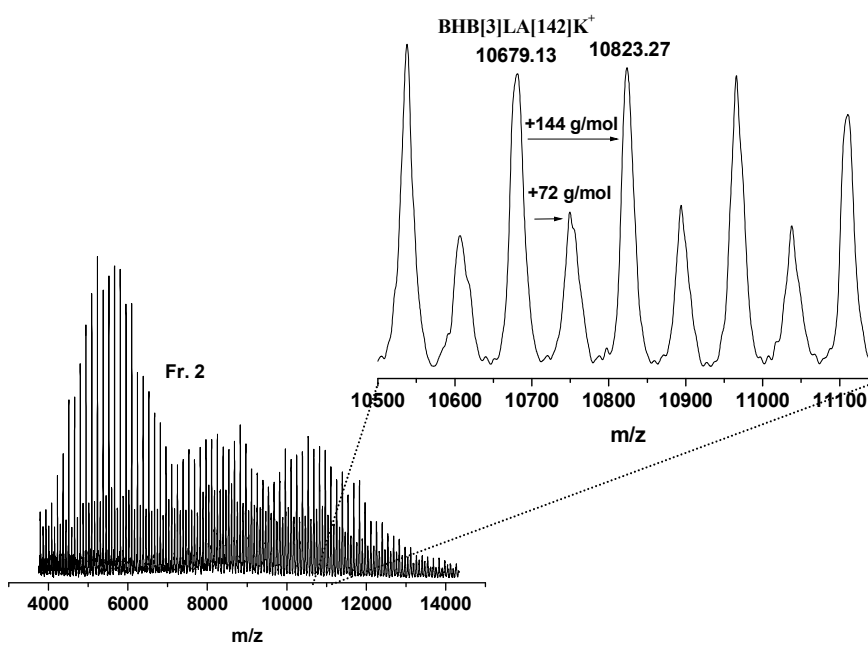


Figure S8. Detailed MALDI-ToF mass spectrum of poly(AB₂-40), fraction 2 measured with dithranol matrix and potassium as counterion.

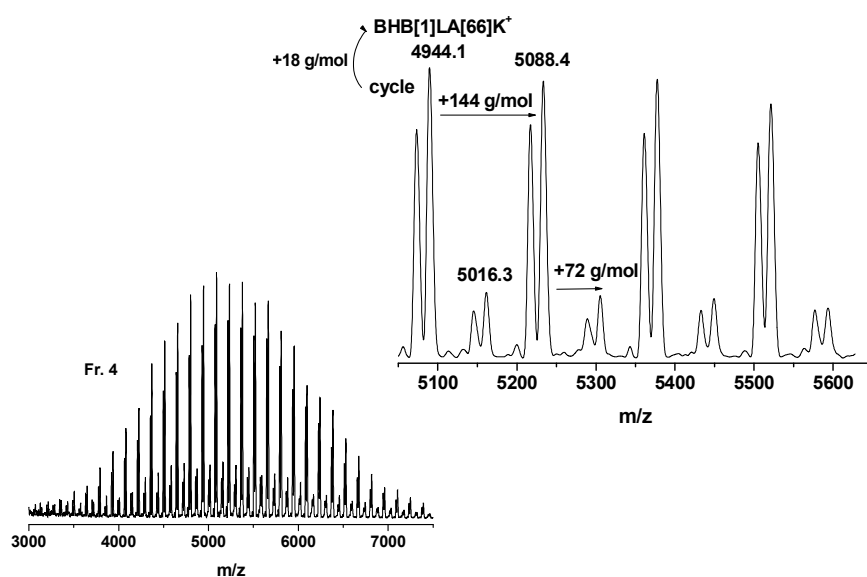


Figure S9. Detailed MALDI-ToF mass spectrum of poly(AB₂-40), fraction 4 measured with dithranol matrix and potassium as counterion.

The molar masses of the branched acyclic and cyclic species were calculated according to the following equations:

$$M = (C_6H_9O_3)_x + (C_3H_4O_2)_n + H_{(x+2)}O + K^+ \quad (S1)$$

$$M_{cycle} = M - 18 \text{ g}\cdot\text{mol}^{-1} \quad (S2)$$

References

1. S. P. Kersey, S. Patel, V. T. Thaller, *Clinical & Experimental Ophthalmology* **2006**, *34*, 152.
2. C. G. Munton, C. I. Phillips, B. Martin, R. S. Bartholomew, I. Capperault, *Br. J. Ophthalmol.* **1974**, *58*, 941.
3. P. Malyala, D. T. O'Hagan, M. Singh, *Advanced Drug Delivery Reviews* **2009**, *61*, 218.
4. J. C. Price, K. Suzuki, *Journal of Pharmaceutical Sciences* **1985**, *74*, 21.
5. K. N. R. Salehi, A. A. Entezami, V. Asgharzadeh, S. Davaran, *Polymers for Advanced Technologies* **2009**, *20*, 416.
6. Y.-K. H. S.H. Kim, Y. H. Kim, S. I. Hong, *Macromol. Chem.* **1992**, *193*, 1623.
7. F. K. Wolf, C. Gottschalk, H. Frey, *Macromol. Chem. Phys.* **2007**, *208*, 1657.
8. Z. Zhong, C. Hiemstra, L. Li, P. J. Dijkstra, J. Feijen, *Biomacromol.* **2006**, *7*, 2790.

9. L. Y. Qiu, Y. H. Bae, *Pharmaceutical Research* **2006**, *23*, 1.
10. I. B. Voit, A. Lederer, *Chem. Rev.* **2009**, *109*, 5924.
11. M. Jikei, M.-a. Kakimoto, *Prog. Polym. Sci.* **2001**, *26*, 1233.
12. M. Trollsås, J. L. Hedrick, *J. Am. Chem. Soc.* **1998**, *120*, 4644.
13. E. Malmström, M. Johansson A. Hult, *Macromolecules* **1995**, *28*, 1698.
14. H. Magnusson, E. Malmström, A. Hult, *Macromolecules* **2000**, *33*, 3099.
15. [15 a] E. Žagar, M. Žigon, *Macromolecules* **2002**, *35*, 9913; [15 b] E. Žagar, M. Žigon, S. Podzimek, *Polymer* **2006**, *47*, 166; [15 c] E. Žagar, M. Žigon, *Prog. Polym. Sci.* **2011**, *36*, 53.
16. J. L. Hedrick, M. Trollsås, *Macromolecules* **1998**, *31*, 4390.
17. J. Choi, S. Y. Kwak, *Macromolecules* **2003**, *36*, 8630.
18. M. Smet, S. Skaria, H. Frey, *Macromol. Rapid Commun.* **2002**, *23*, 292.
19. C. Gottschalk, M. Smet, S. Skaria, H. Frey, *Macromol. Chem. Phys.* **2005**, *206*, 2421.
20. C. Gottschalk, H. Frey, *Macromolecules* **2006**, *39*, 1719.
21. L. M. Pitet, S. B. Hait, T. J. Lanyk, D. M. Knauss, *Macromolecules* **2007**, *40*, 2327.
22. R.-X. Zhao, L. Li, B. Wang, W.-W. Yang, Y. Chen, X.-H. He, F. Cheng, *Polymer* **2012**, *53*, 719.
23. M. Trollsås, P. Löwenhielm, V. Y. Lee, M. Möller, R. D. Miller, J. L. Hedrick, *Macromolecules* **1999**, *32*, 9062.
24. F. K. Wolf, H. Frey, *Macromolecules* **2009**, *42*, 9443.
25. T. Fukuoka, H. Habe, K. Kitamoto, K. Skakai, *J. Oleo Sci.* **2011**, *60*, 369.
26. T. R. Cooper, R. F. Storey, *Macromolecules* **2008**, *41*, 655.
27. Velthoen, I. W., Dijkstra, P. J., Feijen, J. *Macromol. Chem. Phys.* **2009**, *210*, 689.
28. G. Lippke, H. Thaler, *Stärke* **1970**, *22*, 344.
29. G. Schwach, J. Coudane, R. Engel, M. Vert, *Polym. Bull.* **1994**, *32*, 617.
30. T. W. Y. He, J. Wei, Z. Fan, S. Li, *J. Polym. Sci. Part B: Polym. Phys.* **2008**, *46*, 959.
31. D. Garlotta, *J. Polym. Env.* **2001**, *9*, 63.
32. R. E. Drumright, P. R. Gruber, D. E. Henton, *Adv. Mater.* **2000**, *12*, 1841.
33. E. W. Fischer, H. J. Sterzel, G. Wegner, *Kolloid Z. Z. Polym.* **1973**, *251*, 980.
34. H. Tsuji, Y. Ikada, *Macromol. Chem. Phys.* **1996**, *197*, 3483.
35. F. Jing, M. R. Smith, G. L. Baker, *Macromolecules* **2007**, *40*, 9304.
36. A. Duda, A. Kowalski, S. Penczek, *Macromol. Rapid Commun.* **1998**, *19*, 567.
37. M. Ryner, K. Stridsberg, A.-C. Albertsson, H. von Schenck, M. Svensson, *Macromolecules* **2001**, *34*, 3877.
38. A. Kowalski, A. Duda, S. Penczek, *Macromolecules* **2000**, *33*, 7359.
39. M. Yin, M., G. L. Baker, *Macromolecules* **1999**, *32*, 7711-7718.
40. H. R. Kricheldorf, O. Stoeber, *Macromolecules* **1995**, *28*, 2118.

41. Burgath, A. Sunder, H. Frey, *Macromol. Chem. Phys.* **2000**, 201, 782.
42. P. J. Flory, *J. Am Chem. Soc.* **1952**, 75, 2718.
43. W. H. Stockmayer, *J. Chem. Phys.* **1943**, 11, 45.
44. A. M. Fischer, H. Frey, *Macromolecules* **2010**, 43, 8539.
45. H. C. Byrd, C. N. McEwen, *Anal. Chem.* **2000**, 72, 4568.

A.2 CURRICULUM VITAE
